DIGITALCOMMONS
@WAYNESTATE

Wayne State University

Wayne State University Dissertations

1-1-2013

Studies On The Physicochemical Properties Of Eu2+ Cryptates: Implications To Contrast Agents For Magnetic Resonance Imaging

Joel Garcia
Wayne State University,

Follow this and additional works at: http://digitalcommons.wayne.edu/oa_dissertations

 Part of the Chemistry Commons

Recommended Citation
Garcia, Joel, "Studies On The Physicochemical Properties Of Eu2+ Cryptates: Implications To Contrast Agents For Magnetic Resonance Imaging" (2013). *Wayne State University Dissertations.* Paper 657.

This Open Access Dissertation is brought to you for free and open access by DigitalCommons@WayneState. It has been accepted for inclusion in Wayne State University Dissertations by an authorized administrator of DigitalCommons@WayneState.

STUDIES ON THE PHYSICOCHEMICAL PROPERTIES OF Eu^{2+} CRYPTATES: IMPLICATIONS TO CONTRAST AGENTS FOR MAGNETIC RESONANCE IMAGING

by

JOEL GARCIA

DISSERTATION

Submitted to the Graduate School

of Wayne State University,

Detroit, Michigan

in partial fulfillment of the requirements

for the degree of

DOCTOR OF PHILOSOPHY

2013

MAJOR: CHEMISTRY

Approved by

_____

Advisor Date

_____

_____

_____

DEDICATION

To my loving parents

ACKNOWLEDGEMENTS

Working on my Ph. D. has been an interesting and overwhelming adventure in an attempt to satisfy my unquenchable thirst for knowledge in chemistry. This part of my thesis is dedicated to those who made my Ph. D. journey as worthwhile as possible. It was a privilege to be in graduate school and I was grateful to do research in an academic environment equipped with excellent facilities and talented individuals.

First and foremost, I am deeply indebted to my research advisor Professor Matthew J. Allen for giving me the opportunity to do research in his laboratory. His incredible work ethic inspired me to work hard and stay on track with my research. It has been a pleasure working with one of the best mentors in the academia.

I would like to thank my committee members: Professor Claudio N. Verani, Professor Sarah Trimpin, and Professor E. M. Haacke for their valuable suggestions and advice throughout my Ph. D. career.

In addition, I have been very grateful to collaborate with many great people. Thank you Dr. Jaladhar Neelavalli and Uday Bhaskar for walking me through the Matlab codes. My special thanks to Dr. Yimin Shen and Latif Zhahid for doing the MR imaging, and Professor Lisa Polin and Kathryn White for their help in the toxicity studies. I also acknowledge Dr. Bashar Ksebati for his assistance with variable-temperature T_1 and ^{17}O NMR measurements and Dr. James Windak for training me on how to use the EPR instrument at the University of Michigan.

I am privileged to be part of a talented research group. My experiments would not have been successful without the valuable insights coming from the past and present members of the Allen group. It was worth the time to spend several hours in group meetings especially when you learned a lot of ideas from group discussions. Beyond serious group discussions, I also enjoyed

all of the activities outside the four corners of the lab – group picnics and parties, watching a baseball game, drinking at Lefty's, and playing new games including laser tag and feather bowling. Thanks to Sashi, Derek, Akhila, and Levi for proofreading a part of my thesis. I am also thankful to work with my hood partners Nipuni Gamage and Zhijin Lin for their company especially during those times when I was running columns day after day to purify my compounds.

Not to be discounted are my friends who made my stay in the U.S. as enjoyable as possible. I would like to thank Didoy and family, Armando, Janir, and Ellen for helping me settle down during my first year in graduate school. My travel buddies–Juvy, Jake, Gigi, Christian, Mayrose, Stephen, Dennis, Morwena, Rommel, Kristian, Farah, Avi, Paul, Rich, and Benson–for all the fun.

I share the credit of my work to Gillian who is always there for me. Your love and support enabled me to stay focused and optimistic with my research. Thank you and I love you!

This thesis would not have been possible without the emotional support and words of encouragement from my relatives. I am forever indebted to my mom for her exceptional guidance and support during my endeavors.

Maraming salamat sa lahat!

TABLE OF CONTENTS

Dedication……...…… ii

Acknowledgements……...…….. iii

List of Tables……..……..... x

List of Figures……...…….…. xii

List of Schemes……..…….... xvi

List of Abbreviations……..……... xvi

List of Symbols……...…..... xxi

CHAPTER ONE: Introduction to Contrast Agents for Magnetic Resonance Imaging. 1

1.1 Introduction……..……..... 1

1.2 Ultra-High Field Strength MRI……..…..…. 1

1.3 Contrast Agents for MRI……..……..……... 2

1.4 Factors Influencing the Efficiency of MRI Contrast Agents……...……. 4

1.5 Eu^{2+}-Containing [2.2.2]cryptates…….……...…….…... 7

1.6 References……..…..……. 10

CHAPTER TWO: Developments in the Coordination Chemistry of Eu^{2+}……. 14

2.1 Introduction…….……... 14

2.1.1. Properties of Eu^{2+}…….……..……..... 14

2.1.2 Early Eu^{2+} Complexes…….……...…… 16

2.2 Synthesis of Recent Eu^{2+}-Containing Complexes……..……..…….. 22

2.2.1 Oxidation of Eu^{0}……. 22

2.2.2 Reduction of Eu^{3+}……...…….……... 28

2.2.3 Metathesis of Eu^{2+} Complexes……..……..……... 30

2.3 Applications of Eu^{2+}-Containing Complexes……...……..…… 34

2.3.1 Reductants……..…….…….. 34

2.3.2 Polymerization Initiators…….……...…… 36

2.3.2.1 Methyl Methacrylate Polymerization…...…….. 36

2.3.2.2 Ring-Opening Polymerization of ε-Caprolactone……...……... 38

2.3.3 Luminescent Complexes…….…….……..…… 40

2.3.4 MRI Contrast Agents…….…..……..…… 43

2.4 Conclusions…..…..……... 45

2.5 References……..…..……. 45

CHAPTER THREE: Eu^{2+}-Containing Cryptates as Contrast Agents for Ultra-High Field Strength MRI…….…...……... 52

3.1 Introduction……...…….…….……... 52

3.2 Imaging Properties of Eu^{2+}-Containing Cryptates……...……..…… 55

3.2.1 Influence of Magnetic Field on Relaxivity……..…….……. 55

3.2.2 Influence of Temperature on Relaxivity…….…..……. 58

3.2.3 Influence of pH on Relaxivity……...…….…… 60

3.2.4 Phantom Imaging Experiments……...…….…….. 61

3.3 Physical Properties of Eu^{2+}-Containing Cryptates……...……..…… 62

3.3.1 Variable-Temperature ^{17}O NMR Spectroscopy……...……. 62

3.3.2 Electron Paramagnetic Resonance (EPR) Spectroscopy……...…….…… 64

3.4 Conclusions……...……. 66

3.5 Experimental Procedures…… 67

3.5.1 Materials…… 67

3.5.2 Characterization…… 67

3.5.3 Imaging and Relaxometric Experiments…… 68

3.5.4 Synthesis…… 95

3.6 References…… 99

3.7 Estimating Rotational Correlation Time (τ_R)…… 102

3.7.1 Theoretical Basis…… 102

3.7.2 Calculating τ_R using Microsoft Excel Spreadsheet…… 103

3.8 ^{1}H and ^{13}C NMR Spectra of **3.4**–**3.8**…… 106

CHAPTER FOUR: Stability of Eu^{2+}-Containing Cryptates…… 116

4.1 Introduction…… 116

4.2 Synthesis…… 117

4.3 Kinetic Stability Studies…… 118

4.4 Conclusions…… 123

4.5 Experimental Section…… 123

4.5.1 Materials…… 123

4.5.2 Characterization…… 124

4.5.3 Synthesis…… 124

4.5.4 Transmetallation Kinetics…… 126

4.6 References…… 126

4.7 ^{1}H and ^{13}C NMR Spectra of **4.3** and **4.4**…… 129

CHAPTER FIVE: Interaction of Biphenyl Functinalized Eu^{2+}-Containing Cryptate with Albumin Binding: Implications to Contrast Agents in MRI…… 133

5.1 Introduction……..…….. 133

5.2 Results and Discussion…….…….. 134

5.2.1 Influence of Magnetic Field on the Relaxivity of **5.1** and **5.1**–HSA……. 135

5.2.2 Albumin Titration……... 136

5.2.3 ^{17}O NMR Spectroscopy…….. 138

5.3 Conclusions……...……. 139

5.4 Experimental Section……. 140

5.4.1 Materials……. 140

5.4.2 Concentrations…… 140

5.4.3 Preparation of HSA Samples…….. 141

5.4.4 Preparation of Sr^{2+} analogue of **5.1**…….……... 141

5.4.5 T_1 and relaxivity measurements……...…….. 141

5.4.6 Variable-temperature ^{17}O NMR experiments……...……. 142

5.5 References…….……. 145

CHAPTER SIX: Summary of Findings and Future Outlook……... 148

6.1 Summary of Findings…….…… 148

6.2 Future Outlook…….…….. 150

Appendix A: Matlab Codes for Generatig T_2^* and T_1 maps..…….…… 153

Appendix B: Calculated Relaxivity of **5.1** and **5.1**–HSA at Different Magnetic Field Strengths……. 159

Appendix C……..……..……. 162

Abstract……...…… 193

Autobiographical Statement…… 196

LIST OF TABLES

Table 1.1 Comparison of Eu^{2+} to Gd^{3+} in terms of charge, ionic radius, and water-exchange rate……... 8

Table 2.1 Luminescence properties of Eu^{2+}-containing complexes in methanol solution and in the solid state (room temperature and 77 K)[6,54,87,88] ……. 42

Table 3.1 r_1 values of GdDOTA and Eu^{II}-containing cryptates……... 56

Table 3.2 Relaxivity parameters (based on ^{17}O NMR and EPR data) and molecular weights of GdDOTA and cryptates **3.1–3.3**…… 63

Table 3.3 ^{17}O NMR data for acidified water and GdDOTA……..…….. 70

Table 3.4 ^{17}O NMR data for Sr^{II} analog of **3.1** and cryptate **3.1**…….…… 72

Table 3.5 ^{17}O NMR data for Sr^{II} analog of **3.2** and cryptate **3.2**…….…… 74

Table 3.6 ^{17}O NMR data for Sr^{II} analog of **3.3** and cryptate **3.3**…….…… 76

Table 3.7 T_{1e} values for GdDOTA and cryptates **3.1**–**3.3** and the corresponding correlation coefficients (R^2) in the ^{17}O NMR fits…..…….. 78

Table 3.8 T_1 data for GdDOTA (1.4 T, Temp = 37 °C)……... 81

Table 3.9 T_1 data for Cryptate **3.1** (1.4 T, Temp = 37 °C)……... 81

Table 3.10 T_1 data for Cryptate **3.2** (1.4 T, Temp = 37 °C)……..…… 82

Table 3.11 T_1 data for Cryptate **3.3** (1.4 T, Temp = 37 °C)……... 82

Table 3.12 T_1 data for GdDOTA (3 T, Temp = 19.8 °C)……... 83

Table 3.13 T_1 data for Cryptate **3.1** (3 T, Temp = 19.8 °C)……... 84

Table 3.14 T_1 data for Cryptate **3.2** (3 T, Temp = 19.8 °C)……... 85

Table 3.15 T_1 data for Cryptate **3.3** (3 T, Temp = 19.8 °C)……... 86

Table 3.16 T_1 data for GdDOTA (7 T, Temp = 19 °C)…….. 87

Table 3.17 T_1 data for Cryptate **3.1** (7 T, Temp = 19 °C)…….. 88

Table 3.18 T_1 data for Cryptate **3.2** (7 T, Temp = 19 °C)…….. 89

Table 3.19 T_1 data for Cryptate **3.3** (7 T, Temp = 19 °C)…….. 90

Table 3.20 T_1 data for GdDOTA (11.7 T, Temp = 37 °C)……. 91

Table 3.21 T_1 data for Cryptate **3.1** (11.7 T, Temp = 37 °C)……. 91

Table 3.22 T_1 data for Cryptate **3.2** (11.7 T, Temp = 37 °C)……. 92

Table 3.23 T_1 data for Cryptate **3.3** (11.7 T, Temp = 37 °C)……. 92

Table 3.24 T_1 data for GdDOTA (11.7 T, Temp = 20 °C)……. 93

Table 3.25 T_1 data for Cryptate **3.1** (11.7 T, Temp = 20 °C)……. 93

Table 3.26 T_1 data for Cryptate **3.2** (11.7 T, Temp = 20 °C)……. 94

Table 3.27 T_1 data for Cryptate **3.3** (11.7 T, Temp = 20 °C)……. 94

Table 4.1 Calculated %Eu^{2+} dechelated via transmetalation in the presence of Ca^{2+}, Mg^{2+}, and Zn^{2+} after 4740 min (Ca^{2+}), 4770 min (Mg^{2+}), and 4800 min (Zn^{2+}) treatment of 2.5 mM of the corresponding endogeneous ions..... 121

Table 4.2 Kinetic index data..... 122

Table 5.1 Results of ^{17}O NMR experiments of cryptate **5.1** with and without albumin…… 139

Table 5.2 Variable-temperature ^{17}O NMR Data for Cryptate **5.1** and Sr^{2+} analogue of **5.1** in the presence of albumin……. 143

Table B.1 Calculated relaxivity values of **5.1** in the presence of HSA at different field strengths at 37 °C……..…..…. 161

LIST OF FIGURES

Figure 1.1 MR images of a human brain taken at (a) 1.5 and (b) 7 T. Improvement in spatial resolution can be seen at 7 T that enables the detection of a cerebral microbleed (noted by the arrow). Reprinted with permission from ref. [3] Copyright (2011) John Wiley and Sons..... 2

Figure 1.2 MR images of mouse brain with an U87MG tumor taken before injection, directly after injection, and 2 min after the injection of gadolinium(III) diethylenetriaminepentaacetate (GdDTPA). The increased permeability of the vasculature in the tumor allows GdDTPA to diffuse into the tumor and resulted in the contrast enhancement. Reprinted with permission from ref. [4] Copyright (2006) Elsevier..... 3

Figure 1.3 Plots of relaxivity (37 °C, plasma) versus field strength for GdDOTA (left) and MS-325–albumin (right)..... 4

Figure 1.4 Plot of proton Larmor frequency versus magnetic field strength. The proton Larmor frequency values were calculated using **Eq 1.5**..... 6

Figure 1.5 Plot of the anodic peak potentials of Eu^{2+} cryptates **1.1**–**1.6**, the Eu^{2+} aqua ion, Fe^{2+} in hemoglobin, and water. A more positive potential means increased oxidative stability. Anodic peak potentials are reported as mean ± standard error of at least three measurements relative to Ag/AgCl[11]..... 8

Figure 1.6 Chemical structure of the unfunctionalized Eu^{2+}-containing [2.2.2]cryptate **1.7**..... 9

Figure 1.7 Chemical structure of the biphenyl-functionalized Eu^{2+}-containing [2.2.2]cryptate **1.8**..... 10

Figure 2.1 Relative reduction potentials for $Ln^{3+} \rightarrow Ln^{2+}$ (V vs NHE)[2]..... 14

Figure 2.2 Structures of Eu^{2+}-containing complexes **2.1**–**2.15**..... 18

Figure 2.3 ^{151}Eu Mössbauer spectrum of **2.9** at 4.2 K. Reprinted with permission from G. W. Rabe, G. P. A. Yap, A. L. Rheingold, *Inorg. Chem*. **1997**, *36*, 3212–3215. Copyright 1997 American Chemical Society……... 20

Figure 2.4 Structures of Eu^{2+}-containing complexes **2.16**–**2.19**, **2.21**–**2.28**, **2.30**–**2.35**, **2.38**, and **2.40** that were prepared from the oxidation of Eu^0…….. 24

Figure 2.5 Structures of Eu^{2+}-containing complexes **2.41**–**2.47**, which were synthesized by the reduction of Eu^{3+}…….. 30

Figure 2.6 Structures of Eu^{2+}-containing complexes **2.48**–**2.62**, which were obtained from the metathesis of Eu^{2+}-containing complexes……. 33

Figure 2.7 Structure of Eu^{2+}-containing reductant **2.63**……... 35

Figure 2.8 Structure of Eu^{2+}-containing complexes **2.64**–**2.82**, which were used as polymerization initiators…… 37

Figure 2.9 Structures of complexes **2.87** and **2.88**…….. 44

Figure 3.1 Structures of GdDOTA (DOTA = 1,4,7,10-tetraazacyclododecane-*N*,*N*',*N*'',*N*'''-tetraacetate) and Eu^{II}-containing cryptates **3.1**–**3.3**. Coordinated water molecules have been omitted for clarity…….. 53

Figure 3.2 Proton longitudinal relaxivity (T = 20 °C, pH = 7.4) of GdDOTA (○) and Eu^{2+}-containing cryptates **3.1** (◊) and **3.2** (□) as a function of magnetic field strength. Error bars represent standard error of the mean.. 57

Figure 3.3 Proton longitudinal relaxivity (T = 37 °C, pH = 7.4) of GdDOTA (○) and Eu^{2+}-containing cryptates **3.1** (◊) and **3.2** (□) as a function of magnetic field strength. Error bars represent standard error of the mean.. 58

Figure 3.4 Proton longitudinal relaxivity (9.4 T and pH = 7.4) of Eu^{2+}-containing cryptates **3.1** (□) and **3.2** (○) as a function of temperature. Error bars represent standard error of the mean..... 59

Figure 3.5 Proton longitudinal relaxivity (11.7 T, pH = 7.4) of Eu^{2+}-containing cryptates **3.1** (□) and **3.2** (○) as a function of temperature. Error bars represent standard error of the mean..... 59

Figure 3.6 Longitudinal relaxivity at 1.4 T at 37 °C (**3.1** (■) and **3.2** (●)) and 7 T at 19 °C (**3.1** (□) and **3.2** (○)) as a function of pH. Error bars represent standard error of the mean..... 61

Figure 3.7 (a) T_1-weighted MR images of solutions of PBS, GdDOTA (1.0 mM in PBS), and **3.1**–**3.3** (1.0 mM in PBS) at 7 T. The diameter of the tubes that were used for imaging was 6 mm. Imaging parameters were T_R = 21 ms; T_E = 3.26 ms; and resolution = 0.27 × 0.27 × 2 mm^3. (b) Comparison of $1/T_1$ values of the samples from (a) at 7 T. Error bars represent standard error of the mean…….. 62

Figure 3.8 X band EPR spectrum of cryptate **3.1** in PBS at 77 K..... 65

Figure 3.9 X band EPR spectrum of GdDOTA in PBS at 77 K..... 65

Figure 3.10 ^{17}O NMR fits for GdDOTA..... 71

Figure 3.11 ^{17}O NMR fits for cryptate **3.1**..... 73

Figure 3.12 ^{17}O NMR fits for cryptate **3.2**..... 75

Figure 3.13 ^{17}O NMR fits for cryptate **3.3**..... 77

Figure 3.14 ^{1}H NMR Spectrum of **3.4**..... 106

Figure 3.15 ^{13}C NMR Spectrum of **3.4**..... 107

Figure 3.16 ^{1}H NMR Spectrum of **3.5**..... 108

Figure 3.17 ^{13}C NMR Spectrum of **3.5**..... 109

Figure 3.18 ^{1}H NMR Spectrum of **3.6**..... 110

Figure 3.19 ^{13}C NMR Spectrum of **3.6**..... 111

Figure 3.20 ^{1}H NMR Spectrum of **3.7**..... 112

Figure 3.21 ^{13}C NMR Spectrum of **3.7**..... 113

Figure 3.22 ^{1}H NMR Spectrum of **3.8**..... 114

Figure 3.23 ^{13}C NMR Spectrum of **3.8**..... 115

Figure 4.1 Structures of cryptands **4.1**–**4.4**…….. 117

Figure 4.2 Evolution of $R_1^p(t)/R_1^p(t=0)$ versus time for the Eu^{2+}-containing cryptates Eu–**4.1** (♦), Eu–**4.2** (■), Eu–**4.3** (▲), and Eu–**4.4** (●) (2.5 mM) in the presence of Ca^{2+} (2.5 mM). The horizontal line at 0.8 is the threshold for the kinetic index. Error bars represent standard error of the mean..... 119

Figure 4.3 Evolution of $R_1^p(t)/R_1^p(t=0)$ versus time for the Eu^{2+}-containing cryptates Eu–**4.1** (♦), Eu–**4.2** (■), Eu–**4.3** (▲), and Eu–**4.4** (●) (2.5 mM) in the presence of Mg^{2+} (2.5 mM). The horizontal line at 0.8 is the threshold for the kinetic index. Error bars represent standard error of the mean..... 120

Figure 4.4 Evolution of $R_1^p(t)/R_1^p(t=0)$ versus time for the Eu^{2+}-containing cryptates Eu–**4.1** (♦), Eu–**4.2** (■), Eu–**4.3** (▲), and Eu–**4.4** (●) (2.5 mM) in the presence of Zn^{2+} (2.5 mM). The horizontal line at 0.8 is the threshold for the kinetic index. Error bars represent standard error of the mean..... 120

Figure 4.5 Contributing resonance structures of cryptands **4.3** and **4.4**…….. 123

Figure 4.6 ^{1}H NMR Spectrum of **4.3**……... 129

Figure 4.7 ^{13}C NMR Spectrum of **4.3**…….. 130

Figure 4.8 ^{1}H NMR Spectrum of **4.4**……... 131

Figure 4.9 ^{13}C NMR Spectrum of **4.4**…….. 132

Figure 5.1 Structure of biphenyl-functionalized Eu^{2+}-containing complex **5.1**…….. 134

Figure 5.2 (a) Proton longitudinal relaxivity (20 °C, pH = 7.4) of biphenyl-functionalized cryptate **5.1** in the absence (○) and presence (□) of HSA as a function of magnetic field strength. (b) Proton longitudinal relaxivity (37 °C, pH = 7.4) of biphenyl-functionalized cryptate **5.1** in the absence (○) and presence (□) of HSA as a function of magnetic field strength. Simulated relaxivity values (■) of a slowly rotating Eu^{2+}-containing complex at 37 °C. Values at 1.4, 3, 7, and 11.7 T without HSA are from Ref. 6. HSA concentration was 4.5% (w/v). Error bars represent standard error of the mean of 3–9 independently prepared samples……... 136

Figure 5.3 (a) T_1-weighted MR images of albumin-containing solutions of biphenyl-functionalized cryptate **5.1** at 7 T and 20 °C. The diameter of the tubes that were used for imaging was 6 mm. Imaging parameters were T_R = 21 ms; T_E = 3.26 ms; and resolution = 0.27 × 0.27 × 2 mm^3. (b) Proton longitudinal relaxation rate (20 °C, pH = 7.4) as a function of % HSA at 7 T. The concentration of cryptate **5.1** was 1 mM. Error bars represent standard error of the mean of three samples. [a]No cryptate……. 138

Figure 5.4 Variable-temperature ^{17}O NMR Fittings for cryptate **5.1** in the presence of albumin…….. 144

LIST OF SCHEMES

Scheme 2.1 Synthetic methods for obtaining Eu^{2+}-containing complexes arranged by source of europium where L is a ligand, N is either Hg or Sn, and M is an alkali metal ion……. 22

Scheme 2.2 Proposed mechanism of polymerization of ε-caprolactone. Ind is the indenyl ligand. Adapted with permission from S. Zhou, S. Wang, E. Sheng, L. Zhang, Z. Yu, X. Xi, G. Chen, W. Luo, Y. Li. *Eur. J. Inorg. Chem.* **2007**, 1519–1528. Copyright 2007 John Wiley and Sons…… 39

Scheme 3.1 Synthesis of biphenyl-based Eu^{2+}-containing cryptate…… 55

Scheme 3.2 Synthetic route to cryptate **3.3**……. 95

Scheme 4.1 Synthesis of **4.3** and **4.4**……... 117

LIST OF ABBREVIATIONS

Abbreviation	Term
MRI	magnetic resonance imaging
EPR	electron paramagnetic resonance
SBM	Solomon–Bloembergen–Morgan
NHE	normal hydrogen electrode
THF	tetrahydrofuran
DME	1,2-dimethoxyethane
DFT	density functional theory
RT	room temperature
ND	no data is available
TLC	thin-layer chromatography
PBS	phosphate-buffered saline
MW	molecular weight
TRIS	amino-2-(hydroxymethyl)propane-1,3-diol
s	singlet
d	doublet
m	multiplet
brs	broad singlet
HRESIMS	high-resolution electrospray ionization mass spectra
ICP-MS	inductively coupled plasma mass spectrometry
SWI	susceptibility weighted imaging
VIBE	volumetric interpolated breath hold examination
HSA	human serum albumin
equiv	equivalents
R_f	retention factor
calcd	calculated
NMRD	nuclear magnetic relaxation dispersion

Abbreviation	Term	Structure
GdDTPA	gadolinium(III) diethylenetriaminepentaacetate	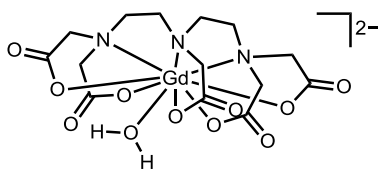

GdDOTA	dadolinium(III) 1,4,7,10-tetraazacyclododecane-1,4,7,10-tetraacetate	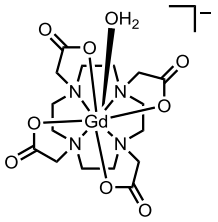
MS-325	5- [trisodium{4-(R)-[(4,4-diphenylcyclohexyl)phosphanooxymethyl]-3,6,9-tri-aza-3,6,9-tris (methoxycarbonyl)undecanedioato} gadolinium(III)	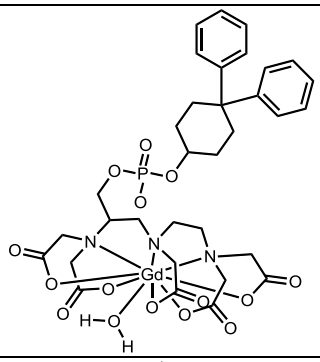
Cp	cyclopentadienyl anion	
Cp*	methyl-substituted Cp	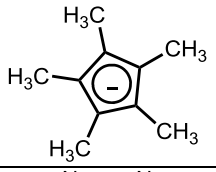
bpy	2,2'-bipyridine	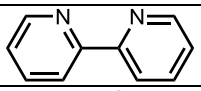
DMPE	1,2-bis-(dimethylphosphino)ethane	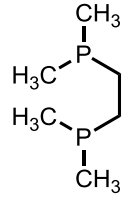
DMPM	1,2-bis-(dimethylphosphino)methane	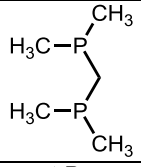
(t-Bu)$_2$pz	3,5-di-*tert*-butylpyrazolate	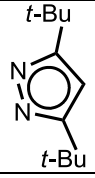
Odip	2,6-diisopropylphenolate	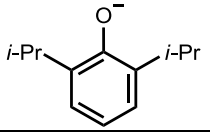

i-Pr_2pz	3,5-diisopropylpyrazolate	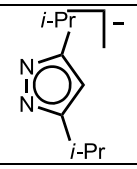
Dmp	2,6-(2,4,6-$(CH_3)_3C_6H_2)_2C_6H_3$	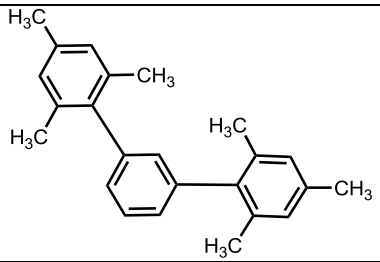
Tph	2-(2,4,6-*i*-$Pr_3C_6H_2)C_6H_4$	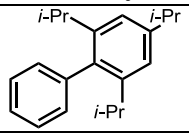
Ph_2pz	3,5-diphenylpyrazolate	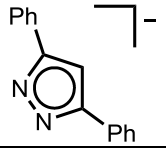
Ar*	2,6-(2,4,6-(*i*-Pr)$_3C_6H_2)_2C_6H_3$	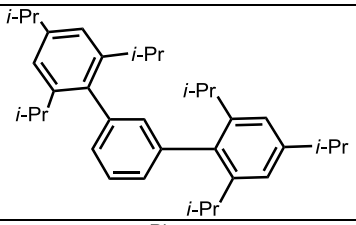
Dpp	2,6-$Ph_2C_6H_3$	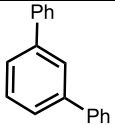
HMPA	hexamethylphosphoric triamide	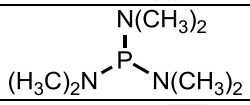
Ap*py	6-methylpyridin-2-yl-[6-(2,4,6-triisopropylphenyl)pyridin-2-yl]amine	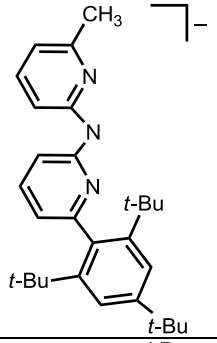
(*i*-$Pr)_2$ATI	*N*-isopropyl-2-(isopropylamino)troponiminate	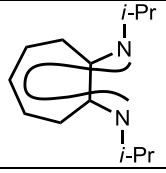

DIP_2pyr	2,5-bis{*N*-2,6-diisopropylphenyl)iminomethyl}pyrrolyl	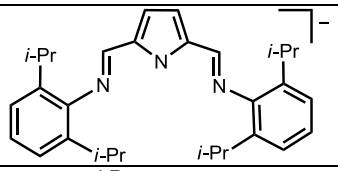
Ar	2,6-diisopropylphenyl	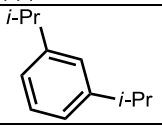
MMA	methyl methacrylate	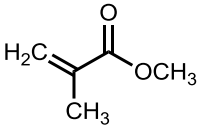
Ind	indenyl ligand	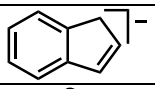
DTPA	diethylenetriaminepentaacetic acid	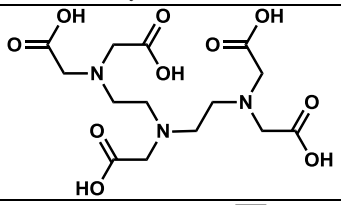
$[EuDOTA]^{2-}$	europium(II) 1,4,7,10-tetraazacyclododecane-1,4,7,10-tetraacetate	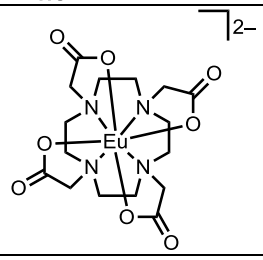
$[EuDTPA]^{3-}$	europium(II) diethylenetriaminepentaacetate	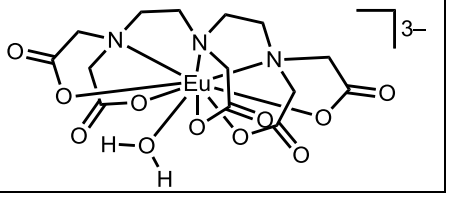

LIST OF SYMBOLS

Symbol	Name
$1/T_1$	roton longitudinal relaxation rate
r_1	relaxivity
q	number of inner-sphere water molecules
$1/\tau_m$ or k_{ex}	exchange rate of coordinated- and bulk-water molecules
$1/\tau_R$	rotational correlation rate
τ_m	mean residency lifetime of coordinated water molecules
ω_I	proton Larmor frequency
B	magnetic field strength
E^o	reduction potential
log K	logarithm of thermodynamic stability constant
T_{1e}^{298}	longitudinal electronic relaxation time
g	electron g factor
$1/T_{2e}$	transverse electronic relaxation rate
B	Bohr magneton constant
ΔH_{pp}	peak-to-peak linewidth
τ_R	rotational correlation time
h	Planck's constant
T_R	repetition time
T_E	echo time
T_2*	effective transverse relaxation time
$A/\hbar$	scalar coupling constant
ΔE	energy of activation of the electron spin relaxation
T_{1e}^{298}	electronic spin relaxation time at 298 K
R_1^p	longitudinal relaxation rates
ΔH	enthalpy of activation of water exchange
c	concentration of the paramagnetic contrast agent
$1/T_{1m}$	longitudinal relaxation rate of the bound water proton
$1/T_1^{DD}$	longitudinal relaxation rate of inner-sphere water by dipole–dipole coupling
$1/T_1^{SC}$	longitudinal relaxation rate of inner-sphere water by scalar coupling
r_{EuH}	Eu–H bond distance
r_1^{IS}	inner sphere longitudinal relaxivity
μ_B	Bohr magneton
μ_0	magnetic permittivity constant
r_{GdH}	Gd–H bond distance
S	total spin of the paramagnetic metal ion
τ_{ci} (i = 1, 2)	longitudinal (i = 1) and transverse (i = 2) correlation times
ω_S	electron Larmor frequency
γ_I	nuclear gyromagnetic ratio

γ_S	electronic gyromagnetic ratio
ZFS	zero field splitting
τ_v	correlation time for the modulation of transient ZFS
B_0	magnetic field strength
Δ	trace of the ZFS tensor
$t_{1/2}$	half life
$R_1^p(t)$	longitudinal relaxation rates of the Eu^{2+}-containing solutions at a time (t)
$R_1^p(t=0)$	longitudinal relaxation rates of the Eu^{2+}-containing solutions at a time (t=0)

Chapter One

Introduction to Contrast Agents for Magnetic Resonance Imaging

1.1 Introduction

To obtain a doctoral degree in chemistry, I have investigated the physical and imaging-relevant properties of Eu^{2+}-containing cryptates using a variety of techniques including magnetic resonance imaging (MRI), ^{17}O NMR spectroscopy, and electron paramagnetic resonance (EPR) spectroscopy. In addition, I examined the stability of these cryptates towards transmetallation in the presence of biologically relevant metal ions. Finally, I studied the binding of a cryptate to human serum albumin to study the relaxivity–molecular weight relationship for Eu^{2+}-containing complexes. The results from all of these studies will be discussed throughout this thesis. This chapter describes the introductory material that will be necessary to appreciate my results. Specifically, I will describe ultra-high field strength MRI, the properties of MRI contrast agents, and Eu^{2+}-containing cryptates as candidates for use as contrast agents for MRI.

1.2 Ultra-High Field Strength MRI

MRI uses radiofrequency and magnetic fields to probe the chemical environment of water protons to produce images. This imaging technique is noninvasive because it does not require cutting or use harmful ionizing radiation to acquire images of the inside of opaque objects. The utility of this technique to study anatomical features stems from its inherent high spatial resolution [0.2–0.8 mm at 1.5–3 Tesla (T)][1] which makes MRI a widely used imaging technique for clinical and preclinical research as well as diagnostic medicine. Most medical imaging is performed at 1.5 and 3 T; however, working at ultra-high fields (≥7 T) enables even higher resolution images (0.05 mm at 7 T) that can be used to study fine anatomical structures including senile plaques in Alzheimer's disease.[1]

Furthermore, ultra-high fields enable the use of shorter acquisition times relative to working at lower field strengths (**Figure 1.1**).[1,2]

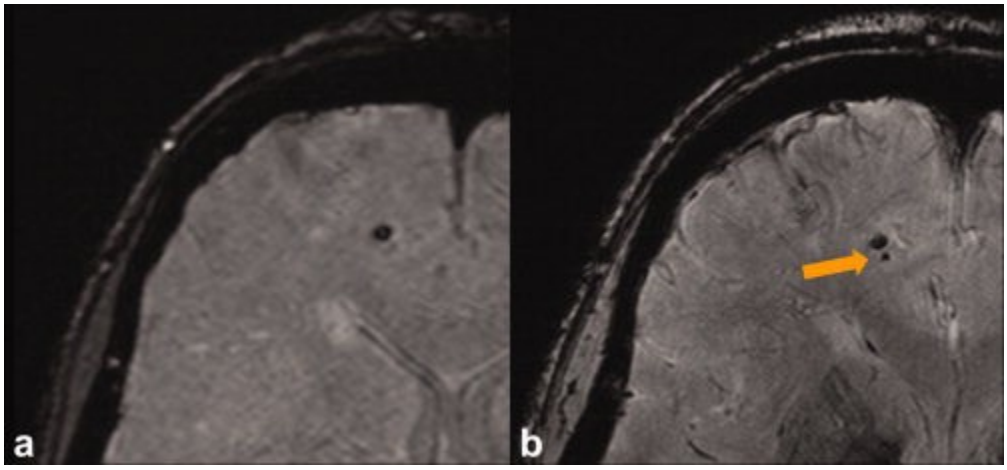

Figure 1.1. MR images of a human brain taken at (a) 1.5 and (b) 7 T. Improvement in spatial resolution can be seen at 7 T that enables the detection of a cerebral microbleed (noted by the arrow). Reprinted with permission from ref. [3] Copyright (2011) John Wiley and Sons.

1.3 Contrast Agents for MRI

Sometimes the contrast brought by MRI is not enough to differentiate pathological tissues from the surrounding healthy tissues. Therefore, contrast agents are used to further enhance image contrast by catalytically reducing the relaxation time of water protons in the vicinity of the contrast agents (**Figure 1.2**).

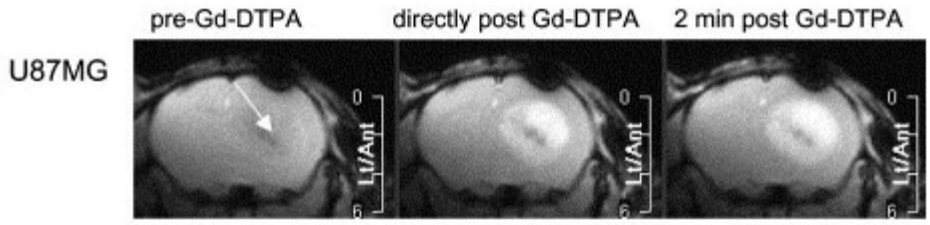

Figure 1.2 MR images of a mouse brain with an U87MG tumor taken before injection, directly after injection, and 2 min after the injection of gadolinium(III) diethylenetriaminepentaacetate (GdDTPA). The increased permeability of the vasculature in the tumor allows GdDTPA to diffuse into the tumor and resulted in the contrast enhancement. Reprinted with permission from ref. [4] Copyright (2006) Elsevier.

The ability of a contrast agent to influence the longitudinal relaxation rate ($1/T_1$) of water protons is known as relaxivity (r_1) and is expressed in units of $mM^{-1}\ s^{-1}$. Relaxivity can be determined as the slope of a plot of proton longitudinal relaxation rate, $1/T_1$, versus the concentration of contrast agent. The relaxivity of common contrast agents, including Gd^{3+}-based contrast agents, decreases as field strength increases, and in the ultra-high field regime, the efficiency of common contrast agents decreases considerably.[6] This observation is demonstrated by the work of Weinmann and coworkers who measured the relaxivity of several Gd^{3+}-based complexes including the clinically approved gadolinium(III) 1,4,7,10-tetraazacyclododecane-1,4,7,10-tetraacetate (GdDOTA) and 5-[trisodium{4-(R)-[(4,4-diphenylcyclohexyl)phosphanooxymethyl]-3,6,9-tri-aza-3,6,9-tris (methoxycarbonyl)undecanedioato}gadolinium(III) (MS-325)–albumin at different field strengths (**Figure 1.3**).[7] The relaxivity values decrease as the field strength increases, indicating that these Gd^{3+}-based complexes become less efficient at higher fields.

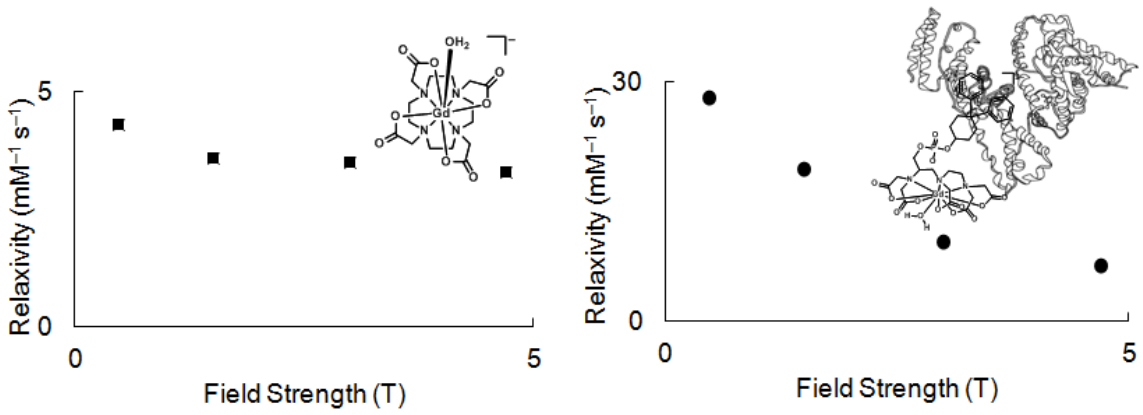

Figure 1.3 Plots of relaxivity (37 °C, plasma) versus field strength for GdDOTA (left) and MS-325–albumin (right).[7]

1.4 Factors Influencing the Efficiency of MRI Contrast Agents

There are several parameters that are crucial to increasing relaxivity including the number of inner-sphere water molecules or the number of water molecules that is directly bound to the metal ion, q; the water-exchange rate or the rate at which inner-sphere water exchanges with bulk water, $1/\tau_m$; and the rotational-correlation rate or the rate at which the complex tumbles in solution, $1/\tau_R$. The way these molecular parameters affect the observed relaxivity of a contrast agent is well described by several intertwined equations known as the Solomon–Bloembergen–Morgan (SBM) equations (**Eqs 1.1–1.4**). It is clear from the SBM equations that relaxivity is influenced by numerous parameters.

Eq 1.1 $$r_1 = \left(\frac{1}{T_{1,obs}} - \frac{1}{T_{1,d}}\right)\left(\frac{1}{[\mathrm{Gd}]}\right) = r_1^{IS} + r_1^{OS}$$

Eq 1.2 $$r_1^{IS} = \frac{\left(\frac{1}{T_1}\right)^{IS}}{[\mathrm{Gd}]} = \frac{q}{55.5}\left(\frac{1}{T_{1m}+\tau_m}\right)$$

Eq 1.3 $$\frac{1}{T_{1m}} = \frac{2}{15}\frac{\gamma_I^2 g^2 \mu_B^2}{r_{\mathrm{GdH}}^6} S(S+1)\left(\frac{\mu_o}{4\pi}\right)^2 \left(7\frac{\tau_{c2}}{1+\omega_S^2\tau_{c2}^2} + 3\frac{\tau_{c1}}{1+\omega_I^2\tau_{c1}^2}\right)$$

Eq 1.4 $$\omega_I = \frac{1}{\tau_{ci}} = \frac{1}{\tau_R} + \frac{1}{T_{ie}} + \frac{1}{\tau_m};\ i{=}1{,}2$$

For example, observed relaxivity is linearly dependent on the number of bound water molecules (**Eq. 1.2**). Therefore, to increase relaxivity, it is desirable for q to be as large as possible. However, increasing the number of inner-sphere water molecules by decreasing the denticity of the ligand generally increases the chance of demetallation. Because unchelated Gd^{3+} is toxic, the value of q needs to be as high as possible as long as the complex is stable to demetallation. In addition to q, the relaxivity of a Gd^{3+}-containing complex is dependent on the bound-water-residency lifetime, τ_m, which is the reciprocal of the water-exchange rate. To increase relaxivity, the optimum value of the water-exchange rate between the inner-sphere water and the bulk solvent water should be slow enough for the metal ion to effectively influence the relaxation of water protons, but fast enough to allow the metal ion to interact with many water molecules. The water residency lifetime of bound water is interdependent on other parameters that include the rate at which the Gd^{3+}-containing complex rotates in solution. This rotational correlation rate is usually the limiting factor influencing relaxivity for small molecules including GdDOTA.

To obtain maximum relaxivity, the molecular parameters need to be simultaneously tuned so that the sum of the rotational correlation rate ($1/\tau_R$), water-exchange rate ($1/\tau_m$), and the electronic spin relaxation rate ($1/T_{1e}$) is equal to that of the proton Larmor frequency, ω_I, or the frequency at which the proton's magnetic moment precesses at a given magnetic field strength (**Eq 1.4**). Because proton Larmor frequency is dependent on magnetic field strength (**Figure 1.4**), the optimum values for these molecular parameters also change as a function of field strength.

Eq 1.5 $\omega_I = \gamma_I B$

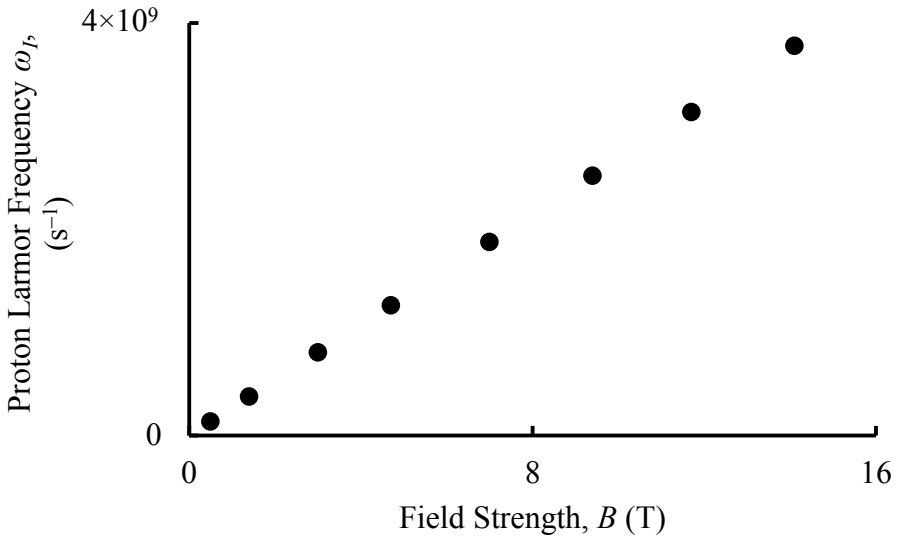

Figure 1.4 Plot of proton Larmor frequency versus magnetic field strength. The proton Larmor frequency values were calculated using **Eq 1.5**.

There are two strategies that have been used to optimize values for rotational correlation rate ($1/\tau_R$) and water-exchange rate ($1/\tau_m$): (1) modifying the ligand such that the paramagnetic complex can bind to macromolecules thereby controlling the rotational correlation rate of the complex[8] and (2) introducing steric bulk in the water-binding site in the metal complex to enable control of the water-exchange rate of the complex.[9] Because most Gd^{3+}-containing complexes have slow water-exchange rates (~10^6 s^{-1}),[10] I took a slightly different approach—changing the metal from Gd^{3+} to Eu^{2+} and adapting the ligand modification strategies that work for Gd^{3+}-based contrast agents. I used Eu^{2+} as an alternative to Gd^{3+} to test the hypothesis that Eu^{2+} is an efficient contrast agent for ultra-high-field-strength MRI. Eu^{2+} is isoelectronic with Gd^{3+}, but differs in some molecular properties, including electronic spin relaxation rate and charge density, which in turn affect water-exchange rates. These molecular properties of Eu^{2+} can be tuned by changing the ligand structure using coordination chemistry principles based from the previous work with

Eu^{2+}-containing complexes.[11] The second chapter of my dissertation surveys the recent developments in the coordination chemistry of Eu^{2+} and applications of Eu^{2+}-containing complexes including the potential use of these complexes as contrast agents for MRI.

1.5 Eu^{2+}-containing [2.2.2]cryptates

A promising feature of Eu^{2+} that makes this ion an excellent candidate for use as a contrast agent for MRI is its lower charge density relative to Gd^{3+}. A lower charge density makes Eu^{2+} to have a faster water-exchange rate than Gd^{3+} (**Table 1.1**). However, research on Eu^{2+} chemistry in aqueous solution is limited because of the oxidative instability of Eu^{2+} in the presence of molecular oxygen. It has been demonstrated in the work of Allen and coworkers, where I was actively involved in synthesizing starting materials, that the divalent state of Eu can be stabilized using modified macrobicyclic ligands known as cryptands. Chelation of Eu^{2+} results in the formation of cryptates, which is the term for metalated cryptands. Using coordination chemistry principles—including Lewis basicity, steric bulk, cavity size, and hard–soft acid–base theory—the most oxidatively stable, aqueous Eu^{2+} complex reported was developed: the benzotetrathia[2.2.2] Eu^{2+}-containing cryptate that is more oxidatively stable than Fe^{2+} in hemoglobin (**Figure 1.5**).[11]

Table 1.1 Comparison of Eu^{2+} to Gd^{3+} in terms of charge, ionic radius, and water-exchange rate.

	Eu^{2+}	Gd^{3+}
Charge	+2	+3
Radius (pm)[12]	125	108
Water-exchange rate (10^9 s^{-1}),[10] $[M(H_2O)_8]^x$	4.4	0.8
Water-exchange rate (10^9 s^{-1}),[10] $[M(DTPA)(H_2O)]^x$	1.3	0.033

M = Gd^{3+} or Eu^{2+}; *x* is the charge of the complex

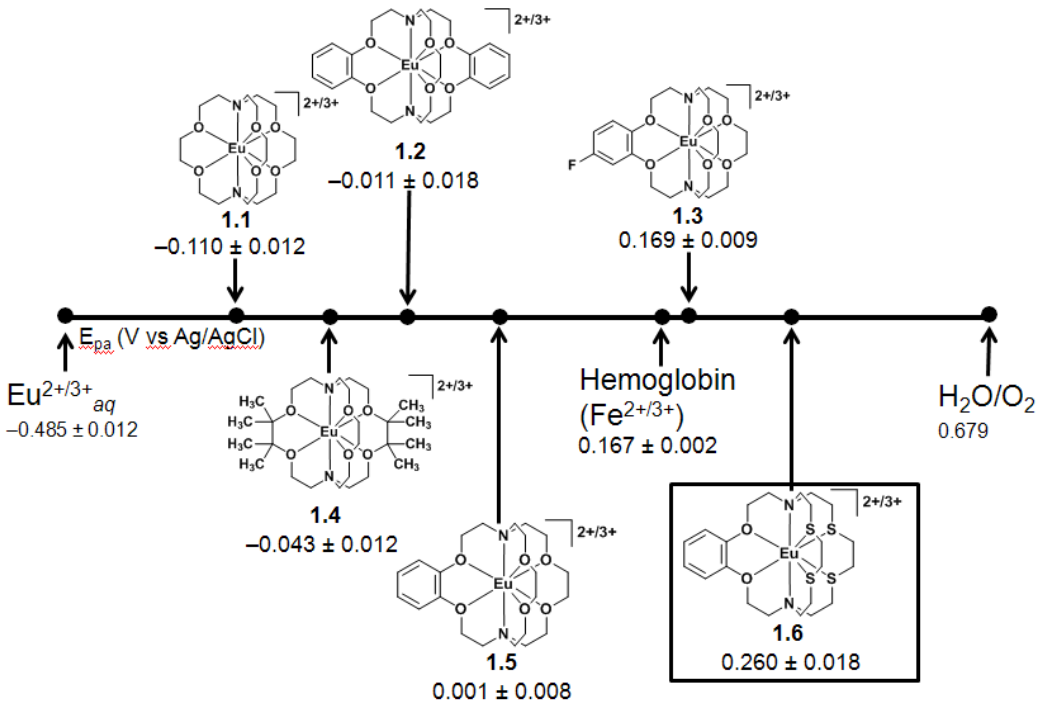

Figure 1.5 Plot of the anodic peak potentials of Eu^{2+} cryptates **1.1**–**1.6**, the Eu^{2+} aqua ion, Fe^{2+} in hemoglobin, and water. A more positive potential means increased oxidative stability. Anodic peak potentials are reported as mean ± standard error of at least three measurements relative to Ag/AgCl.[11]

In addition to stabilizing the divalent state of Eu, the unfunctionalized Eu^{2+}-containing [2.2.2]cryptate (**Figure 1.6**) was reported to have two inner-sphere water molecules and fast water-exchange rate (~10^8 s^{-1}).[13] These favorable properties prompted me to hypothesize that Eu^{2+}-containing crypates would be candidates for contrast agents at ultra-high field MRI. I investigated the contrast-enhancing ability of Eu^{2+}-containing cryptates at different field strengths, temperature, and pH because these factors influence the relaxivity of contrast agents. The efficacy of Eu^{2+}-containing cryptates at different temperatures and field strengths as well as the physical properties of Eu^{2+}-containing cryptates are presented in the third chapter of this thesis.

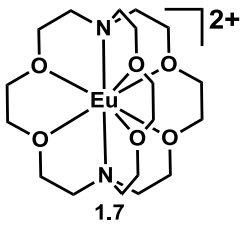

1.7

Figure 1.6 Chemical structure of the unfunctionalized Eu^{2+}-containing [2.2.2]cryptate **1.7**.

Another critical feature that should be considered for complexes to be used as contrast agents for MRI is their stability towards demetallation. For contrast agents to be safe, they should be kinetically inert for at least long enough to be excreted. The stability towards demetallation is important for these Eu^{2+}-containing cryptates because uncomplexed Eu^{2+} oxidizes easily, and Eu^{3+} is toxic.[14] One possible pathway for dechelation of Eu^{2+} from a complex is by transmetallation induced by other ions. Ions that are found in blood plasma that could exchange with Eu^{2+} include Ca^{2+}, Mg^{2+}, and Zn^{2+}.[14] These ions are of particular concern because of their abundance and their tendency to be complexed by ligands. Therefore, I examined the stability of several Eu^{2+}-containing

cryptates towards transmetallation in the presence of Ca^{2+}, Mg^{2+}, and Zn^{2+}, and the details of the transmetallation studies are presented in the fourth chapter of this document.

The transmetallation studies demonstrated that amine-containing cryptates are inert to transmetallation, and because relaxivity tends to increase with molecular weight for these cryptates, I hypothesized that increasing the molecular weight by binding to human serum albumin produces a more efficient contrast agent. The fifth chapter of this thesis discusses the effect of the interaction of biphenyl cryptate **1.8** (**Figure 1.7**) with albumin and the resulting relaxometric properties of the cryptate.

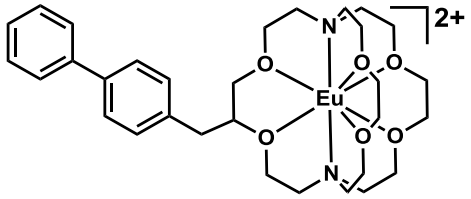

1.8

Figure 1.7 Chemical structure of the biphenyl-functionalized Eu^{2+}-containing [2.2.2]cryptate **1.8**.

The final chapter summarizes my graduate research and discusses the future directions to establish relaxivity–molecular weight relationship for the Eu^{2+}-containing cryptates using macromolecular and supramolecular systems and to evaluate the toxicity profile of these cryptates to assess their potential use for in vivo applications.

1.6 References

(1) Wada, H.; Sekino, M. *IEEE Trans. Appl. Supercond.* **2010,** *20,* 115–122.

(2) (a) Blow, N. *Nature* **2009,** *458,* 925–928. (b) Moser, E. *World J. Radiol.* **2010,** *2,* 37–40. (c) Pitt, D.; Boster, A.; Pei, W.; Wohleh, E.; Jasne, A.; Zachariah C. R.; Rammohan, K.; Knopp, M. V.; Schmalbrock, P. *Arch. Neurol.* **2010,** *67,* 812–818.

(3) Theysohn, J. M.; Kraff, O.; Maderwald, S.; Barth, M. B.; Ladd, S. C.; Forsting, M.; Ladd, M. E.; Gizewski, E. R. *J. Magn. Reson. Imaging* **2011,** *33,* 782–791.

(4) Kemper, E. M.; Leenders, W.; Küsters, B.; Lyons, S.; Buckle, T.; Heerschap, A.; Boogerd, W.; Beijnen, J. H.; van Tellingen, O. *Eur. J. Cancer* **2006,** *42,* 3294–3303.

(5) Aime, S., Caravan, P. *J. Magn. Reson. Imaging* **2009,** *30,* 1259–1267.

(6) Caravan, P. *Chem. Soc. Rev.* **2006,** *35,* 512–523.

(7) Rohrer, M.; Bauer, H.; Mintorovitch, J.; Requardt, M.; Weinmann, H.-J. *Invest. Radiol.* **2005,** *40,*715–724.

(8) (a) Armitage, F. E.; Richardson, D. E.; Li, K. C. P. *Biconjugate Chem.* **1990,** *1,* 365–374. (b) Aime, S.; Botta, M.; Crich, S. G.; Giovenzana, G.; Palmisano, G.; Sisti, M.; *Bioconjugate Chem.* **1990,** *10,* 192–199. (c) Nicolle, G. M.; Tóth, É.; Eisenwiener, K.-P.; Mäcke, H. R.; Merbach, A. E. *J. Biol. Inorg. Chem.* **2002,** *7,* 757–769. (d) Torres, S.; Martin, J. A.; André, J. P.; Geraldes, C. F. G. C.; Merbach, A. E.; Tóth, É. *Chem. Eur. J.* **2006,** *12,* 940–948. (e) Laus, S.; Sour, A.; Ruloff, R.; Tóth, É.; Merbach, A. E. *Chem. Eur. J.* **2005,** *11,* 3064–3076. (f) Yang, J. Y.; Yang, J.; Wei, L.; Zurkiya, O.; Yang, W.; Li, S.; Zou, J.; Zhou, Y.; Maniccia A. K. W.; Mao, H.; Zhao, F.; Malchow, R.; Zhao, S.; Johnson, J.; Hu, X.; Krogstad, E.; Liu, Z.-R. *J. Am. Chem. Soc.* **2008,** *130,* 9260–9267. (g) Kundu, A.; Peterlik, H.; Krssak, M.; Bytek, A. K.; Pashkunova-Martic, I.; Arion, V. B.; Helbich, T. H.; Keppler, B. K. *J. Inorg. Biochem.* **2011,** *105,* 250–255. (h) Avedano, S.; Tei, L.; Lombardi, A.; Giovenzana, G. B.; Aime, S.; Longo, D.; Botta, M. *Chem. Commun.* **2007,** 4726–4728. (i) Henoumont, C.; Vander Elst, L.; Laurent, S.; Muller, R. N. *J. Biol. Inorg. Chem.* **2009,** *14,* 683–691. (j) Gianolio, E.; Giovenzana, G. B.; Longo, D.; Longo, I.; Menegotto, I.; Aime, S. *Chem. Eur. J.* **2007,** *13,* 5785–5797. (k) Ou, M.-H.; Tu, C.-H.; Tsai, S.-C.; Lee, W.-T.; Liu, G.-C.; Wang, Y.-M. *Inorg. Chem.* **2006,** *45,* 244–254. (l)

Aime, S.; Botta, M.; Fasana, M.; Geninatti, C.; Terreno, E. *J. Biol. Inorg. Chem.* **1999,** *4,* 766–774. (m) Aime, S.; Chiaussa, M.; Digilio, G.; Gianolio, E.; Terreno, E. *J. Biol. Inorg. Chem.* **1999,** *4,* 766–774. (n) Parac-Vogt, T. N.; Kimpe, K.; Laurent, S.; Vander Elst, L.; Burtea, C.; Chen, F.; Muller, R. N.; Ni, Y.; Verbruggen, A.; Binnemans, K. *Chem. Eur. J.* **2005,** *11,* 3077–3086. (o) Aime, S.; Gianolio, E.; Terreno, E.; Giovenzana, G. B.; Pagliarin, R.; Sisti, M.; Palmisano, G.; Botta, M.; Lowe, M. P.; Parker, D. *J. Biol. Inorg. Chem.* **2000,** *5,* 488–497. (p) Dumas, S.; Troughton, J. S.; Cloutier, N. J.; Chasse, J. M.; McMurry, T. J.; Caravan. P. *Aust. J. Chem.* **2008,** *61,* 682–686. (q) Nivorozhkin, A. L.; Kolodziej, A. F.; Caravan, P.; Greenfield, M. T.; Lauffer, R. B.; McMurry, T. J. *Angew. Chem. Int. Ed.* **2001,** *40,* 2903–2906. (r) Strijkers, G. J.; Mulder, W. J. M.; van Heeswijk, R. B.; Frederik, P. M.; Bomans, P.; Magusin, P. C. M. M.; Nicolay, K. Magma **2005,** *18,* 186–192.

(9) (a) Torres, S.; Martins, J. A.; André, J. P.; Giovannia, A. P.; Kiraly, R.; Brücher, E.; Helm, L.; Tóth, É.; Geraldes, C. F. G. *Eur. J. Inorg. Chem.* **2007,** 5489–5499. (b) Laus, S.; Ruloff, R.; Tóth, É.; Merbach, A. E. *Chem. Eur. J.* **2003,** *9,* 3555–3566. (c) Ruloff, R.; Tóth, É.; Scopelliti, R.; Tripier, R.; Handel, H.; Merbach, A. E. *Chem. Commun.* **2002,** 2630–2631. (d). Laurent, S.; Botterman, F.; Vander Elst, L.; Muller, R. N. Magma **2004,** *16,* 235–245. (e) Jászberényi, Z.; Sour, A.; Tóth, É.; Benmelouka M.; Merbach, A. E. *Dalton Trans.* **2005,** 2713–2719. (f) Aime, S.; Barge, A.; Borel, A.; Botta, M.; Chemerisov, S.; Merbach, A. E.; Müller, U.; Pubanz, D. *Inorg. Chem.* **1997,** *36,* 5104–5112.

(10) Burai, L.; Tóth, É.; Moreau, G.; Sour, A.; Scopelliti, R.; Merbach, A. E. *Chem. Eur. J.* **2003**, *9*, 1394–1404.

(11) Gamage, N. H.; Mei, Y.; Garcia, J.; Allen, M. J. *Angew. Chem. Int.* **2010,** *49,* 8923–8925.

(12) (a) Tóth, É.; Burai, L.; Merbach, A. E. *Coord. Chem. Rev.* **2001,** *216–217,* 363–382. (b) Idée, J.-M.; Port, M.; Raynal, I.; Schaefer, M.; Le Greneur, S.; Corot, C. *Fundam. Clin. Pharmacol.* **2006,** *20,* 563–576.

(13) Burai, L.; Scopelliti, R.; Tóth, É. *Chem. Commun.* **2002,** 2366–2367.

(14) Garcia, J.; Kuda-Wedagedara, A. N. W.; Allen, M. J. *Eur. J. Inorg. Chem.* **2012,** *2012,* 2135–2140.

Chapter Two

Developments in the Coordination Chemistry of Eu^{2+}

Portions of this chapter were reprinted with permission from Garcia, J.; Allen, M. J. Developments in the Coordination Chemistry of Europium(II). *Eur. J. Inorg. Chem.* **2012,** *2012,* 4550–4563.

DOI: 10.1002/ejic.201200159

link: http://onlinelibrary.wiley.com/doi/10.1002/ejic.201200159/pdf

Copyright © 2012 WILEY-VCH Verlag GmbH & Co. KGaA, Weinheim.

2.1 Introduction

2.1.1 Properties of Eu^{2+}

Among the divalent lanthanides, Eu^{2+} has the most accessible divalent oxidation state because of its half-filled $4f^7$ electronic configuration and, consequently, a high stabilization from exchange energy (**Figure 2.1**).[1] While Eu^{2+} is the most accessible of the divalent lanthanides, outside of the solid state it has a propensity to oxidize [reduction potential, $Eu^{o}(Eu^{3+}/Eu^{2+})$ = –0.35 V vs normal hydrogen electrode (NHE)],[2] which necessitates handling under an inert atmosphere. Four decades ago, there were only a few discrete Eu^{2+}-containing complexes reported. Most of these complexes were halides, chalcogenides, and organometallic compounds that are generally insoluble in organic solvents such as tetrahydrofuran (THF) because of the formation of extended structures.[3]

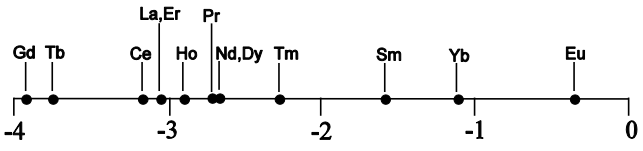

Figure 2.1 Relative reduction potentials for $Ln^{3+} \rightarrow Ln^{2+}$ (V vs NHE).[2]

Despite oxidation and oligomerization presenting obstacles to the preparation and characterization of Eu^{2+}-containing complexes, the interesting catalytic, photophysical, and magnetic properties of this ion have spurred a great deal of research. The unique properties of Eu^{2+} are influenced largely by the spacing of the energy levels of the 4*f* and 5*d* orbitals and the reducing properties of the ion.

The *f* orbitals make the electronic properties of Eu^{2+} unique compared to elements in the *d* block. For example, using spectroscopic techniques, Adin and Sykes demonstrated that electron transfer from *f* orbitals is more difficult than from *d* orbitals.[4] They observed a rate constant for the reaction of Eu^{2+} with V^{3+} of 0.013 M^{-1} s^{-1} (1.0 N $HClO_4$, 25 °C, ionic strength of 2.0 M), while the reaction of Cr^{2+} with V^{3+} under the same conditions is 0.85 M^{-1} s^{-1}.[4] The smaller rate constant observed for Eu^{2+} relative to Cr^{2+} can be attributed to the valence 4*f* orbitals being shielded from the environment by the electrons in the fully occupied 5*s* and 5*p* orbitals. An additional influence of the *f* orbitals is exemplified by the photophysical properties of Eu^{2+} that stem from the lowest-energy and first-excited-state configurations of $4f^7$ and $4f^6 5d^1$, respectively.[5] While the 4*f* orbitals of Eu^{2+} remain largely unperturbed by the presence of ligands, the energy of the 5*d* orbitals is influenced readily by ligands. Consequently, the luminescence properties of Eu^{2+} can be tuned using coordination chemistry, and the characteristic emission properties of this divalent ion include a broad emission band (390–580 nm)[6] and a short radiative lifetime (~1 μs) that are attributed to the Laporte allowed $4f^6 5d^1 \rightarrow 4f^7$ transitions.[5] In addition to these allowed transitions, sharp emission bands, which appear between 354 and 376 nm,[7,8] and longer radiative emission lifetimes (~1 ms) are observed that correspond to the Laporte forbidden $4f \rightarrow 4f$ transitions, similar to those observed in the Eu^{3+} ion.[5] Beyond the unique luminescence properties of Eu^{2+}, the *f* orbitals are responsible for the interesting magnetic

characteristics of this divalent ion that include a high magnetic moment (7.63–8.43 μ_B) associated with seven unpaired electrons in an $^8S_{7/2}$ ground-state configuration.[3,9]

In addition to the desirable optical and magnetic properties of Eu^{2+}, this ion displays interesting redox chemistry. Divalent lanthanides including Eu^{2+} act as one-electron reductants, and detailed discussions of the reductive chemistry of divalent lanthanides were published by Evans in 2000 and 2002.[2,10] Since then, research efforts have been directed toward developing Eu^{2+}-containing species that act as multielectron reductants in synthetic chemistry.[11] Additionally, there is interest in studying the influence of ligands on the redox properties of Eu^{2+}.[12]

2.1.2 Early Eu^{2+} Complexes

Discrete Eu^{2+}-containing complexes were reported as early as 1964.[13] However, the number of these complexes is small relative to their Eu^{3+} analogues, which form air-stable complexes with most electronegative atoms such as oxygen and nitrogen, partially because Eu^{3+} is a hard Lewis acid. Eu^{2+} is a softer Lewis acid than Eu^{3+} because of its lower charge density; consequently, Eu^{2+}-containing complexes often include ligands with relatively soft atoms such as carbon and phosphorous.

Among the first discrete Eu^{2+}-containing complexes prepared was the metallocene-like complex Cp_2Eu, where Cp is cyclopentadiene. This complex did not garner much interest because of its insolubility in polar organic solvents such as THF.[14] This insolubility was ascribed to a polymerization that can be prevented with the use of bulkier ligands.[9,14,15] Templeton and coworkers were able to isolate crystals from THF or toluene of Cp^*_2Eu, **2.1**, where Cp* is methyl-substituted Cp (**Figure 2.2**).[9] Evans and coworkers investigated the bond characteristics and the electronic spin–spin paramagnetic relaxation rate of Eu in $Cp^*_2Eu(THF)$, **2.2**, and $Cp^*_2Eu(THF)(Et_2O)$, **2.3**. The Eu–ligand bonds of **2.2** and **2.3** are

ionic in character as indicated by the isomer shifts of these complexes: from ^{151}Eu Mössbauer spectroscopy, a technique used to study the oxidation state and the local environment of Eu in the solid state, the shifts of **2.2** and **2.3** are not different from those of ionic Eu^{2+} halide complexes.[16] Moreover, the data obtained from the spherical relaxation model fits of the ^{151}Eu Mössbauer spectra of the **2.2**, **2.3**, and $[Cp^*Eu(THF)_2(\mu\text{-}I)]_2$, **2.4**, in the solid state indicate that the Eu–Eu distances affect the electronic spin–spin paramagnetic relaxation of these complexes, with longer Eu–Eu distances leading to slower spin–spin relaxation rates.[16] In addition to Cp*, the sterically demanding ligand bis(trimethylsilyl)amide, $[((CH_3)_3Si)_2N]^-$, was used as a precursor in preparing Eu^{2+} complexes. The six-coordinate complex $[((CH_3)_3Si)_2N]_2Eu(CH_3OCH_2CH_2OCH_3)_2$, **2.5**, and the four-coordinate complex $[((CH_3)_3Si)_2N]_2Eu(bpy)$, **2.6**, where bpy is 2,2'-bipyridine, are both soluble in THF, pentane, toluene, and 1,2-dimethoxyethane (DME).[3] In general, the problem of insolubility in hydrocarbons is addressed using sterically demanding ligands to increase hydrophobicity and to prevent the formation of coordination polymers.[9,14,15]

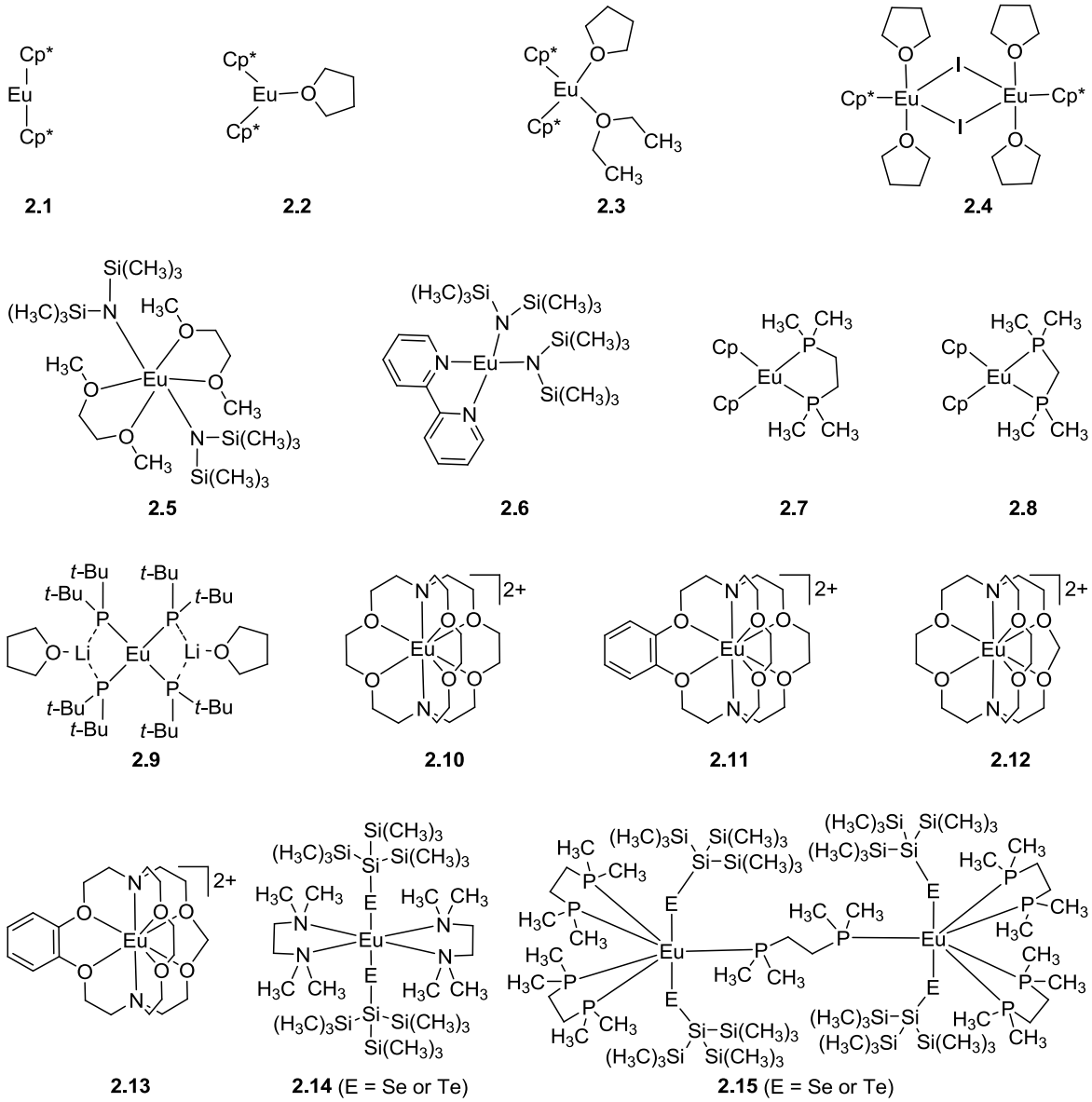

Figure 2.2 Structures of Eu^{2+}-containing complexes **2.1**–**2.15**.

Phosphine complexes of Eu^{2+} have been investigated since the early 1980s and display unique structural and electronic properties.[17–19] In some cases, phosphorous-containing ligands form dative bonds with Eu^{2+} in the presence of oxygen-containing bases.[20] Templeton and coworkers reported the synthesis of phosphine complexes of Eu^{2+}: in their procedure, $NaEu[N(Si(CH_3)_3)_2]_3$ was prepared from EuI_2 and $NaN(Si(CH_3)_3)_2$ in diethyl ether, and the relatively weak donor ligand $[N(Si(CH_3)_3)_2]^-$ was displaced by a

phosphorous-containing ligand such as 1,2-bis-(dimethylphosphino)ethane (DMPE) to give a complex with an empirical formula of $Eu[N(Si(CH_3)_3)_2]_2(DMPE)_{1.5}$.[19] Another Eu^{2+}-containing phosphine complex was reported by the same group with Cp* in place of $[N(Si(CH_3)_3)_2]^-$. The resulting complex, $EuCp^*_2(DMPE)$, **2.7**, was not soluble in noncoordinating solvents, potentially because of the role of DMPE in bridging complexes to form coordination polymers. To reduce the potential for aggregation, ethylene-bridged DMPE was replaced with methylene-bridged 1,2-bis-(dimethylphosphino)methane (DMPM).[21] The resulting complex $EuCp^*_2(DMPM)$, **2.8**, was isolated, but analogous complexes with monodentate phosphines such as $P(CH_3)_3$ or $P(n\text{-}Bu)_3$ were not reported, likely because the steric bulk of these phosphines prevented the formation of a coordinatively saturated metal ion.[21] Another Eu^{2+}-containing phosphine complex was reported by Rabe and coworkers.[18] Their four-coordinate, homoleptic Eu^{2+}-containing phosphine complex $Eu[(\mu\text{-}P(t\text{-}Bu)_2)_2\text{-}Li(THF)]_2$, **2.9**, assumes a heavily distorted tetrahedral geometry. The oxidation state of Eu in the complex was confirmed by ^{151}Eu Mössbauer spectroscopy with an isomer shift of –11.7 mm s^{-1} as opposed to isomer shifts of 0–1 mm s^{-1} for compounds that contain Eu^{3+} (**Figure 2.3**).[18] One interesting feature of this complex is that an alkali ion, Li^+, interacts with phosphorous in $P(t\text{-}Bu)_2$ and oxygen in THF similar to the complex $NaEu[N(Si(CH_3)_3)_2]_3$ where Na^+ interacts with the nitrogen of $[N(Si(CH_3)_3)_2]^-$.[15,18] Also, an agostic interaction between Eu^{2+} and the *tert*-butyl groups in $P(t\text{-}Bu)_2$ was observed in **2.9**.[18] The authors postulated that this interaction is driven by the tendency of the metal to form a coordinatively saturated environment and also by crystal packing forces because this interaction is only observed in the solid state.[15,18]

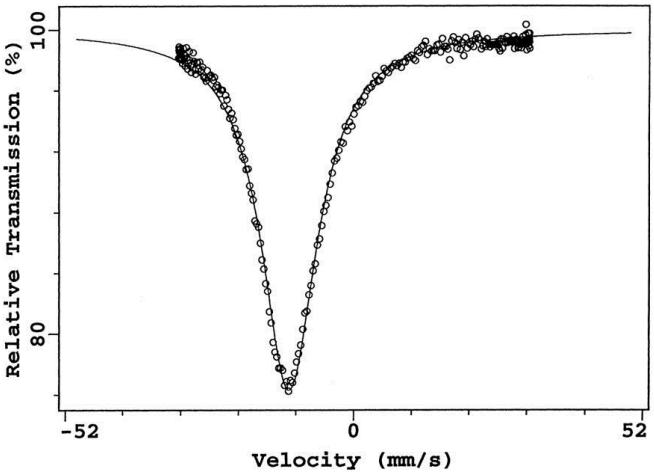

Figure 2.3 ^{151}Eu Mössbauer spectrum of **2.9** at 4.2 K. Reprinted with permission from G. W. Rabe, G. P. A. Yap, A. L. Rheingold, *Inorg. Chem*. **1997**, *36*, 3212–3215. Copyright 1997 American Chemical Society.

In addition to the softer C- and P-containing ligands, polyoxadiazamacrobicyclic ligands (cryptands) form stable complexes (cryptates) of Eu^{2+}, **2.10–2.13**, which were first reported in the late 1970s. Cryptands are used to encapsulate Eu^{2+} to oxidatively stabilize this ion and enable studies of the luminescence properties of Eu^{2+}. Gansow and coworkers demonstrated the oxidative stabilization of Eu^{2+} using cyclic voltammetry when the ion is bound by cryptands.[22] This stabilization was attributed to a good fit of the Eu^{2+} ion in the cryptand cavity,[22] and the thermodynamic stability constants (log K) for some Eu^{2+}-containing cryptates were reported by Burns and Baes to be 10.2–13.0.[23] Besides the thermodynamic properties of these cryptates, these Eu^{2+}-containing cryptates are substitutionally inert towards Na^{+}, Ba^{2+}, Ca^{2+}, Mg^{2+}, Zn^{2+}, and tetraethylammonium cations.[24,25] Beyond stabilizing the Eu^{2+} ion thermodynamically and kinetically, cryptands also exclude a large number of solvent molecules from the inner-sphere of the ion. This solvent exclusion is important because coordinated solvent molecules quench the

luminescence of Eu^{2+}, thus this ion does not exhibit strong luminescence in aqueous solution at room temperature when not chelated.[26]

In the 1990s, Eu^{2+} complexes with a wide variety of ligands were synthesized. Shore and coworkers reported Eu^{2+}-containing borohydrides $(NH_3)_xEu(B_{10}H_{14})$, $(CH_3CN)_2Eu(BH_4)_2$, and $(C_5H_5N)_{1.8}Eu(BH_4)_2$ as precursors for preparing metal borides.[20,27] However, all complexes that contain borohydrides are unstable as solids and tend to decompose to produce *closo*-$[B_{10}H_{10}]^{2-}$.[20] The conversion from Eu^{2+} borohydrides to Eu^{2+} borides was performed successfully at high temperatures (>200 °C) under vacuum to obtain the stable boride phase, EuB_6.[27] Although Eu^{2+}-containing complexes with borohydrides as ligands were successfully synthesized, the coordination modes of Eu^{2+} in these complexes were not fully explored due to the lack of X-ray crystallographic data. In addition to Eu^{2+} borohydrides, Eu^{2+} selenolates and tellurolates were also prepared. For example, $Eu[ESi(Si(CH_3)_3)_3]_2(TMEDA)_2$, **2.14**, and $\{Eu[ESi(Si(CH_3)_3)_3]_2(DMPE)_2\}_2(\mu$-DMPE), **2.15**, were reported by Arnold and coworkers where TMEDA is $(CH_3)_2NCH_2CH_2N(CH_3)_2$ and E is Se or Te.[28] The crystal structure of **2.15** reveals a seven-coordinate Eu^{2+} ion that is bridged by DMPE to form a dimeric complex that was not observed for the TMEDA-containing complex. The difference in coordination chemistry of the two complexes was attributed to the larger covalent radius of P relative to N and, consequently, a less crowded metal center in complex **2.15**.[28]

The seminal studies of the coordination chemistry of Eu^{2+} from the 1960's through the 1990's built a foundation for the design of new ligands that will be driven by the functions of the resulting Eu^{2+}-containing complexes. While Eu^{2+}-containing clusters and polymers are reported in the literature,[29–33] these compounds are not described in this chapter because the focus of this chapter is recent advances in the coordination chemistry

of discrete Eu^{2+} complexes. Synthetic strategies reported in the 21st century are presented followed by a description of the reactivity and applications of the resulting Eu^{2+}-containing complexes.

2.2 Synthesis of Recent Eu^{2+}-Containing Complexes

The rapid increase in the reporting of Eu^{2+}-containing complexes over the last two decades has resulted in the publication of several synthetic pathways to prepare these complexes (**Scheme 2.1**). These methods fall into three categories based on the europium-based starting materials used: metallic europium; europium(III) salts including halides, triflates, oxides, or nitrates; or europium(II) halides. This section is organized based on these three types of starting materials: oxidation of Eu metal, reduction of Eu^{3+}, and metathesis of Eu^{2+}.

Scheme 2.1 Synthetic methods for obtaining Eu^{2+}-containing complexes arranged by source of europium where L is a ligand, N is either Hg or Sn, and M is an alkali metal ion.

Oxidation of Eu metal

$$Eu^0 + nL \xrightarrow{\text{activating agent}} Eu^{2+}(L_n)^{2-}$$

or

$$Eu^0 + NL_n \xrightarrow{\text{activating agent}} Eu^{2+}(L_n)^{2-} + N$$

or

$$Eu^0 + nLI \longrightarrow L_n^{-}Eu^{2+}I_n^{-}$$

Reduction of Eu^{3+}

$$Eu^{3+} + (n+1)L \longrightarrow Eu^{2+}L_n + L^{+}$$

or

$$Eu^{3+} + nL \xrightarrow[\text{reduction}]{\text{chemical or electrochemical}} Eu^{2+}L_n$$

Metathesis of Eu^{2+} complexes

$$Eu^{2+}L_1 + ML_2 \longrightarrow Eu^{2+}L_2 + ML_1$$

2.2.1 Oxidation of Eu^0

Oxidation of Eu metal can be accomplished by activation of Eu^0 using Hg, iodine, or liquid ammonia; redox transmetallation; or pseudo-Grignard formation. It is crucial to

perform this type of synthesis under an inert atmosphere because Eu metal will oxidize uncontrollably in air to produce mixtures of Eu^{2+}- and Eu^{3+}-containing complexes.

Syntheses of Eu^{2+} complexes from Eu^0 often require activation. Mercury, which activates Eu^0 through amalgamation, was used to prepare the homoleptic and tetranuclear Eu^{2+} complex $Eu_4[(t\text{-}Bu)_2pz)]_8$, **2.16**, where $(t\text{-}Bu)_2pz$ is 3,5-di-*tert*-butylpyrazolate (**Figure 2.4**).[34] Structural elucidation of the linear complex **2.16** revealed different coordination modes (η^2, $\mu\text{-}\eta^5\text{:}\eta^2$, and $\mu\text{-}\eta^2\text{:}\eta^2$) for the pyrazolates to Eu^{2+}. The outer Eu^{2+} ions are bonded in a η^2 fashion by the two terminal pyrazolates; a $\mu\text{-}\eta^5\text{:}\eta^2$ coordination mode is observed for the four pyrazolates that bridge the inner and outer Eu^{2+} ions; and a $\mu\text{-}\eta^2\text{:}\eta^2$ binding mode is exhibited by the two pyrazolates that bridge the two inner Eu^{2+} centers.[34]

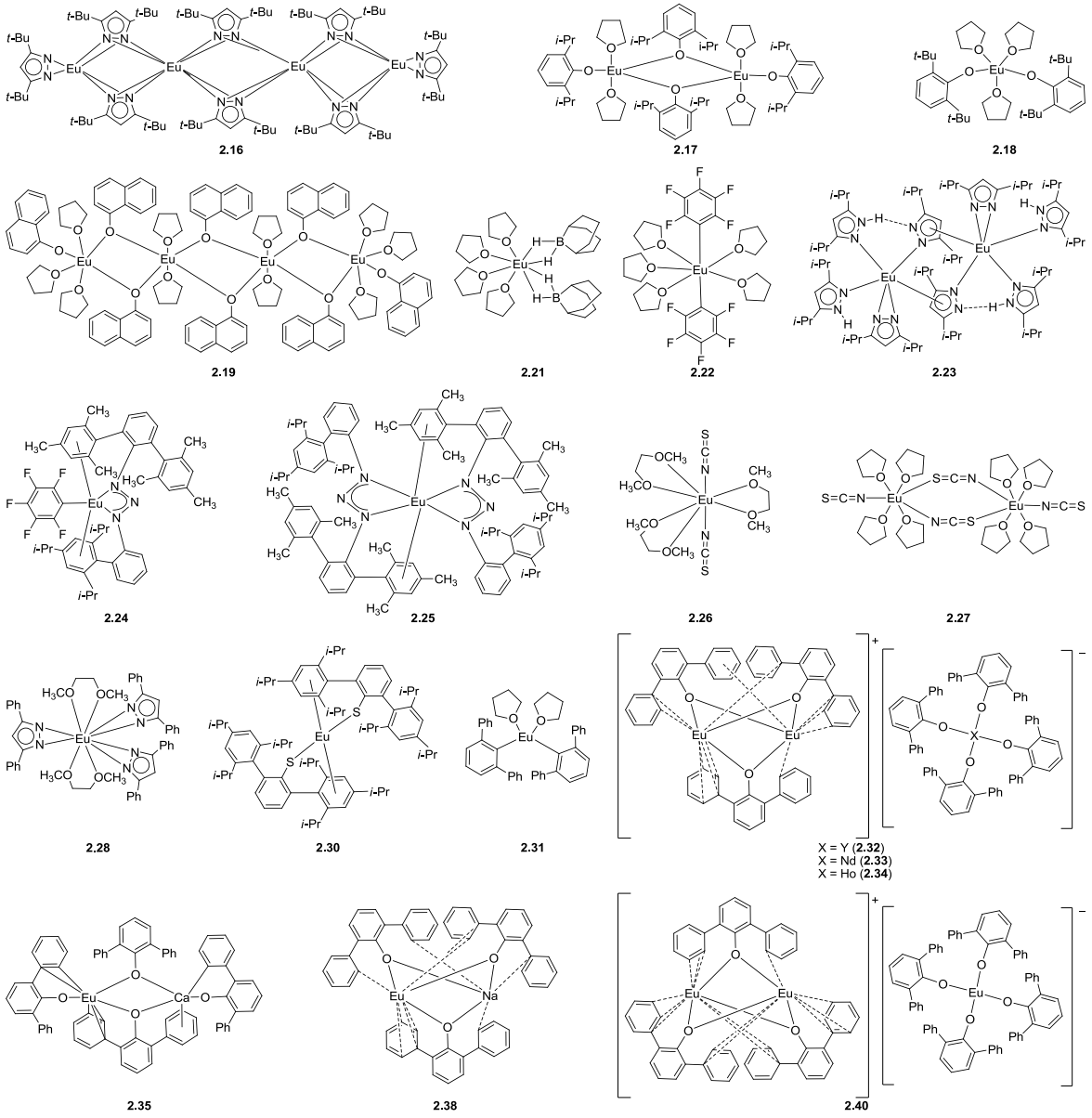

Figure 2.4 Structures of Eu^{2+}-containing complexes **2.16**–**2.19**, **2.21**–**2.28**, **2.30**–**2.35**, **2.38**, and **2.40** that were prepared from the oxidation of Eu^0.

An alternative to Hg as an activating agent is iodine, which was reported to be crucial in the preparation of several lanthanide-based complexes including the dimeric $[Eu(Odip)(\mu\text{-}Odip)(THF)_2]_2$, **2.17**, where Odip is 2,6-diisopropylphenolate.[35] In addition to mercury and iodine, dissolution in liquid ammonia can be used in the activation of Eu^0. Such is the case in the preparation of Eu^{2+}-containing alkoxide $Eu[OC_6H_3\text{-}2,6\text{-}(t\text{-}$

$Bu)_2]_2(THF)_3 \cdot 0.75C_7H_8$, **2.18**, and aryloxides $[Eu_4(\mu\text{-}OC_{10}H_7)_6(OC_{10}H_7)_2(THF)_{10}] \cdot 2THF$, **2.19**, and $Eu(OC_6H_4OCH_3)_2$, **2.20**.[36–38] Activation of Eu^0 was also employed using liquid ammonia for the synthesis of $\{Eu_2[(t\text{-}Bu)_2pz)]_4(THF)_2\}$ that is characterized by having centrosymmetric Eu^{2+} centers bonded in $\mu\text{-}\eta^2\text{:}\eta^5$ and η^2 modes by the bridging and terminal pyrazolate ligands, respectively.[39] These coordination modes can also be found in pyrazolate-based Eu^{2+} complex **2.16** and demonstrate the ability of pyrazolate ligands to coordinatively saturate Eu^{2+}. Liquid ammonia was also used in the one-pot synthesis of the organohydroborate complex of Eu^{2+} $(THF)_4Eu\{(\mu\text{-}H)_2BC_8H_{14}\}_2$, **2.21**, that features an agostic interaction between Eu^{2+} and a hydrogen atom in one of the hydroborate ligands. Structural and IR data suggest the presence of agostic interaction in solution and solid state, and this interaction may have influenced the *cis* arrangement of the hydroborate ligands in the octahedral complex.[40]

The preparation of Eu^{2+} complexes through redox transmetallation sometimes uses mercury- and tin-based complexes as oxidants, and activating agents such as Hg are used to improve the yields of this type of synthesis. The preparation of the (perfluoroaryl)europium(II) complex $Eu(C_6F_5)_2(OC_4H_8)_5$, **2.22**, entails the oxidation of Eu^0 using bis(pentafluorophenyl)mercury, $Hg(C_6F_5)_2$, in THF. Complex **2.22**, characterized by a pentagonal bipyramidal geometry with axial C_6F_5 groups and five THF molecules in the equatorial position, has relatively long Eu–C bonds (2.82 Å) that are likely due to the inductive electron-withdrawing effect of the fluorine substituents of the two phenyl groups.[41] The same oxidant, $Hg(C_6F_5)_2$, was used to prepare the homoleptic and dinuclear $\{Eu(i\text{-}Pr_2pz)_2(i\text{-}Pr_2pzH)_2\}_2$, **2.23**, where $i\text{-}Pr_2pz$ is 3,5-diisopropylpyrazolate. An x-ray crystal structure of the pyrazolato Eu^{2+} complex **2.23** shows a different coordination mode ($\mu\text{-}\eta^5\text{:}\eta^1$) to Eu^{2+} by the bridging 3,5-diisopropylpyrazolates centers. This coordination

mode of the bridging pyrazolates in addition to the η^1 binding mode of the terminal pyrazolates was ascribed to intramolecular hydrogen binding.[42] It is worth noting that redox transmetallation reactions carried out in nonpolar solvents including toluene (for example, in the preparation of complex **2.23**) can produce homoleptic Eu^{2+} complexes. In addition to complexes **2.22** and **2.23**, $Hg(C_6F_5)_2$ was used as oxidant in the preparation of Eu^{2+}-containing complexes with triazanides as ligands [Dmp(Tph)$N_3EuC_6F_5$], **2.24**, and [Eu{N_3Dmp(Tph)}$_2$], **2.25** where Dmp is 2,6-(2,4,6-$(CH_3)_3C_6H_2)_2C_6H_3$ and Tph is 2-(2,4,6-*i*-$Pr_3C_6H_2)C_6H_4$. Of particular note are the coordination modes of the terphenyl and biphenyl groups in complexes **2.24** and **2.25** that exhibit π-arene–Eu interactions with Eu–C distances of 3.088–3.233 and 3.011–3.311 Å in complex **2.24** and **2.25**, respectively. In complex **2.24**, both the mesityl ring of the terphenyl group and the triisopropylphenyl ring of the biphenyl moiety show an η^5 interaction with the metal, whereas in complex **2.25**, the mesityl rings of terphenyl groups exhibit η^5 and η^3 binding modes. The assignment of hapticity was based on the shortest metal–centroid separation or the smallest angle of the M–centroid vector and the normal of the arene plane.[43,44]

When $Hg(SCN)_2$ was used as oxidant, $[Eu(NCS)_2(DME)_3]$, **2.26**, was obtained from redox transmetallation with Eu^0 in DME, and bimetallic $[Eu(NCS)_2(THF)_4]_2$, **2.27**, was obtained when THF was used as solvent. The crystal structure of the eight-coordinate **2.26** shows configurational isomers, and the relative amount of each isomer is dependent on temperature. Racemic mixtures in a single crystal can be obtained at lower temperature (5 °C) while a mixture of enantionamerically pure Λ (left hand) or Δ (right hand) products was observed in a single crystal at room temperature.[45] The coordination environment in **2.27** features bridging two thiocyanate ligands and terminal THF molecules, adapting a distorted pentagonal bipyramidal geometry in each Eu^{2+} center.

Besides mercury-based oxidants, trialkyltin(IV) compounds were explored for redox transmetallation with Eu^0. Either the trivalent $[Eu^{3+}(Ph_2pz)_3(DME)_2]\cdot 2DME$, **2.28**, or the divalent *cis*-$[Eu^{2+}(Ph_2pz)_2(DME)_2]$, **2.29**, can be made from the reaction of $Sn(CH_3)_3(Ph_2pz)$, where Ph_2pz is 3,5-diphenylpyrazolate, with Eu^0 in DME by changing the amount of excess Eu^0.[46,47]

In contrast to redox transmetallation, the route toward the formation of a pseudo-Grignard compound has been successful in preparing Eu^{2+} complexes even without the use of Hg, iodine, or ammonia. Thiolate-containing complex $Eu(SAr^*)_2(THF)_{0.5}$, **2.30**, where Ar* is 2,6-(2,4,6-(*i*-Pr)$_3C_6H_2)_2C_6H_3$ was prepared from Eu^0, Ar*SH, and 2-iodobenzotrifluoride.[48] This thiolate complex is characterized by η^6-π interactions of Eu^{2+} with two *o*-2,4,6-triisopropylphenyl rings of the terphenyl groups as evidenced by IR spectroscopy and X-ray crystallography.[48] Another example of a Eu^{2+}-containing complex that shows η^1-π interactions with Eu^{2+} and was prepared from europium metal is $Eu(Dpp)(THF)_2$, **2.31**, where Dpp is 2,6-$Ph_2C_6H_3$. Complex **2.31** was synthesized from Eu^0 and DppI in THF and exhibits a distorted tetrahedral geometry with two aryl ligands and two THF molecules.[49]

While the oxidation of Eu^0 through activation of the metal surface, redox transmetallation, and formation of pseudo-Grignard compounds are used to prepare homometallic Eu^{2+} complexes, charged-separated and neutral heterobimetallic Eu^{2+}-containing complexes can also be synthesized from Eu^0. Treatment of Eu^0 and another lanthanide metal (Y^0, Nd^0, or Ho^0) with 2,6-diphenylphenol (OHdpp) at elevated temperature (190 °C) in the presence of Hg yielded charged-separated complexes, $[Eu_2(Odpp)_3][Y(Oddp)_4]$, **2.32**; $[Eu_2(Odpp)_3][Nd(Oddp)_4]$, **2.33**; and $[Eu_2(Odpp)_3][Ho(Oddp)_4]$, **2.34**. The Eu^{2+} centers in the $[Eu_2(Odpp)_3]^+$ are bridged by

aryloxide ligands and have coordination modes of η^4:η^2:η^1 and η^1:η^6:η^3 with π-arene–Eu interactions.[50] In contrast to the charged-separated complexes, heterobimetallic complexes [CaEu(Oddp$_4$)], **2.35**; [SrEu(Oddp)$_4$], **2.36**; and [BaEu(Oddp)$_4$], **2.37**, were produced upon reaction of Eu^0 and an alkaline-earth metal (Ca^0, Sr^0, or Ba^0) with OHdpp at high temperatures (210–235 °C). However, when Eu^0 was reacted with HOdpp in the presence of MOdpp (M = Na^0, K^0, and Li^0) at elevated temperature (210 °C), heterobimetallic Eu^{2+}-containing complexes [NaEu(Oddp)$_3$]·PhCH$_3$, **2.38**, and [KEu(Oddp)$_3$]·2.5PhCH$_3$, **2.39,** and the mixed-valent complex [Eu$_2$(Oddp)$_3$][Eu(Oddp)$_4$], **2.40**, were obtained. These heterobimetallic complexes also show π-arene–Eu interactions that coordinatively saturate Eu^{2+}. The coordination mode of the Eu^{2+} center is similar for **2.35** and **2.36** (η^2:η^3) while a different binding mode was observed in **2.37** (η^3:η^5). The coordination modes in the Eu^{2+}-containing complexes with alkaline metals are η^4:η^2:η^1 (complex **2.38**) and η^3:η^1:η^1 (complex **2.39**) and are similar to that of $[Eu_2(Odpp)_3]^+$ in the charged-separated complexes **2.32**–**2.34**.[51] Structural data for the $[Eu_2(Oddp)_3]^+$ unit in **2.40** depict the aryloxides binding in η^1:η^4:η^2 and η^3:η^2:η^3 fashions.[51] Purification of charged-separated or heterobimetallic complexes requires solvent extraction to remove the unreacted metal and homometallic coproducts.[50,51]

Despite of the propensity of Eu metal to undergo uncontrolled oxidation to both Eu^{2+} and Eu^{3+}, the use of Eu metal can produce modest to excellent yields (23–96%) in the preparation of Eu^{2+}-containing complexes. Also, activating Eu^0 using Hg has been shown to increase the yield of the desired Eu^{2+} complexes.

2.2.2 Reduction of Eu^{3+}

The reduction of Eu^{3+} by either a ligand that is also a reductant or by chemical or electrochemical methods is more common than the oxidation of Eu metal. Eu^{3+} halides,

triflates, oxides, or nitrates are typically used as the precursors for the preparation of Eu^{2+}-containing complexes with a variety of ligands including aryloxides, aminodiboranates, crown ethers, and cryptands.[25,52–58] An example of a Eu^{2+}-containing complex that was prepared from Eu^{3+} chlorides with a reducing species is the dinuclear, distorted pentagonal bipyramidal complex $\{Eu(H_3BN(CH_3)_2BH_3)_2(THF)_2\}_2$, **2.41**, which used *N,N*-dimethylaminodiboranate as the reductant (**Figure 2.5**).[52] However, the preparation of **2.41** produced mixtures of divalent and trivalent species.[52] In contrast, only divalent species were obtained when EuI_2 was used as a precursor instead of $EuCl_3$.[52] Qi and coworkers used Eu^{3+} chlorides as starting materials and a Na–K alloy as reductant to prepare $[LEu(HMPA)_2]_2(THF)_4$, **2.42**, where L is 2,2'-methylene bis(6-*t*-butyl-4-methylphenoxo) and HMPA is hexamethylphosphoric triamide. Complex **2.42** is characterized by two phenolate moieties bridging two Eu^{2+} atoms.[53] Each Eu^{2+} in **2.42** adopts a distorted trigonal bipyramidal geometry and a slightly asymmetric bridging mode of the phenolate ligand. This asymmetry is also observed in the bond length of Eu–O, where the axial Eu–O bond (2.44 Å) is shorter than the equatorial Eu–O bond (2.52 Å).[53] Also, the variation of the Eu–O–C angles in **2.42** have been associated with the existence of agostic interaction in this coordinatively unsaturated complex.[53] In addition to the use of Na–K alloy as a noncoordinating reductant in the preparation of Eu^{2+}-containing complexes, Zn was used as reductant in the synthesis of complexes **2.10** and Eu^{2+}–18-crown-6, **2.43**, from Eu^{3+} triflate.[54] The reduction of Eu^{3+} by Zn in the presence of 18-crown-6 or [2.2.2]cryptand was monitored using the absorption bands at 250 and 330 nm, which were assigned to the Eu^{2+} species.[54] Additionally, Eu^{3+} oxides serve as starting materials for preparing Eu^{2+}-containing complexes using electrochemical reduction. For example, Eu_2O_3 was reduced electrochemically in the syntheses of the Eu^{2+} complex of benzo-18-crown-6 and of

triethanolamine.[55,56] With the reduction of Eu^{3+} strategy, our laboratory prepared several Eu^{2+}-containing cryptates, **2.10**, **2.11**, and **2.44**–**2.47**.[57] In general, the advantage of using the reduction approach is that the metal source is air-stable, so the problem of surface oxidation is avoided. Nevertheless, the possibility of incomplete reduction of Eu^{3+} can limit the yield and purity of the desired Eu^{2+}-containing complexes.

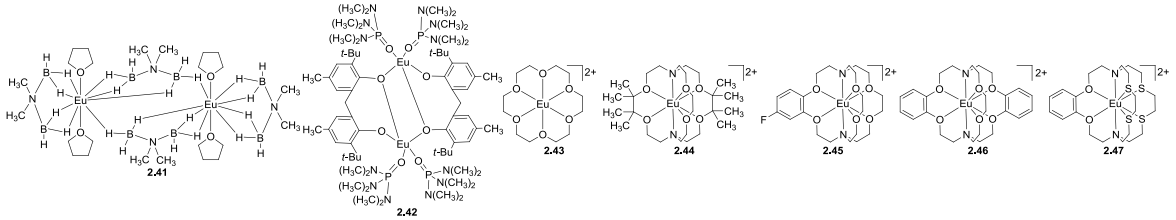

Figure 2.5 Structures of Eu^{2+}-containing complexes **2.41**–**2.47**, which were synthesized by the reduction of Eu^{3+}.

2.2.3 Metathesis of Eu^{2+} Complexes

While the other synthetic methods involve redox reactions to obtain Eu^{2+}, the metathesis approach makes use of Eu^{2+} halides and alkali metal-containing ligands as precursors to generate the desired Eu^{2+}-containing complex. The metathesis reaction has been successful in preparing several Eu^{2+}-containing complexes including the bimetallic $Eu_2(Ap^*py)_3I(THF)$, **2.48**, where Ap*py is deprotonated 6-methylpyridin-2-yl-[6-(2,4,6-triisopropylphenyl)pyridin-2-yl]amine;[59] a monometallic Eu^{2+}-containing *trans-N,N'*-dimethyl-*meso*-octaethylporphyrinogen complex, **2.49**;[60] a Eu^{2+}-containing benzamidinate complex $Eu[PhC(NSi(CH_3)_3)(2,6\text{-}(i\text{-}Pr)_2NC_6H_3)]_2(THF)_2$, **2.50**;[61] a Eu^{2+} complex with olefin-substituted cyclopentadienyl ligands $[C_5(CH_3)_4Si(CH_3)_2CH_2CH{=}CH_2]_2Eu$, **2.51**;[62] the bis(diphosphanylamido complex $[\{(Ph_2P)_2N\}_2Eu(THF)_3]$, **2.52**;[63] a Eu^{2+} complex containing bis(phosphinimino)methanides ligands $[\{(CH_3)_3SiNPPh_2)_2CH\}EuI(THF)]_2$, **2.53**;[64] the aminotroponiminate complex of compostion [{(*i*-Pr)$_2$ATI}Eu{N-

$(Si(CH_3)_2\}(THF)_2]$, **2.54**, where $(i\text{-Pr})_2$ATI is *N*-isopropyl-2-(isopropylamino)troponiminate;[65] and a monometallic, heteroleptic $[(DIP_2pyr)Eu(THF)_3]$, **2.55**, where DIP_2pyr is 2,5-bis{*N*-2,6-diisopropylphenyl)iminomethyl}pyrrolyl (**Figure 2.6**).[66] Complexes **2.48**–**2.55** were prepared from the metathesis reaction of $EuI_2(THF)_x$, where labile THF, iodine, or both are displaced by the desired ligand. Complex **2.50** exhibits *cisoid* and *transoid* isomers with respect to the position of coordinated THF.[61] The bidentate diphospanylamides, $(Ph_2P)_2N^-$, in complex **2.52** are η^2 coordinated to the Eu^{2+} center through the phosphorous and nitrogen. The structure of the bimetallic Eu^{2+}-containing complex **2.53** displays the tridentate bis(phosphinimino)methanide ligands bound to Eu^{2+} via two nitrogen atoms and a methine carbon atom. Two of these ligands are coordinated to a Eu^{2+} center to form a six membered metallacycle with a twist boat conformation.[64] When complex **2.53** was treated with $K\{CH(PPh_2NSi(CH_3)_2\}$, the six-coordinate amido Eu^{2+}-containing complex $[\{(CH_3)_3SiNPPh_2)_2CH\}Eu\{(Ph_2P)_2N\}(THF)]$, **2.56**, was obtained. As observed in **2.53**, the methine carbon was coordinated to Eu^{2+} in **2.56**, and the reported Eu–C (methine carbon) bond lengths were 2.945 Å and 2.878 Å for complexes **2.53** and **2.56**, respectively.[64] In contrast to **2.53** where iodine bridged two Eu^{2+} centers, complex **2.56** is monometallic with a nonbridging iodine atom and THF occupying the axial positions and the tridentate $(DIP_2pyr)^-$ ligand that is bound to Eu^{2+} through its three nitrogen atoms affording a distorted pentagonal pyramidal complex. As an alternative to the metathesis reaction of $EuI_2(THF)_x$ in preparing Eu^{2+}-containing complexes, we used the commercially available EuI_2 to prepare cryptates **2.10**, **2.11**, and **2.57**–**2.59**.[25,58] A similar europium halide salt was used to generate four-coordinate $\{Eu[(ArN)_2CN(i\text{-Pr})_2]_2\}$, **2.60**, where Ar is 2,6-diisopropylphenyl.[67] Roesky and coworkers used a bimetallic Eu^{2+}-containing complex $[\{CH(PPh_2NSiMe_3)_2\}Eu(THF)(\mu\text{-I})]_2$ and $NaBPh_4$ as precursors to

prepare [{CH(PPh$_2$NSi(CH$_3$)$_3$)$_2$}Eu(THF)$_3$]BPh$_4$, **2.61**.[68] The resulting complex was used to prepare other Eu^{2+}-containing complexes via metathesis of the labile borate ligand.[68] Another example of a borate-containing Eu^{2+} complex [Cp*(μ-η^6:η^1-Ph)$_2$EuBPh$_2$], **62**, was prepared from Eu(Cp*)$_2$ in the presence of [Et$_3$NH][BPh$_4$]. The structural motif of complex **2.62** features one coordinated Cp* and two of the phenyl rings of BPh_4^- ligand showing a μ-η^6:η^1 binding mode, with the ligands arranged in a pyramidal geometry around the coordination sphere of Eu^{2+}. While density functional theory (DFT) calculations predicted a trigonal planar shape for complex **2.62**, the large size of Eu^{2+} prefers intermolecular packing over intramolecular packing in the solid state, and agostic interactions may also have contributed to this deviation of geometry.[69] In general, with the metathesis approach of preparing Eu^{2+}-containing complexes, the presence of other oxidation states of Eu is not a problem as long as synthesis is performed under an inert atmosphere. The success of this third approach of metathesis relies on the completeness of the displacement of the alkali metal or a practical method of purification to remove byproduct salts. Steric limitations introduced by the incoming ligand may pose a problem in preparing the target Eu^{2+} complex.

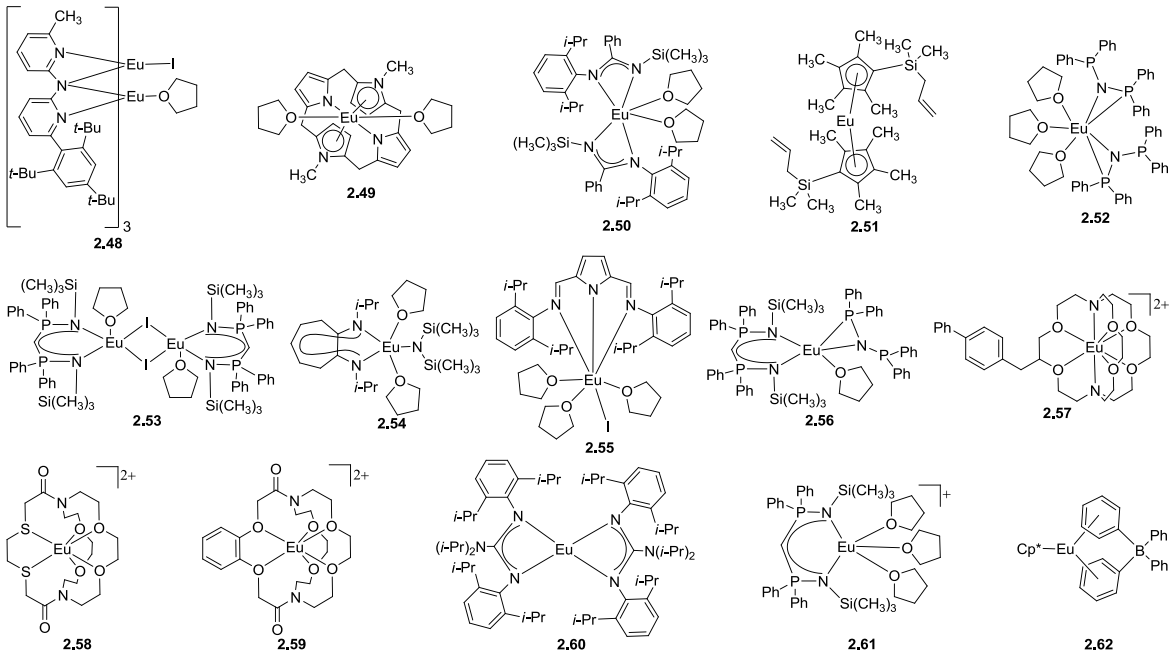

Figure 2.6 Structures of Eu^{2+}-containing complexes **2.48**–**2.62**, which were obtained from the metathesis of Eu^{2+}-containing complexes.

Each of the three synthetic methods described here have distinct advantages and limitations, and each route must be carefully considered when choosing a method to synthesize a new complex. In addition, structural studies of the recently synthesized Eu^{2+}-containing complexes presented in this section demonstrate the rich coordination chemistry of Eu^{2+}. Differences in the coordination environment in Eu^{2+}-containing complexes can be attributed to steric and electronic effects of the coordinated ligands as well as the size and electronic properties of Eu^{2+} that is responsible, in part, to the agostic interaction observed in some Eu^{2+} complexes.

The development of other Eu^{2+}-containing complexes in conjunction with the use of other divalent lanthanides in generating complexes with Ln^{2+}–Ga^{+} or Ln^{2+}–Al^{+} (Ln = Sm, Eu, Yb, or Tm) bonds is an active area of research.[70–72] Their applications for use as reductants are currently being explored.[70]

2.3 Applications of Eu^{2+}-Containing Complexes

The growing interest in Eu^{2+}-containing complexes stems from the unique catalytic, photophysical, and magnetic properties of these complexes. The remainder of this review describes the use of Eu^{2+}-containing complexes in four different applications.

2.3.1 Reductants

Eu^{2+} is a one-electron reductant for many systems. However, it was reported that a bimetallic Sm^{2+}-containing complex has the potential to be a two-electron reductant per molecule.[73] This discovery led to the pursuit of divalent lanthanide species, including Eu^{2+}-containing complexes, that could act as multielectron reductants. This active area of research is important in establishing a more complete understanding in the reduction chemistry of Eu^{2+}. Lee and coworkers reported a Eu^{2+}-containing complex **2.50** that serves as a one-electron reductant to a diphenyl dichalcogenide PhSeSePh to produce $\{Eu([PhC(NSi(CH_3)_3)(2,6\text{-}(i\text{-}Pr)_2NC_6H_3)])_2(\mu\text{-}SePh_2)\}_2$, **2.63**, in which the two Eu^{3+} centers are bridged by diphenyl diselenides (**Figure 2.7**).[61] Each Eu^{3+} ion in **2.63** assumed a distorted octahedral geometry and was coordinated by two η^2-bound benzamidinate ligands. However, when the same Eu^{2+}-containing bisamidinate complex was allowed to react with diphenyl ditellurides and iodine, both reactions were unsuccessful, indicating that the reducing strength of Eu^{2+} was not sufficient to reduce diphenyl ditellurides and iodine.[61] Also, in the case of the macrocylic ligand system *trans-N,N'*-dimethyl-*meso*-octaethylporphyrinogen, the Eu^{2+}-containing complex cannot reduce *t*-butyl-1,4-diazabuta-1,3-diene (*t*-Bu-DAB).[60] However, the analogous Sm^{2+} complex forms a bimetallic complex when reacted with *t*-Bu-DAB.[60] The formation of the bimetallic Sm^{3+} complex bridged by the reduced $[t\text{-Bu-DAB}]^{2-}$ is driven by the reducing power of Sm^{2+} towards *t*-Bu-DAB, but the steric constraints due to the bulky *t*-butyl moieties makes this reaction

reversible.[60] Because Eu^{2+} has a more positive Ln^{2+}/Ln^{3+} oxidation potential (–0.35 V vs NHE) than Sm^{2+} (–1.55 V vs NHE), the driving force to form an analogous bimetallic Eu^{3+} complex is hindered, presumably because the reducing strength of Eu^{2+} is not sufficient to reduce *t*-Bu-DAB. These examples of controlled redox potential could be useful in selective reductions during multistep syntheses and for developing the first Eu^{2+}-containing complex that could act as multielectron reductant.

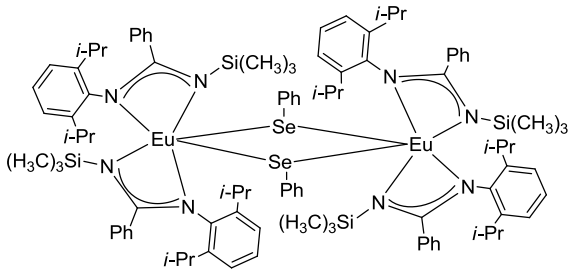

2.63

Figure 2.7 Structure of Eu^{2+}-containing reductant **2.63**.

An important factor that can control the reducing properties of Eu^{2+} is the nature of the ligands. As an example, the reaction with $Cp^*_2Eu(OEt_2)$ with C_6F_5-substituted diazabutadiene $(DADC_6F_5)^-$ led to the oxidation of Eu^{2+} and formation of the radical anion $(DADC_6F_5)^{\bullet-}$.[74] The presence of Eu^{3+} in the resulting complex was characterized by crystallographic data, magnetic susceptibility measurements, and IR spectroscopy. The electron-withdrawing characteristic of the C_6F_5 moiety and its proximity to the metal center is likely the cause of the facile oxidation of Eu^{2+}. On the other hand, neither oxidation of Eu^{2+} nor formation of radical anion was observed when *t*-butyl-substituted diazabutadiene was used.[74] In general, the diazabutadienyl ligand can have rich redox chemistry when coupled with Eu^{2+} by modifying this ligand using substituents of different electronic properties.

2.3.2 Polymerization Initiators

As discussed in the previous section, ligands can influence the rich reduction chemistry of Eu^{2+} where the resulting complex can play an important role in several applications including polymer chemistry. In the preparation of polymers, Eu^{2+}-containing complexes can act as electron-transfer agents to initiate several polymerization processes. An example of this application is the activity of several Eu^{2+}-containing complexes that contain indenyl ligands in the initiation of the polymerization of methyl methacrylate (MMA) and ε-caprolactone.[11,12]

2.3.2.1 Methyl Methacrylate Polymerization

Eu^{2+}-containing complexes **2.64**–**2.73** that contain functionalized indenyl ligands are used in the polymerization of MMA (**Figure 2.8**).[11,75–77] The activity of these complexes in polymerizations and the stereochemistries of the resulting polymers are dependent on temperature and solvent (**Figure 2.7**). High activity is observed at low temperatures (–30 to –60 °C for complexes **2.64** and **2.65**; 0 to –60 °C for complexes **2.66**–**2.69**, **2.72**, and **2.73**; –30 to –45 °C for complexes **2.70** and **2.71**), and these complexes have solvent-dependent activities. Complexes **2.64, 2.65**, and **2.72** have high activities when THF or dimethoxyethane is used as solvent instead of toluene. Complex **2.66** has high activity in dimethoxyethane, THF, and toluene; **2.67** show good activity in THF; and complexes **2.68**, **2.69**, and **2.73** have high activity in dimethoxyethane. The molecular weights of the resulting MMA polymers were high (up to 443 kDa) at low temperatures indicating that chain propagation is favored at low temperatures.[11,75–77] The mechanism of MMA polymerization was postulated to initiate through reductive dimerization of MMA via electron transfer from Eu^{2+}, resulting in the formation of Eu^{3+} enolates.[11,75–77] Propagation

did not go through an insertion mechanism because the indenyl ligand was not detected on the polymer chains by ^{1}H NMR spectroscopy.[11,76]

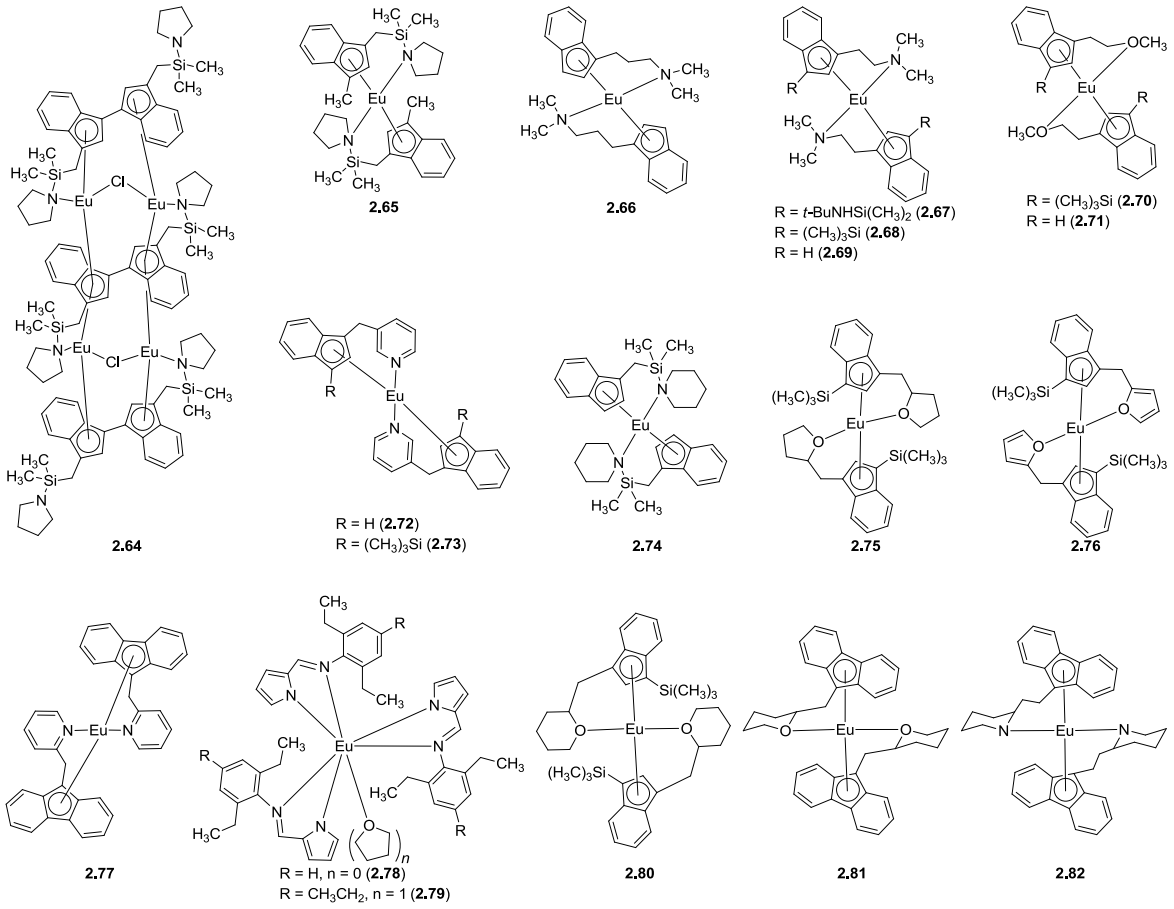

Figure 2.8 Structure of Eu^{2+}-containing complexes **2.64**–**2.82**, which were used as polymerization initiators.

The stereochemistry of the MMA polymers is determined by ^{1}H NMR spectroscopy. The majority of the MMA polymers produced using Eu^{2+}-containing functionalized indenyl complexes **2.64**, **2.65**, **2.72** and **2.73** as initiators is syndiotactic.[11,77] However, when complexes **2.66**–**2.68** were used in dimethoxethane or THF, a 1:1:1 ratio of isotactic, syndiotactic, and atactic polymers was obtained. But, predominantly syndiotactic polymers was obtained using **2.66** in toluene, and a decrease in the ratio of syndiotactic to isotactic polymers was observed using **2.70** when the solvent was changed from THF or

dimethoxyethane to toluene suggesting a solvent effect influences the stereochemistry of these polymers. The presence of several tacticities in the synthesized polymers was attributed to the *rac*/*meso* interconversion, which is favored by solvents including THF and dimethoxyethane.[77] While the stereochemistry of the polymers showed solvent dependency, it is still unclear if this stereoregularity is influenced by the nature of the initiator, specifically on the metal and ligands. A similar study that uses different initiators (for example, different divalent lanthanide metal ions or a ligand system other than indene compounds) could answer this question.

2.3.2.2 Ring-Opening Polymerization of ε-Caprolactone

Eu^{2+}-containing complexes **2.74**–**2.79** that contain indenyl, fluorenyl, and iminopyrrolyl ligands showed catalytic activity in the ring-opening polymerization of ε-caprolactone.[12,78–80] With these catalysts, high activity is observed at high temperatures (0 to 30 °C for complexes **2.75** and **2.76**; –30 to 60 °C for complex **2.74**; 0 to 60 °C for complex **2.77**; and 30 to 60 °C for complexes **2.78** and **2.79**), and the activities of these complexes depend on solvent. Complexes **2.77**–**2.79** have high activities when THF or toluene is the solvent; complex **2.74** exhibits high activity in dimethoxyethane, THF, and toluene; and **2.75** and **2.76** show good activity in toluene. Furthermore, the steric bulk of the substituents in the ligands may have an effect on the activity of the complexes and the molecular weights of the resulting polymers. When the silyl substituent in the furfuryl- or tetrahydrofurfuryl-functionalized indenyl ligands of complexes **2.75** and **2.76** was absent, no activity using the two complexes was observed. However, it is not clear what the role of the silyl substituent is in the polymerization process.[78] The use of more sterically bulky ligands in **2.79** relative to the ligands in **2.78** has been implicated to affect the chain propagation process, thus affecting the molecular weights of the polymers.[80] Wang and

coworkers proposed that the polymerization of ε-caprolactone is initiated by the formation of Eu^{3+}-containing alkoxyl radical species formed from the oxidation of the Eu^{2+} metal center (**Scheme 2.2**).[12] The alkoxyl radical species is believed to take a second Eu^{2+}-containing complex and produce a bimetallic Eu^{3+}-containing complex that is bridged by the opened caprolactone.[12] Subsequently, chain propagation occurs when subsequent molecules of ε-caprolactone are added to the Eu^{3+} complex via a coordination–insertion process.[12]

Scheme 2.2 Proposed mechanism of polymerization of ε-caprolactone.[12] Ind is the indenyl ligand. Adapted with permission from S. Zhou, S. Wang, E. Sheng, L. Zhang, Z. Yu, X. Xi, G. Chen, W. Luo, Y. Li. *Eur. J. Inorg. Chem.* **2007**, 1519–1528. Copyright 2007 John Wiley and Sons.

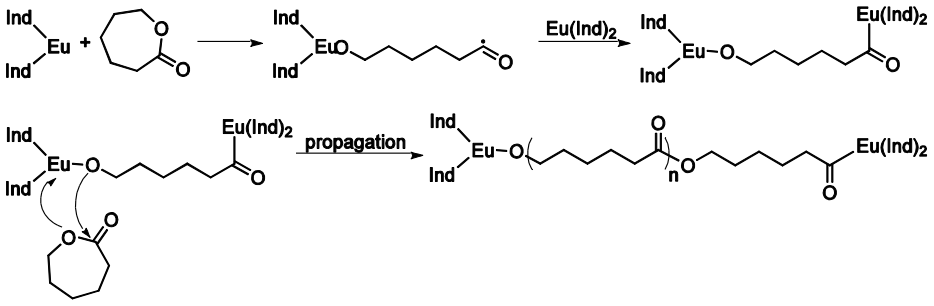

Because the role of the ligands on the polymerization of MMA and ε-caprolactone has yet to be elucidated, several Eu^{2+} complexes $\{\eta^5{:}\eta^1\text{-}[1\text{-}(CH_3)_3Si\text{-}3\text{-}(C_5H_9OCH_2)C_9H_5]\}_2Eu$, **2.80**;[81] $(\eta^5{:}\eta^1\text{-}C_5H_9OCH_2C_{13}H_8)_2Eu$, **2.81**;[82] and $(\eta^5{:}\eta^1\text{-}C_5H_{10}NCH_2CH_2C_{13}H_8)_2Eu$, **2.82**,[82] containing functionalized indenyl and fluorenyl ligands were investigated in terms of their activity towards MMA and ε-caprolactone polymerization. The silyl substituent in the indenyl ligands in complex **2.80** is likely a key factor in the two polymerization processes.[81] Without the silyl substituent in **2.80**, no activity was observed for any reaction condition.[81] However, high activity was observed for **2.80** for both MMA and ε-

caprolactone polymerizations. The effect of the ligand is also evident in the case of complexes **2.81** and **2.82**. Complex **2.81** with *N*-piperidineethyl functionalized fluorenyl ligands has higher activity in ε-caprolactone polymerization than complex **2.81** with tetrahydro-2H-pyranyl ligands under the same reaction conditions. However, this ligand effect was not observed on the polymerization of MMA.

In general, Eu^{2+}-containing complexes using fluorenyl ligands are more effective as catalysts for both MMA and ε-caprolactone polymerizations than indenyl ligands with similar substituents. While Eu^{2+}-containing complexes **2.64**–**2.82** initiate the polymerization of MMA or ε-caprolactone, it would be useful to investigate the mechanistic role of the different ligands in initiation. Also, exploration of a broader ligand system would enable an in depth understanding of how to better control the properties of the synthesized polymers. Although a Eu^{2+} complex has been used in the cyclotrimerization of isocyanates, the scope of the ligands used is still limited.[83] These ligand-centered studies would expand our understanding of the reduction chemistry of Eu^{2+} and its application to synthetic and polymer chemistry.

2.3.3 Luminescent Complexes

Aside from the rich reduction properties of Eu^{2+}, this ion produces complexes that are luminescent both in solution and in the solid state. Current research efforts are directed towards developing Eu^{2+}-containing complexes that have high luminescence efficiency.

The luminescence of uncomplexed Eu^{2+} and Eu^{3+} in protic solvents is quenched by O–H oscillators of coordinated solvent molecules.[84] Thus, macrocyclic ligands including crown ethers and cryptands are used to encapsulate Eu^{2+}, protecting this ion from luminescence quenching by solvent molecules. The luminescence properties of Eu^{2+}-containing crown ethers, azacrown ethers, cryptands, and polymers were reviewed by

Adachi and coworkers in 1998.[6] Since then, efforts have focused on developing luminescent complexes with high quantum yields by introducing functional groups into macrocyclic ethers or by using other ligands that better encapsulate Eu^{2+}.[85–88] There is also a growing interest in the comparison of spectroscopic properties of Eu^{2+} in the solid state to Eu^{2+}-containing complexes in solution.

A variety of functional groups have been used to study the contribution of antenna effects and conjugated π systems on the luminescence efficiency of Eu^{2+}-containing complexes.[86–87] Pyridine groups, known for exhibiting an antenna effect in Eu^{3+}-containing complexes, were introduced into 18-crown-6. When bis-pyridino-18-crown-6 was complexed with Eu^{2+}, the emission of the complex in the solid state was quenched at room temperature, and only a weak emission at 430 nm was observed at 77 K, which is typical for Eu^{2+}-containing crown ethers.[86] This quenching is likely due to the energy transfer from the excited state quasi-5*d* energy level of Eu^{2+} to the π* levels of pyridine, and this quenching is not observed when unfunctionalized 18-crown-6, **2.83**, was used.[86] However, a blue luminescence was observed when benzo-15-crown-5, **2.84**, and benzo-18-crown-6, **85**, were used as ligands.[54,87] The Eu^{2+}-containing complex with benzo-15-crown-5 is characterized by a Eu^{2+} metal center that is sandwiched by two benzo-15-crown-5 ligands.[86] In the solid state, Eu^{2+}–**2.85** shows an emission peak that is similar to what is observed in methanol at room temperature. This observation is also true for Eu^{2+}-containing 15-crown-5, Eu–**2.86**. These observations suggest that similar structures exist in the solid state and in solution.[88] The mean lifetime of the excited state of Eu^{2+}–**2.84** at room temperature is 0.65 μs in the solid state and 0.14 μs in methanol (**Table 2.1**).[87] This difference in excited state lifetime is likely due to the additional relaxation processes caused by the methanolic O–H oscillators.[87] Furthermore, a phenyl moiety in the crown

ether might contribute to a reduction in the lifetime because this moiety could rigidify the crown ether and lead to structural changes making Eu^{2+} more exposed to luminescence quenchers relative to unmodified crown ethers.[6] Also, the cavity size of the crown ether affects the luminescence lifetime of the excited state. Among the three crown ethers studied, the cavity size of **2.86** is most efficient at reducing the number of coordinating anions or solvent molecules that decrease luminescence lifetime.[88]

Table 2.1 Luminescence properties of Eu^{2+}-containing complexes in methanol solution and in the solid state (room temperature and 77 K).[6,54,87,88]

Complex	Maximum emission band, nm (solid)	Maximum emission band, nm (methanol)	Luminescence lifetime, μs (solid)	Luminescence lifetime, μs (methanol)
Eu^{2+}–**2.83**	ND (RT)	ND	ND	ND
	411.5 (77 K)		ND	
Eu^{2+}–**2.84**	422 (RT)	417	0.65 (RT)	0.14
	427 (77 K)		0.59 (77 K)	
Eu^{2+}–**2.85**	425 (RT)	447	8.34 (RT)	0.028
	430 (77 K)		8.01 (77 K)	
Eu^{2+}–**2.86**	433 (RT)	432	0.922 (RT)	0.800
	417 (77 K)		0.745 (77 K)	

Legend: RT is room temperature, ND is no data available

In general, macrocylic ligands with cavity sizes that closely match the ionic radius of Eu^{2+} are the best ligands to insulate Eu^{2+} from solvent-based luminescence quenchers. Rigidifying ligands by adding phenyl groups and the addition of substituents like pyridine,

leads to a decrease in luminescence emission. These factors should be taken into consideration when designing Eu^{2+}-based luminescent materials.

2.3.4 MRI Contrast Agents

In addition to the reducing and luminescence properties of Eu^{2+}, the magnetic properties of this ion are important in the development of Eu^{2+}-based contrast agents for magnetic resonance imaging (MRI). In the last two decades, research on the properties of Eu^{2+} that are relevant to MRI has been reported. A fast water-exchange rate and an isoelectronic ground state to Gd^{3+} are properties that make Eu^{2+} an excellent candidate for use as a contrast agent for MRI.[89] This area started when Merbach and coworkers reported the fast water-exchange rate of the Eu^{2+} aqua ion that is in the order of 10^9 s^{-1}. After detailed mechanistic studies on the water exchange of the Eu^{2+} aqua ion,[90] investigations of the nuclear and electronic relaxation processes of Eu^{2+} chelated by polyaminopolycarboxylates, commonly used with Gd^{3+}, were performed.[91] When chelated to diethylenetriamine pentaacetate (DTPA), Eu^{2+} has a water-exchange rate that is three orders of magnitude faster than the clinically approved contrast agent $[GdDTPA]^{2-}$, **2.87**, (**Figure 2.9**).[91] In addition to water-exchange rate, other molecular parameters including rotational correlation time and electronic spin relaxation time are important factors that influence the efficiency of contrast agents, known as relaxivity. For example, despite the fast water-exchange of $[EuDTPA]^{3-}$, **2.88**, the reported relaxivity of **2.88** at 20 MHz is 20% lower than that of **2.87** because relaxivity is influenced by fast rotation and by fast electronic spin relaxation.[91] The same observation was implicated for the higher relaxivity of Eu^{2+}-containing 1,4,7,10-tetraazacyclododecane-1,4,7,10-tetraacetate $[EuDOTA]^{2-}$ (4.74 $mM^{-1}s^{-1}$) than $[EuDTPA]^{3-}$ (3.49 $mM^{-1}s^{-1}$) at 20 MHz and 298 K.[92] Results with other Eu^{2+}-containing complexes indicate that the unfavorable fast electronic spin

relaxation rate is not observed with all Eu^{2+} complexes.[91,93] Tóth and coworkers reported that the electron paramagnetic resonance line widths of **2.10**, are narrower by a factor of 8–10 compared to **2.88**, indicating a slower electronic spin relaxation of Eu^{2+} in cryptate **2.10** relative to **2.88**.[94] Consequently, the observed electronic spin relaxation for Eu^{2+}-containing cryptates does not limit relaxivity. In addition to slow electronic spin relaxation, this Eu^{2+}-containing cryptate has a fast water-exchange rate (10^8 s^{-1}) and contains two inner-sphere water molecules in a ten-coordinate complex.[94] These properties are promising because they present an opportunity to develop Eu^{2+}-containing cryptates as effective contrast agents for MRI. A review of the similarities and differences in terms of these molecular parameters for several Eu^{2+}- and Gd^{3+}-containing complexes and their implications to research on MRI contrast agents was written by Merbach and coworkers in 2001.[93]

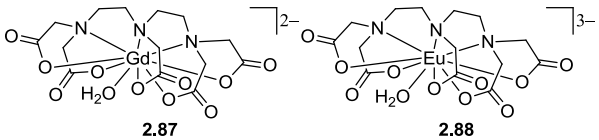

Figure 2.9 Structures of complexes **2.87** and **2.88**.

While Eu^{2+} has properties that make it a candidate for use as a contrast agent for MRI, its propensity to oxidize prevents in vivo applications.[57] It was demonstrated in the work of Allen and coworkers that Eu^{2+} can be oxidatively stabilized using coordination chemistry principles, including hard–soft acid–base theory, to the extent that it is more oxidatively stable than Fe^{2+} in hemoglobin.[57] These studies raised the possibility of using Eu^{2+}-containing cryptates for in vivo applications.

In addition to using modified cryptands as ligands to stabilize Eu^{2+}, I investigated the relaxivity of several Eu^{2+}-containing cryptates **2.10–2.11** at different field strengths (1.4, 3,

7, 9.4, and 11.7 T).[25,58] These cryptates showed higher relaxivity at higher fields (7 and 9.4 T) relative to lower fields (1.4 and 3 T) unlike common Gd^{3+}-containing contrast agents.[25,58] While high relaxivity is a requirement for effective contrast agents, other properties including kinetic stability need to be considered for utility in vivo. I demonstrated that Eu^{2+}-containing cryptates **2.10** and **2.11** are stable to transmetallation in the presence of endogenous ions such as Ca^{2+}, Mg^{2+}, and Zn^{2+},[25] and the Allen group is currently investigating the thermodynamic stability and toxicity of several other Eu^{2+}-containing cryptates.

2.4 Conclusions

The rapid increase in the number of Eu^{2+}-containing complexes reported in the past few decades has paved the way to making these complexes commonplace in coordination chemistry. New information regarding the stability and utility of Eu^{2+}-containing complexes using a variety of ligands has opened new frontiers in lanthanide chemistry. Careful control of ligand properties produces Eu^{2+}-containing complexes that are useful in synthetic, materials, and medicinal applications.

2.5 References

(1) Huheey, J. E.; Keiter, E. A.; Keiter, R. L. in *Inorganic Chemistry: Principles of Structure & Reactivity* HarperCollins College Publishers, **1993**, 4th ed., p 601.

(2) Evans, W. J. Evans, *Coord. Chem. Rev.* **2000**, *206–207*, 263–283.

(3) Tilley, T. D.; Zalkin, A.; Andersen, R. A.; Templeton, D. H. Templeton, *Inorg. Chem.* **1981**, *20*, 551–554.

(4) Adin, A.; Sykes, A. G. *Nature* **1966**, *209*, 804–804.

(5) Sabbatini, N.; Ciano, M.; Dellonte, S.; Bonazzi, A.; Bolletta, F. Balzani, V. *J. Phys. Chem.* **1984**, *88*, 1534–1537.

(6) Jiang, J.; Higashiyama, N.; Machida, K.; Adachi, G. *Coord. Chem. Rev.* **1998**, *170*, 1–29.

(7) Hoffman, M. V. *J. Electrochem. Soc*. **1971**, *118*, 933–936.

(8) Ryan, F. M.; Lehmann,W.; Feldman, D. W.; Murphy, J. *J. Electrochem. Soc.* **1974**, *121*, 1475–1481.

(9) Tilley, T. D.; Andersen, R. A.; Spencer, B.; Ruben, H.; Zalkin, A. Templeton, D. H.; *Inorg. Chem.* **1980**, *19*, 2999–3003.

(10) Evans, W. J. *J. Organomet. Chem.* **2002**, *652*, 61–68.

(11) Wang, S.; Zhou, S.; Sheng, E.; Xie, M.; Zhang, K.; Zheng, L.; Feng, Y.; Mao, L. Huang, Z. *Organometallics* **2003**, *22*, 3546–3552.

(12) Zhou, S.; Wang, S.; Sheng, E.; Zhang, L.; Yu, Z.; Xi, X.; Chen, G.; Luo, W.; Li, Y. *Eur. J. Inorg. Chem.* **2007**, 1519–1528.

(13) Fischer, E. O.; Fischer, H. *Angew. Chem, Internat. Edit.* **1964**, *3*, 132–133.

(14) Nief, F. *Dalton Trans.* **2010**, *39*, 6589–6598.

(15) Tilley, T. D.; Andersen, R. A.; Zalkin, A. *Inorg. Chem.* **1984**, *23*, 2271–2276.

(16) Williams, A. F. Grandjean, F.; Long, G. J.; Ulibarri, T. A.; Evans,W. J. *Inorg. Chem.* **1989**, *28*, 4584–4588.

(17) Rabe, G. W.; Yap, G. P. A.; Rheingold, A. L. *Inorg. Chim. Acta* **1998**, *267*, 309–311.

(18) Rabe, G. W.; Yap, G. P. A.; Rheingold, A. L. *Inorg. Chem.* **1997**, *36*, 3212–3215.

(19) Tilley, T. D.; Andersen, R. A.; Zalkin, A. *J. Am. Chem. Soc.* **1982**, *104*, 3725–3727.

(20) White, III, J. P.; Shore, S. G. *Inorg. Chem.* **1992**, *31*, 2756–2761.

(21) Tilley, T. D.; Andersen, R. A.; Zalkin, A. *Inorg. Chem.* **1983**, *22*, 856–859.

(22) Gansow, O. A.; Kausar, A. R.; Triplett, K. M.; Weaver, M. J.; Yee, E. L. *J. Am. Chem. Soc.* **1977**, *99*, 7087–7089.

(23) Burns, J. H.; Baes, Jr., C. F. *Inorg. Chem.* **1981**, *20*, 616–619.

(24) Yee, E. L.; Gansow, O. A.; Weaver, M. J. *J. Am. Chem. Soc.* **1980**, *102*, 2278–2285.

(25) Garcia, J.; Kuda-Wedagedara, A. N. W.; Allen, M. J. *Eur. J. Inorg. Chem*. **2012**, 2135–2140.

(26) Adachi, G.-Y.; Tomokiyo, K.; Sorita, K.; Shiokawa, J. *J. Chem. Soc., Chem. Commun.* **1980**, 914–915.

(27) White, III, J. P.; Deng, H.; Shore, S. G. *Inorg. Chem.* **1991**, *30*, 2337–2342.

(28) Cary, D. R.; Arnold, J. *Inorg. Chem.* **1994**, *33*, 1791–1796.

(29) Maudez, W.; Meuwly, M.; Fromm, K. M. *Chem. Eur. J.* **2007**, *13*, 8302–8316.

(30) Plečnik, C. E.; Liu, S.; Chen, X. Meyers, E. A.; Shore, S. G. *J. Am. Chem. Soc.* **2004**, *126*, 204–213.

(31) Rybak, J.-C.; Müller-Bushbaum, K. *Z. Anorg. Allg. Chem.* **2010**, *636*, 126–131.

(32) Janicki, R.; Mondry, A.; Starynowicz, P. *Z. Anorg. Allg. Chem.* **2005**, *631*, 2475–2477.

(33) Hou, Z.; Zhang, Y.; Nishiura, M.; Wakatsuki, Y. *Organometallics* **2003**, *22*, 129–135.

(34) Deacon, G. B. A. Gitlits, P. W. Roesky, M. R. Bürgstein, K. C. Lim, B. W. Skelton, A. H. White, *Chem. Eur. J.* **2001**, *7*, 127–138.

(35) Hamidi, S.; Deacon, G. B.; Junk, P. C.; Neumann, P. *Dalton Trans.* **2012**, *41*, 3541–3552.

(36) Carretas, J.; Branco, J. ; Marçalo, J.; Domingos, Â. ; Pires de Matos, A. *Polyhedron* **2003**, *22*, 1425–1429.

(37) Carretas, J.; Branco, J.; Marčalo, J.; Isolani, P.; Domingos, A.; de Matos, A. P. *J. Alloys Compd*, **2001**, *323–324*, 169–172.

(38) Carretas, J.; Branco, J.; Marčalo, J.; Valente, N.; Waerenborgh, J. C.; Carvalho, A.; Marques, N.; Domingos, Â.; de Matos, A. P. *J. Alloys Compd*, **2004**, *374*, 289–292.

(39) Hitzbleck, J.; O'Brien, A. Y.; Deacon, G. B.; Ruhlandt-Senge, K. *Inorg. Chem.* **2006**, *45*, 10329–10337.

(40) Chen, X.; Lim, S.; Plečnik, C. E.; Liu, S.; Du, B.; Meyers, E.; Shore, A. S. G. *Inorg. Chem.* **2004**, *43*, 692–698.

(41) Forsyth, C. M.; Deacon, G. B. *Organometallics* **2000**, *19*, 1205–1207.

(42) Hitzbleck, J.; Deacon, G. B.; Ruhlandt-Senge, K. *Eur. J. Inorg. Chem.* **2007**, 592–601.

(43) Hauber, S.-O.; Niemeyer, M. *Inorg. Chem.* **2005**, *44*, 8644–8646.

(44) Lee, H. S.; Niemeyer, M. *Inorg. Chem.* **2010**, *49*, 730–735.

(45) Bakker, J. M.; Deacon, G. B.; Forsyth, C. M.; Junk, P. C.; Wiecko, M. *Eur. J. Inorg. Chem.* **2010**, 2813–2825.

(46) Beaini, S.; Deacon, G. B.; Hilder, M.; Junk, P. C.; Turner, D. R. *Eur. J. Inorg. Chem.* **2006**, 3434–3441.

(47) Beaini, S.; Deacon, G. B.; Delbridge, E. E.; Junk, P. C.; Skelton, B. W.; White, A. H.; *Eur. J. Inorg. Chem.* **2008**, 4586–4596.

(48) Niemeyer, M. *Eur. J. Inorg. Chem.* **2001**, 1969–1981.

(49) Heckmann, G.; Niemeyer, M. *J. Am. Chem. Soc*. **2000**, *122*, 4227–4228.

(50) Deacon, G. B.; Junk, P. C.; Moxey, G. J.; Ruhlandt-Senge, K.; St. Prix, C.; Zuniga, M. F. *Chem. Eur. J.* **2009**, *15*, 5503–5519.

(51) Deacon, G. B.; Junk, P. C.; Moexy, G. J. *Chem. Asian J.* **2009**, *4*, 1309–1317.

(52) Daly, S. R.; Girolami, G. S. *Inorg. Chem.* **2010**, *49*, 4578–4585.

(53) Bao, L.; Yingming, Y.; Mingyu, D.; Yong, Z.; Qi, S. *J. Rare Earths* **2006**, *24*, 264–267.

(54) Shinoda, S.; Nishioka, M.; Tsukube, H. *J. Alloys Compd*. **2009**, *488*, 603–605.

(55) Starynowicz, P.; Bukietyńska, K.; Goląb, S.; Ryba-Romanowski, W.; Sokolnicki, J. *Eur. J. Inorg. Chem*. **2002**, 2344–2347.

(56) Starynowicz, P. *J. Alloys Compd*, **2001**, *323–324*, 159–163.

(57) Gamage, N.-D. H.; Mei, Y.; Garcia, J.; Allen, M. J. *Angew. Chem., Int. Ed*. **2010**, *49*, 8923–8925.

(58) Garcia, J.; Neelavalli, J.; Haacke, E. M.; Allen, M. J. *Chem. Commun.* **2011**, *47*, 12858–12860.

(59) Dietel, A. M.; Döring, C.; Glatz, G.; Butovskii, M. V.; Tok, O.; Schappacher, F. M.; Pöttgen, R.; Kempe, R. *Eur. J. Inorg. Chem.* **2009**, 1051–1059.

(60) Dick, A. K. J.; Frey, A. S. P.; Gardiner, M. G.; Hilder, M.; James, A. N.; Junk, P. C.; Powanosorn, S.; Skelton, B. W.; Wang, J.; White, A. H. *J. Organomet. Chem.* **2010**, *695*, 2761–2767.

(61) Yao, S.; Chan, H.-S.; Lam, C.-K.; Lee, H. K. *Inorg. Chem*. **2009**, *48*, 9936–9946.

(62) Evans, W. J.; Perotti, J. M.; Brady, J. C.; Ziller, J. W. *J. Am. Chem. Soc.* **2003**, *125*, 5204–5212.

(63) Roesky, P. W. *Inorg. Chem.* **2006**, *45*, 798–802.

(64) Panda, T. K.; Zulys, A.; Gamer, M. T.; Roesky, P. W. *J. Organomet. Chem.* **2005**, *690*, 5078–5089.

(65) Datta, S.; Gamer, M. T.; Roesky, P. W. *Organometallics* **2008**, *27*, 1207–1213.

(66) Jenter, J.; Gamer, M. T.; Roesky, P. W. *Organometallics* **2010**, *29*, 4410–4413.

(67) Heitmann, D.; Jones, C.; Mills, D. P.; Stasch, A. *Dalton Trans.* **2010**, *39*, 1877–1882.

(68) Wiecko, M.; Roesky, P. W. *Organometallics* **2009**, *28*, 1266–1269.

(69) Evans, W. J.; Walensky, J. R.; Furche, F.; DiPasquale, A. G.; Rheingold, A. L. *Organometallics* **2009**, *28*, 6073–6078.

(70) Jones, C.; Stasch, A.; Woodul, W. D. *Chem. Commun.* **2009**, 113–115.

(71) Wiecko, M.; Roesky, P. W. *Organometallics* **2007**, *26*, 4846–4848.

(72) Gamer, M. T.; Roesky, P. W.; Konchenko, S. N.; Nava, P.; Ahlrichs, R. *Angew. Chem. Int. Ed.* **2006**, *45*, 4447–4451.

(73) Evans, W. J.; Clark, R. D.; Ansari, M. A.; Ziller, J. W. *J. Am. Chem. Soc*. **1998**, *120*, 9555–9563.

(74) Moore, J. A.; Cowley, A. H.; Gordon, J. C. *Organometallics* **2006**, *25*, 5207–5209.

(75) Sheng, E.; Zhou, S.; Wang, S.; Yang, G.; Wu, Y.; Feng, Y.; Mao, L.; Huang, Z. *Eur. J. Inorg. Chem.* **2004**, 2923–2932.

(76) Zhang, K.; Zhang, W.; Wang, S.; Sheng, E.; Yang, G.; Xie, M.; Zhou, S.; Feng, Y.; Mao, L.; Huang, Z. *Dalton Trans.* **2004**, 1029–1037.

(77) Wang, S.; Feng, Y.; Mao, L.; Sheng, E.; Yang, G.; Xie, M.; Wang, S.; Wei, Y.; Huang, Z. *J. Organomet. Chem.* **2006**, *691*, 1265–1274.

(78) Wu, Y.; Wang, S.; Qian, C.; Sheng, E.; Xie, M.; Yang, G.; Feng, Q.; Zhang, L.; Tang, X. *J. Organomet. Chem.* **2005**, *690*, 4139–4149.

(79) Miao, H.; Wang, S.; Zhou, S.; Wei, Y.; Zhou, Z.; Zhu, H.; Wu, S.; Wang, H. *Inorg. Chim. Acta* **2010**, *363*, 1325–1331.

(80) Zhou, S.; Yin, C.; Wang, H.; Zhu, X.; Yang, G.; Wang, S. *Inorg. Chem. Commun.* **2011**, *14*, 1196–1200.

(81) Wang, S.; Zhou, S.; Yang, G.; Luo, W.; Hu, N.; Zhou, Z.; Song, H.-B. *J. Organomet. Chem.* **2007**, *692*, 2099–2106.

(82) Wei, Y.; Yu, Z.; Wang, S.; Zhou, S.; Yang, G.; Zhang, L.; Chen, G.; Qian, H.; Fan, J. *J. Organomet. Chem.* **2008**, *693*, 2263–2270.

(83) Zhu, X.; Fan, J.; Wu, Y.; Wang, S.; Zhang, L.; Yang, G.; Wei, Y.; Yin, C.; Zhu, H.; Wu, S.; Zhang, H. *Organometallics* **2009**, *28*, 3882–3888.

(84) Kropp, J. L.; Windsor, M. W. *J. Chem. Phys*. **1963**, *39*, 2769–2770.

(85) Starynowicz, P. *Polyhedron* **2003**, *22*, 2761–2765.

(86) Christoffers, J.; Starynowicz, P. *Polyhedron* **2008**, *27*, 2688–2692.

(87) Starynowicz, P.; Bukietyńska, K. *Eur. J. Inorg. Chem*. **2002**, 1835–1838.

(88) Starynowicz, P. *Polyhedron* **2003**, *22*, 337–345.

(89) Caravan, P.; Merbach, A. E. *Chem. Commun.* **1997**, 2147–2148.

(90) Caravan, P.; Tóth, É.; Rockenbauer, A.; Merbach, A. E. *J. Am. Chem. Soc.* **1999**, *121*, 10403–10409.

(91) Seibig, S.; Tóth, É.; Merbach, A. E. *J. Am. Chem. Soc.* **2000**, *122*, 5822–5830.

(92) Burai, L.; Tóth, É.; Moreau, G.; Sour, A.; Scopelliti, R.; Merbach, A. E. *Chem. Eur. J.* **2003**, *9*, 1394–1404.

(93) Tóth, É.; Burai, L.; Merbach, A. E. *Coord. Chem. Rev.* **2001**, *216–217*, 363–382.

(94) Burai, L.; Scopelliti, R.; Tóth, É. *Chem. Commun.* **2002**, 2366–2367.

Chapter Three

Eu^{2+}-Containing Cryptates as Contrast Agents for Ultra-High Field Strength MRI

Portions of this chapter were reprinted or adapted with permission from:

(1) Garcia, J.; Neelavalli, J.; Haacke, E. Mark; Allen, M. J. Eu^{II}-containing cryptates as contrast agents for ultra-high field strength magnetic resonance imaging. *Chem. Commun.* **2011,** *47,* 12858–12860. Reproduced by permission of The Royal Society of Chemistry.

Link: http://pubs.rsc.org/en/Content/ArticleLanding/2011/CC/C1CC15219J

(2) Garcia, J.; Kuda-Wedagedara, A. N. W.; Allen, M. J. Physical Properties of Eu^{2+}-Containing Cryptates as Contrast Agents for Ultrahigh-Field Magnetic Resonance Imaging *Eur. J. Inorg. Chem.* **2012,** *2012,* 2135–2140.

DOI: 10.1002/ejic.201101166

Link: http://onlinelibrary.wiley.com/doi/10.1002/ejic.201101166/pdf

Copyright © 2012 WILEY-VCH Verlag GmbH & Co. KGaA, Weinheim

3.1 Introduction

Contrast-agent-enhanced magnetic resonance imaging (MRI) is a widely used, noninvasive imaging technique for clinical and preclinical research as well as diagnostic medicine. Most clinical imaging is performed at high field strengths (1.5 or 3 T); however, a shift to ultra-high field strength MRI (≥7 T) is desirable because of the increased signal-to-noise ratio, spatial resolution, and shorter acquisition times enabled at these fields, which offer the potential to lead to early diagnoses of diseases and more accurate imaging in vivo.[1–4] Consequently, preclinical research relies heavily on ultra-high field strengths. A major limitation is that common T_1-reducing (positive) contrast agents at lower field strengths, such as Gd^{III}-containing complexes, become inefficient at ultra-high field strengths.[2,5] Multiple parameters—including the water-exchange rate, the number of

inner-sphere water molecules, the rotational correlation time, and the relaxation times of the electron spins of Gd^{III}—are in a complex interplay that is crucial to increasing relaxivity, r_1, which is a measure of contrast-enhancing ability of a contrast agent.[2–4] An alternative to Gd^{III} is Eu^{II}, which is isoelectronic with Gd^{III} but has a faster water-exchange rate due to its lower charge density. However, until recently, research on Eu^{II} chemistry in aqueous solution was limited because of its tendency to oxidize to Eu^{III}.[6–8] Modified [2.2.2]cryptands were used to increase the oxidative stability of Eu^{II},[6] and here, the molecular properties and imaging profiles of a series of Eu^{II}-containing [2.2.2]cryptates (**3.1**–**3.3** in **Figure 3.1**) that are, to the best of my knowledge, among a few reported contrast agents, and the first lanthanide-based contrast agents, that are more effective at ultra-high field strengths than at lower fields were reported.[9]

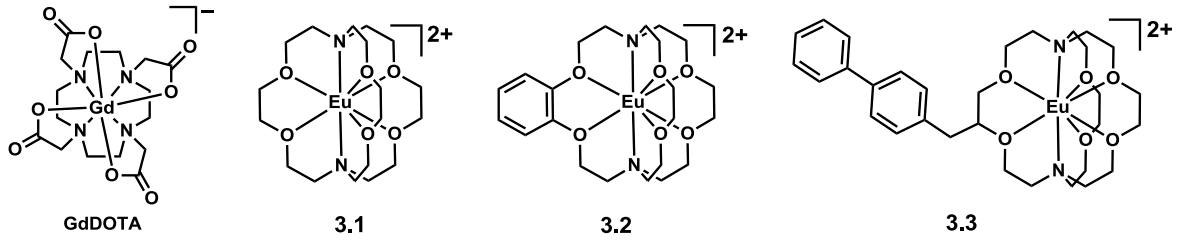

Figure 3.1 Structures of GdDOTA (DOTA = 1,4,7,10-tetraazacyclododecane-*N*,*N*',*N*'',*N*'''-tetraacetate) and Eu^{II}-containing cryptates **3.1**–**3.3**. Coordinated water molecules have been omitted for clarity.

I hypothesized that Eu^{II}-containing [2.2.2]cryptates in aqueous solution could be used as the basis for efficient positive contrast agents for ultra-high field strength MRI because Eu^{II} and Gd^{III} are isoelectronic but differ in other molecular parameters that influence relaxivity. This hypothesis is supported by studies of Eu^{II}-containing complexes: for example, Eu^{II}-containing [2.2.2]cryptate, **3.1**, has been reported to have a fast water-

exchange rate.[8] The water-exchange rate of **3.1** is 3×10^8 s^{-1}, which is faster than most Gd^{III}-based complexes and is very close to the optimal value (~10^8 s^{-1} at 7 T) for developing efficient MRI contrast agents at ultra-high fields.[2,8] Attempts to increase the water-exchange rate of Gd^{III}-containing complexes have been made by altering the coordination number of ligands for Gd^{III} or by increasing steric bulk at the site where inner-sphere water binds.[10] However, because of the complicated interplay between water-exchange rate and other parameters that affect relaxivity, there is a need to simultaneously optimize all factors to increase the efficacy of contrast agents. In addition to its optimal water-exchange rate, **3.1** has two inner-sphere water molecules in a ten-coordinate complex, which should enable higher relaxivity than an equivalent complex with only one inner-sphere water molecule according to Solomon–Bloembergen–Morgan (SBM) theory. These favorable molecular properties prompted me to hypothesize that Eu^{II}-containing cryptates would be candidates for contrast agents at ultra-high field MRI.

To test my hypothesis, I investigated the imaging (longitudinal relaxivity, r_1, at 3 and 7 T) and physical (water-exchange rate, electron-spin relaxation rate, and number of inner-sphere water molecules) properties of a series of Eu^{II}-containing [2.2.2]cryptates (**Figure 3.1**). Cryptands of **3.1** and **3.2** are commercially available, and I synthesized cryptate **3.3** (**Scheme 3.1**).

Scheme 3.1 Synthesis of biphenyl-based Eu^{2+}-containing cryptate.

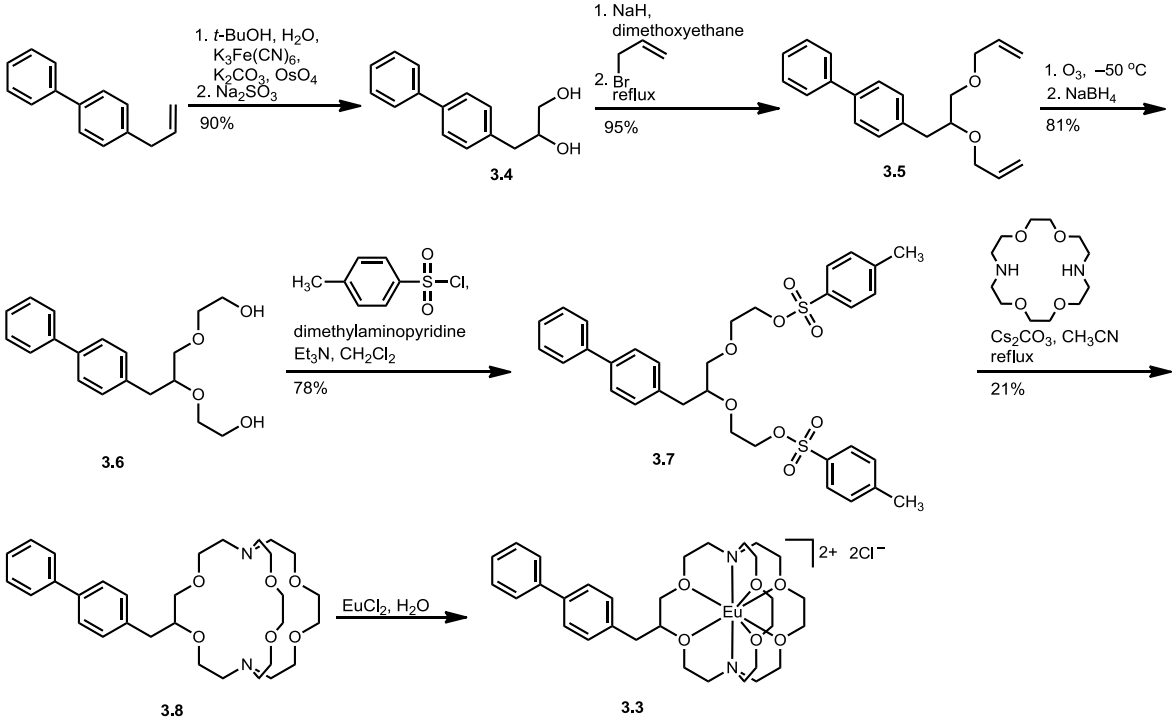

3.2 Imaging Properties of Eu^{2+}-Containing Cryptates

3.2.1 Influence of Magnetic Field on Relaxivity

Relaxivity was determined using multiple flip angles in gradient echo imaging experiments performed between 19 and 20 °C at 3 and 7 T (**Table 3.1**) and inversion recovery experiments at either 20 or 37 °C at 1.4 T.[11] At all of these field strengths, Eu^{II}-containing cryptates **3.2** and **3.3** displayed higher r_1 than clinically approved GdDOTA (up to 46, 71, and 92 higher at 1.4, 3, and 7 T, respectively). Furthermore, cryptate **3.1** displayed a higher relaxivity than GdDOTA at 7 T. I found that the r_1 values of GdDOTA were not different at 3 and 7 T (Student *t* test). This result was expected based on what is known about fast rotating Gd^{III}-containing complexes.[3] However, Eu^{II}-containing complexes **3.1–3.3** showed an increase in r_1 values at 7 relative to 3 T.[12]

Additionally, the r_1 values of cryptates **3.1–3.3** increased as a function of molecular weight at all field strengths. These cryptates are two of a few examples of paramagnetic materials that demonstrate an increase in relaxivity at ultrahigh field strengths relative to lower field strengths.[13]

Table 3.1 r_1 values of GdDOTA and Eu^{II}-containing cryptates

	r_1 at 1.4 T ($mM^{-1}s^{-1}$) T = 37 °C	r_1 at 3 T ($mM^{-1}s^{-1}$) T = 19.8 °C	r_1 at 7 T ($mM^{-1}s^{-1}$) T = 19 °C
GdDOTA	3.00 ± 0.06	3.69 ± 0.06	3.73 ± 0.01
3.1	2.09 ± 0.02	3.94 ± 0.12	5.01 ± 0.03
3.2	3.67 ± 0.09	4.84 ± 0.08	6.47 ± 0.17
3.3	4.39 ± 0.10	6.31 ± 0.07	7.17 ± 0.04

All complexes were in phosphate buffered saline (PBS, pH = 7.4). Results are reported as mean ± standard error.

To establish a more complete understanding of the behavior of the efficacy of these cryptates as a function of field strength, we measured the relaxivity of **3.1** and **3.2** at field strengths of 1.4, 3, 7, 9.4, and 11.7 T. These measurements allowed us to compare the efficiency of Eu^{2+}-containing complexes at clinically relevant field strengths (1.4 and 3 T) with that at higher field strengths, which are commonly used in preclinical research (> 3 T). Because relaxivity is dependent on temperature,[12b] we compared field strengths at the same temperature.

On comparing the efficacy of Eu^{2+}-containing cryptates at field strengths of 3, 7, 9.4, and 11.7 T (20 °C, pH = 7.4), the relaxivity of **3.2** is higher than that of **3.1** at all field strengths (**Figure 3.2**). This difference in relaxivity is likely due to the difference in

rotational correlation rate, which is the rate at which these molecules tumble in solution. This rate is proportional to the molecular weight for structurally similar compounds.[14] The relaxivity of **3.1** increases from 3 to 7 T followed by a decrease above 9.4 T and that of Eu-**3.2** shows an increase in relaxivity from 3 to 7 T followed by a decrease above 7 T. This "bump" could be similar to the bump with a maximum value between 7 and 9.4 T observed at lower field strengths in the NMR dispersion plots of slowly rotating Gd^{3+}-based contrast agents.[2] An attempt to explain this increase in relaxivity at higher fields was made using a simulation of the Solomon–Bloembergen–Morgan (SBM) equations. Although the relaxivity values from this simulation matched the trend observed for GdDOTA, they did not fit the experimental data for Eu^{2+}-containing complexes. The results of this simulation indicate that SBM theory alone cannot explain our observations.

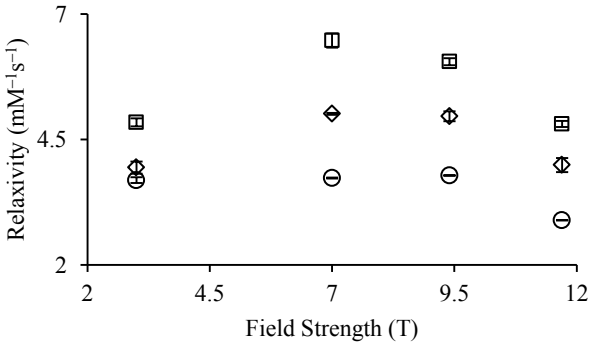

Figure 3.2 Proton longitudinal relaxivity (T = 20 °C, pH = 7.4) of GdDOTA (○) and Eu^{2+}-containing cryptates **3.1** (◊) and **3.2** (□) as a function of magnetic field strength. Error bars represent standard error of the mean.

At a higher temperature (T = 37 °C, pH = 7.4, **Figure 3.3**), **3.1** displays an increase in relaxivity from 1.4 to 7 T and a decrease above 9.4 T. However, at 37 °C, the relaxivity of **3.2** at 1.4 and 9.4 T is the same. At all field strengths and temperatures measured (except 1.4 T), **3.1**and **3.2** have higher relaxivities than GdDOTA. To further explain the

influence of temperature on the relaxivity of **3.1** and **3.2**, I measured relaxivity as a function of temperature at constant field strength.

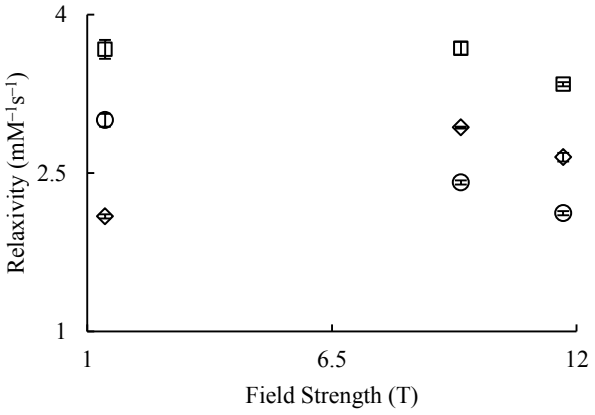

Figure 3.3 Proton longitudinal relaxivity (T = 37 °C, pH = 7.4) of GdDOTA (○) and Eu^{2+}-containing cryptates **3.1** (◊) and **3.2** (□) as a function of magnetic field strength. Error bars represent standard error of the mean.

3.2.2 Influence of Temperature on Relaxivity

Temperature can have a dramatic influence on the relaxivity of contrast agents. To explore the temperature dependence of the relaxivity of **3.1** and **3.2**, I measured the relaxivity at 15, 20, 30, 37, and 50 °C at 9.4 and 11.7 T at pH = 7.4 (**Figures 3.4** and **3.5**).

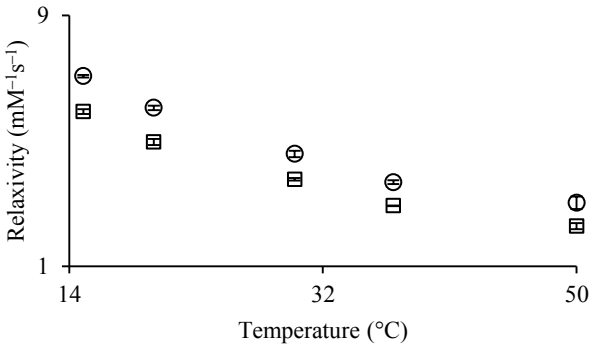

Figure 3.4 Proton longitudinal relaxivity (9.4 T and pH = 7.4) of Eu^{2+}-containing cryptates **3.1** (□) and **3.2** (○) as a function of temperature. Error bars represent standard error of the mean.

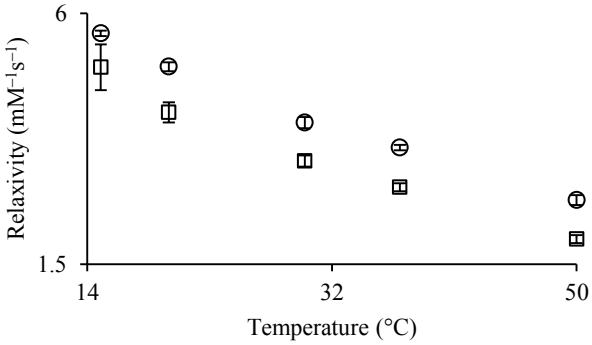

Figure 3.5 Proton longitudinal relaxivity (11.7 T, pH = 7.4) of Eu^{2+}-containing cryptates **3.1** (□) and **3.2** (○) as a function of temperature. Error bars represent standard error of the mean.

Another temperature-dependent parameter that contributes to relaxivity is water-exchange rate, which is important when it approaches the magnitude of the relaxation rate of the bound water. When this happens, the plot of relaxivity versus temperature should show a plateau or a positive slope in the low temperature region. This case was not observed for either **3.1** or **3.2**, implying that the water-exchange rates of **3.1** and **3.2** are fast enough to not limit relaxivity even at low temperatures. This conclusion is supported

by the results of variable temperature ^{17}O NMR studies, which revealed that cryptates **3.1** and **3.2** have water-exchange rates of 3.3×10^8 s^{-1} and 0.85×10^8 s^{-1}, respectively. In general, the variation in the relaxivities of these cryptates with temperature is likely due to the changes in the rotational correlation rate of the complexes as temperature changes, similar to what is observed with Gd^{3+}-containing complexes.

3.2.3 Influence of pH on Relaxivity

The effect of pH on the relaxivity of Eu^{2+}-containing cryptates as contrast agents was examined as a gauge of their performance in vivo and to explore the potential of these complexes to behave as pH responsive agents (**Figure 3.6**).

At 7 T and 19 °C, the relaxivity of **3.1** did not change significantly at any of the pH values measured from 3 to 10 ($p = 0.01$). The relaxivity of **3.2** exhibited the same behavior. These observations are expected for complexes that do not have functional groups that are sensitive to pH changes. Also, at 1.4 T and 37 °C, the relaxivity of **3.1** is independent of pH value ($p = 0.01$). However, the relaxivity of **3.2** remained constant below pH 7.4, but between pH values of 7.4 and 8, the relaxivity of **3.2** decreased by 22% (from 3.67 ± 0.09 to 2.86 ± 0.02 $mM^{-1}s^{-1}$) and remained constant above pH 8. In summary, the experiments at different pH values for **3.1** and **3.2** under two different sets of conditions (7 T at 19 °C and 1.4 T at 37 °C) indicate that the relaxivity of these cryptates is not influenced by pH over a physiologically relevant range.

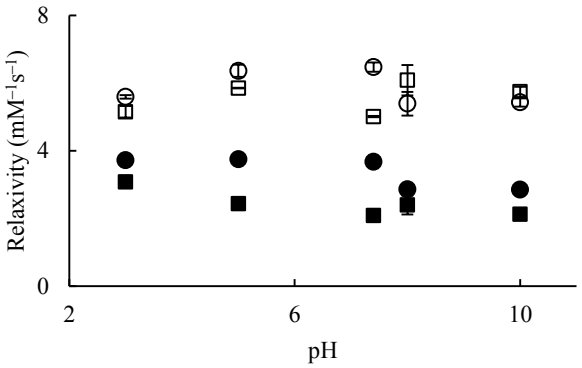

Figure 3.6 Longitudinal relaxivity at 1.4 T at 37 °C (**3.1** (■) and **3.2** (●)) and 7 T at 19 °C (**3.1** (□) and **3.2** (○)) as a function of pH. Error bars represent standard error of the mean.

3.2.4 Phantom Imaging Experiments

To demonstrate the consequence of having higher relaxivity, I obtained phantom images (images of solutions) of GdDOTA and Eu^{II}-containing complexes **3.1**–**3.3** using T_1-weighted imaging at 7 T (**Figure 3.7**). The MR images of Eu^{II} cryptates **3.1**–**3.3** showed higher signal intensity relative to PBS. This observation is indicative that Eu^{II} cryptates are effective at influencing the relaxation of water protons in solution. The signal intensities of the Eu^{II} complexes are different from each other (Student *t* test) with **3.3** giving rise to the highest signal intensity. The $1/T_1$ values were between 29 and 89% higher for cryptates **3.1**–**3.3** relative to GdDOTA. An increase in $1/T_1$ corresponds to higher signal intensity and, therefore, is advantageous for imaging. These imaging experiments demonstrate that cryptates **3.1**–**3.3** are effective contrast agents at ultra-high field strengths.

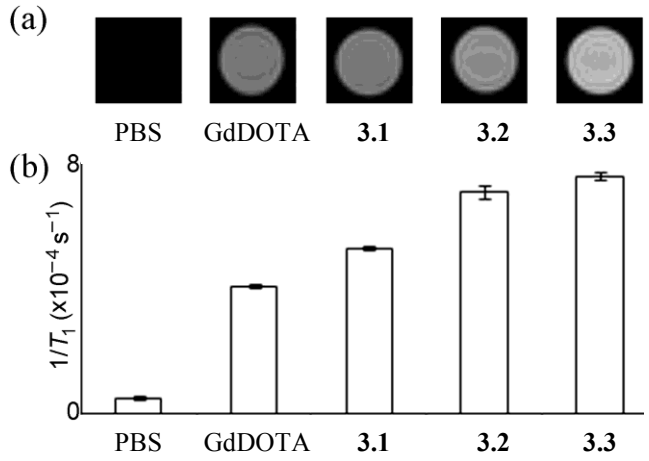

Figure 3.7 (a) T_1-weighted MR images of solutions of PBS, GdDOTA (1.0 mM in PBS), and **3.1**–**3.3** (1.0 mM in PBS) at 7 T. The diameter of the tubes that were used for imaging was 6 mm. Imaging parameters were T_R = 21 ms; T_E = 3.26 ms; and resolution = 0.27 × 0.27 × 2 mm^3. (b) Comparison of $1/T_1$ values of the samples from (a) at 7 T. Error bars represent standard error of the mean.

3.3 Physical Properties of Eu^{2+}-Containing Cryptates

3.3.1 Variable-Temperature ^{17}O NMR Spectroscopy

To understand the observations of r_1 values, I used variable temperature ^{17}O NMR spectroscopy to determine the molecular parameters expected to influence relaxivity (**Table 3.2**): the residence lifetime of bound water molecules, τ_m^{298}, where water-exchange rate, k_{ex}^{298}, is equal to $1/\tau_m^{298}$; the longitudinal electronic relaxation time, T_{1e}^{298}; and the number of inner-sphere water molecules, q. To attain the highest relaxivity at ultra-high field strengths, water-exchange rate must be ~10^8 s^{-1}.[2] The water-exchange rates of the Eu^{II} complexes are 6–94 times faster than GdDOTA and, consequently, are closer to being optimal at ultra-high field strengths as described by SBM theory. However, our observed water-exchange rate does not limit the relaxation enhancement for fast rotating complexes even at ultra-high fields. As seen from the data in **Tables 3.1** and **3.2**, r_1 values

were larger for cryptates **3.2** and **3.3** relative to **3.1** despite **3.2** and **3.3** having slower water-exchange rates than **3.1**. The differences in water-exchange rates among **3.1**, **3.2**, and **3.3** could be attributed to the flexibility of the cryptates because having a flexible structure may lead to changes in steric bulk at the water-binding site thereby affecting water-exchange rate. The relaxivity differences among cyptates **3.1**–**3.3** are likely due to differences in molecular weight because increases in molecular weight correspond to decreases in rotational correlation rates for structurally similar monomeric complexes.[13]

Table 3.2 Relaxivity parameters (based on ^{17}O NMR and EPR data) and molecular weights of GdDOTA and cryptates **3.1**–**3.3**.

	GdDOTA	**3.1**	**3.2**	**3.3**
τ_m^{298} (ns)	287 ± 10	3.0 ± 0.4	11.7 ± 0.3	48 ± 4
k_{ex}^{298} (10^8 s^{-1})	0.035	3.3	0.85	0.21
q	1	2	2	2
T_{1e} (ns)	29	120	41	1100
g	1.9847	1.9774	1.9790	1.9786
$1/T_{2e}$ (10^9 s^{-1})	0.91	2.7	3.4	4.0
τ_R (ns)[a]	–	19.6	2.72	2.27
MW (Da)	591	564	657	731

[a] See Section 3.7 of this chapter for the method of estimating τ_R.

SBM theory also describes the dependence of relaxivity on the electron spin relaxation, which we investigated with ^{17}O NMR studies. Data acquired from variable temperature ^{17}O NMR experiments were refitted using 63 unique values of T_{1e}^{298} in the range of 10^{-8}–10^{-3} s, and the T_{1e}^{298} values that were associated with the best correlation coefficient are

reported in **Table 3.2**. The electron-spin relaxation rates of the Eu^{II} ion in cryptates **3.1**–**3.3** were in the range of 10^6–10^7 s^{-1} and were not limiting as evidenced by the change in relaxivity with molecular weight. The differences in the obtained electronic relaxation rates among **3.1**, **3.2**, and **3.3** could be attributed to the symmetry differences among the cryptates. However, the influence of structural factors to correlation times that describe electronic spin relaxation is not yet fully understood.[15] Another key parameter in increasing relaxivity at ultra-high fields is the number of inner-sphere water molecules. Eu^{II} cryptates have two inner-sphere water molecules, which corresponds to higher efficiency of a contrast agent relative to complexes with fewer inner-sphere water molecules. In general, the superiority of the Eu^{II} cryptates over GdDOTA in enhancing relaxivity at ultra-high field strengths is likely due to a combination of factors. I have determined k_{ex}^{298}, q, and T_{1e}^{298} for cryptates **3.1**–**3.3** in an attempt to explain the molecular basis for our observations; however, the results cannot be satisfactorily interpreted using SBM theory.

3.3.2 Electron Paramagnetic Resonance (EPR) Spectroscopy

In addition to relaxivity and ^{17}O NMR experiments, I also performed EPR experiments to investigate the electronic properties of these cryptates that include the g factor and the transverse electronic spin relaxation rate, $1/T_{2e}$, of the metal ion. The g factor values for all the complexes are almost close to 2 (**Table 3.2**). This value is expected for complexes of which the metal ion has an f^7 electronic configuration.

The EPR peak of Eu^{2+} shown in **Figure 3.8** at X-band is likely to be a superposition of 12 lines, which could become visible at higher frequencies (~225 GHz), as a result of coupling of Eu^{2+} isotopes, ^{151}Eu and ^{153}Eu, with similar spin (I = 5/2) and natural abundance (47.82 and 52.18%, respectively).[16] The presence of a shoulder in the EPR

profile could also be attributed to the presence of a mixture of species–a cryptate with one inner-sphere water molecule and a species with two coordinated water molecules. Comparing the X-band EPR profile of the unfunctionalized cryptate **3.1** to that of GdDOTA, the peak-to-peak linewidth in the EPR plot of cryptate **3.1** is wider relative to that of GdDOTA (**Figures 3.8 and 3.9)**. This translates to a faster electron spin relaxation for Eu^{2+} relative to Gd^{3+} as implied in **Eq 3.1**:

Eq 3.1 $$\frac{\mathbf{1}}{\boldsymbol{T_{2e}}} = \frac{\boldsymbol{g\beta\pi\sqrt{3}\Delta H_{pp}}}{\boldsymbol{h}}$$

where β is the Bohr magneton constant, ΔH_{pp} is the peak-to-peak linewidth, and h is the Planck's constant. Using the *g* factor, the transverse electron spin relaxation rate can be calculated, and looking at the $1/T_{2e}$ values on **Table 3.2**, these cryptates have faster electronic spin relaxation rate (2.97–4.40 times faster) than GdDOTA.

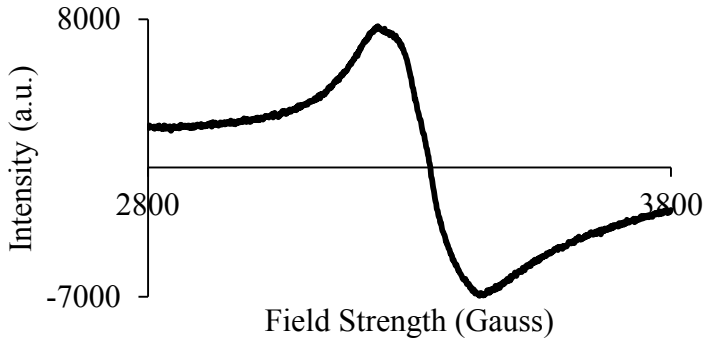

Figure 3.8 X band EPR spectrum of cryptate **3.1** in PBS at 77 K.

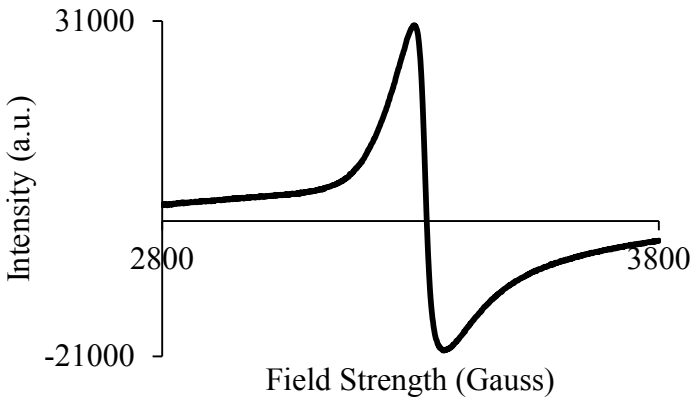

Figure 3.9 X band EPR spectrum of GdDOTA in PBS at 77 K.

3.4 Conclusions

This study demonstrated that Eu^{II}-based complexes **3.1**–**3.3** are effective contrast agents at ultra-high field strengths likely because of the interplay of water-exchange rate, rotational correlation rate, and the presence of two inner-sphere water molecules. To the best of our knowledge, these complexes are among a few reported examples of contrast agents that display increased r_1 values at ultra-high field strengths relative to lower fields.

Relaxometric studies of **3.1** and **3.2** showed that the efficiencies of these cryptates were higher at 7 and 9.4 T at 20 °C. Furthermore, the relaxivities of these complexes decreased as the temperature increased from 15 to 50 °C, likely due to the increase in rotational correlation rate with increasing temperature. In addition, the efficacy of **3.1** and **3.2** did not vary significantly in the pH range of 3–10, which suggests that these complexes are expected to display constant relaxivity in biologically relevant pH ranges. These studies lay the foundation for the use of Eu^{2+}-containing cryptates as contrast agents for MRI.

3.5 Experimental Procedures

3.5.1 Materials

Commercially available chemicals were of reagent-grade purity or better and were used without further purification unless otherwise noted. Water was purified using a PURELAB Ultra Mk2 water purification system (ELGA). Dicholoromethane was dried using a solvent purification system (Vacuum Atmospheres Company) and degassed under vacuum. Triethylamine was distilled from CaH_2 under an atmosphere of Ar.[17] 4-Allylbiphenyl was prepared according to a published procedure.[18] Ozone was generated using an apparatus from Ozone Research and Equipment Corporation. For ozone generation, oxygen was passed through a column of anhydrous calcium sulfate before the ozone apparatus, and the oxygen flow rate and current were held constant at 1.0 L/min and 0.8 A, respectively. *p*-Toluenesulfonyl chloride was recrystallized prior to use.[17]

Flash chromatography was performed using silica gel 60, 230–400 mesh (EMD Chemicals).[19] Analytical thin-layer chromatography (TLC) was carried out on ASTM TLC plates precoated with silica gel 60 F_{254} (250 μm layer thickness). TLC visualization was accomplished using a UV lamp followed by charring with potassium permanganate stain (2 g $KMnO_4$, 20 g K_2CO_3, 5 mL 5% w/v aqueous NaOH, 300 mL H_2O).

The following commercially available buffers were degassed and used in relaxometric experiments: glycine/HCl (pH = 3), acetate (pH = 5), PBS (pH = 7.4), 2-amino-2-(hydroxymethyl)propane-1,3-diol (TRIS) (pH = 8), and glycine/NaOH (pH = 10).

3.5.2 Characterization

^{1}H NMR spectra were obtained using a Varian Unity 400 (400 MHz) spectrometer, and ^{13}C NMR spectra were obtained using a Varian Unity 400 (101 MHz) spectrometer. Chemical shifts are reported relative to residual solvent signals (CD_3OD: ^{1}H: δ 3.30, ^{13}C: δ

49.00; CD_3CN: ^1H: δ 1.94, ^{13}C: δ 118.26 and 1.30). ^1H NMR data are assumed to be first order, and the apparent multiplicity is reported as "s" = singlet, "m" = multiplet, and "brs" = broad singlet. Italicized elements are those that are responsible for the shifts. High-resolution electrospray ionization mass spectra (HRESIMS) were obtained using an electrospray time-of-flight high-resolution Waters Micromass LCT Premier XE mass spectrometer.

Samples for inductively coupled plasma mass spectrometry (ICP–MS) were diluted using aqueous 2% nitric acid. Standard solutions were prepared by serial dilution using Eu, Gd, and Sr standards (High-Purity Standards). ICP–MS measurements were conducted on a PE Sciex Elan 9000 ICP–MS instrument with a cross-flow nebulizer and Scott-type spray chamber.

3.5.3 Imaging and Relaxometric Experiments

Susceptibility weighted imaging (SWI) and Volumetric Interpolated Breath Hold Examination (VIBE) were performed at 3 (Siemens TRIO) and 7 (ClinScan) Tesla (T). The acquisition parameters for SWI were as follows: T_R = 37 ms, T_E = 5.68–31.18 ms, and resolution = 0.5 × 0.5 × 2 mm^3 for 3 T; T_R = 21 ms, T_E = 3.26–15.44 ms, and resolution = 0.27 × 0.27 × 2 mm^3 for 7 T. Multiple flip angles (5, 10, 15, 20, 25, and 30°) were used in the SWI experiments to allow for the determination of longitudinal relaxation time, T_1.[20] On the other hand, the parameters used for VIBE were as follows: T_R = 5 ms, T_E = 1.71 ms, and resolution = 0.27 × 0.27 × 2 mm^3 for 7 T. MR images were processed using SPIN software (SVN Revision 1751). Matlab (7.12.0.635 R2011a) was used to generate effective transverse relaxation time, T_2^*, and corrected T_1 maps. The T_1 values from the corrected T_1 maps were plotted vs the concentration of Gd or Eu in the samples to calculate longitudinal

relaxivities, r_1. The Matlab codes for T_2* and T_1 (with T_2* correction) maps are shown in Appendix A.

Inverse recovery experiments were performed using Bruker minispec mq (1.4 T), a Varian Unity 400 (9.4 T) at 400 MHz, and Varian–500S (11.7 T) spectrometer using GdDOTA, **3.1**, **3.2**, and **3.3** as samples, which were dissolved in degassed phosphate buffered saline (PBS) solutions (pH = 7.4). All the T_1 measurements were made at 37 °C. The relaxivity of the complexes were calculated from the slopes of the linear plots of $1/T_1$ versus concentration.

Longitudinal relaxation times, T_1, were also measured using inverse recovery methods with a Varian Unity 400 (9.4 T) at 400 MHz and 15, 20, 30, 37, and 50 °C, and a Varian 500S instrument (11.7 T) at 500 MHz and 15, 20, 30, 37, and 50 °C.

Variable-temperature ^{17}O NMR measurements of degassed solutions of GdDOTA (20 mM); **3.1** (5.0 mM); **3.2** (0.50 mM); **3.3** (0.42 mM), and their Sr^{II} analogues of **3.1** (5.0 mM), **3.2** (0.50 mM), and **3.3** (0.42 mM) in phosphate buffered saline (PBS, pH = 7.4) as well as acidified water ($HClO_4$, pH 3.4) were obtained on a Varian–500S (11.7 T) spectrometer. ^{17}O-enriched water (10% $H_2{}^{17}O$, Cambridge Isotope Laboratories, Inc.) was added to samples to yield 1% ^{17}O enrichment. Transverse and longitudinal ^{17}O relaxation rates and chemical shifts were measured at 15, 20, 30, 40, 50, 60, and 70 °C. The Sr^{II} analogues of **3.1**, **3.2**, **3.3**, and the acidified water were used as diamagnetic references. $A/\hbar$, q, and ΔE were fixed to -3.8×10^{-6} rad/s, 2, and 2.5×10^{-11} J/mol, respectively, for Eu^{II}-containing cryptates. Data acquired from variable-temperature ^{17}O NMR experiments were fitted using sixty unique values of T_1e^{298} in the range of 10^{-8}–10^{-3} s, and the T_1e^{298} values that were associated with the best correlation coefficients were reported. The least-squares fits of the ^{17}O NMR relaxation data were calculated using Origin software (8.0951

B951) following published procedures.[21] The variable temperature ^{17}O NMR data and fits are presented in **Tables 3.3–3.6** and **Figures 3.8–3.11**.

Table 3.3 ^{17}O NMR data for acidified water and GdDOTA.

Temperature (°C)	**Linewidth (Hz)**	
	Acidified water	**GdDOTA**
70	33	97
60	39	137
50	50	197
40	68	249
30	99	281
20	137	256
15	160	241

⊞ *Notes*

⊞ *Input Data*

⊟ *Parameters*

		Value	Standard Error
1overT2P	T1e298	2.9E-8	0
	taum298	2.8731E-7	1.44761E-8
	deltaH	70278.52868	1737.2312
	deltaE	2.5E-11	0
	q	1	0
	Gd	0.02	0

Iterations Performed = 8
Total Iterations in Session = 8
Fit converged - tolerance criterion satisfied.
Some parameter values were fixed.

⊟ *Statistics*

	1overT2P
Number of Points	7
Degrees of Freedom	5
Reduced Chi-Sqr	355.87249
Residual Sum of Squares	1779.36246
Adj. R-Square	0.98372
Fit Status	Succeeded(100)

Fit Status Code :
100 : Fit converged

⊞ *Summary*

⊞ *ANOVA*

⊟ *Fitted Curves Plot*

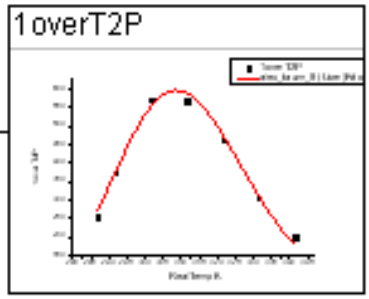

⊞ *Residual vs. Independent Plot*

Figure 3.10 ^{17}O NMR fits for GdDOTA.

Table 3.4 ^{17}O NMR data for Sr^{II} analog of **3.1** and cryptate **3.1**.

Temperature (°C)	**Linewidth (Hz)**	
	Sr analog of 3.1	**3.1**
70	30	31
60	34	37
50	40	46
40	53	57
30	64	73
20	91	111
15	107	142

⊞ *Notes*

⊞ *Input Data*

⊟ *Parameters*

		Value	Standard Error
1overT2P	T1e298	1.2E-7	0
	taum298	3.0316E-9	3.61557E-10
	deltaH	60371.25707	8482.41449
	deltaE	2.5E-11	0
	q	2	0
	Eu	0.005	0

Iterations Performed = 5
Total Iterations in Session = 5
Fit converged - Chi-sqr no longer changed.
Some parameter values were fixed.

⊟ *Statistics*

	1overT2P
Number of Points	7
Degrees of Freedom	5
Reduced Chi-Sqr	51.7001
Residual Sum of Squares	258.50051
Adj. R-Square	0.96503
Fit Status	Succeeded(101)

Fit Status Code :
101 : Fit converged

⊞ *Summary*

⊞ *ANOVA*

⊟ *Fitted Curves Plot*

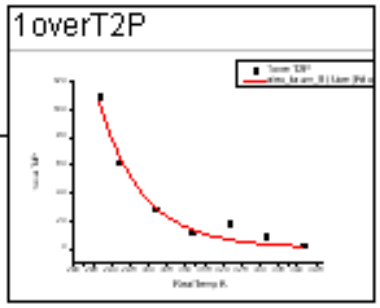

⊞ *Residual vs. Independent Plot*

Figure 3.11 ^{17}O NMR fits for cryptate **3.1**.

Table 3.5 ^{17}O NMR data for Sr^{II} analog of **3.2** and cryptate **3.2**.

Temperature (°C)	**Linewidth (Hz)**	
	Sr analog of 3.2	**3.2**
70	30	37
60	34	45
50	41	57
40	52	75
30	71	105
20	102	154
15	126	183

⊞ *Notes*

⊞ *Input Data*

⊟ *Parameters*

		Value	Standard Error
1overT2P	T1e298	4.1E-8	0
	taum298	1.16602E-8	2.57992E-10
	deltaH	33732.12485	1360.89106
	deltaE	2.5E-11	0
	q	2	0
	Eu	0.005	0

Iterations Performed = 6
Total Iterations in Session = 6
Fit converged - Chi-sqr no longer changed.
Some parameter values were fixed.

⊟ *Statistics*

	1overT2P
Number of Points	7
Degrees of Freedom	5
Reduced Chi-Sqr	19.20064
Residual Sum of Squares	96.0032
Adj. R-Square	0.99503
Fit Status	Succeeded(101)

Fit Status Code :
101 : Fit converged

⊞ *Summary*

⊞ *ANOVA*

⊟ *Fitted Curves Plot*

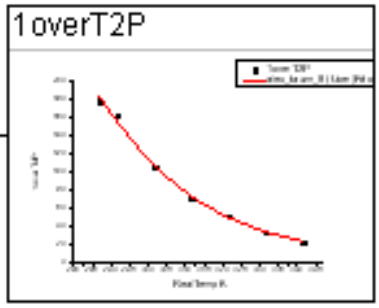

⊞ *Residual vs. Independent Plot*

Figure 3.12 ^{17}O NMR fits for cryptate **3.2**.

Table 3.6 ^{17}O NMR data for Sr^{II} analog of **3.3** and cryptate **3.3**.

Temperature (°C)	**Linewidth (Hz)**	
	Sr analog of 3.3	**3.3**
70	29	30
60	33	35
50	39	43
40	48	55
30	63	75
20	90	108
15	112	134

⊞ *Notes*

⊞ *Input Data*

⊟ *Parameters*

		Value	Standard Error
1overT2P	T1e298	1.1E-6	0
	taum298	4.78533E-8	3.77746E-9
	deltaH	48872.87829	5457.16633
	deltaE	2.5E-11	0
	q	2	0
	Eu	4.2E-4	0

Iterations Performed = 11
Total Iterations in Session = 11
Fit converged - tolerance criterion satisfied.
Some parameter values were fixed.

⊟ *Statistics*

	1overT2P
Number of Points	7
Degrees of Freedom	5
Reduced Chi-Sqr	9.39458
Residual Sum of Squares	46.97288
Adj. R-Square	0.98571
Fit Status	Succeeded(100)

Fit Status Code :
100 : Fit converged

⊞ *Summary*

⊞ *ANOVA*

⊟ *Fitted Curves Plot*

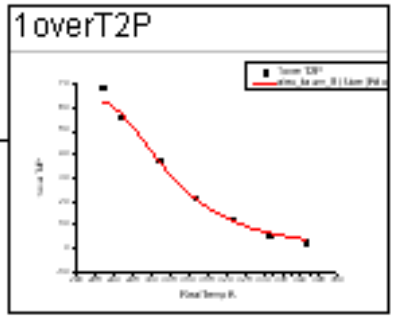

⊞ *Residual vs. Independent Plot*

Figure 3.13 ^{17}O NMR fits for cryptate **3.3**.

The T_{1e} value for each complex corresponds to the T_{1e} that gave the best correlation coefficient. A table is presented below that shows unique T_{1e} values in the range 10^{-8} to 10^{-3} s and their corresponding correlation coefficient for each of the four complexes when they were used in the fitting of the NMR data. The reported T_{1e} values are shown in bold in the table.

Table 3.7 T_{1e} values for GdDOTA and cryptates **3.1**–**3.3** and the corresponding correlation coefficients (R^2) in the ^{17}O NMR fits.

T_{1e} (s)	Correlation coefficient (R^2)			
	GdDOTA	**3.1**	**3.2**	**3.3**
1×10^{-8}	–8.51	0.91	0.67	–1.04
2×10^{-8}	0.69	0.95	0.99	–0.47
3×10^{-8}	**0.98**	0.96	0.99	–0.11
4×10^{-8}	0.70	0.96	**1**	0.12
5×10^{-8}	0.21	0.96	0.99	0.29
6×10^{-8}	–0.33	0.96	0.99	0.42
7×10^{-8}	–0.87	0.96	0.99	0.51
8×10^{-8}	–1.37	0.96	0.99	0.58
9×10^{-8}	–1.83	0.96	0.99	0.64
1×10^{-7}	–2.24	0.96	0.99	0.69
2×10^{-7}	–4.79	**0.97**	0.99	0.88
3×10^{-7}	–4.82	0.97	0.99	0.94
4×10^{-7}	–4.84	0.97	0.99	0.96
5×10^{-7}	–4.85	0.97	0.99	0.97

6×10^{-7}	–4.86	0.97	0.99	0.97
7×10^{-7}	–4.86	0.97	0.99	0.98
8×10^{-7}	–4.86	0.97	0.99	0.98
9×10^{-7}	–4.86	0.97	0.99	0.98
1×10^{-6}	–4.87	0.97	0.99	0.98
2×10^{-6}	–4.87	0.97	0.99	**0.99**
3×10^{-6}	–4.87	0.97	0.99	0.99
4×10^{-6}	–4.87	0.97	0.99	0.99
5×10^{-6}	–4.87	0.97	0.99	0.99
6×10^{-6}	–4.87	0.97	0.99	0.99
7×10^{-6}	–4.87	0.97	0.99	0.99
8×10^{-6}	–4.87	0.97	0.99	0.99
9×10^{-6}	–4.88	0.97	0.99	0.99
1×10^{-5}	–4.88	0.97	0.99	0.99
2×10^{-5}	–4.88	0.97	0.99	0.99
3×10^{-5}	–4.88	0.97	0.99	0.99
4×10^{-5}	–4.88	0.97	0.99	0.99
5×10^{-5}	–4.88	0.97	0.99	0.99
6×10^{-5}	–4.88	0.97	0.99	0.99
7×10^{-5}	–4.88	0.97	0.99	0.99
8×10^{-5}	–4.88	0.97	0.99	0.99
9×10^{-5}	–4.88	0.97	0.99	0.99
1×10^{-4}	–4.88	0.97	0.99	0.99

2×10^{-4}	–4.88	0.97	0.99	0.99
3×10^{-4}	–4.88	0.97	0.99	0.99
4×10^{-4}	–4.88	0.97	0.99	0.99
5×10^{-4}	–4.88	0.97	0.99	0.99
6×10^{-4}	–4.88	0.97	0.99	0.99
7×10^{-4}	–4.88	0.97	0.99	0.99
8×10^{-4}	–4.88	0.97	0.99	0.99
9×10^{-4}	–4.88	0.97	0.99	0.99
1×10^{-3}	–4.88	0.97	0.99	0.99
2×10^{-3}	–4.88	0.97	0.99	0.99
3×10^{-3}	–4.88	0.97	0.99	0.99
4×10^{-3}	–4.88	0.97	0.99	0.99
5×10^{-3}	–4.88	0.97	0.99	0.99
6×10^{-3}	–4.88	0.97	0.99	0.99
7×10^{-3}	–4.88	0.97	0.99	0.99
8×10^{-3}	–4.88	0.97	0.99	0.99
9×10^{-3}	–4.88	0.97	0.99	0.99

Table 3.8 T_1 data for GdDOTA (1.4 T, Temp = 37 °C).

Concn (mM)	$1/T_1$ (s^{-1})	T_1 (s)
1	3.18	0.31
0.5	1.69	0.59
0.25	0.96	1.05
0.125	0.58	1.71
0.0625	0.40	2.51
0	0.22	4.63

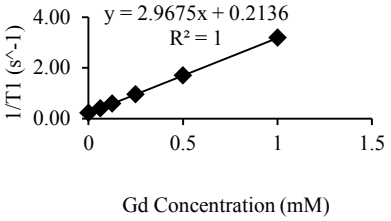

Concn (mM)	$1/T_1$ (s^{-1})	T_1 (s)
1	3.13	0.32
0.5	1.67	0.60
0.25	0.93	1.07
0.125	0.58	1.74
0.0625	0.40	2.52
0	0.22	4.63

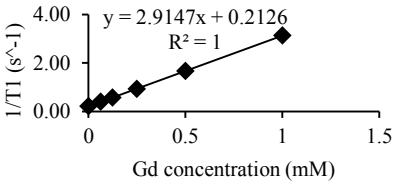

Concn (mM)	$1/T_1$ (s^{-1})	T_1 (s)
1	3.33	0.30
0.5	1.79	0.56
0.25	1.00	1.00
0.125	0.60	1.66
0.0625	0.41	2.45
0	0.22	4.63

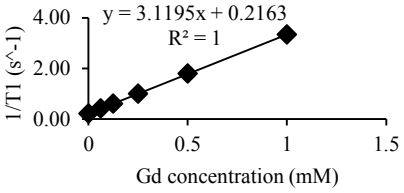

Table 3.9 T_1 data for Cryptate **3.1** (1.4 T, Temp = 37 °C).

Concn (mM)	$1/T_1$ (s^{-1})	T_1 (s)
1	2.30	0.43
0.5	1.24	0.81
0.25	0.73	1.37
0.125	0.44	2.26
0.0625	0.30	3.38
0	0.22	4.63

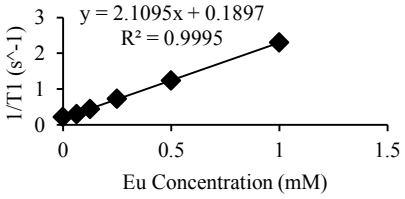

Concn (mM)	$1/T_1$ (s^{-1})	T_1 (s)
1	2.31	0.43
0.5	1.27	0.79
0.25	0.65	1.54
0.125	0.47	2.13
0.0625	0.29	3.39
0	0.22	4.63

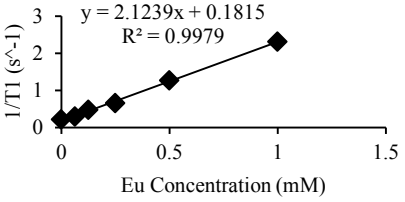

Concn (mM)	$1/T_1$ (s^{-1})	T_1 (s)
1	2.31	0.43
0.5	1.27	0.79
0.25	0.65	1.54
0.125	0.47	2.13
0.0625	0.29	3.39
0	0.22	4.63

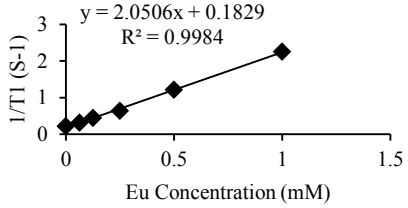

Table 3.10 T_1 data for Cryptate **3.2** (1.4 T, Temp = 37 °C).

Concn (mM)	$1/T_1$ (s^{-1})	T_1 (s)
1	3.97	0.25
0.5	2.13	0.47
0.25	1.14	0.88
0.125	0.69	1.46
0.0625	0.45	2.21
0	0.22	4.63

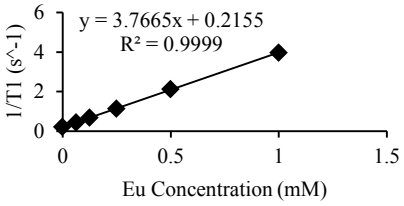

Concn (mM)	$1/T_1$ (s^{-1})	T_1 (s)
1	3.96	0.25
0.5	2.00	0.50
0.25	1.15	0.87
0.125	0.68	1.48
0.0625	0.36	2.76
0	0.22	4.63

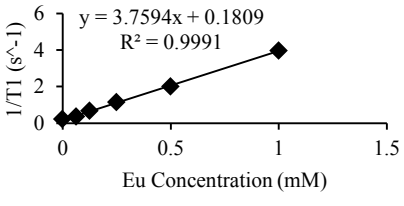

Concn (mM)	$1/T_1$ (s^{-1})	T_1 (s)
1	3.69	0.27
0.5	2.02	0.50
0.25	1.11	0.90
0.125	0.66	1.51
0.0625	0.44	2.30
0	0.22	4.63

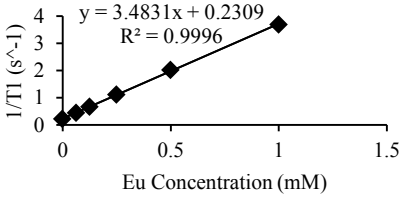

Table 3.11 T_1 data for Cryptate **3.3** (1.4 T, Temp = 37 °C).

Concn (mM)	$1/T_1$ (s^{-1})	T_1 (s)
1	4.57	0.22
0.5	2.36	0.42
0.25	1.25	0.80
0.125	0.72	1.40
0.0625	0.47	2.14
0	0.22	4.63

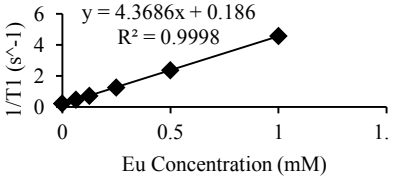

Concn (mM)	$1/T_1$ (s^{-1})	T_1 (s)
1	4.77	0.21
0.5	2.45	0.41
0.25	1.33	0.75
0.125	0.75	1.33
0.0625	0.47	2.12
0	0.22	4.63

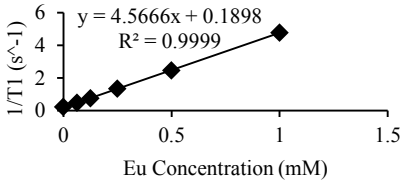

Concn (mM)	$1/T_1$ (s^{-1})	T_1 (s)
1	4.41	0.23
0.5	2.30	0.43
0.25	1.23	0.81
0.125	0.70	1.43
0.0625	0.44	2.27
0	0.22	4.63

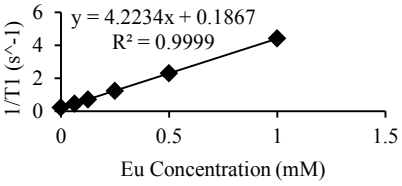

Table 3.12 T_1 data for GdDOTA (3 T, Temp = 19.8 °C).

Concn (mM)	$1/T_1$ (s^{-1})	T_1 (s)
1	3.86	0.26
0.5	1.88	0.53
0.25	0.95	1.06
0.125	0.53	1.90
0.0625	0.45	2.24
0	0.23	4.36

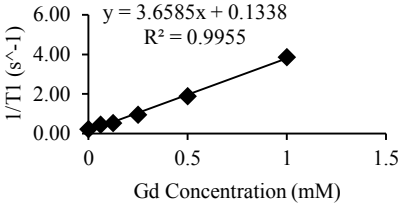

Concn (mM)	$1/T_1$ (s^{-1})	T_1 (s)
1	3.98	0.25
0.5	1.90	0.53
0.25	1.07	0.93
0.125	0.58	1.71
0.0625	0.38	2.65
0	0.21	4.78

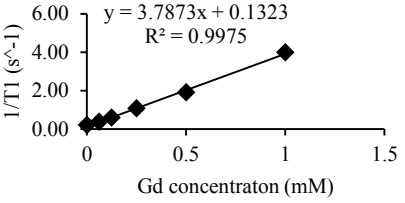

Concn (mM)	$1/T_1$ (s^{-1})	T_1 (s)
1	3.97	0.25
0.5	1.93	0.52
0.25	1.05	0.95
0.125	0.63	1.58
0.0625	0.34	2.91
0	0.22	4.62

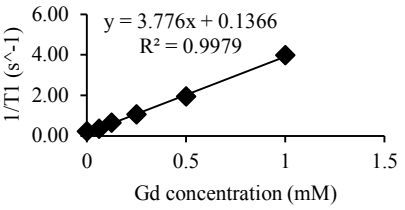

Concn (mM)	$1/T_1$ (s^{-1})	T_1 (s)
1	3.73	0.27
0.5	1.96	0.51
0.25	1.02	0.98
0.125	0.60	1.66
0.0625	0.36	2.78
0	0.24	4.19

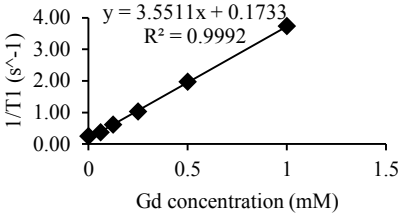

Table 3.13 T_1 data for Cryptate **3.1** (3 T, Temp = 19.8 °C).

Concn (mM)	$1/T_1$ (s^{-1})	T_1 (s)
1	3.88	0.26
0.5	2.11	0.48
0.25	1.10	0.91
0.125	0.64	1.55
0.0625	0.47	2.11
0	0.23	4.36

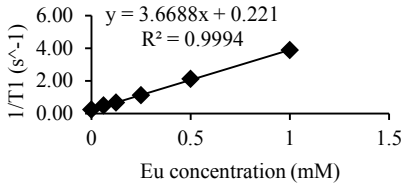

Concn (mM)	$1/T_1$ (s^{-1})	T_1 (s)
1	4.44	0.23
0.5	2.17	0.46
0.25	1.18	0.85
0.125	0.65	1.55
0.0625	0.44	2.27
0	0.21	4.78

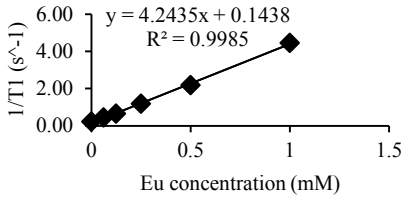

Concn (mM)	$1/T_1$ (s^{-1})	T_1 (s)
1	4.10	0.24
0.5	2.13	0.47
0.25	1.07	0.93
0.125	0.66	1.51
0.0625	0.48	2.09
0	0.22	4.62

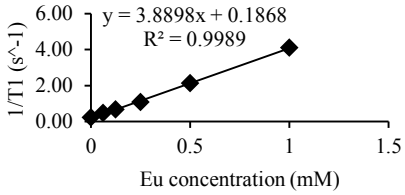

Concn (mM)	$1/T_1$ (s^{-1})	T_1 (s)
1	4.17	0.24
0.5	2.16	0.46
0.25	1.08	0.92
0.125	0.63	1.60
0.0625	0.46	2.18
0	0.24	4.19

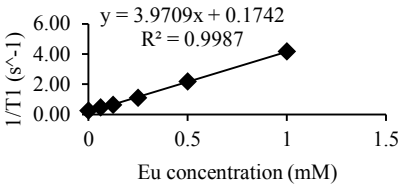

Table 3.14 T_1 data for Cryptate **3.2** (3 T, Temp = 19.8 °C).

Concn (mM)	$1/T_1$ (s^{-1})	T_1 (s)
1	5.29	0.19
0.5	2.34	0.43
0.25	1.26	0.79
0.125	0.74	1.35
0.0625	0.48	2.07
0	0.23	4.36

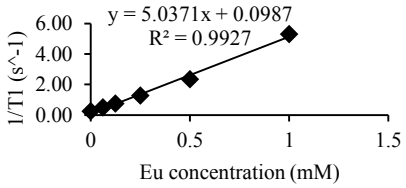

Concn (mM)	$1/T_1$ (s^{-1})	T_1 (s)
1	5.03	0.20
0.5	2.46	0.41
0.25	1.33	0.75
0.125	0.72	1.38
0.0625	0.45	2.22
0	0.21	4.78

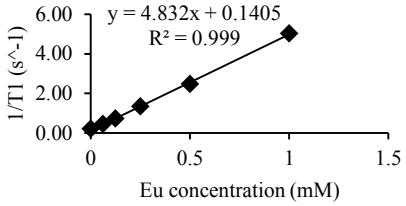

Concn (mM)	$1/T_1$ (s^{-1})	T_1 (s)
1	4.98	0.20
0.5	2.56	0.39
0.25	1.23	0.81
0.125	0.73	1.38
0.0625	0.41	2.42
0	0.22	4.62

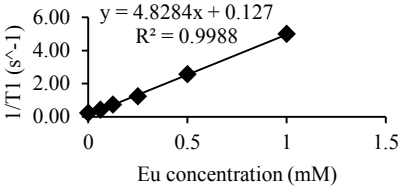

Concn (mM)	$1/T_1$ (s^{-1})	T_1 (s)
1	4.83	0.21
0.5	2.48	0.40
0.25	1.23	0.82
0.125	0.68	1.48
0.0625	0.48	2.08
0	0.24	4.19

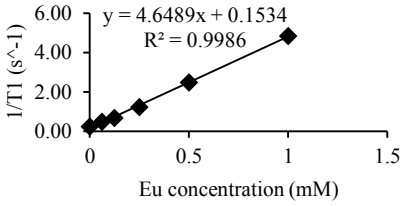

Table 3.15 T_1 data for Cryptate **3.3** (3 T, Temp = 19.8 °C).

Concn (mM)	$1/T_1$ (s^{-1})	T_1 (s)
1	6.58	0.15
0.5	3.05	0.33
0.25	1.69	0.59
0.125	0.86	1.16
0.0625	0.60	1.68
0	0.23	4.36

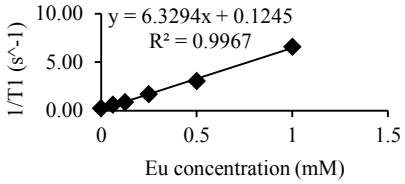

Concn (mM)	$1/T_1$ (s^{-1})	T_1 (s)
1	6.62	0.15
0.5	3.07	0.33
0.25	1.62	0.62
0.125	0.85	1.17
0.0625	0.54	1.85
0	0.21	4.78

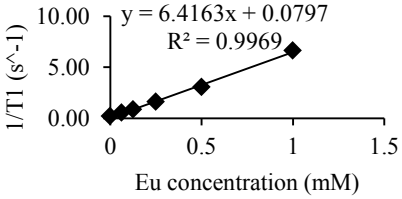

Concn (mM)	$1/T_1$ (s^{-1})	T_1 (s)
1	6.29	0.16
0.5	3.24	0.31
0.25	1.83	0.55
0.125	0.83	1.20
0.0625	0.53	1.90
0	0.22	4.62

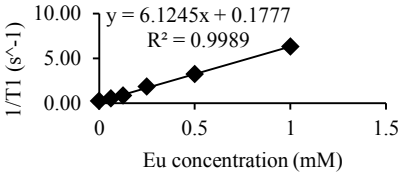

Concn (mM)	$1/T_1$ (s^{-1})	T_1 (s)
1	6.58	0.15
0.5	3.06	0.33
0.25	1.52	0.66
0.125	0.83	1.20
0.0625	0.52	1.93
0	0.24	4.19

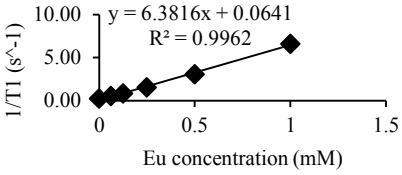

Table 3.16 T_1 data for GdDOTA (7 T, Temp = 19 °C).

Concn (mM)	$1/T_1$ (s^{-1})	T_1 (s)
1	4.07	0.25
0.5	2.16	0.46
0.25	1.25	0.80
0.125	0.70	1.42
0.0625	0.46	2.20
0	0.51	1.96

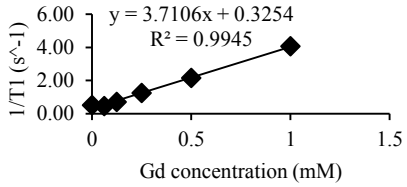

Concn (mM)	$1/T_1$ (s^{-1})	T_1 (s)
1	4.08	0.25
0.5	2.19	0.46
0.25	1.25	0.80
0.125	0.70	1.43
0.0625	0.46	2.18
0	0.56	1.77

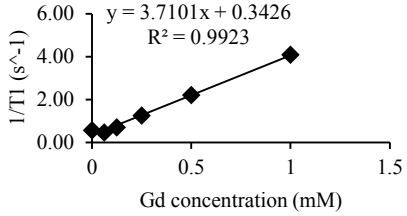

Concn (mM)	$1/T_1$ (s^{-1})	T_1 (s)
1	4.08	0.25
0.5	2.19	0.46
0.25	1.24	0.80
0.125	0.70	1.43
0.0625	0.45	2.20
0	0.50	1.99

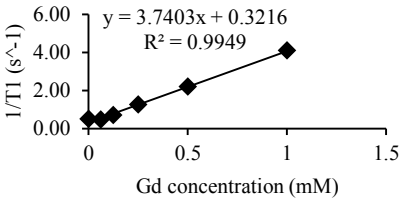

Concn (mM)	$1/T_1$ (s^{-1})	T_1 (s)
1	4.10	0.24
0.5	2.22	0.45
0.25	1.24	0.81
0.125	0.71	1.42
0.0625	0.46	2.17
0	0.54	1.86

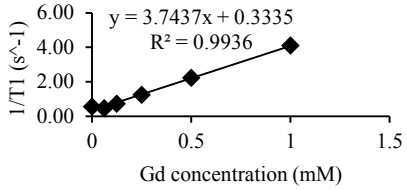

Table 3.17 T_1 data for Cryptate **3.1** (7 T, Temp = 19 °C).

Concn (mM)	$1/T_1$ (s^{-1})	T_1 (s)
1	5.26	0.19
0.5	2.96	0.34
0.25	1.55	0.65
0.125	0.87	1.15
0.0625	0.55	1.83
0	0.51	1.96

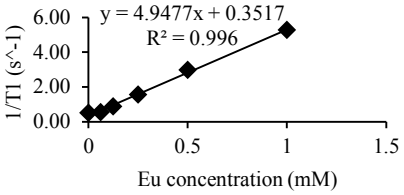

Concn (mM)	$1/T_1$ (s^{-1})	T_1 (s)
1	5.32	0.19
0.5	3.15	0.32
0.25	1.59	0.63
0.125	0.89	1.13
0.0625	0.57	1.77
0	0.56	1.77

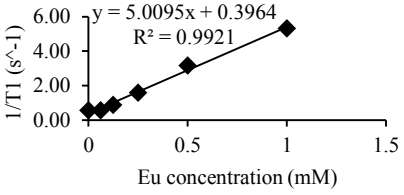

Concn (mM)	$1/T_1$ (s^{-1})	T_1 (s)
1	5.32	0.19
0.5	3.15	0.32
0.25	1.59	0.63
0.125	0.89	1.13
0.0625	0.57	1.77
0	0.56	1.77

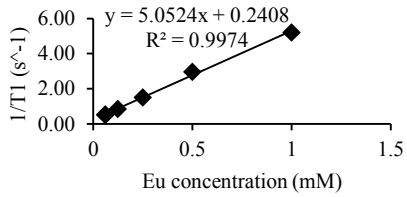

Concn (mM)	$1/T_1$ (s^{-1})	T_1 (s)
1	5.32	0.19
0.5	3.15	0.32
0.25	1.59	0.63
0.125	0.89	1.13
0.0625	0.57	1.77
0	0.56	1.77

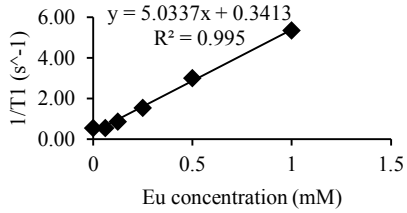

Table 3.18 T_1 data for Cryptate **3.2** (7 T, Temp = 19 °C).

Concn (mM)	$1/T_1$ (s^{-1})	T_1 (s)
1	7.14	0.14
0.5	3.73	0.27
0.25	2.10	0.48
0.125	1.63	0.61
0.0625	1.04	0.96
0	0.51	1.96

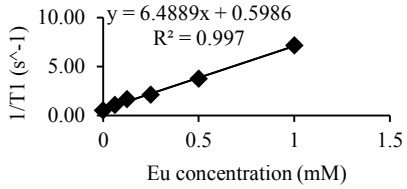

Concn (mM)	$1/T_1$ (s^{-1})	T_1 (s)
1	7.58	0.13
0.5	3.97	0.25
0.25	2.18	0.46
0.125	1.81	0.55
0.0625	1.16	0.86
0	0.56	1.77

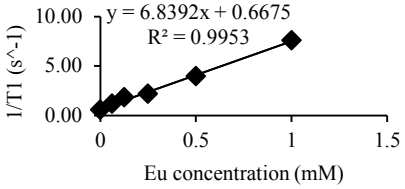

Concn (mM)	$1/T_1$ (s^{-1})	T_1 (s)
1	6.67	0.15
0.5	3.60	0.28
0.25	2.01	0.50
0.125	1.56	0.64
0.0625	1.04	0.96
0	0.50	1.99

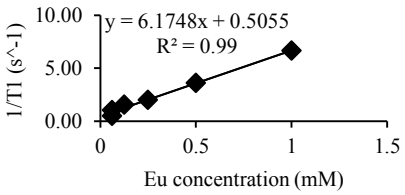

Concn (mM)	$1/T_1$ (s^{-1})	T_1 (s)
1	7.09	0.14
0.5	3.66	0.27
0.25	2.11	0.48
0.125	1.71	0.59
0.0625	1.10	0.91
0	0.54	1.86

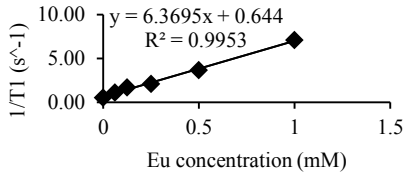

Table 3.19 T_1 data for Cryptate **3.3** (7 T, Temp = 19 °C).

Concn (mM)	$1/T_1$ (s^{-1})	T_1 (s)
1	7.58	0.13
0.5	3.46	0.29
0.25	1.78	0.56
0.125	1.03	0.97
0.0625	0.65	1.54
0	0.51	1.96

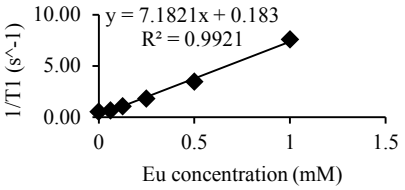

Concn (mM)	$1/T_1$ (s^{-1})	T_1 (s)
1	7.63	0.13
0.5	3.51	0.29
0.25	1.79	0.56
0.125	1.04	0.96
0.0625	0.67	1.49
0	0.56	1.77

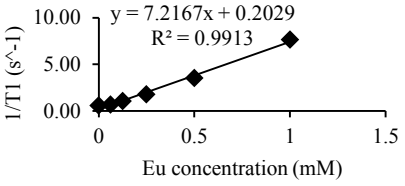

Concn (mM)	$1/T_1$ (s^{-1})	T_1 (s)
1	7.58	0.13
0.5	3.51	0.29
0.25	1.79	0.56
0.125	1.01	0.99
0.0625	0.64	1.55
0	0.50	1.99

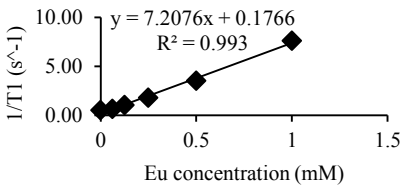

Concn (mM)	$1/T_1$ (s^{-1})	T_1 (s)
1	7.46	0.13
0.5	3.50	0.29
0.25	1.77	0.56
0.125	1.02	0.98
0.0625	0.67	1.50
0	0.54	1.86

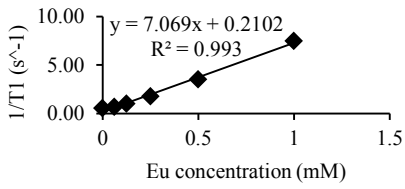

Table 3.20 T_1 data for GdDOTA (11.7 T, Temp = 37 °C).

Concn (mM)	$1/T_1$ (s^{-1})	T_1 (s)
5	13.08	0.08
2.5	6.89	0.15
1.25	3.93	0.25
0	3.01	0.33

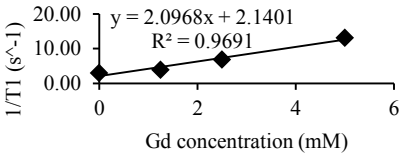

Concn (mM)	$1/T_1$ (s^{-1})	T_1 (s)
5	13.21	0.08
2.5	7.10	0.14
1.25	4.07	0.25
0	3.01	0.33

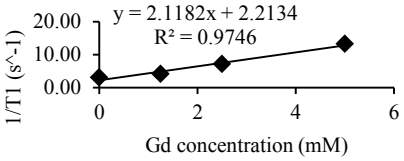

Concn (mM)	$1/T_1$ (s^{-1})	T_1 (s)
5	13.24	0.08
2.5	7.24	0.14
1.25	3.62	0.28
0	3.01	0.33

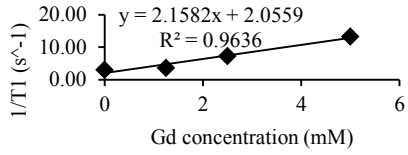

Table 3.21 T_1 data for Cryptate **3.1** (11.7 T, Temp = 37 °C).

Concn (mM)	$1/T_1$ (s^{-1})	T_1 (s)
10	29.08	0.03
5	13.28	0.08
2.5	8.08	0.12
0	3.01	0.33

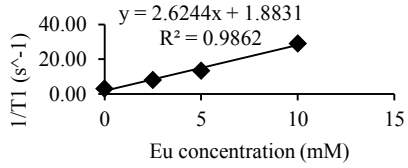

Concn (mM)	$1/T_1$ (s^{-1})	T_1 (s)
10	28.54	0.04
5	14.02	0.07
2.5	7.97	0.13
0	3.01	0.33

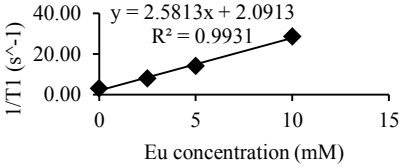

Concn (mM)	$1/T_1$ (s^{-1})	T_1 (s)
7.63	23.53	0.04
3.825	11.21	0.09
1.9125	6.52	0.15
0	3.01	0.33

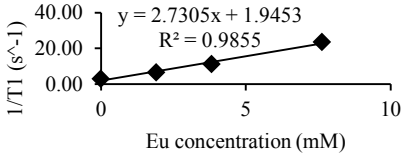

Table 3.22 T_1 data for Cryptate **3.2** (11.7 T, Temp = 37 °C).

Concn (mM)	$1/T_1$ (s^{-1})	T_1 (s)
10	36.19	0.03
5	17.03	0.06
2.5	9.23	0.11
0	3.01	0.33

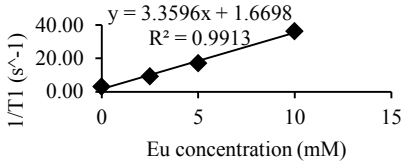

Concn (mM)	$1/T_1$ (s^{-1})	T_1 (s)
10	35.54	0.03
5	18.34	0.05
2.5	9.29	0.11
0	3.01	0.33

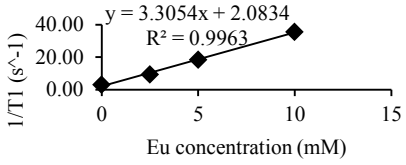

Concn (mM)	$1/T_1$ (s^{-1})	T_1 (s)
7.63	27.93	0.04
3.825	13.88	0.07
1.9125	7.05	0.14
0	3.01	0.33

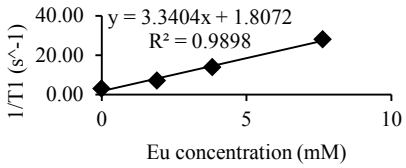

Table 3.23 T_1 data for Cryptate **3.3** (11.7 T, Temp = 37 °C).

Concn (mM)	$1/T_1$ (s^{-1})	T_1 (s)
13	63.86	0.02
6.5	28.23	0.04
3.25	14.52	0.07
0	3.01	0.33

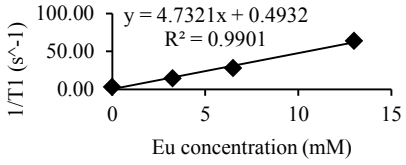

Concn (mM)	$1/T_1$ (s^{-1})	T_1 (s)
13	65.36	0.02
6.5	29.06	0.03
3.25	14.45	0.07
0	3.01	0.33

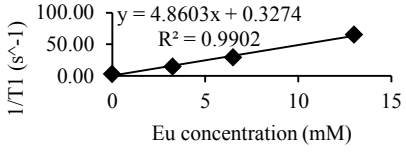

Table 3.24 T_1 data for GdDOTA (11.7 T, Temp = 20 °C).

Concn (mM)	$1/T_1$ (s^{-1})	T_1 (s)
5	16.89	0.06
2.5	8.79	0.11
1.25	4.73	0.21
0	2.84	0.35

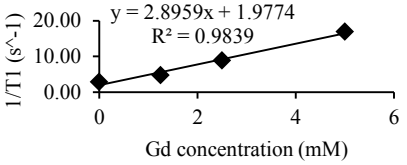

Concn (mM)	$1/T_1$ (s^{-1})	T_1 (s)
5	16.83	0.06
2.5	8.77	0.11
1.25	4.72	0.21
0	3.01	0.35

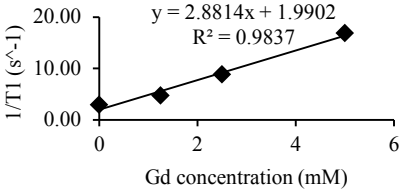

Concn (mM)	$1/T_1$ (s^{-1})	T_1 (s)
5	16.88	0.06
2.5	8.77	0.11
1.25	4.71	0.21
0	3.01	0.35

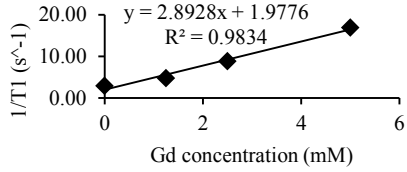

Table 3.25 T_1 data for Cryptate **3.1** (11.7 T, Temp = 20 °C).

Concn (mM)	$1/T_1$ (s^{-1})	T_1 (s)
10	41.19	0.02
5	22.20	0.05
2.5	10.90	0.09
0	2.84	0.35

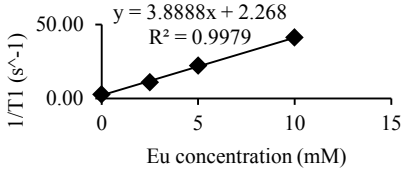

Concn (mM)	$1/T_1$ (s^{-1})	T_1 (s)
10	40.78	0.02
5	18.47	0.05
2.5	10.41	0.10
0	3.01	0.35

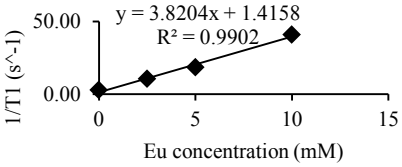

Concn (mM)	$1/T_1$ (s^{-1})	T_1 (s)
7.63	34.89	0.03
3.825	16.88	0.06
1.9125	8.87	0.11
0	3.01	0.35

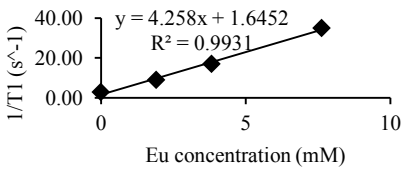

Table 3.26 T_1 data for Cryptate **3.2** (11.7 T, Temp = 20 °C).

Concn (mM)	$1/T_1$ (s^{-1})	T_1 (s)
10	49.70	0.02
5	24.30	0.04
2.5	12.57	0.08
0	2.84	0.35

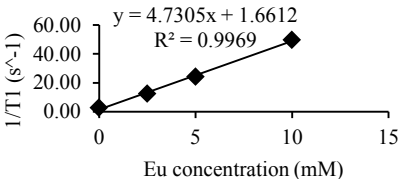

Concn (mM)	$1/T_1$ (s^{-1})	T_1 (s)
10	50.10	0.02
5	26.12	0.04
2.5	12.70	0.08
0	3.01	0.35

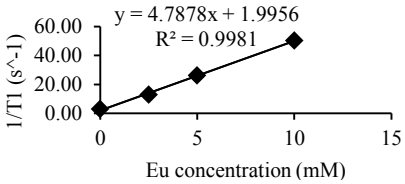

Concn (mM)	$1/T_1$ (s^{-1})	T_1 (s)
7.63	39.98	0.03
3.825	19.83	0.05
1.9125	10.40	0.10
0	3.01	0.35

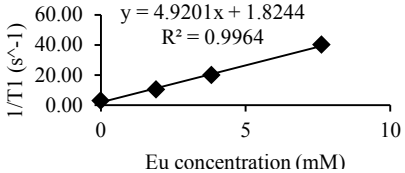

Table 3.27 T_1 data for Cryptate **3.3** (11.7 T, Temp = 20 °C).

Concn (mM)	$1/T_1$ (s^{-1})	T_1 (s)
13	84.75	0.01
6.5	39.64	0.03
3.25	19.77	0.05
0	2.84	0.35

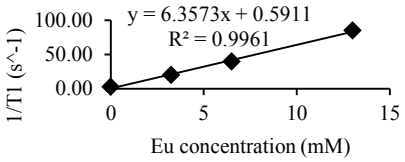

Concn (mM)	$1/T_1$ (s^{-1})	T_1 (s)
13	84.82	0.01
6.5	38.62	0.03
3.25	20.01	0.05
0	3.01	0.35

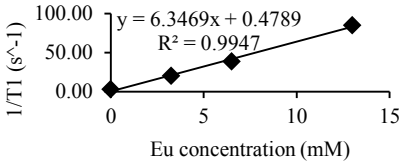

3.5.4 Synthesis

Scheme 3.2 Synthetic route to cryptate **3.3**.

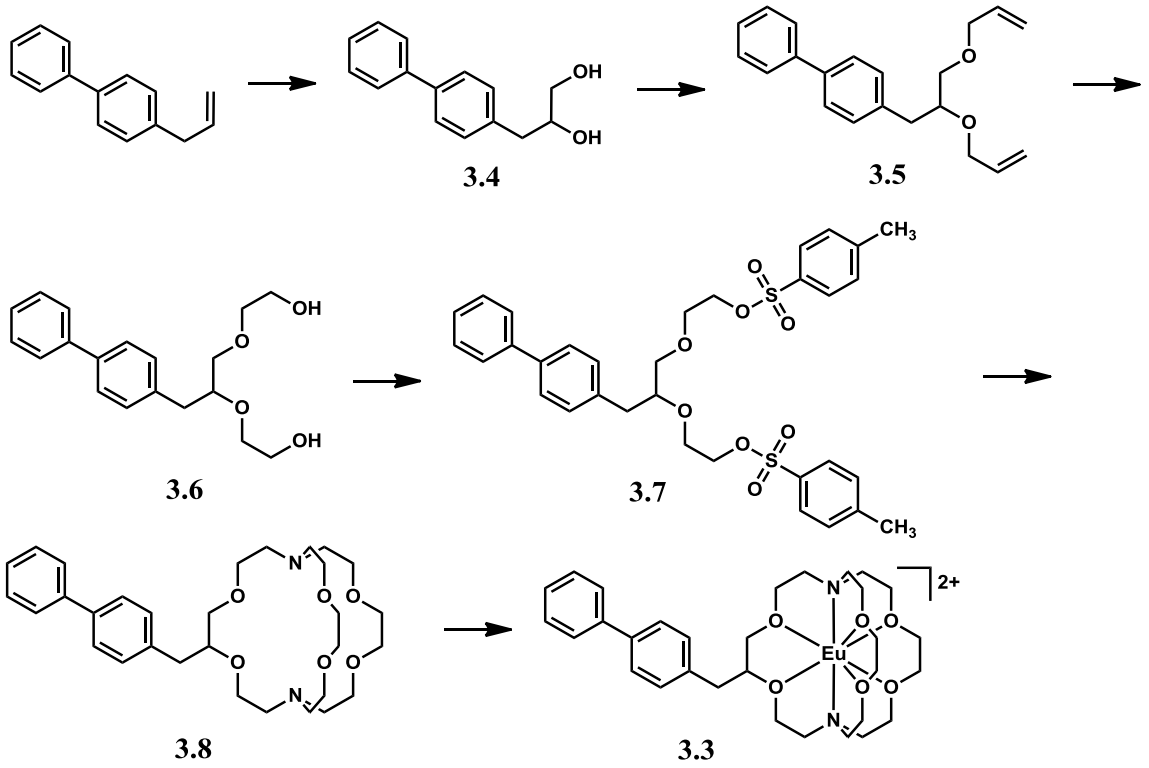

3-(Biphenyl-4-yl)propane-1,2-diol (3.4): To a mixture of 4-allylbiphenyl (4.00 g, 20.6 mmol, 1 equiv), *t*-BuOH (150 mL), and H_2O (150 mL) was added sequentially $K_3Fe(CN)_6$ (20.3 g, 61.8 mmol, 3 equiv), $K_2CO_3 \cdot H_2O$ (9.65 g, 61.8 mmol, 3 equiv), and a solution of OsO_4 in *t*-BuOH (95.9 mM, 2.70 mL, 0.0129 equiv). The reaction mixture was stirred for 20 h at ambient temperature at which point Na_2SO_3 (7.79 g, 61.8 mmol, 3 equiv) was added, and stirring was continued for 4 h. The resulting solution was concentrated to dryness under reduced pressure, and the residue was extracted with Et_2O (6 × 50 mL). After removal of Et_2O under reduced pressure, purification was performed using silica gel chromatography (1:1 hexanes/ethyl acetate) to yield 4.25 g (90%) of **3.4** as white solid. ^{1}H NMR (400 MHz, CD_3OD, δ): 2.66–2.90 (m, CH_2, 2H), 3.44–3.56 (m, CH_2, 2H), 3.81–3.89 (m, C*H*, 1H), 7.24–7.58 (m, C*H*, 9H); ^{13}C NMR (101 MHz, CD_3OD, δ): 40.5 (*C*H_2), 66.6

(*C*H_2), 74.4 (*C*H), 127.80 (*C*H), 127.81 (*C*H), 128.1 (*C*H), 129.8 (*C*H), 130.9 (*C*H), 139.3, 140.3, 142.2; TLC: R_f = 0.33 (1:1 hexanes/ethyl acetate); HRESIMS (*m*/*z*): $[M + Na]^+$ calcd for $C_{15}H_{16}O_2Na$, 251.1048; found, 251.1046.

4-(1,2-Bis(allyloxy)ethyl)biphenyl (3.5): To a solution of **3.4** (3.10 g, 13.5 mmol, 1 equiv) in anhydrous dimethoxyethane (60 mL) under Ar at ambient temperature was added NaH (2.53 g, 52.6 mmol, 4 equiv) followed by the dropwise addition of 1-bromoprop-2-ene (4.45 mL, 52.6 mmol, 4 equiv). The resulting reaction mixture was heated at reflux for 23 h and allowed to cool to ambient temperature before excess NaH was quenched with methanol (2 mL). Solvent was removed under reduced pressure; the resulting residue was extracted with ethyl acetate (3 × 20 mL); and the combined ethyl acetate solutions were washed with water (3 × 20 mL). The organic phase was dried over Na_2SO_4 and concentrated under reduced pressure. Purification was performed using silica gel chromatography (9:1 hexanes/ethyl acetate) to yield 3.85 g (95%) of **3.5** as a yellow oil. ^{1}H NMR (400 MHz, CD_3CN, δ): 2.79–2.91 (m, CH_2, 2H), 3.37–3.48 (m, CH_2, 2H), 3.68–3.76 (m, C*H*, 1H), 3.93–4.11 (m, CH_2, 4H), 5.04–5.32 (m, CH_2, 4H), 5.78–5.98 (m, C*H*, 2H), 7.28–7.66 (m, C*H*, 9H); ^{13}C NMR (101 MHz, CD_3CN, δ): 38.1 (*C*H_2), 72.3 (*C*H_2), 72.6 (*C*H_2), 79.8 (*C*H), 116.4 (*C*H_2), 116.7 (*C*H_2), 127.6 (*C*H), 127.7 (*C*H), 128.1 (*C*H), 129.8 (*C*H), 131.0 (*C*H), 136.2 (*CH*), 136.6 (*C*H), 139.2, 139.5, 141.6; TLC: R_f = 0.53 (9:1 hexanes/ethyl acetate); HRESIMS (*m*/*z*): $[M + Na]^+$ calcd for $C_{21}H_{24}O_2Na$, 331.1674; found, 331.1669.

2,2'-(Propane-1,2-diylbisoxy-3-biphenyl-4-yl)-diethanol (3.6): Ozone was passed through a solution of **5** (4.00 g, 12.9 mmol, 1 equiv) in methanol (100 mL) at –50 °C until the starting compound was consumed (55 min). The resulting reaction mixture was purged

with Ar, and $NaBH_4$ (4.87 g, 129 mmol, 10 equiv) was added. The mixture was stirred for 1 h, a mixture of HOAc/H_2O 1:10 (v/v) (18 mL) was added, and the resulting solution was stirred for 2 h. Volatile components were removed under reduced pressure, and the residue was extracted with ethyl acetate (6 × 20 mL). The extract was concentrated under reduced pressure, and purification was performed using silica gel chromatography (ethyl acetate) to yield 3.31 g (81%) of **3.6** as pale yellow oil. ^{1}H NMR (400 MHz, CD_3CN, δ): 2.75–2.90 (m, C*H*$_2$, 2H), 3.01 (brs, O*H*, 2H), 3.25–3.77 (m, C*H* and C*H*$_2$, 11H), 7.29–7.68 (m, C*H*, 9H); ^{13}C NMR (101 MHz, CD_3CN, δ): 38.1 (*C*H$_2$), 61.9 (*C*H$_2$), 62.2 (*C*H$_2$), 72.3 (*C*H$_2$), 73.3 (*C*H$_2$), 73.6 (*C*H$_2$), 80.8 (*C*H), 127.6 (*C*H), 127.7 (*C*H), 128.2 (*C*H), 129.8 (*C*H), 131.0 (*CH*), 139.1, 139.6, 141.6; TLC: R_f = 0.44 (ethyl acetate); HRESIMS (*m*/*z*): [M + H]$^+$ calcd for $C_{19}H_{25}O_4$, 317.1753; found, 317.1745.

2,2'-(Propane-1,2-diylbisoxy-3-biphenyl-4-yl)-ditosylate (3.7): A solution of tosyl chloride (3.71 g, 19.5 mmol, 3 equiv) in CH_2Cl_2 (22 mL) was added in a dropwise manner to an ice-cooled solution of **3.6** (2.06 g, 6.51 mmol, 1 equiv), triethylamine (5.45 mL, 39.1 mmol, 6 equiv), and dimethylaminopyridine (0.030 mL, 0.25 mmol, 0.038 equiv) in CH_2Cl_2 (33 mL), and the resulting mixture was stirred for 24 h while warming to ambient temperature. The reaction mixture was washed sequentially with water (2 × 33 mL), saturated aqueous Na_2CO_3 (2 × 22 mL), and saturated aqueous citric acid (2 × 22 mL); dried over Na_2SO_4; and concentrated under reduced pressure. Purification was performed using silica gel chromatography (stepwise gradient of 3:1→1:1 hexanes/ethyl acetate) to yield 3.15 g (78%) of **3.7** as a light yellow oil. ^{1}H NMR (400 MHz, CD_3CN, δ): 2.37 (s, C*H*$_3$, 6H), 2.60–2.74 (m, C*H*$_2$, 2H), 3.20–3.35 (m, C*H*$_2$, 2H), 3.47–3.58–3.67 (m, C*H* and C*H*$_2$, 5H), 3.97–4.12 (m, C*H*$_2$, 4H), 7.18–7.81 (m, C*H*, 17H); ^{13}C NMR (101 MHz,

CD_3CN, δ): 21.6 (*C*H_3), 37.7 (*C*H_2), 68.2 (*C*H_2), 69.3 (*C*H_2), 70.8 (*C*H_2), 71.1 (*C*H_2), 73.1 (*C*H_2), 80.7 (*C*H), 127.6 (*C*H), 127.7 (*C*H), 128.2 (*C*H), 128.7 (*C*H), 129.8 (*CH*), 131.0 (*C*H), 133.8, 138.6, 139.5, 141.6, 146.3; TLC: R_f = 0.21 (3:1 hexanes/ethyl acetate); HRESIMS (*m*/*z*): $[M + Na]^+$ calcd for $C_{33}H_{36}O_8S_2Na$, 647.1749; found, 647.1735.

5-(Biphenyl-4-ylmethyl)-4,7,13,16,21,24-hexaoxa-1,10-diazabicyclo[8.8.8]hexacosane (3.8): Under an atmosphere of Ar, 4,13-diaza-18-crown-6-ether (0.177 g, 0.675 mmol, 1 equiv) was added to a suspension of Cs_2CO_3 (1.08 g, 3.33 mmol, 4.93 equiv) in anhydrous acetonitrile (37 mL). The mixture was heated to 60 °C, and a solution of **7** (0.478 g, 0.765, 1.13 equiv) in anhydrous acetonitrile (13 mL) was added. The reaction mixture was heated at reflux for 115 h, cooled to ambient temperature, and filtered through celite. Solvent was removed under reduced pressure, and purification was performed using silica gel chromatography (stepwise gradient of 20:1→10:1 CH_2Cl_2/methanol) to yield 73.6 mg (21%) of **3.8** as a pale yellow oil. ^{1}H NMR (400 MHz, CD_3CN, δ): 2.55–2.88 (m, 10H), 3.03–3.11 (m, 1H), 3.32–3.82 (m, 26H), 7.30–7.66 (m, C*H*, 9H); ^{13}C NMR (101 MHz, CD_3CN, δ): 38.4 (*C*H_2), 53.4 (*C*H_2), 53.5 (*C*H_2), 53.7 (*C*H_2), 53.8 (*C*H_2), 54.1 (*C*H_2), 54.3 (*C*H_2), 66.1 (*C*H_2), 68.0 (*C*H_2), 68.1 (*C*H_2), 68.57 (*C*H_2), 68.59 (*C*H_2), 68.8 (*C*H_2), 68.9 (*C*H_2), 69.2 (*C*H_2), 69.6 (*C*H_2), 71.4 (*C*H_2), 79.4 (*C*H), 126.7 (*C*H), 127.7 (*C*H), 127.8 (*C*H), 128.3 (*C*H), 129.2 (*CH*), 129.9 (*C*H), 131.0 (*C*H), 138.4, 139.6, 141.5; TLC: R_f = 0.23 (10:1 CH_2Cl_2/methanol); HRESIMS (*m*/*z*): $[M + H]^+$ calcd for $C_{31}H_{47}O_6N_2$, 543.3434; found, 543.3425.

General Procedure for the synthesis of Eu^{II}-containing cryptates (3.1–3.3): A degassed aqueous solution of $EuCl_2$ (1 equiv) was mixed with a degassed aqueous solution of a cryptand (2 equiv). The resulting mixture was stirred for 12 h at ambient temperature under

Ar. Degassed PBS (10×) was added to make the entire reaction mixture 1× in PBS, and stirring was continued for 30 min. The concentration of Eu was verified by ICP-MS.

3.6 References

(1) (a) Moser, E. *World J. Radiol.* **2010,** *2,* 37–40. (b) Pitt, D.; Boster, A.; Pei, W.; Wohleb, E.; Jasne, A.; Zachariah, C. R.; Rammohan, K.; Knopp, M. V.; Schmalbrock, P. *Arch. Neurol.* 2010, 67, 812–818. (c) Blow, N. *Nature,* **2009,** *458,* 925–928.

(2) Helm, L. *Future Med. Chem.* **2010,** *2,* 385–396.

(3) Caravan, P. *Chem. Soc. Rev.* **2006,** *35,* 512–523.

(4) Costa, J.; Ruloff, R.; Burai, L.; Helm, L.; Merbach, A. E. *J. Am. Chem. Soc.* **2005,** *127,* 5147–5157.

(5) (a) Livramento, J. B.; Weidensteiner, C.; Prata, M. I. M.; Allegrini, P. R.; Geraldes, C. F. G. C.; Helm, L.; Kneuer, R.; Merbach, A. E.; Santos, A. C.; Schmidt, P.; Tóth, É. *Contrast Media Mol. Imaging* **2006,** *1,* 30–39. (b) Livramento, J. B.; Helm, L.; Sour, A.; O'Neil, C.; Merbach, A. E.; Tóth, É. *Dalton Trans.* **2008,** 1195–1202. (c) Moriggi, L.; Cannizzo, C.; Prestinari, C.; Berrière, F.; and Helm, L. *Inorg. Chem.* **2008,** *47,* 8357–8366. (d) Mamedov, I.; Táborsky, P.; Lubal, S.; Laurent, L.; Elst, V.; Mayer, H. A.; Logothetis, N. K.; Angelovski, G. *Eur. J. Inorg. Chem.* **2009,** 3298–3306.

(6) Gamage, N.-D. H.; Mei, Y.; Garcia, J.; Allen, M. J. *Angew. Chem., Int. Ed*. **2010,** *49,* 8923–8925.

(7) (a) Tóth, É.; Burai, L.; Merbach, A. E. *Coord. Chem. Rev.* **2001,** *216–217,* 363–382. (b) Caravan, P.; Tóth, É.; Rockenbauer, A.; Merbach, A. E. *J. Am. Chem. Soc.* **1999,** *121,* 10403–10404. (c) Caravan, P.; Merbach, A. E. *Chem. Commun.* **1997,** 2147–2148.

(8) Burai, L.; Scopelliti, R.; Tóth, É. *Chem. Commun.* **2002,** 2366–2367.

(9) (a) Kowalewski, J.; Egorov, A.; Laaksonen, A.; Nikkhou Aski, S.; Parigi, G.; Westlund, P.-O. *J. Magn. Reson.* **2008,** *195,* 103–111. (b) Kruk, D.; Kowalewski, J. *J. Chem. Phys.* **2002,** *116,* 4079–4086. (c) Nilsson,T.; Parigi, G.; Kowalewski, J. *J. Phys. Chem. A* **2002,** *18,* 4476–4488. (d) Svoboda, J.; Nilsson, T.; Kowalewski, J.; Westlund, P.-O.; Larsson, P. T. *J. Magn. Reson., Ser. A* **1996,** *121,* 108–113.

(10) (a) Werner, E. J.; Avedano, S.; Botta, M.; Hay, B. P.; Moore, E. G.; Aime, S; Raymond, K. N. *J. Am. Chem. Soc.* **2007,** *129,* 1870–1871. (b) Torres, S.; Martins, J. A.; André, J. P.; Pereira, G. A.; Kiraly, R.; Brücher; Helm, E. L.; Tóth, É.; Geraldes, C. F. G. C. *Eur. J. Inorg. Chem.* **2007,** 5489–5499. (c) Pierre, V. C.; Botta, M.; Raymond, K. N. *J. Am. Chem. Soc.* **2005,** *127,* 504–505. (d) Laus, S.; Ruloff, R.; Tóth, É.; Merbach, A. E. *Chem.–Eur. J.* **2003,** *9,* 3555–3556. (e) Doble, D. M. J.; Botta, M.; Wang, J.; Aime, S.; Barge, A.; Raymond, K. N. *J. Am. Chem. Soc.* **2001,** *123,* 10758–10759. (f) Cohen, S. M.; Xu, J.; Radkov, E.; Raymond, K. N. *Inorg. Chem.* **2000,** *39,* 5747–5756. (g) Aime, S.; Barge, A.; Borel, A.; Botta, M.; Chemerisov, S.; Merbach, A. E.; Müller, U.; Pubanz, D. *Inorg. Chem.* **1997,** *36,* 5104–5112.

(11) Haacke, E. M.; Brown, R. W.; Thompson, M. R.; Venkatesan, R. Magnetic Resonance Imaging Physical Principles and Sequence Design, John Wiley & Sons, Inc., New York, **1999,** p. 654.

(12) (a) The temperatures at 3 and 7 T differed by 0.8 °C. To examine the influence of this temperature variation on relaxivity, we measured cryptate **3.3** at 11.7 T at temperatures of 19 and 19.8 °C. The relaxivity values were 6.82 ± 0.01 and 6.72 ± 0.01, respectively. (b) Averill, D. J.; Garcia, J.; Siriwardena-Mahanama, B. N.; Vithanarachchi, S. M.; Allen, M. J. *J. Vis. Exp.* **2011,** *53,* e2844.

(13) (a) Kowalewski, J.; Egorov, A.; Kruk, D.; Laaksonen, A.; Nikkhou Aski, S.; Parigi, G.; Westlund, P.-O. *J. Magn. Reson.* **2008,** *195,* 103–111. (b) Kruk, D.; Kowalewski, J. *J. Chem. Phys.* **2002,** *116,* 4079–4086. (c) Nilsson, T.; Parigi, G.; Kowalewski, J. *J. Phys Chem. A* **2002,** *106,* 4476–4488. d) Svoboda, J.; Nilsson, T.; Kowalewski, J.; Westlund, P.-O. P.; Larsson, T. *J. Magn. Reson., Ser. A* **1996,** *121,* 108–113.

(14) (a) Chan, K. W.-Y.; Wong, W.-T. *Coord. Chem. Rev.* **2007,** *251,* 2428–2451; (b) Reichert, D. E.; Hancock, R. D.; Welch, M. J. *Inorg. Chem.* **1996,** *35,* 7013–7020.

(15) Borel, D. A.; Bean, J. F.; Clarkson, R. B.; Helm, L.; Moriggi, L.; Sherry, A. D.; Woods, M. *Chem. Eur. J.* **2008,** *14,* 2658–2667.

(16) Burai, L.; Tóth, É.; Moreau, G.; Sour, A.; Scopelliti, R.; Merbach, A. E. *Chem. Eur. J.* **2003,** *9,* 1394–1404.

(17) Armarego, W. L. F.; Chai, C. L. L. Purification of Laboratory Chemicals, Fifth Edition; Elsevier: Burlington, MA, **2003**.

(18) Lin, S.; Song, C.-X.; Cai, G.-X.; Wang, W.-H.; Shi, Z.-J. *J. Am. Chem. Soc.* **2008,** *130,* 12901−12903.

(19) Still, W. C.; Kahn, M.; Mitra, A. *J. Org. Chem.* **1978,** *43,* 2923–2925.

(20) Haacke, E. M.; Brown, R. W.; Thompson, M. R.; Venkatesan, R. Magnetic Resonance Imaging Physical Principles and Sequence Design; John Wiley & Sons, Inc.: New York, **1999;** p 654.

(21) Urbanczyk-Pearson, L. M.; Femia, F. J.; Smith, J.; Parigi, G.; Duimstra, J. A.; Eckermann, A. L.; Luchinat, C.; Meade, T. *J. Inorg. Chem.* **2008,** *47,* 56–68.

3.7 Estimating Rotational Correlation Time (τ_R)

3.7.1 Theoretical Basis

Inner-sphere relaxivity can be expressed by the following equation:

Eq 3.2 inner-sphere relaxivity, $r_1^{IS} = \frac{q}{55.5}\left(\frac{1}{T_{1m}+\tau_m}\right)$

where q is the number of inner-sphere water molecules, T_1m is the longitudinal relaxation time of a bound water molecule, τ_m is the residence lifetime of bound water molecules. Assuming that the inner-sphere relaxivity of a sample is contributing to half the observed relaxivity, $r_{1,obs}$, **Eq 3.2** can be rewritten as:

Eq 3.3 $0.5r_{1,obs}(1000) = \frac{q}{55.5}\left(\frac{1}{T_{1m}+\tau_m}\right)$

where 1000 was used as a factor to convert mM unit in relaxivity to M.

Solving for T_{1m}:

Eq 3.4 $T_{1m} = \frac{q}{(0.5r_{1,obs})(1000)(55.5)} - \tau_m$

There are two relaxation mechanisms of the bound water protons that depend on the interaction between the paramagnetic metal and the water proton—dipole–dipole (through space) and scalar (through bonds) and are expressed by the equation below:

Eq 3.5 $\frac{1}{T_{1m}} = \frac{1}{T_1^{DD}} + \frac{1}{T_1^{SC}}$ note: $\frac{1}{T_1^{SC}}$ goes to zero at frequencies above 10 MHz

The longitudinal relaxation rate of water proton due to dipole-dipole mechanism is described by the following equation:

Eq 3.6 $\frac{1}{T_1^{DD}} = \frac{2}{15}\left(\frac{\gamma_I^2 g^2 \mu_B^2}{r_{EuH}^6}\right) S(S+1)\left(\frac{\mu_o}{4\pi}\right)^2 \left(3\frac{\tau_{c1}}{1+\omega_I^2\tau_{c1}^2} + 7\frac{\tau_{c2}}{1+\omega_S^2\tau_{c2}^2}\right)$

where γ_I is the proton gyromagnetic ratio (2.67×10^8 rad s^{-1} T^{-1}), μ_B is Bohr magneton (9.27×10^{-24} J T^{-1}), r_{EuH} is the distance between Eu^{2+} and water proton (3.22×10^{-10} m), S is the spin number (3.5 for Eu^{2+}), $\mu_o$is the magnetic permeability constant ($4\pi \times 10^{-7}$ T•m

A^{-1}), τ_{c1} and τ_{c2} are the longitudinal and transverse correlation times, respectively, ω_I is the nuclear Larmor frequency (γ_I multiplied with magnetic field strength), and ω_S is the electronic Larmor frequency (γ_S multiplied with magnetic field strength).

The longitudinal and transverse correlation rates, $1/\tau_{c1}$ and $1/\tau_{c2,}$ respectively, are mathematically described as:

Eq 3.7 $$\frac{1}{\tau_{c1}} = \frac{1}{\tau_R} + \frac{1}{T_{1e}} + \frac{1}{\tau_m}$$

Eq 3.8 $$\frac{1}{\tau_{c2}} = \frac{1}{\tau_R} + \frac{1}{T_{2e}} + \frac{1}{\tau_m}$$

where τ_R is the rotational correlation time, and T_{1e} and T_{2e} are longitudinal and transverse electronic relaxation times, respectively.

3.7.2 Calculating τ_R using Microsoft Excel Spreadsheet

1. Input the values of ***q*** (cell F1), ***r1(obs)*** (cell F2), ***taum*** (cell F3), ***g-factor*** (cell H1), ***r(EuH)*** (cell H2), and ***S*** (cell H3). Values for T1m (cell B1) and (1/T1m)/c (cell B4) will be automatically calculated.

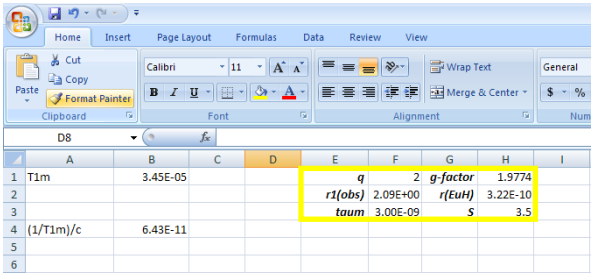

Note: Shown below are the MS excel functions for T1m (cell B1) and (1/T1m)/c (cell B4):

Eq 3.9 T1m (cell B1): =(F1/(0.7*55.5*F2*1000))-F3

where **Eq 3.9** was based from **Eq 3.4**. (1/T1m)/c (cell B4) has the following formula:

Eq 3.10 (1/T1m)/c (cell B4): =(1/B1)/((2/15)*(((267000000^2)*(H1^2)*((9.27E-24)^2))/((H2)^6))*((0.0000001)^2)*(H3*(H3+1)))

Eq 3.10 is derived from **Eq 3.6** and has the following equation:

Eq 3.11 $$\frac{\frac{1}{T_{1m}}}{c} = \frac{\frac{1}{T_1^{DD}}}{\frac{2}{15}\left(\frac{\gamma_I^2 g^2 \mu_B^2}{r_{EuH}^6}\right) S(S+1)\left(\frac{\mu_o}{4\pi}\right)^2}$$

The derived equation shown in **Eq 3.11** is equivalent to **Eq 3.12**

Eq 3.12 $$\left(3\frac{\tau_{c1}}{1+\omega_I^2\tau_{c1}^2} + 7\frac{\tau_{c2}}{1+\omega_S^2\tau_{c2}^2}\right)$$

which is the basis for the function in cell B8:

Eq 3.13 (1/T1m)/c (cell B4): =(3*B12/(1+((F8)^2)*B12^2))+(7*B13)/(1+((F9)^2)*B13^2)

2. Input the magnetic field strength, ***B***, (cell H8) to compute for the nuclear and electronic Larmor frequency, ***proton LF*** (cell F8) and ***electron LF*** (cell F9), respectively.

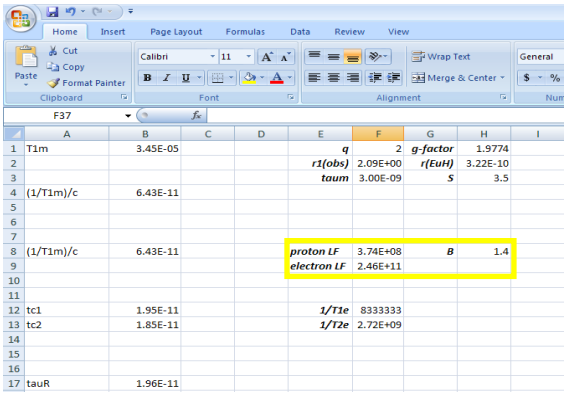

	A	B	C	D	E	F	G	H	I
1	T1m	3.45E-05			*q*	2	*g-factor*	1.9774	
2					*r1(obs)*	2.09E+00	*r(EuH)*	3.22E-10	
3					*taum*	3.00E-09	*S*	3.5	
4	(1/T1m)/c	6.43E-11							
5									
6									
7									
8	(1/T1m)/c	6.43E-11			*proton LF*	3.74E+08	*B*	1.4	
9					*electron LF*	2.46E+11			
10									
11									
12	tc1	1.95E-11			*1/T1e*	8333333			
13	tc2	1.85E-11			*1/T2e*	2.72E+09			
14									
15									
16									
17	tauR	1.96E-11							

Note: Shown below are the MS excel functions for tc1 (cell B12) and tc2 (cell B12):

Eq 3.14 tc1 (cell B12): =B17/(1+((1/F3)+(F12))*B17)

Eq 3.15 tc2 (cell B13): =B17/(1+((1/F3)+(F13))*B17)

Eq 3.14 and **3.15** are based from **Eq 3.7** and **3.8**.

3. Input the ***1/T1e*** and ***1/T2e*** values.

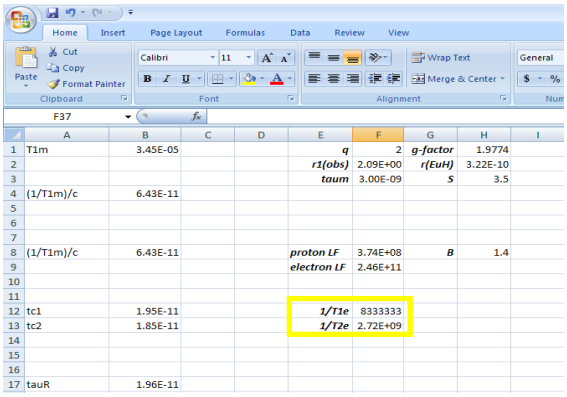

	A	B	C	D	E	F	G	H	I
1	T1m	3.45E-05			*q*	2	*g-factor*	1.9774	
2					*r1(obs)*	2.09E+00	*r(EuH)*	3.22E-10	
3					*taum*	3.00E-09	*S*	3.5	
4	(1/T1m)/c	6.43E-11							
5									
6									
7									
8	(1/T1m)/c	6.43E-11			*proton LF*	3.74E+08	*B*	1.4	
9					*electron LF*	2.46E+11			
10									
11									
12	tc1	1.95E-11			*1/T1e*	8333333			
13	tc2	1.85E-11			*1/T2e*	2.72E+09			
14									
15									
16									
17	tauR	1.96E-11							

4. Input **tauR** values until (1/T1m)/c value in cell B8 is equal to that in cell B4.

3.8 ^{1}H and ^{13}C NMR Spectra of 3.4–3.8

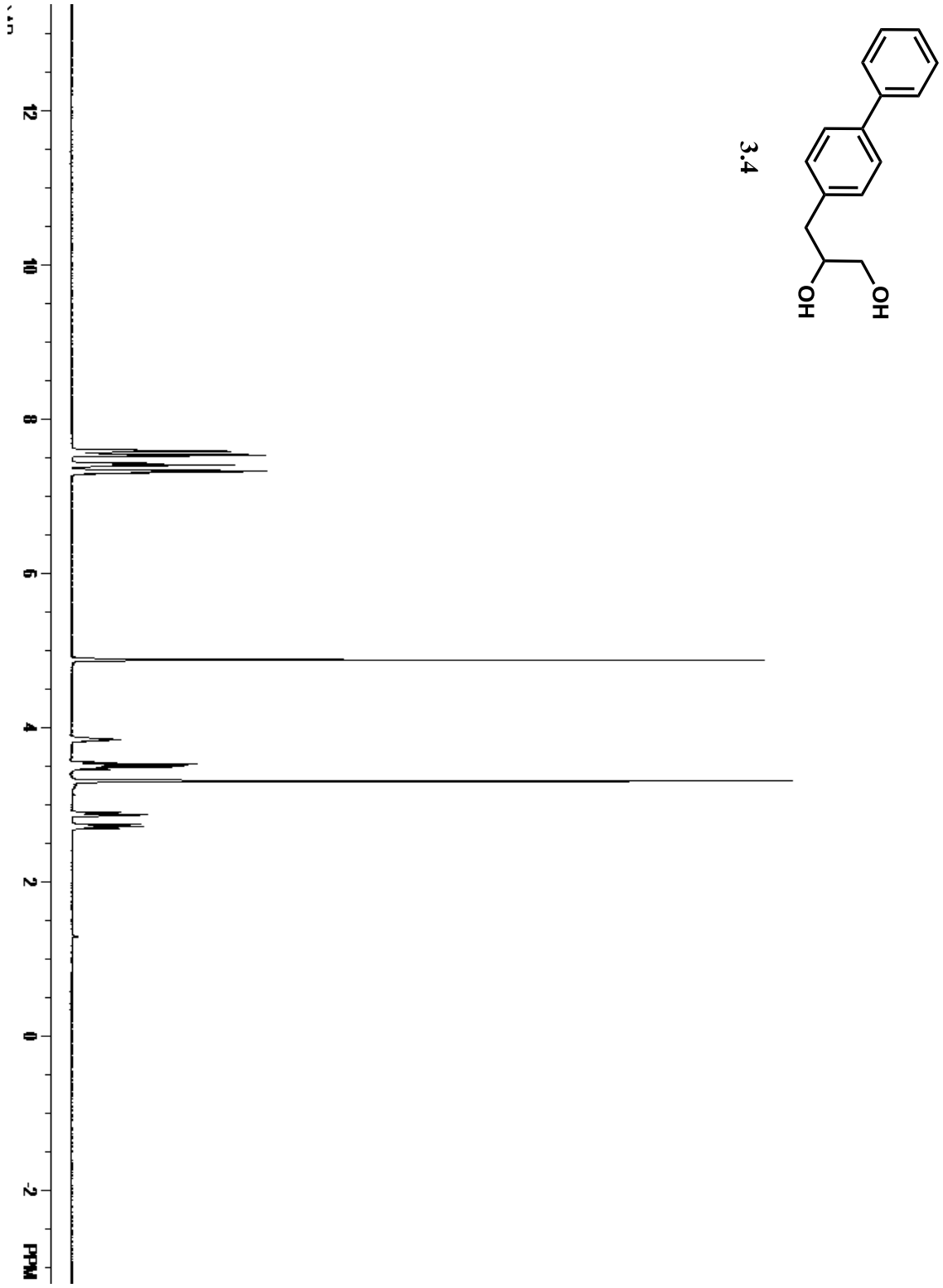

Figure 3.14 ^{1}H NMR Spectrum of **3.4**.

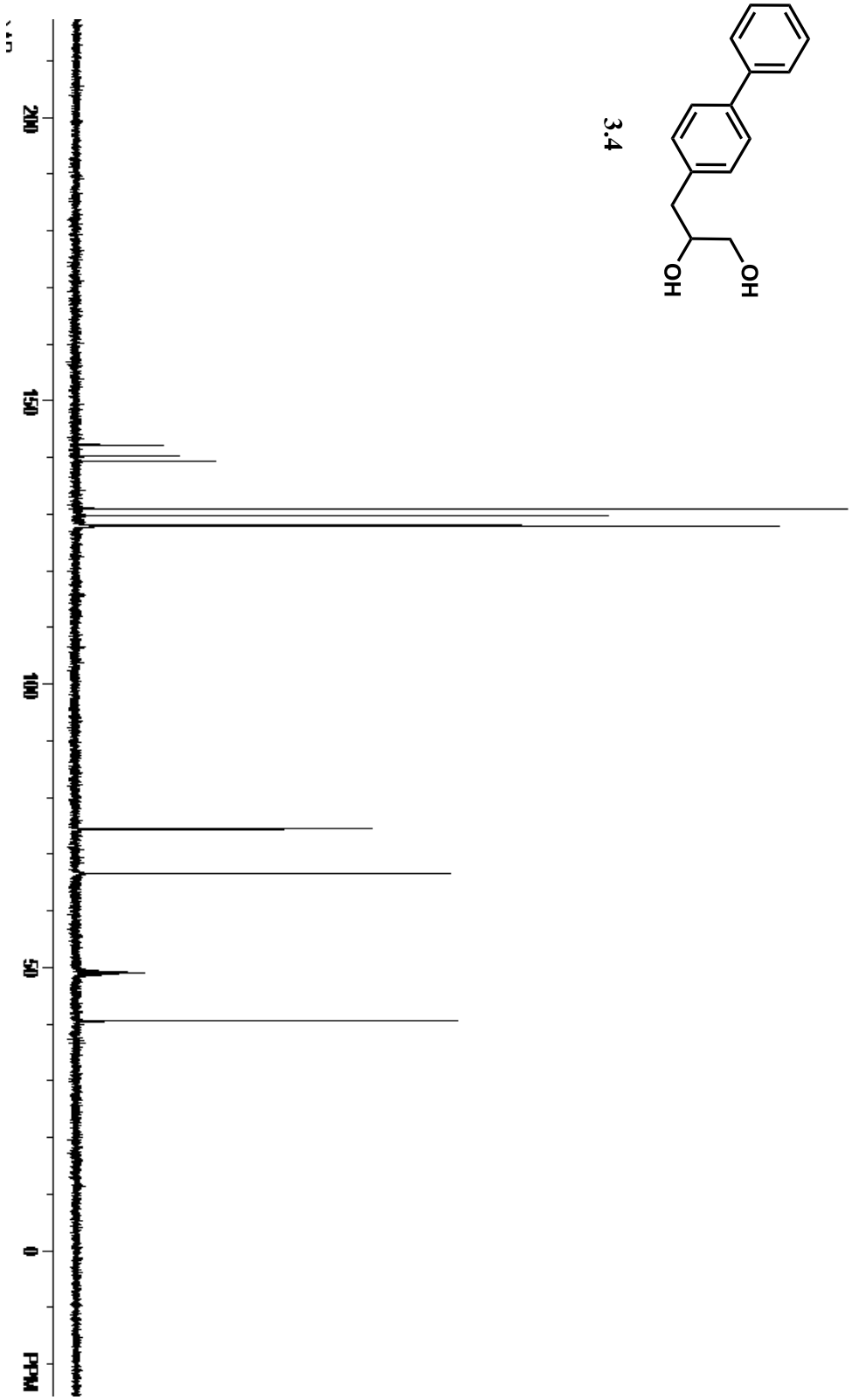

Figure 3.15 ^{13}C NMR Spectrum of **3.4**.

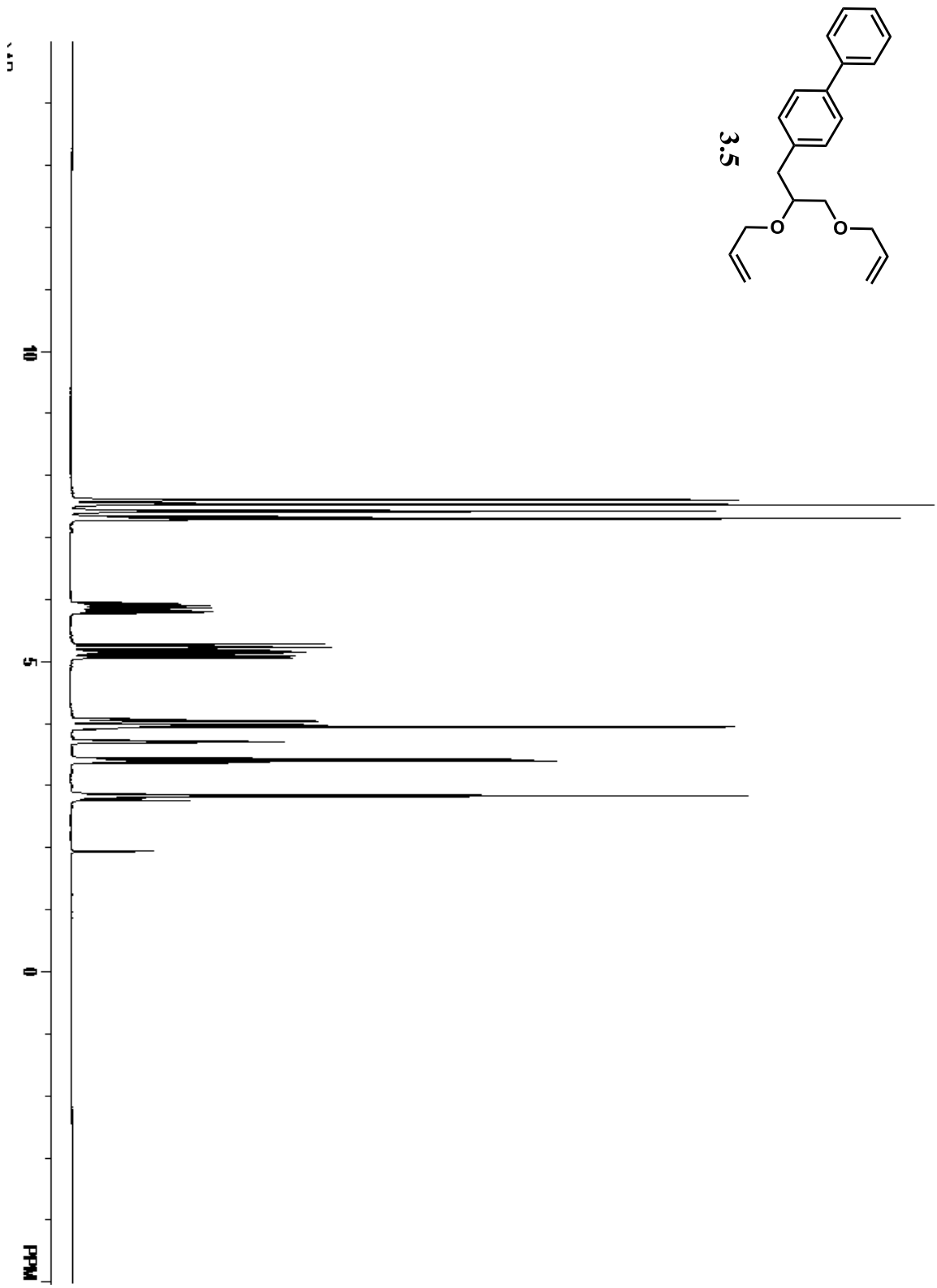

Figure 3.16 ^{1}H NMR Spectrum of **3.5**.

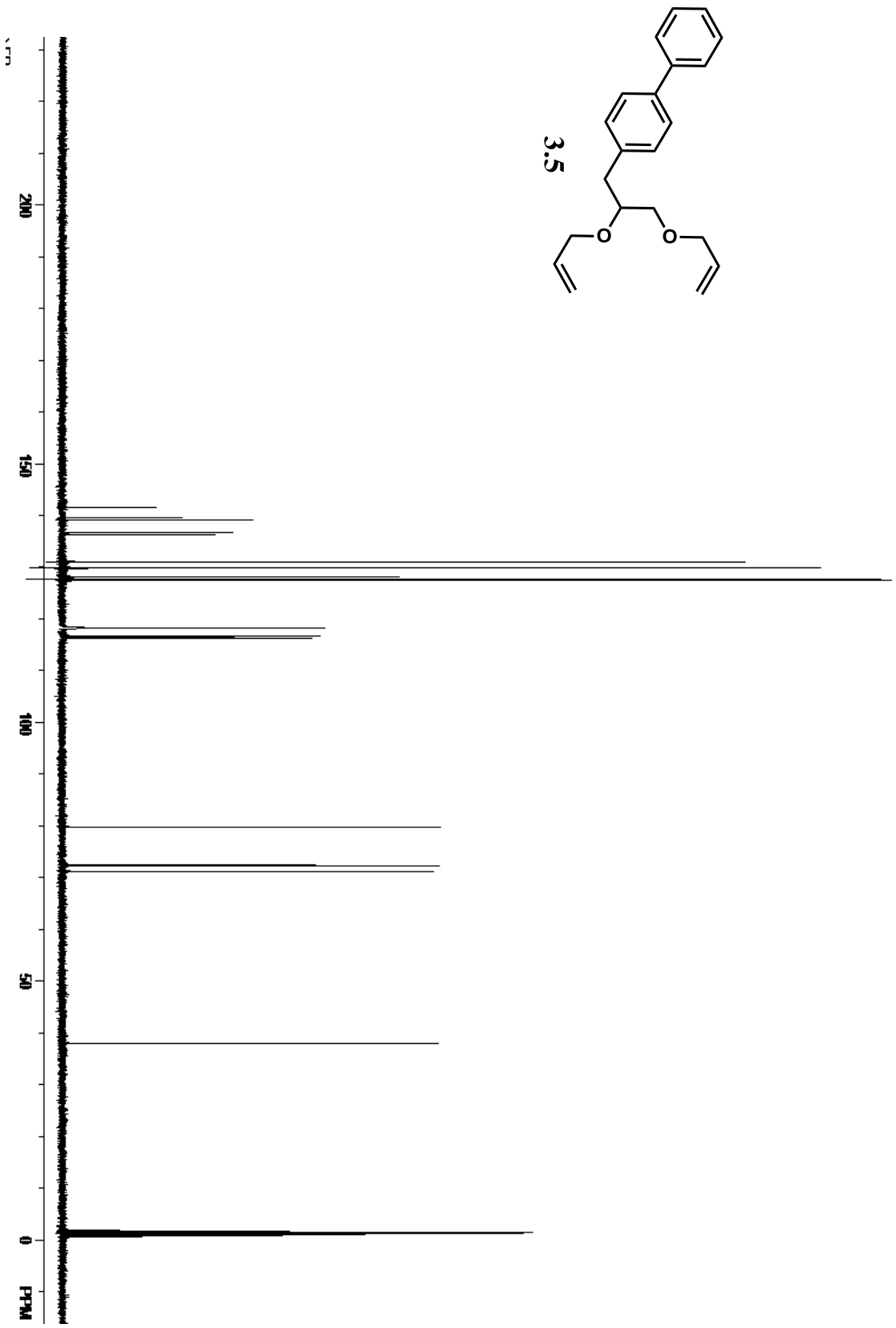

Figure 3.17 ^{13}C NMR Spectrum of **3.5**.

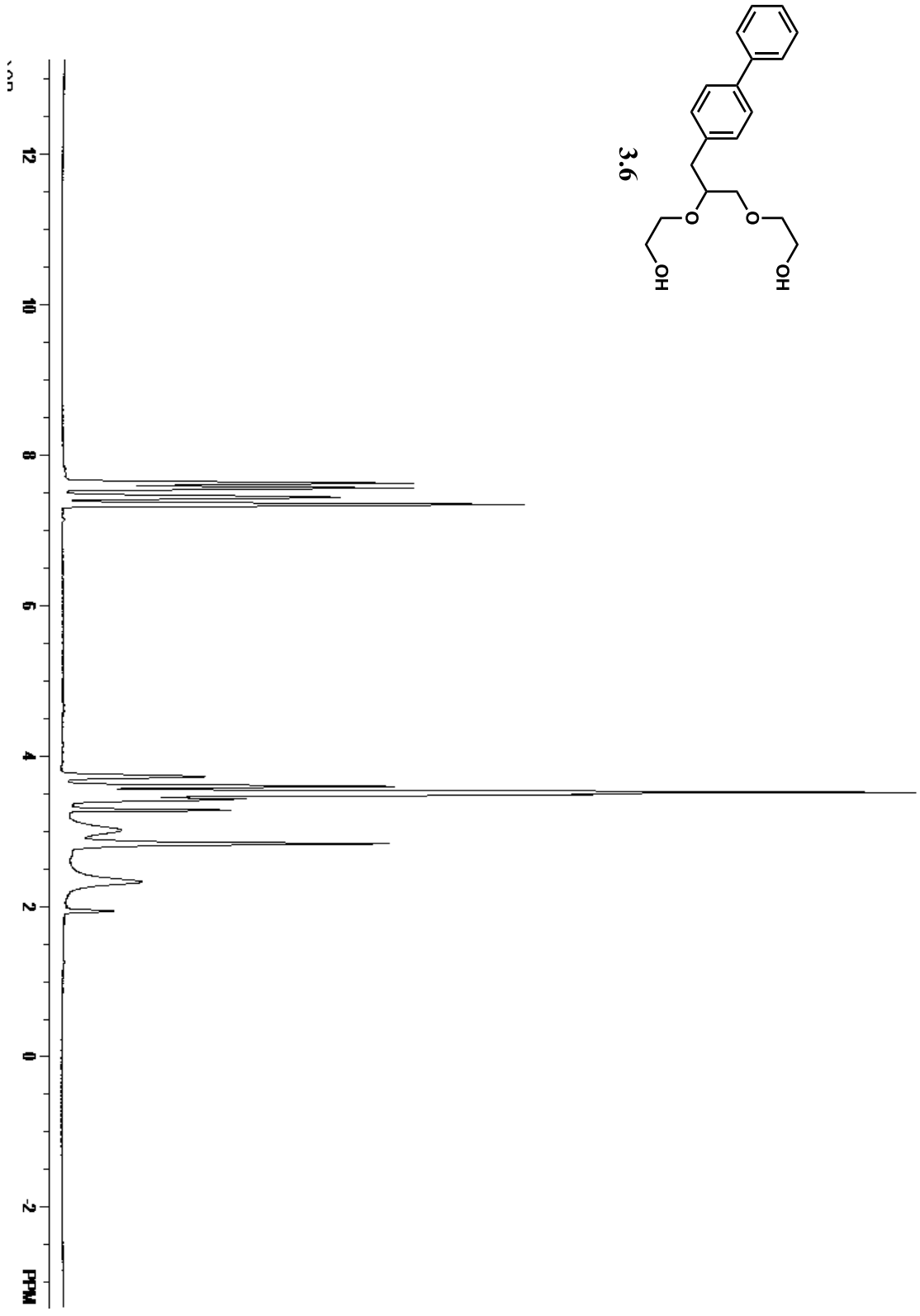

Figure 3.18 ^{1}H NMR Spectrum of **3.6**.

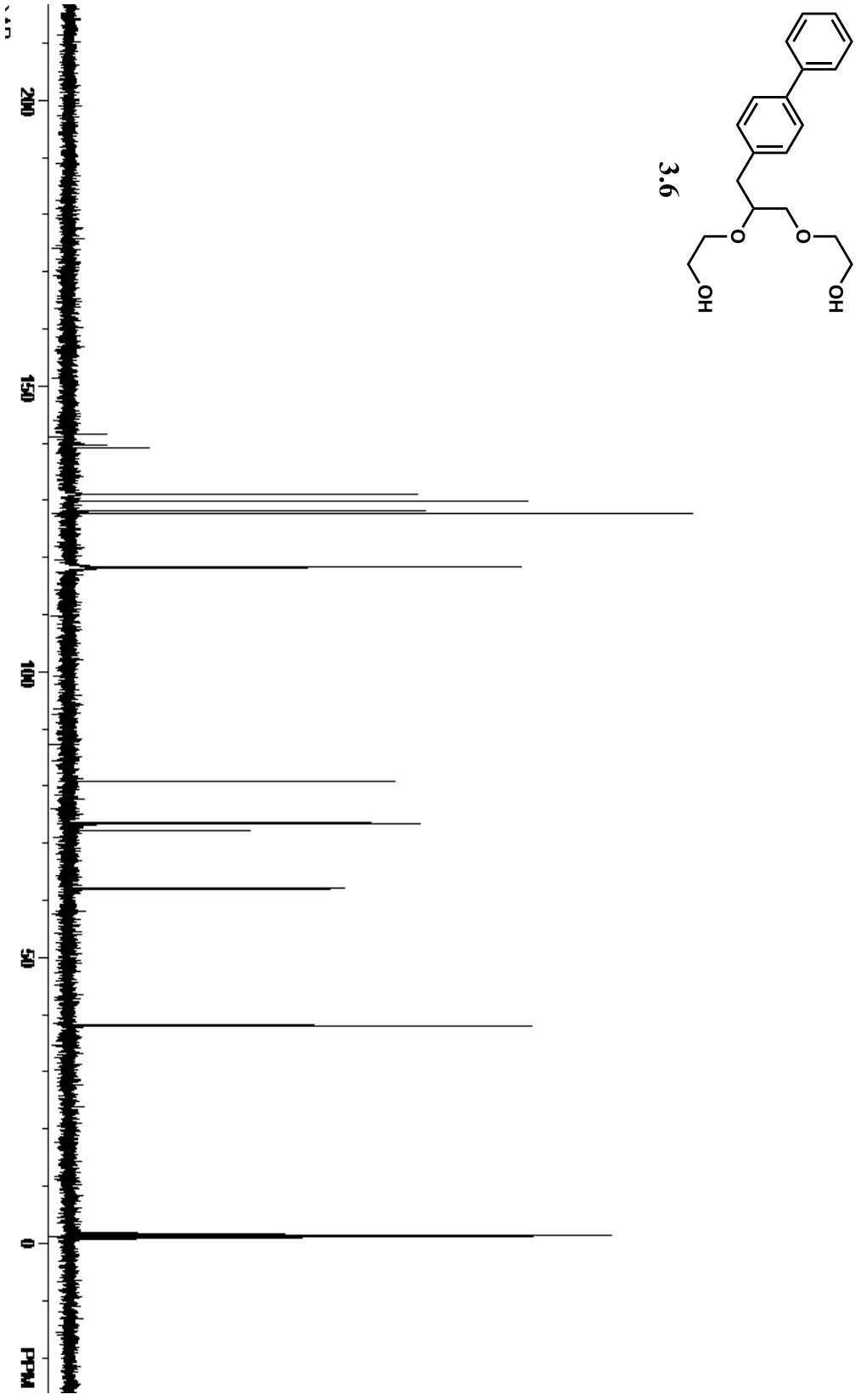

Figure 3.19 ^{13}C NMR Spectrum of **3.6**.

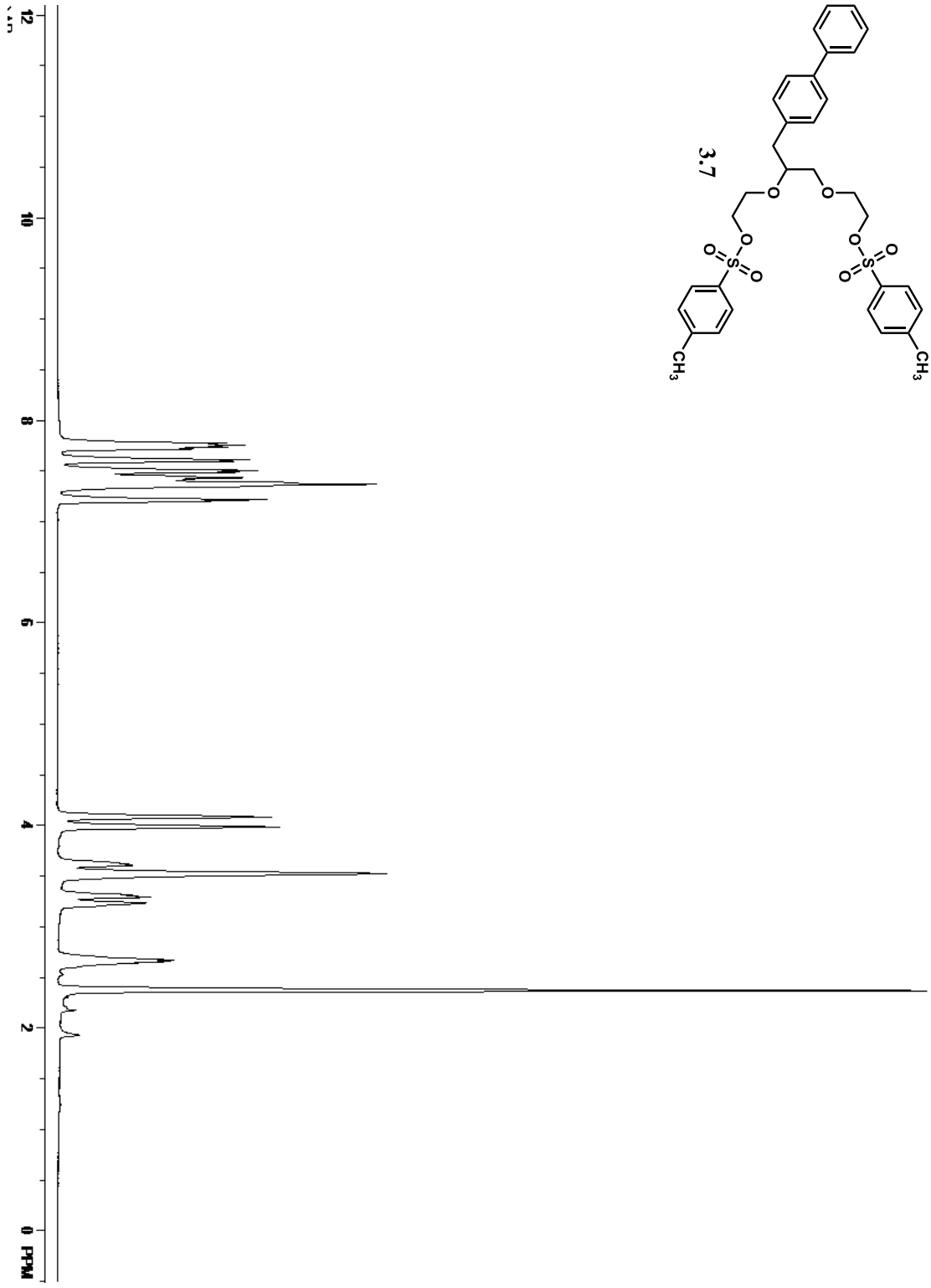

Figure 3.20 ^{1}H NMR Spectrum of **3.7**.

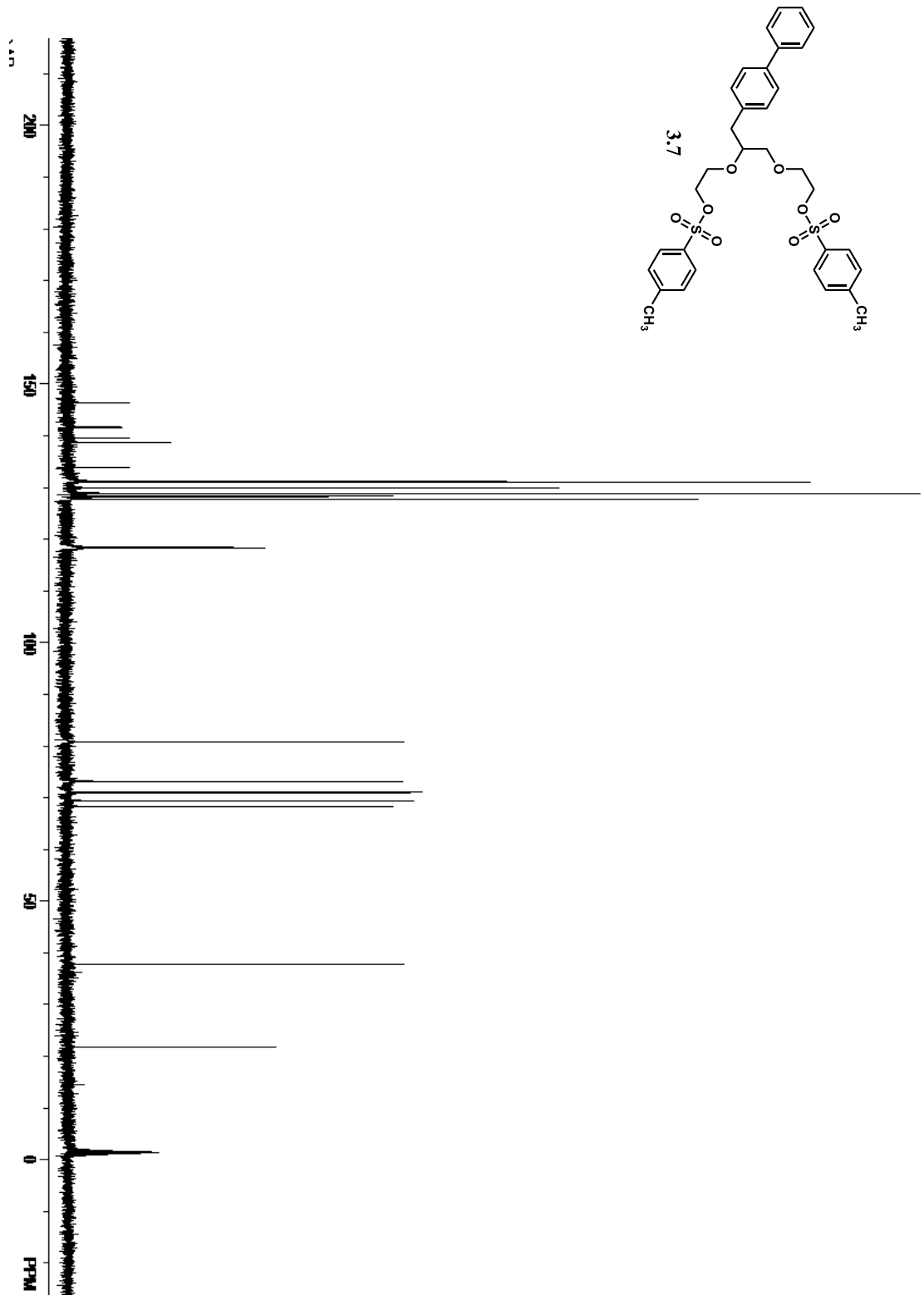

Figure 3.21 ^{13}C NMR Spectrum of **3.7**.

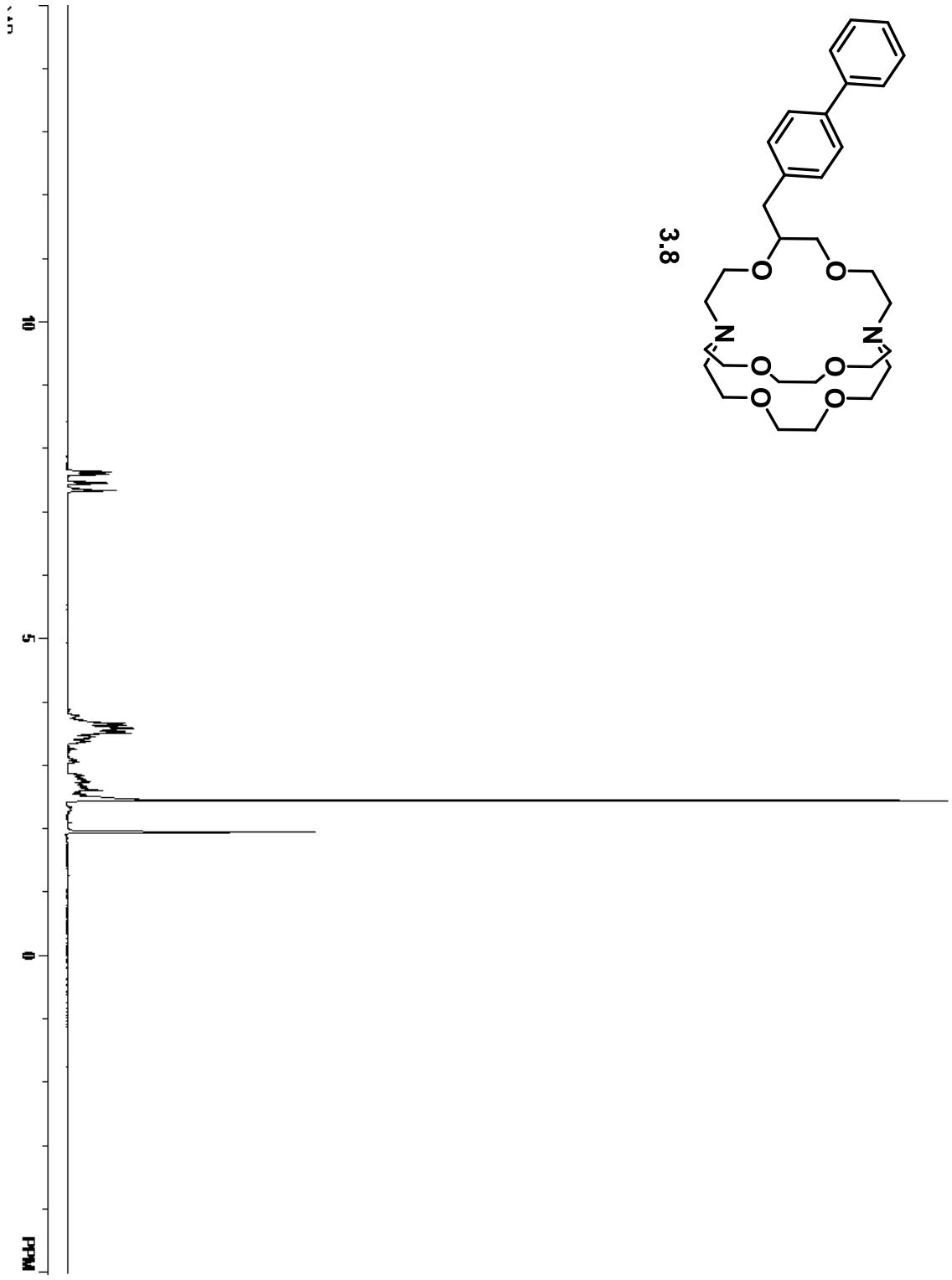

Figure 3.22 ^{1}H NMR Spectrum of **3.8**.

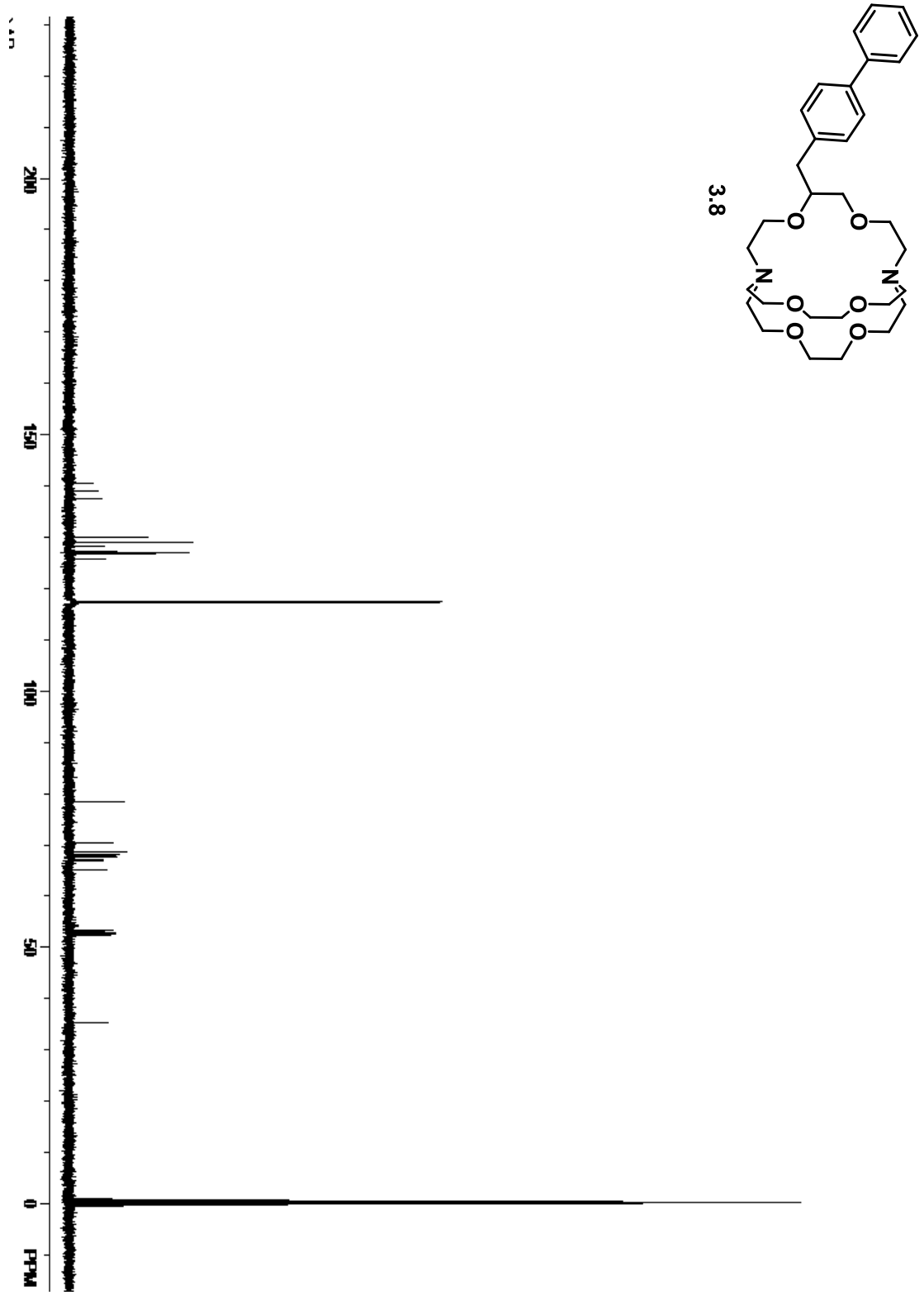

Figure 3.23 ^{13}C NMR Spectrum of **3.8**.

Chapter Four

Stability of Eu^{2+}-Containing Cryptates

Portions of this chapter were reprinted or adapted with permission from:

Garcia, J.; Kuda-Wedagedara, A. N. W.; Allen, M. J. Physical Properties of Eu^{2+}-Containing Cryptates as Contrast Agents for Ultrahigh-Field Magnetic Resonance Imaging *Eur. J. Inorg. Chem.* **2012,** *2012,* 2135–2140.

DOI: 10.1002/ejic.201101166

Link: http://onlinelibrary.wiley.com/doi/10.1002/ejic.201101166/pdf

Copyright © 2012 WILEY-VCH Verlag GmbH & Co. KGaA, Weinheim

4.1 Introduction

Kinetic stability, which relates to the inertness of a complex to transmetallation in vivo, is a critical parameter for contrast agents. Weaver and coworkers have reported the stability of cryptate Eu-**4.1** in the presence of Na^+, Ba^{2+}, and tetraethylammonium cations, which are components of electrolytes in cyclic voltammetric experiments.[1] However, the kinetic stability of Eu^{2+}-containing cryptates in the presence of biologically relevant ions, which include Ca^{2+}, Mg^{2+}, and Zn^{2+}, is of the utmost importance due to the toxicity of uncomplexed europium.[2] Therefore, our kinetic studies explored the stability of the Eu^{2+}-containing complexes of cryptands **4.1**–**4.4**, which contain a variety of functional groups (**Figure 4.1**), in the presence of Ca^{2+}, Mg^{2+}, and Zn^{2+}. The use of these ligands allowed us to establish the relationship between the ligand structure and kinetic stability. Additionally, understanding the structural characteristics of Eu^{2+}-containing cryptates that influence relaxivity as a function of pH value, temperature, and magnetic field strength is important because this knowledge should enable the design of improved ligands for use at ultrahigh field strengths.

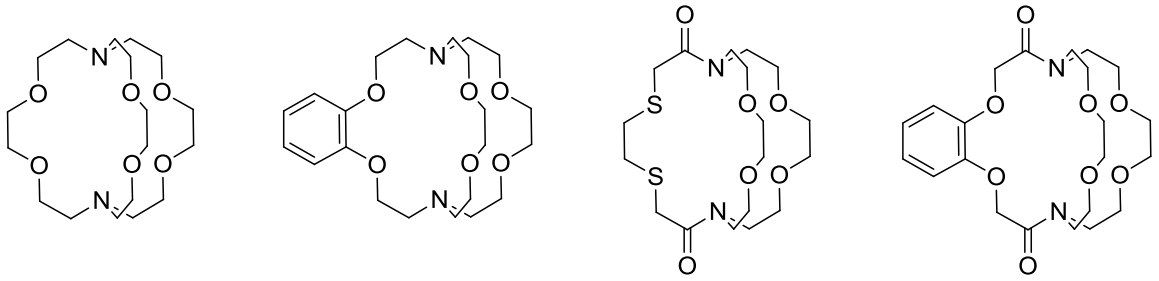

4.1 **4.2** **4.3** **4.4**

Figure 4.1 Structures of cryptands **4.1**–**4.4**.

4.2 Synthesis

The synthesis of cryptands **4.3** and **4.4** was performed by Akhila Kuda-Wedagedara, a graduate student of the Allen laboratory. To synthesize cryptands **4.3** and **4.4**, a two-step synthetic procedure was used that involved thionyl chloride and 1,4,10,13-tetraoxa-7,16-diazacyclooctadecane (diazacrown ether). Briefly, the diacids were converted into diacid chlorides followed by immediate reaction with diazacrown ether to produce the desired cryptands (**Scheme 4.1**).

Scheme 4.1 Synthesis of **4.3** and **4.4**.

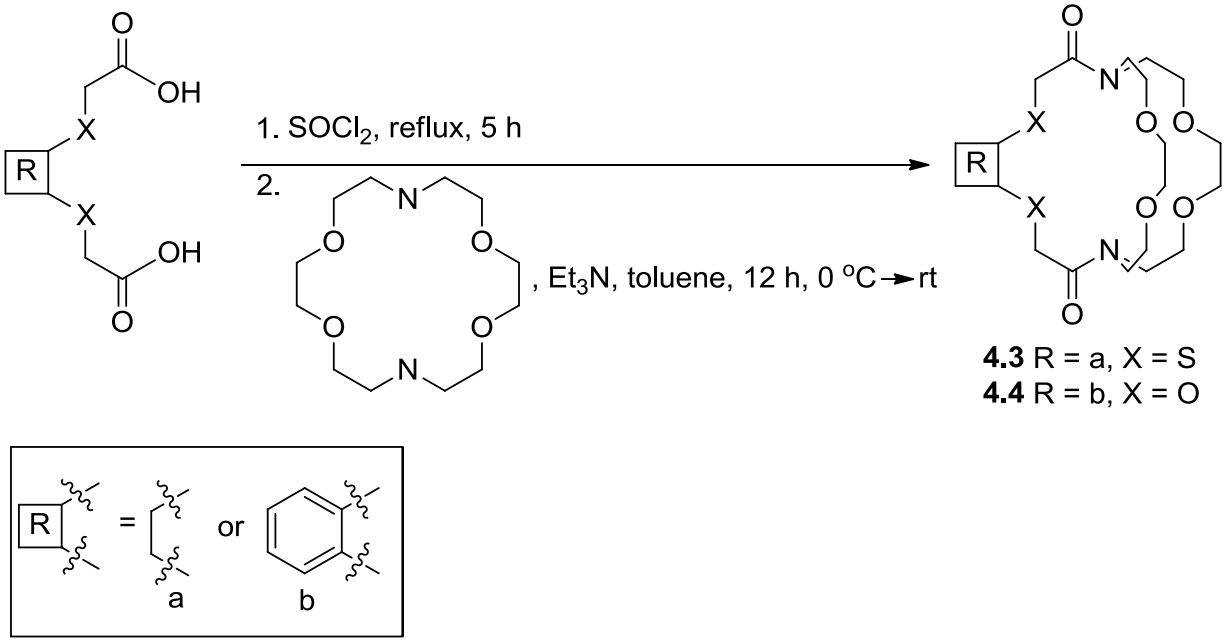

4.3 Kinetic Stability Studies

One critical feature of a useful contrast agent is its stability towards dechelation under physiological conditions. Although the thermodynamic stability constant of Eu–**4.1** is high (log K = 13.0),[3] kinetic stability is also crucial to evaluate the possibility of demetallation of contrast agents in the presence of endogenous ions. For a small-molecule contrast agent to be used in vivo, it should be kinetically inert for at least long enough to be excreted ($t_{1/2} \approx$ 5–6 min in mice, $t_{1/2} \approx$ 90 min in humans).[4] Kinetic stability is important because uncomplexed Eu^{2+} oxidizes to Eu^{3+} more easily than Eu^{2+} that is encapsulated in cryptands,[5] and Eu^{3+} is toxic.[2] Prior to excretion, one possible pathway for the release of Eu^{2+} is through transmetallation with endogenous ions. Ions that are found in blood plasma include Ca^{2+}, Mg^{2+}, and Zn^{2+} and these are of particular concern because of their abundance in serum and their tendency to be complexed by ligands. Uncomplexed Ca^{2+} and Mg^{2+} ions, despite having a lower affinity than Zn^{2+} for many ligands,[6] are present in higher concentrations than Zn^{2+} in blood serum (1.05, 1.34, and 0.125 mM for Ca^{2+}, Mg^{2+}, and Zn^{2+}, respectively).[6–8] However, the relatively low concentration of zinc in serum is sufficient to displace gadolinium in diethylenetriamine pentaacetate.[6,9] Therefore, we have examined the stability of Eu^{2+}-containing cryptates Eu–**4.1**–Eu–**4.4** towards transmetallation by monitoring the change in the longitudinal relaxation rate of water protons at 60 MHz in the presence of Ca^{2+}, Mg^{2+}, and Zn^{2+} following the procedure of Muller and coworkers.[6,9] An Eu^{2+}-containing complex was prepared in degassed phosphate buffered saline (PBS) and other metals were added to the solution. The Eu^{2+} complexes are soluble in PBS, however, uncomplexed Eu^{2+} is insoluble, and upon transmetallation, it immediately precipitates.[10] Once Eu^{2+}precipitates, a measurable decrease in the relaxation rate of the water protons is detected. A plot of the ratio of the longitudinal relaxation rates

(R_1p) of the Eu^{2+}-containing solutions at a time (t) relative to initial values ($t = 0$) vs. t allows the extent of transmetallation to be monitored. Muller and coworkers developed this technique as a way to measure the degree of transmetallation in terms of the kinetic index, which is defined as the time required to reach 80% (at this point 80% of the Eu^{2+} is dechelated by transmetallion with the endogenous ions) of the initial longitudinal relaxation rate of water protons. We used concentrations of Ca^{2+}, Mg^{2+}, and Zn^{2+} that are 2.38, 1.87, and 20 times greater than normal in vivo levels, respectively, and the results of our experiments are shown in **Figures 4.2**, **4.3**, **4.4**, and **Table 4.1**.

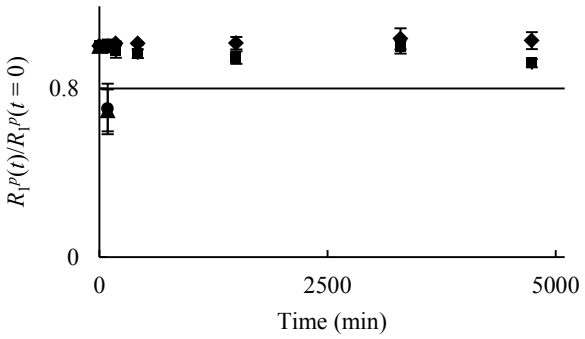

Figure 4.2 Evolution of $R_1^p(t)/R_1^p(t=0)$ versus time for the Eu^{2+}-containing cryptates Eu–**4.1** (♦), Eu–**4.2** (■), Eu–**4.3** (▲), and Eu–**4.4** (●) (2.5 mM) in the presence of Ca^{2+} (2.5 mM). The horizontal line at 0.8 is the threshold for the kinetic index. Error bars represent standard error of the mean.

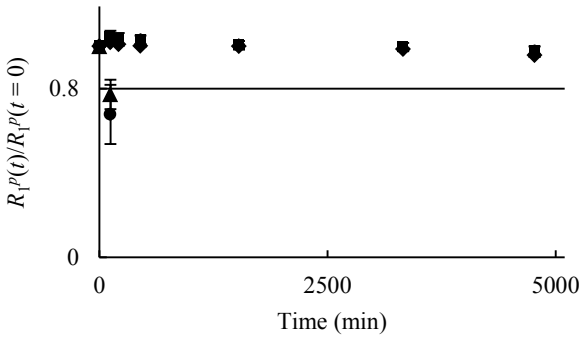

Figure 4.3 Evolution of $R_1^p(t)/R_1^p(t=0)$ versus time for the Eu^{2+}-containing cryptates Eu–**4.1** (♦), Eu–**4.2** (■), Eu–**4.3** (▲), and Eu–**4.4** (●) (2.5 mM) in the presence of Mg^{2+} (2.5 mM). The horizontal line at 0.8 is the threshold for the kinetic index. Error bars represent standard error of the mean.

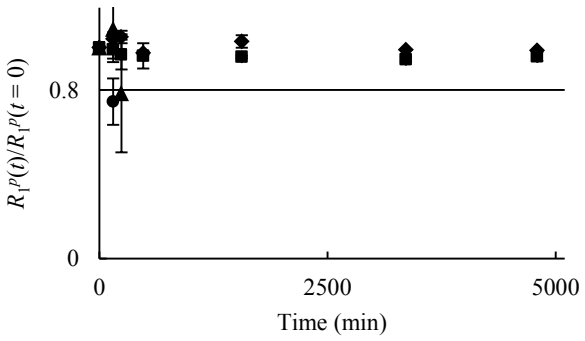

Figure 4.4 Evolution of $R_1^p(t)/R_1^p(t=0)$ versus time for the Eu^{2+}-containing cryptates Eu–**4.1** (♦), Eu–**4.2** (■), Eu–**4.3** (▲), and Eu–**4.4** (●) (2.5 mM) in the presence of Zn^{2+} (2.5 mM). The horizontal line at 0.8 is the threshold for the kinetic index. Error bars represent standard error of the mean.

Table 4.1 Calculated %Eu^{2+} dechelated via transmetalation in the presence of Ca^{2+}, Mg^{2+}, and Zn^{2+} after 4740 min (Ca^{2+}), 4770 min (Mg^{2+}), and 4800 min (Zn^{2+}) treatment of 2.5 mM of the corresponding endogeneous ions.

Complexes	Ca^{2+} (%)	Mg^{2+} (%)	Zn^{2+} (%)
Eu–**4.1**	9	4	7
Eu–**4.2**	17	8	14

As seen from the ratio of the longitudinal relaxation rates vs. *t* (**Figures 4.2**, **4.3**, and **4.4**), the kinetic indices of Eu–**4.1** and Eu–**4.2** are greater than 4740 min in the presence of Ca^{2+}, Mg^{2+}, and Zn^{2+}(**Table 4.2**), which is more than 53 times longer than the half-life of small molecules in vivo. This kinetic index indicates that Eu–**4.1** and Eu–**4.2** did not fall below 80% of their efficacy during this time, which suggests that these complexes are inert to transmetallation in the presence of Ca^{2+}, Mg^{2+}, and Zn^{2+} at greater than normal in vivo levels. Interestingly, the values in the presence of Zn^{2+} appeared to decrease initially and then increase again; however, analysis of the variance revealed that all of the data points for Eu–**4.1** and Eu–**4.2** in the presence of Zn^{2+} are not different (α = 0.01). The stability of these Eu^{2+}-containing complexes is likely due to the effective binding of the cryptand to the metal ion.

Table 4.2 Kinetic index data.

Complexes	Ca^{2+} (min)	Mg^{2+} (min)	Zn^{2+} (min)
Eu–**4.1**	>4740	>4770	>4800
Eu–**4.2**	>4740	>4770	>4800
Eu–**4.3**	>0,<90	>0,<120	>0,<240
Eu–**4.4**	>0,<90	>0,<120	>150,<240

Although Eu–**4.1** and Eu–**4.2** showed stability towards transmetallation in the presence of endogenous metal ions, precipitates were observed as soon as PBS was added to Eu–**4.3** and Eu–**4.4**, consequently, these data are not included in **Figures 4.1**, **4.2**, and **4.3**. This observation suggests a weaker interaction between Eu^{2+} and amide-containing **4.3** and **4.4** relative to **4.1** and **4.2**. A further decrease in the longitudinal relaxation rate was observed in the presence of Ca^{2+}, Mg^{2+}, and Zn^{2+}. Studies with Eu–**3** and Eu–**4** were stopped once the longitudinal relaxation rate fell below 80 % of the initial value.

The weak binding of Eu^{2+} to **4.3** and **4.4** can be attributed to the presence of amide groups in the cryptand structure. Amides have resonance structures (**Figure 4.5**) that change both the electronic and structural properties of the ligands relative to **4.1** and **4.2**. Because of the presence of partial positive charges on nitrogen atoms, it is unlikely that these nitrogen atoms serve as donors. Thus, the denticity of **4.3** and **4.4** is decreased relative to that of **4.1** and **4.2**. Furthermore, when the lone pairs on the nitrogen atoms are delocalized, the geometry of the nitrogen atoms changes from pyramidal to trigonal planar, and this change in geometry could also make it harder for Eu^{2+} to coordinate with **4.3** and **4.4** relative to **4.1** and **4.2**. Consequently, a decrease in the kinetic stability is observed.

Although amide-containing cryptands are not good ligands for Eu^{2+}, Eu–**4.1** and Eu–**4.2** were observed to have high kinetic stabilities in the presence of Ca^{2+}, Mg^{2+}, and Zn^{2+} in concentrations higher than those found in vivo, a promising result for their potential use as contrast agents.

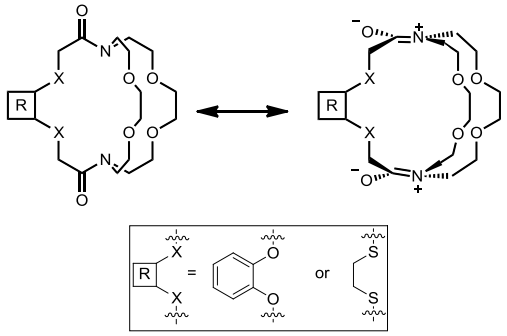

Figure 4.5 Contributing resonance structures of cryptands **4.3** and **4.4**.

4.4 Conclusion

Eu^{2+}-containing cryptates that have no amide moieties in their structures were kinetically stable in the presence of Ca^{2+}, Mg^{2+}, and Zn^{2+}at concentrations 1.87–20 times higher than biological concentrations. In addition, transmetallation studies demonstrated that the kinetic stability of Eu^{2+}-containing cryptates is affected by the presence of amides.

4.5 Experimental Section

4.5.1 Materials

Commercially available chemicals were of reagent-grade purity or better and were used without further purification unless otherwise noted. Water was purified using a PURELAB Ultra Mk2 water purification system (ELGA). Dicholoromethane was dried using a solvent purification system (Vacuum Atmospheres Company) and degassed under vacuum. Triethylamine was distilled from CaH_2 under an atmosphere of Ar.[11] Flash chromatography was performed using silica gel 60, 230–400 mesh (EMD Chemicals).[12] Analytical TLC was carried out with ASTM TLC plates precoated with

silica gel 60 F_{254} (250 μm layer thickness). TLC visualization was accomplished using a UV lamp followed by charring with potassium permanganate stain (2 g of $KMnO_4$, 20 g of K_2CO_3, 5 mL of 5% w/v aqueous NaOH, 300 mL of H_2O).

4.5.2 Characterization

^{1}H NMR spectra were obtained with a Varian Unity 400 (400 MHz) spectrometer, and ^{13}C NMR spectra were obtained with a Varian Unity 400 (101 MHz) spectrometer. Chemical shifts are reported relative to residual solvent signals ($CDCl_3$: ^{1}H: δ = 7.27, ^{13}C: δ = 77.23 ppm). ^{1}H NMR spectroscopic data are assumed to be first order, and the apparent multiplicity is reported as d = doublet and m = multiplet. HRMS (ESI) were obtained with an electrospray time-of-flight high-resolution Waters Micromass LCT Premier XE mass spectrometer. Samples for inductively coupled plasma mass spectrometry (ICP-MS) were diluted using aqueous nitric acid (2 % v/v). Standard solutions were prepared by serial dilution of a Eu standard (High-Purity Standards). ICP-MS measurements were conducted with a PE Sciex Elan 9000 ICP-MS instrument with a cross-flow nebulizer and Scott-type spray chamber. Longitudinal relaxation times, T_1, were measured using standard recovery methods with a Bruker Minispec mq 60 [1.4 T] at 60 MHz and 37 °C.

4.5.3 Synthesis

4,7,21,24-tetraoxa-13,16-dithia-1,10-diazabicyclo[8.8.8]hexacosane-11,18-dione (4.3). A solution of (ethylenedithio)diacetic acid (0.500 g, 2.38 mmol) in thionyl chloride (5.0 mL, 68 mmol) under Ar was heated at reflux for 5 h. Excess thionyl chloride was removed under reduced pressure, and the residue was dissolved in anhydrous toluene (40 mL). The resulting solution and a solution of 1,4,10,13-tetraoxa-7,16-diazacyclooctadecane and triethylamine (1.5 mL, 0.010 mol, 4.2 equiv) in anhydrous toluene (40 mL) were added

simultaneously (50 mL/h) to a separate flask containing anhydrous toluene (100 mL) at 0–5 ^{o}C under an Ar atmosphere. The resulting solution was stirred for 12 h at ambient temperature. A yellow–orange suspension formed and was filtered, and the solvent from the filtrate was removed under reduced pressure. Purification using silica gel chromatography (10:1 CH_2Cl_2/methanol) yielded 0.215 g (43%) of **4.3** a fluffy yellow solid. ^{1}H NMR (400 MHz, $CDCl_3$, δ): 2.77–4.32 (m, C*H*$_2$); ^{13}C NMR (101 MHz, $CDCl_3$, δ): 32.9 (*C*H_2), 33.6 (*C*H_2), 49.7 (*C*H_2), 50.5 (*C*H_2), 69.2 (*C*H_2), 69.5 (*C*H_2), 71.2 (*C*H_2), 71.4 (*C*H_2), 170.7; TLC: R_f = 0.54 (10:1 CH_2Cl_2/methanol); HRESIMS (*m*/*z*): $[M + Na]^+$ calcd for $NaC_{18}H_{32}N_2S_2O_6$, 459.1600; found, 459.1602.

5,6-benzo-4,7,13,16,20,23-hexaoxa-1,10-diazabicyclo[8.8.8]hex-acosane-2,9-dione (4.4). A solution of catechole-1,4-*o,o*-diacetic acid (0.40 g, 1.8 mmol) in thionyl chloride (5.0 mL, 68 mmol) under Ar was heated at reflux for 5 h. Excess thionyl chloride was removed under reduced pressure, and the residue was dissolved in anhydrous toluene (25 mL). The resulting solution and a solution of 1,4,10,13-tetraoxa-7,16-diazacyclooctadecane (0.32 g, 1.2 mmol, 1.0 equiv) and triethylamine (0.50 mL, 3.3 mmol, 2.4 equiv) in anhydrous toluene (25 mL) were added simultaneously (50 mL/h) to a separate flask containing anhydrous toluene (60 mL) at 0–5 ^{o}C under an Ar atmosphere. The solution was stirred for 12 h at ambient temperature. An orange suspension formed and was filtered, and the solvent was removed under reduced pressure. Purification using silica gel chromatography (9:1 CH_2Cl_2/methanol) yielded 0.144 g (36%) of **4.4** a fluffy white solid. ^{1}H NMR (400 MHz, $CDCl_3$, δ): 2.77–3.22 (m, C*H*$_2$, 2H), 3.37–3.83 (m, C*H*$_2$, 20H), 4.08–4.35 (m, C*H*$_2$, 2H), 4.64–4.91 (m, C*H*$_2$, 2H), 5.15–5.23 (d, *J* = 14.4 Hz, C*H*$_2$, 2H), 6.86–7.10 (m, C*H*, 4H); ^{13}C NMR (101 MHz, $CDCl_3$, δ): 48.5 (*C*H_2), 48.9 (*C*H_2), 68.1 (*C*H_2), 69.4 (*C*H_2), 69.7 (*C*H_2), 71.1 (*C*H_2), 71.3 (*C*H_2), 116.1 (*C*H), 122.2 (*C*H),

148.3, 169.0; TLC: R_f = 0.8 (9:1 CH_2Cl_2/methanol); HRESIMS (*m*/*z*): $[M + Na]^+$ calcd for $NaC_{22}H_{32}N_2O_8$, 475.2062; found, 475.2060.

General Procedure for the Synthesis of Eu–**4.1**–Eu–**4.4:** A degassed aqueous solution of $EuCl_2$ (1 equiv.) was mixed with a degassed aqueous solution of a cryptand (2 equiv.). The resulting mixture was stirred for 12 h at ambient temperature under Ar. Degassed PBS (10×) was added, and stirring was continued for 30 min. The concentration of Eu in the resulting solution was verified by ICP-MS, and the solution was used directly for relaxivity measurements. For transmetallation experiments, the same procedure was followed with only 1 equiv. of ligand.

4.5.4 Transmetallation Kinetics

The following procedure was adapted from Muller and coworkers.[9] A stock solution of the Eu^{2+}-containing cryptate (5 mM) was prepared in degassed PBS under an Ar atmosphere. To an aliquot of this solution was added a solution of Ca^{2+} (12.1 mM) in degassed PBS such that the resulting solution was 2.5 mM in both Eu^{2+} and Ca^{2+}. This solution was stirred at 37 °C under Ar. Aliquots were taken at 90, 180, 420, 1500, 3300, and 4740 min after the addition of Ca^{2+}. All aliquots were filtered using 0.2 μm filters prior to T_1 measurements. The t_1 value of these aliquots (60 MHz, 37 °C) was immediately measured at each time point. The experiment was triplicated with independently prepared solutions. The entire procedure was repeated using Mg^{2+} (16.4 mM) and Zn^{2+} (9.97 mM) in place of Ca^{2+} (12.1 mM). Statistical analysis of variance was performed using the program found at faculty.vassar.edu/lowry/anova1u.html.

4.6 References

(1) Yee , E. L.; Gansow, O. A.; Weaver, M. J. *J. Am. Chem. Soc.* **1980,** *102,* 2278–2285.

(2) (a) Wolfson, J. M.; Kearns, D. R. *Biochemistry* **1975,** *14,* 1436–1444. (b) Ogawa, Y.; Suzuki, S.; Naito, K.; Saito, M.; Kamata, E.; Hirose, A.; Ono, A.; Kaneko, T.; Chiba, M.; Inaba, Y.; Kurokawa, Y. *J. Environ. Pathol. Toxicol. Oncol.* **1995,** *14,* 1–9.

(3) Burns, J. H.; Baes Jr., C. F. *Inorg. Chem.* **1981,** *20,* 616–619.

(4) (a) Penfield, J. G.; Reilly Jr., R. F. *Nat. Clin. Pract. Nephrol.* **2007,** *3,* 654–668. (b) Tweedle, M. F.; Wedeking, P.; Kumar, K. *Invest. Radiol.* **1995,** *30,* 372–380.

(5) Gamage, N.-D. H.; Mei, Y.; Garcia, J.; Allen, M. J. *Angew. Chem. Int. Ed.* **2010,** *49,* 8923–8925.

(6) Laurent, S.; Vander Elst, L.; Henoumont, C.; Muller, R. N. *Contrast Media Mol. Imaging* **2010,** *5,* 305–308 .

(7) (a) Deng, B.; Zhu, P.; Wang,Y.; Feng, J.; Li, X.; Xu, X.; Lu, H.; Xu, Q. *Anal. Chem.* **2008,** *80,* 5721–5726. (b) Pors Nielsen, S. *Scand. J. Clin. Lab. Invest.* **1969,** *23,* 219–225.

(8) Cu^{2+} and Fe^{3+} were not considered in the transmetallation studies because free Cu^{2+} in human plasma is very low (3–9 μM)[14] and Fe^{3+} is tightly bound to storage proteins (ferritin and hemosiderin), consequently, making this ion unavailable for transmetallation.[15]

(9) Laurent, S.; Vander Elst, L.; Muller, R. N. *Contrast Media Mol. Imaging* **2006,** *1,* 128–137.

(10) A xylenol orange-based colorimetric assay was used to test for the presence of free europium as described in ref.[13] When a solution of $EuCl_2$ (2.5 mM) in PBS was prepared, a precipitate immediately formed. The filtrate of the mixture was exposed to air to allow oxidation of Eu^{2+} to Eu^{3+}, and the Eu^{3+} concentration was measured with xylenol orange as

an indicator using a calibration curve made from a purchased Eu standard. A concentration of 1.63 μM was measured, which corresponds to 0.07% of the original Eu in solution.

(11) Armarego, W. L. F.; Chai, C. L. L. Purification of Laboratory Chemicals, Fifth Edition; Elsevier: Burlington, MA, **2003**.

(12) Still, W. C.; Kahn, M.; Mitra, A. *J. Org. Chem.* **1978,** *43,* 2923–2925.

(13) Averill, D. J.; Garcia, J.; Siriwardena-Mahanama, B. N.; Vithanarachchi, S. M.; Allen, M. J. *J. Vis. Exp.* **2011,** *53,* e2844.

(14) Tedeschi, A.; Arquati, M.; Lorini, M.; Milazzo, N.; Miadonna, A. *Agents Actions* **1992,** *1–2,* 16–24.

(15) Cacheris, W. P.; Quay, S. C.; Rocklage, S. M. *J. Magn. Reson. Im.* **1990,** *8,* 467–481.

4.7 ^{1}H and ^{13}C NMR Spectra of 4.3 and 4.4

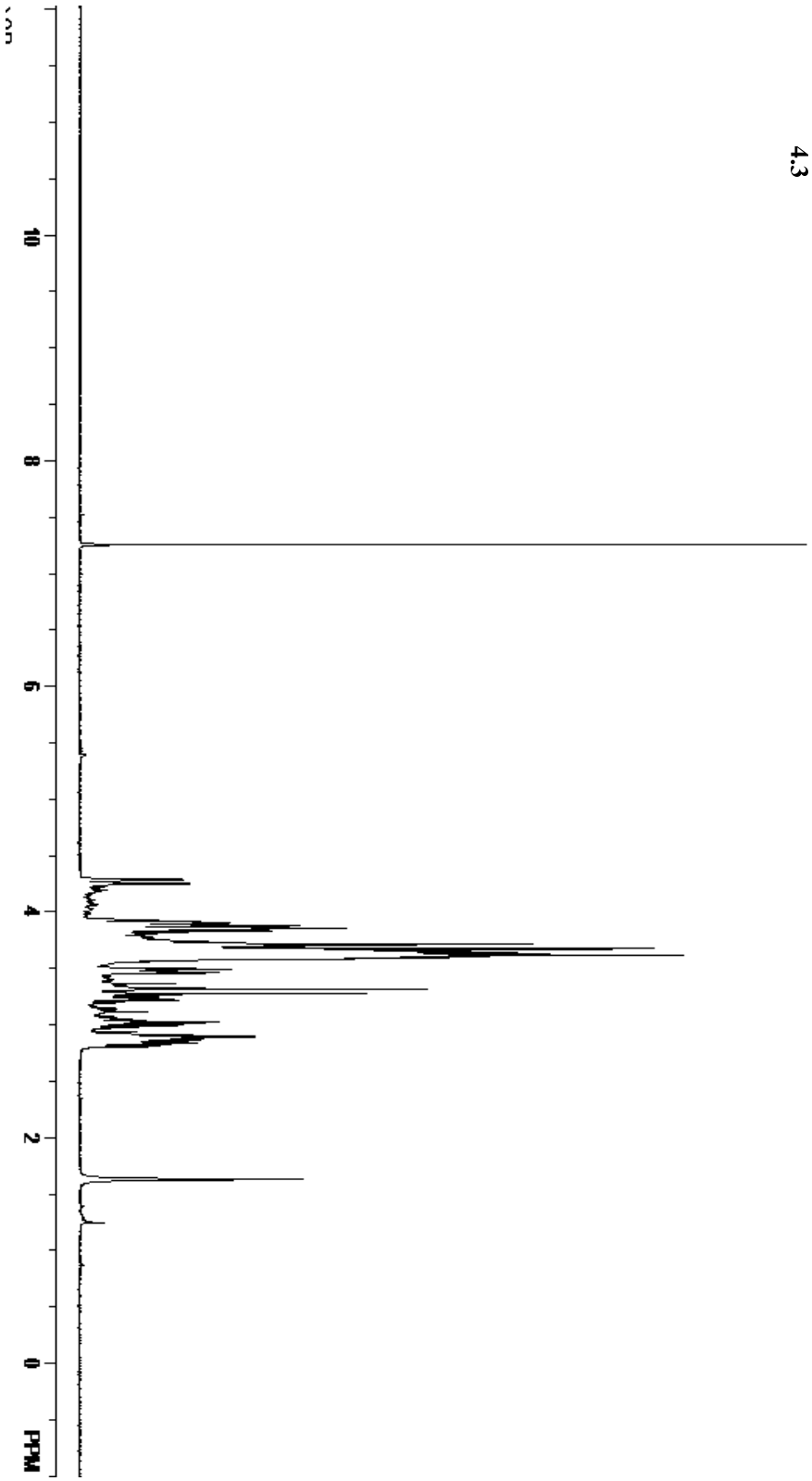

Figure 4.6 ^{1}H NMR Spectrum of **4.3**.

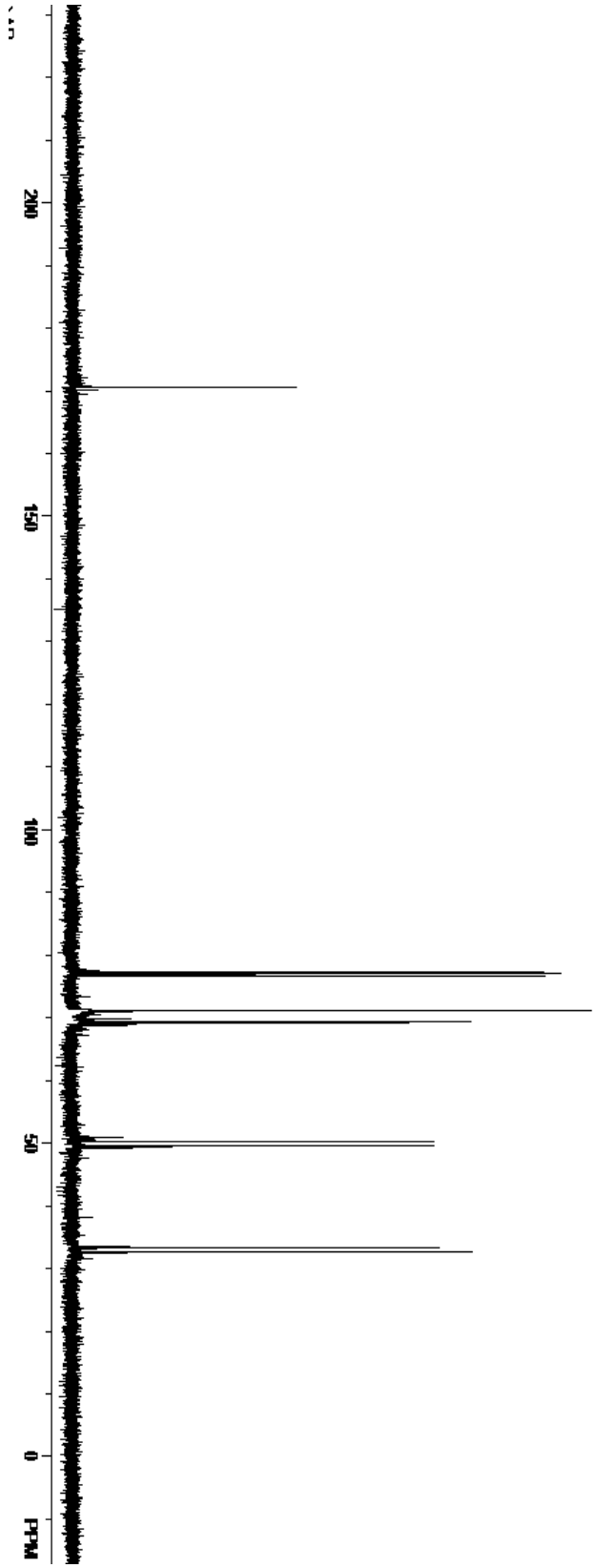

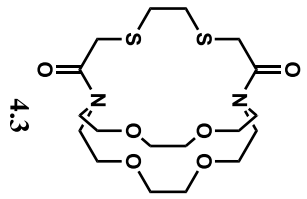

4.3

Figure 4.7 ^{13}C NMR Spectrum of **4.3**.

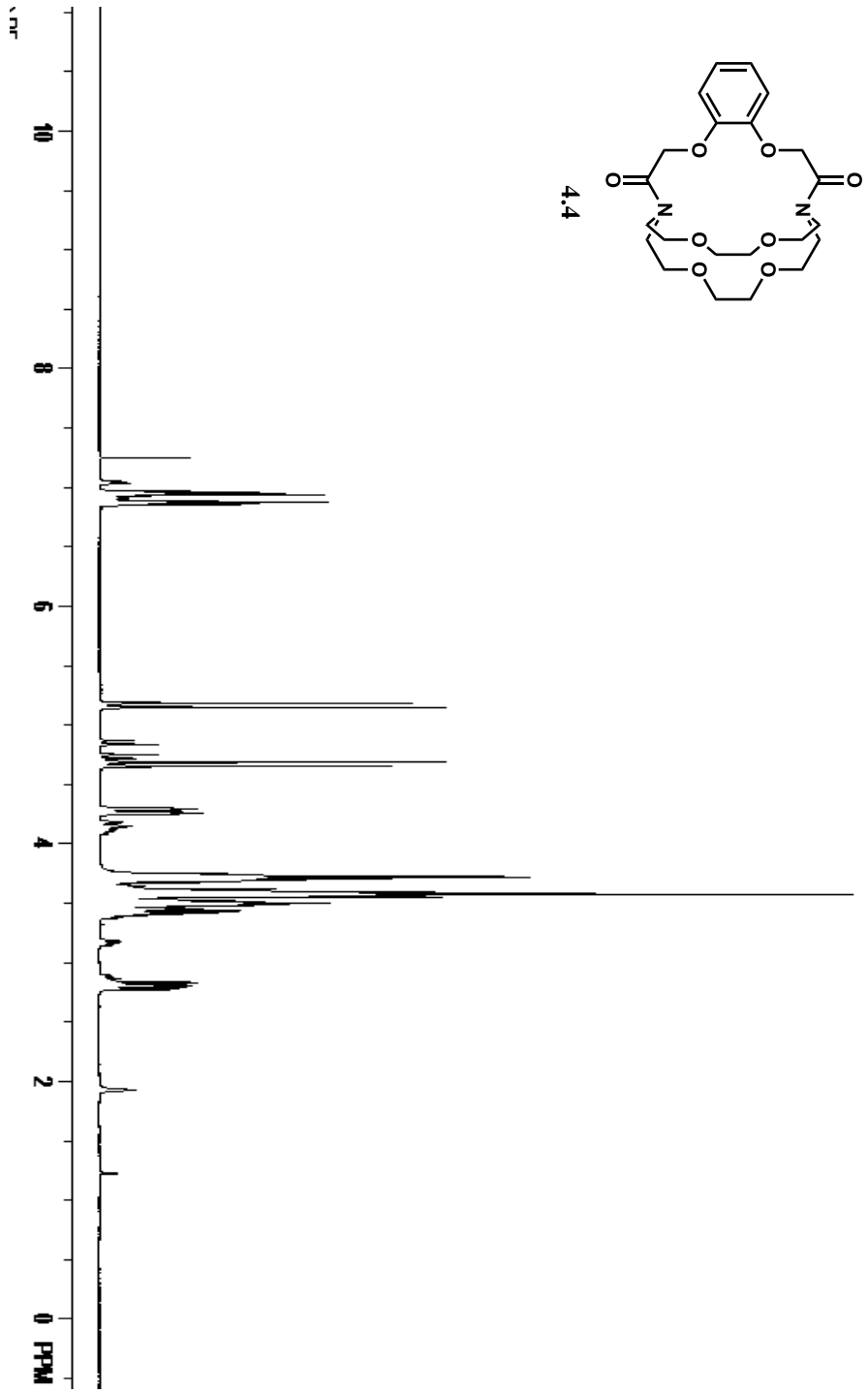

Figure 4.8 ^{1}H NMR Spectrum of **4.4**.

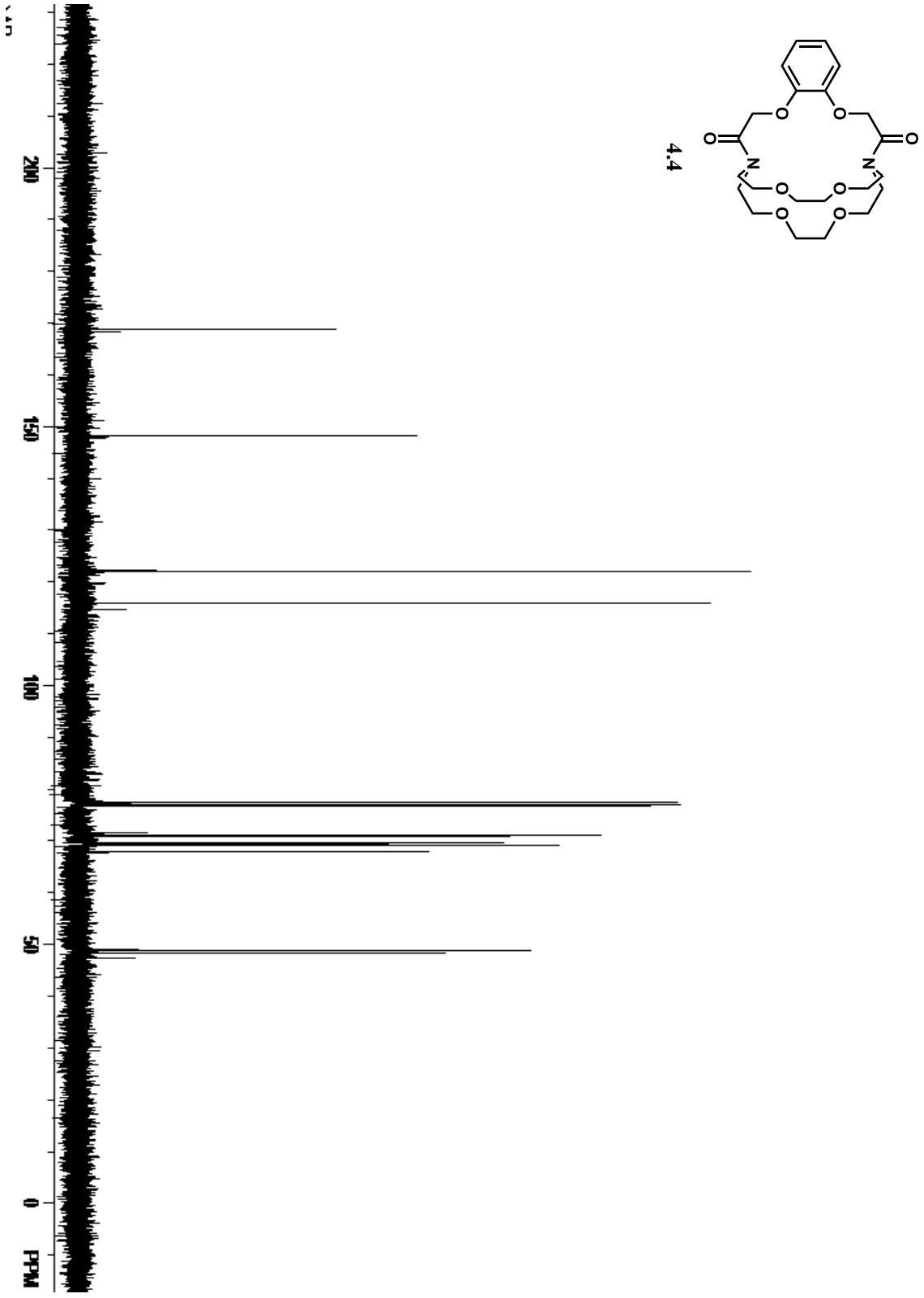

Figure 4.9 ^{13}C NMR Spectrum of **4.4**.

Chapter Five

Interaction of Biphenyl Functionalized Eu^{2+}-Containing Cryptate with Albumin Binding: Implications to Contrast Agents in MRI

Reprinted from Inorg. Chim. Acta, 393, Garcia, J.; Allen, M. J., Interaction of biphenyl-functionalized Eu^{2+}-containing cryptate with albumin: Implications to contrast agents in magnetic resonance imaging, 324–327, 2012. Copyright (2012), with permission from Elsevier.

5.1 Introduction

Magnetic resonance imaging (MRI) is a noninvasive imaging modality that can be used to study anatomical structures,[1] and the use of ultra-high field strength (≥7 T) magnets enables faster acquisition of MR images with increased spatial resolution.[2–4] However, common contrast agents such as low-molecular-weight Gd^{3+}-containing complexes become less efficient at ultra-high field strengths relative to lower field strengths.[5] Unlike these Gd^{3+}-based contrast agents, Eu^{2+}-containing cryptates have higher relaxivity values at ultra-high field strengths (7 and 9.4 T) than at lower field strengths (1.4 and 3 T).[6–7]

I hypothesized that the relaxivity of Eu^{2+}-containing cryptates could be increased by using strategies that improve the relaxivity of Gd^{3+}-based agents. One of these strategies is the slowing of molecular-tumbling rate that can be influenced by covalent or noncovalent interactions with macromolecules including proteins.[1,8–27] Human serum albumin (HSA), the most abundant protein in plasma with concentration of ~670 μM or 4.5% (w/v),[16] noncovalently binds to some contrast agents that contain lipophilic moieties.[16–25] McMurry and coworkers reported an increase in relaxivity of over 200% as a result of the noncovalent interaction of albumin with a Gd^{3+}-containing complex functionalized with

biphenyl.[25] Because of the work with Gd^{3+} and the ability to influence the properties of Eu^{2+} with functionalized cryptands,[28] we hypothesized that a cryptand with a biphenyl group would produce a Eu^{2+}complex that interacts with albumin to result in an increase in relaxivity.

To test my hypothesis, I synthesized biphenyl-modified Eu^{2+}-containing cryptate **5.1** (**Figure 5.1**), and measured the relaxivity of cryptate **5.1** in the presence and absence of HSA at different field strengths (1.4, 3, 7, 9.4, and 11.7 T). I compared the resulting relaxivity values to estimates calculated using the Solomon–Bloembergen–Morgan equations.[29] I also illustrated the effect of albumin on the contrast-enhancing ability of **5.1** using phantom images acquired at 7 T. Finally, I performed variable-temperature ^{17}O NMR experiments that probed the molecular basis of the relaxivity values of complex **5.1** in the presence and absence of HSA.

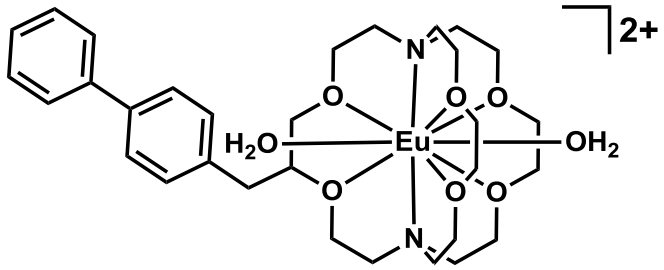

5.1

Figure 5.1 Structure of biphenyl-functionalized Eu^{2+}-containing complex **5.1**.

5.2 Results and Discussion

Biphenyl-functionalized cryptate **5.1** was designed based on the structure of Gd^{3+}-based contrast agents that interact with HSA. These Gd^{3+}-containing albumin-binding contrast agents contain lipophilic aryl groups such as the biphenyl moiety that enable them to interact with HSA.[16–25] Therefore, I expected that the lipophilic biphenyl moiety in

cryptate **5.1** would enable investigation of the effect of albumin binding on the relaxivity of Eu^{2+} at different field strengths.

5.2.1 Influence of Magnetic Field on the Relaxivity of 5.1 and 5.1–HSA

The relaxivity, r_1, of **5.1** in PBS in the presence and absence of HSA was measured at multiple field strengths, and because not all of the magnets were capable of variable-temperature measurements, I separated data into **Figure 5.2a** and **5.2b** so that measurements obtained at each temperature could be compared. In the absence of HSA, the r_1 of **5.1** at 20 °C is higher at 7 and 9.4 T than at 3 T suggesting that this complex is more efficient at ultra-high field strengths than at lower field strengths (**Figure 5.2a**). However, I found that the r_1 values at 3 and 11.7 T were not different (Student *t* test). Moreover, the relaxivity of **5.1** as a function of field strength is similar to other Eu^{2+}-containing cryptates in the same conditions.[7] In the presence of HSA (4.5% w/v), the relaxivity of **5.1** decreased by 24.8 ± 0.6% to 40.2 ± 0.2% at field strengths of 3, 7, 9.4, and 11.7 T (**Figure 5.2a**). However, at 37 °C and 1.4 T, the r_1 of **5.1** in the presence of albumin was 171 ± 11% higher than in the absence of HSA (**Figure 5.2b**). An increase of 218% in relaxivity (measured at 37 °C and 0.47 T MHz) was reported by McMurry and coworkers for a Gd^{3+}-containing complex functionalized with biphenyl in the presence of albumin.[25] McMurry's report and the relaxation data of **5.1** at 1.4 T indicate that the observed relaxation enhancement of **5.1** in the presence of HSA is likely due to the interaction of the biphenyl moiety of Eu^{2+}cryptate with albumin.[30] However, the relaxivity of **5.1** was 15.2 ± 0.5% and 49.8 ± 0.2% lower in the presence of HSA at 37 °C and 9.4 T and 11.7 T, respectively. The observed decreasing trend in relaxivity of **5.1** in the presence of HSA at 37 °C as a function of field strength is consistent with the trend obtained by calculating the

relaxivity of a slowly rotating Eu^{2+}-containing cryptate at multiple field strengths using the Solomon–Bloembergen–Morgan equations (**Figure 5.2b** and **Table 5.1**).

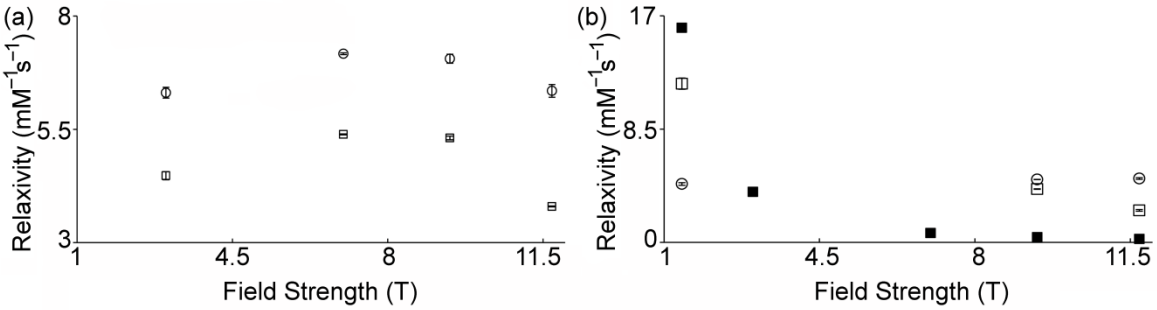

Figure 5.2 (a) Proton longitudinal relaxivity (20 °C, pH = 7.4) of biphenyl-functionalized cryptate **5.1** in the absence (○) and presence (□) of HSA as a function of magnetic field strength. (b) Proton longitudinal relaxivity (37 °C, pH = 7.4) of biphenyl-functionalized cryptate **5.1** in the absence (○) and presence (□) of HSA as a function of magnetic field strength. Simulated relaxivity values (■) of a slowly rotating Eu^{2+}-containing complex at 37 °C. Values at 1.4, 3, 7, and 11.7 T without HSA are from Ref. 6. HSA concentration was 4.5% (w/v). Error bars represent standard error of the mean of 3–9 independently prepared samples.

5.2.2 Albumin Titration

To better understand the effect of albumin on the relaxivity of **5.1**, titration experiments were performed using different percentages (2, 4.5, 6, 10, 15, and 25% w/v) of HSA while keeping the concentration (1 mM) of cryptate **5.1** constant. In preparation of **5.1**, two equivalents of the biphenyl cryptand were used for each equivalent of Eu^{2+} to facilitate metalation of the biphenyl cryptand; therefore, the samples 2, 4.5, 6, and 10% HSA have an excess of biphenyl relative to HSA (HSA/**5.1** < 1 except 10% HSA sample) and samples with 15 and 25% HSA have a subcess of biphenyl relative to HSA (HSA/**5.1** > 1). The MR images (**Figure 5.3a**) of **5.1** with HSA/**5.1** ratios less than one have higher signal

intensities as compared to the images of samples with HSA/**5.1** ratios greater than 1. To quantify this observation, the proton longitudinal relaxation rate, $1/T_1$, of the sample with the lowest HSA/**5.1** ratio is $102.7 \pm 0.3\%$ higher than the sample with the highest HSA/**5.1** ratio and $47.0 \pm 0.2\%$ higher than the other sample (15% HSA) that has an excess of HSA relative to biphenyl (**Figure 5.3b**). The difference in signal intensity and $1/T_1$ values among the samples indicate that the presence of albumin affects the relaxivity of complex **5.1** and does not translate to a higher signal intensity and higher efficacy of **5.1** at ultra-high fields. These observations support the relaxivity measurements described in **Figure 5.1**.

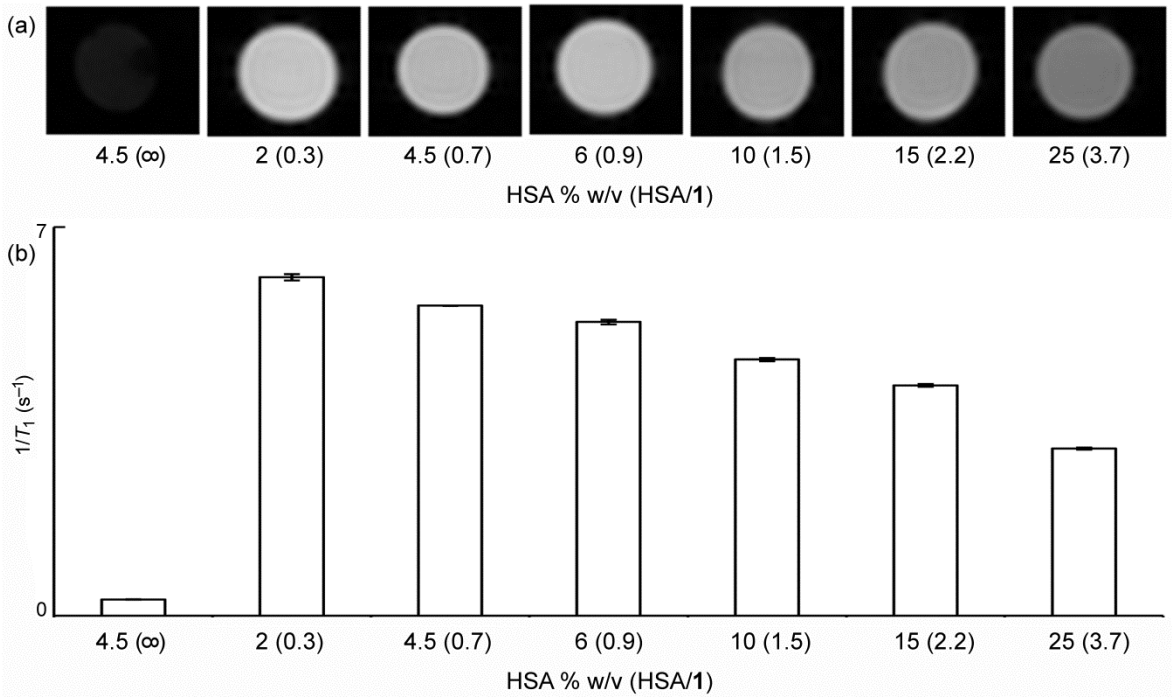

Figure 5.3 (a) T_1-weighted MR images of albumin-containing solutions of biphenyl-functionalized cryptate **5.1** at 7 T and 20 °C. The diameter of the tubes that were used for imaging was 6 mm. Imaging parameters were T_R = 21 ms; T_E = 3.26 ms; and resolution = 0.27 × 0.27 × 2 mm^3. (b) Proton longitudinal relaxation rate (20 °C, pH = 7.4) as a function of % HSA at 7 T. The concentration of cryptate **5.1** was 1 mM. Error bars represent standard error of the mean of three samples. [a]No cryptate.

5.2.3 ^{17}O NMR Spectroscopy

To explain the observations of relaxivity, I performed variable-temperature ^{17}O NMR measurements using a sample of **5.1** in PBS and **5.1** in PBS with 25% HSA. I chose 25% HSA because the majority of **5.1** was expected to be bound to albumin at this percentage,[25] and the ^{17}O NMR data obtained from this sample would be representative of the molecular properties of cryptate **5.1** that is bound to HSA. The molecular properties that influence relaxivity that were studied using variable-temperature ^{17}O NMR spectroscopy were the residence lifetime of bound water molecules, τ_m^{298}; the water-exchange rate, k_{ex}^{298} =

$1/\tau_m^{298}$; and the number of inner-sphere water molecules, q (**Table 5.1**). While the residence lifetime of bound water of cryptate **5.1** was not different (Student t test) in the presence and absence of albumin, the number of inner-sphere water molecules was reduced from two to one upon addition of albumin indicating that the observed decrease in relaxivity for cryptate **5.1** in the presence of albumin at 3, 7, 9.4, and 11.7 T is likely caused by the displacement of inner-sphere water molecules from the Eu^{2+} complex. Moreover, the residence lifetime of bound water was not different in the presence or absence of albumin suggesting that protein side chains do not hinder the remaining bound water molecule from exchanging with the bulk solvent. With the water-exchange rate and the number of inner-sphere water molecules of **5.1** in the presence of HSA remaining constant at different field strengths, the relaxivity enhancement observed at 1.4 T likely can be attributed to the enhanced contribution of rotational correlation rate at this field strength.

Table 5.1 Results of ^{17}O NMR experiments of cryptate **5.1** with and without albumin.

	5.1[a]	**5.1**–HSA[b]
τ_m^{298} (ns)	48 ± 4	40 ± 7
k_{ex}^{298} (10^8 s^{-1})	0.21	0.25
q	2	1
ΔH (kJ/mol)	70 ± 2	62 ± 8

[a] Reference 6, [b]HSA concentration was 25% (w/v)

5.3 Conclusions

The relaxation profile of Eu^{2+}-containing cryptate **5.1** in the absence of albumin shows that cryptate **5.1** is more efficient at higher field strengths (7 and 9.4 T) than at lower field

strengths (1.4 and 3 T). MR images and $1/T_1$ values of samples with different HSA/**5.1** ratios suggest that possible interaction of **5.1** with HSA occurs, but this interaction does not lead to an increase in relaxivity of Eu^{2+} at higher field strengths ($\geqslant$3 T). However, in the presence of albumin, an increase in relaxivity of **5.1** is only observed at 1.4 T likely due to decreased rotational correlation rate values, and a decrease in relaxivity was observed at 3, 7, 9.4, and 11.7 T because of a decreased water-coordination number. These data are in agreement with calculations made using the Solomon–Bloembergen–Morgan equations. Studies using different lengths of linkers between the biphenyl and cryptate could provide a good insight on the influence of albumin interaction on the relaxivity of cryptate **5.1**. Also, binding a Eu^{2+}-containing cryptate to different sizes of macromolecules could provide a better understanding on the effect of macromolecular binding on the relaxivity of Eu^{2+}-containing cryptates at higher fields. These studies are currently underway in our laboratory.

5.4 Experimental Section

5.4.1 Materials

Commercially available chemicals were of reagent-grade purity or better and were used without further purification unless otherwise noted. Biphenyl-functionalized cryptand and cryptate **5.1** were prepared following a published procedure presented in chapter 3 of this thesis.

5.4.2 Concentrations

Samples for inductively coupled plasma mass spectrometry (ICP-MS) were diluted using aqueous nitric acid (2% v/v). Standard solutions were prepared by serial dilution of a Eu standard (high-purity standards). ICP-MS measurements were conducted on a PE Sciex Elan 9000 ICP-MS instrument with a cross-flow nebulizer and Scott-type spray chamber.

5.4.3 Preparation of HSA samples

Stock solutions of HSA (30% w/v) and (35% w/v) were prepared by dissolving 300 and 350 mg of HSA, respectively in 1 mL of 1× degassed phosphate buffered saline (PBS). An aliquot of the stock HSA solution was added to a solution of **5.1** in degassed PBS to produce the desired concentrations of **5.1** and HSA.

5.4.4 Preparation of Sr^{2+} analogue of 5.1

A degassed aqueous solution of $SrCl_2$ (1 equiv, 41.2 mM) was mixed with a degassed aqueous solution of the biphenyl cryptand (2 equiv, 34.2 mM). The resulting mixture (1 mM $SrCl_2$ and 2 mM cryptand) was stirred for 12 h at ambient temperature under Ar. Degassed PBS (10×) was added to make the entire reaction mixture 1× in PBS, and stirring was continued for 30 min. The concentration of Sr in the resulting solution was verified by ICP-MS.

5.4.5. T_1 and relaxivity measurements

Longitudinal relaxation times, T_1, were measured using standard recovery methods with a Bruker Minispec mq 60 (1.4 T) at 60 MHz and 37 °C; a Varian Unity 400 (9.4 T) at 400 MHz and 20 and 37 °C; and a Varian 500S (11.7 T) at 500 MHz and 20 and 37 °C. The slope of a plot of $1/T_1$ versus concentration of Eu was used to calculate relaxivity. Four to six different concentrations of Eu (0–10 mM) were used, and measurements were repeated 3–9 times with independently prepared samples.

Susceptibility weighted imaging (SWI) was performed at 3 (Siemens TRIO) and 7 T (ClinScan) using volume coils. The acquisition parameters were as follows: T_R = 37 ms, T_E = 5.68–31.18 ms, and resolution = 0.5 × 0.5 × 2 mm^3 for 3 T; and T_R = 21 ms, T_E = 3.26–15.44 ms, and resolution = 0.27 × 0.27 × 2 mm^3 for 7 T. Multiple flip angles (5, 10, 15, 20, 25, and 30°) were used in the SWI experiments to allow

for the determination of longitudinal relaxation time, T_1.[31] MR images were processed using SPIN software (SVN Revision 1751). Matlab (7.12.0.635 R2011a) was used to generate effective transverse relaxation time, T_2^*, and corrected T_1 maps. The $1/T_1$ values from the corrected T_1 maps were plotted versus the concentration of Eu in the samples to calculate longitudinal relaxivities, r_1, as previously reported in chapter 3 of this document.[6]

5.4.6. Variable-temperature ^{17}O NMR experiments

Variable-temperature ^{17}O NMR measurements of solutions of **5.1**-HSA (1 mM **5.1**, 25% HSA) and its Sr^{2+}analogue (1 mM Sr^{2+}-cryptate, 25% HSA) in degassed PBS (pH 7.4) were obtained on a Varian-500S (11.7 T) spectrometer. ^{17}O-enriched water (10% $H_2{}^{17}O$, Cambridge Isotope Laboratories, Inc.) was added to samples to yield 1% ^{17}O enrichment. Transverse ^{17}O relaxation rates were measured at 15, 25, 30, 35, 40, 45, and 50 °C. The Sr^{2+} analogue of **5.1**-HSA was used as diamagnetic reference. $A/\hbar$ was fixed to -4.1×10^{-6} rad/s.[32] The least-squares fits of the ^{17}O NMR relaxation data were calculated using Origin software (8.0951 B951) following published procedures.[33]

Table 5.2. Variable-temperature ^{17}O NMR Data for Cryptate **5.1** and Sr^{2+} analogue of **5.1** in the presence of albumin**.**

Temperature (°C)	**Linewidth of $^{17}OH_2$ (Hz)**	
	Sr^{2+} analogue of **5.1**–HSA	**5.1**–HSA
50	57.85	60.44
45	65.03	68.09
40	73.78	77.40
35	84.57	89.24
30	96.26	102.35
25	111.44	119.16
15	151.97	160.28

Parameters

		Value	Standard Error
1overT2P	T1e298	2.44399E-8	1.75994E-9
	taum298	3.9744E-8	6.85832E-9
	deltaH	61984.56106	8163.02663
	deltaE	2.5E-11	0
	q	1	0
	Eu	1E-3	0

Iterations Performed = 4
Total Iterations in Session = 4
Fit converged - Chi-sqr no longer changed.
Some parameter values were fixed.

Statistics

	1overT2P
Number of Points	7
Degrees of Freedom	4
Reduced Chi-Sqr	1.4706
Residual Sum of Squares	5.88242
Adj. R-Square	0.97113
Fit Status	Succeeded(101)

Fit Status Code :
101 : Fit converged

Fitted Curves Plot

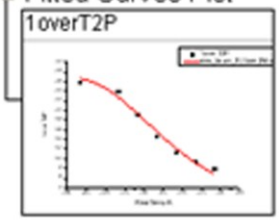

Figure 5.4. Variable-temperature ^{17}O NMR Fittings for cryptate **5.1** in the presence of albumin**.**

5.5 References

(1) Villaraza, A. J. L.; Bumb, A.; Brechbiel, M. W. *Chem. Rev.* **2010,** *110,* 2921–2959.

(2) Moser, E. *World J. Radiol.* **2010,** *2,* 37–40.

(3) Pitt, D.; Boster, A.; Pei, W.; Wohleb, E.; Jasne, A.; Zachariah, C. R.; Rammohan, K.; Knopp, M. V.; Schmalbrock, P. *Arch. Neurol.* **2010,** 812–818.

(4) Blow, N. *Nature* **2009,** *458,* 925–928.

(5) Caravan, P.; Farrar, C. T.; Frullano, L.; Uppal, R. *Contrast Media Mol. Imaging* **2009,** *4,* 89–100.

(6) Garcia, J.; Neelavalli, E.; Haacke, E. M.; Allen, M. J. *Chem. Commun.* **2011,** *47,* 12858–12860.

(7) Garcia, J.; Kuda-Wedagedara, A. N. W.; Allen, M. J. *Eur. J. Inorg. Chem.* **2012,** *2012,* 2135–2140.

(8) Amitage, F. E.; Richardson, D. E.; Li, K. C. P. *Bioconjugate Chem.* **1990,** *1,* 365–374.

(9) Aime, S.; Botta, M.; Crich, S. G.; Giovenzana, G.; Palmisano, G.; Sisti, M. *Bioconjugate Chem.* **1999,** *10,* 192–199.

(10) Nicolle, G. M.; Tóth, É.; Eisenwiener, P.; Mäcke, H. R.; Merbach, A. E. *J. Biol. Inorg. Chem.* **2000**, *7,* 757–769.

(11) Torres, S.; Martins, J. A.; André, J. P.; Geraldes, C. F. G. C.; Merbach, A. E.; Tóth, É. *Chem. Eur. J.* **2006,** *12,* 940–948.

(12) Laus, S.; Sour, A.; Ruloff, R.; Tóth, É.; Merbach, A. E. *Chem. Eur. J.* **2005,** *11,* 3064–3076.

(13) Yang, J. J.; Yang, J.; Wei, L.; Zurkiya, O.; Yang, W.; Li, S.; Zou, J.; Zhou, Y.; Maniccia, A. L. W.; Mao, H.; Zhao, F.; Malchow, R.; Zhao, S.; Johnson, J.; Hu, X.; Krogstad, E.; Liu, Z.-R. *J. Am. Chem. Soc.* **2008,** *130,* 9260–9267.

(14) Kundu, A.; Peterlik, H.; Krssak, M.; Bytzek, A. K.; Pashkunova-Martic, I.; Arion, V. B.; Helbich, T. H.; Keppler, B. K. *J. Inorg. Biochem.* **2011,** *105,* 250–255.

(15) Avedano, S.; Tei, L.; Lombardi, A.; Giovenzana, G. B.; Aime, S.; Longo, D.; Botta, M. *Chem. Commun.* **2007,** 4726–4728.

(16) Caravan, P.; Cloutier, N. J.; Greenfield, M. T.; McDemid, S. A.; Dunham, S. U.; Bulte, J. W. M.; Amedio Jr., J. C.; Looby, R. J.; Supkowski, R. M.; DeW Horrocks Jr.; W.; McMurry, T. J.; Lauffer, R. B. *J. Am. Chem. Soc.* **2002,** *124,* 3152–3162.

(17) Henoumont, C.; Vander Elst, L.; Laurent, S.; Muller, R. N. *J. Biol.Inorg. Chem.* **2009**, *14,* 683–691.

(18) Gianolio, E.; Giovenzana, G. B.; Longo, D.; Longo, I.; Menegotto, I.; Aime, S. *Chem. Eur. J.* **2007,** *13,* 5785–5797.

(19) Ou, M.-H.; Tu, C.-H.; Tsai, S.-U.; Lee, W.-T.; Liu, G.-C.; Wang, Y.-M. *Inorg. Chem.* **2006,** *45,* 244–254.

(20) Aime, S.; Botta, M.; Fasano, M.; Crich, S. G.; Terreno, E. *J. Biol. Inorg. Chem.* **1996,** *1,* 312–319.

(21) Aime, S.; Chiaussa, M.; Digilio, G.; Gianolio, E.; Terreno, E. *J. Biol. Inorg. Chem.* **1999,** *44,* 766–774.

(22) Parac-Vogt, T. N.; Kimpe, K.; Laurent, S.; Elst, L. V.; Burtea, C.; Chen, F.; Muller, R. N.; Ni, Y.; Verbruggen, A.; Binnemans, K. *Chem. Eur. J.* **2005,** 3077–3086.

(23) Aime, S.; Gianolio, E.; Terreno, E.; Giovenzana, G. B.; Pagliarin, R.; Sisti, M.; Palmisano, G.; Botta, M.; Lowe, M. P.; Parker, D. *J. Biol. Inorg. Chem.* **2006,** *5,* 488–497.

(24) Dumas, S.; Troughton, J. S.; Cloutier, N. J.; Chasse, J. M.; McMurry, T. J.; Caravan, P. *Aust. J. Chem.* **2008,** *61,* 682–686.

(25) Nivorozhkin, A. L.; Kolodziej, A. F.; Caravan, P.; Greenfield, M. T.; Lauffer, R. B.; McMurry, T. J. *Angew. Chem., Int Ed.* **2001,** *40,* 2903–2906.

(26) Strijkers, G. J.; Mulder, W. J. M.; van Heeswijk, R. B.; Frederick, P. M.; Bomans, P.; Magusin, P. C. M. M.; Nicolay, K. *MAGMA,* **2005,** *18,* 186–192.

(27) Anderson, E. A.; Isaacman, S.; Peabody, D. S.; Wang, E. Y.; Canary, J. W.; Kirshenbaum, K. *Nano Lett.* **2006,** *6,* 1160–1164.

(28) Gamage, N.-D.H.; Mei, Y.; Garcia, J.; Allen, M. J. *Angew. Chem., Int Ed.* **2010,** *49,* 8923–8925.

(29) Caravan, P.; Ellison, J. J.; McMurry, T. J.; Lauffer, R. B. *Chem. Rev.* **1999,** *99,* 2293–2352.

(30) To confirm that the increase in relaxivity was not due to nonspecific binding of the cryptate with HSA, we repeated the measurement at 1.4 T using Eu^{2+}[2.2.2] cryptate (without biphenyl) and observed a relaxivity value of 3.31 ± 0.07 mM^{-1} s^{-1}.

(31) Haacke, E. M.; Brown, R. W.; Thompson, M. R.; Venkatesan, R. Magnetic Resonance Imaging Physical Principles and Sequence Design. John Wiley & Sons, Inc., New York, pp. 451–460.

(32) Burai, L.; Scopelliti, R.; Töth, É. *Chem. Commun.* **2002,** 2366–2367.

(33) Urbanczyk-Pearson, L. M.; Femia, F. J.; Smith, J.; Parigi, G.; Duimstra, J. A.; Eckmann, A. L.; Eckemann, A. L.; Luchinat, C.; Meade, T. J. *Inorg. Chem.* **2008,** *47,* 56–68.

Chapter Six

Summary of Findings and Future Outlook

6.1 Summary of Findings

Magnetic resonance imaging (MRI) cannot always differentiate pathological from healthy tissues, and therefore contrast agents are used to enhance image contrast. However, the contrast-enhancing ability of clinically approved contrast agents decreases dramatically at higher field strengths where better resolution and shorter scan times are accessible. Therefore, there is a need to develop T_1-reducing (positive) contrast agents that perform well in the ultra-high field strength regime. This thesis describes my efforts with respect to the coordination chemistry necessary to pursue an answer to this need.

I measured the relaxivity of small Eu^{2+}-containing cryptates at field strengths that are commonly used for clinical imaging and at field strengths that are used in preclinical research. These studies demonstrated that these cryptates have higher relaxivity at ultra-high field strengths relative to lower fields. In addition, these cryptates showed higher efficiency at high and ultra-high field strengths relative to a clinically approved contrast agent, gadolinium(III) 1,4,7,10-tetraazacyclododecane-1,4,7,10-tetraacetate. Because of these promising results, I also measured the relaxivity of small Eu^{2+}-containing cryptates at different temperatures and pH values. Relaxivity data showed that the contrast-enhancing ability of these cryptates decreases as temperature increases, as predicted by theory, but is not affected by changes in pH under physiologically relevant range.

The relaxometric studies described in this thesis demonstrated the basis of using Eu^{2+}-containing cryptates as contrast agents at ultra-high field strength MRI. Through my studies, the scientific community is able to gain additional understanding of the performance of Eu^{2+}-containing cryptates at field strengths accessible to clinical and

preclinical imaging. This knowledge should aid in the design of more efficient Eu^{2+}-containing cryptates.

To explain the results of my relaxometric experiments, I performed variable-temperature ^{17}O NMR and electron paramagnetic resonance (EPR) spectroscopy. These spectroscopic techniques are crucial in understanding the influence of molecular parameters including the number of inner-sphere water molecules, water-exchange rate, electron-spin relaxation times, and rotational-correlation rate to the relaxivity of Eu^{2+}-containing cryptates. These experiments demonstrated the presence of two inner-sphere water molecules in each cryptate and near-optimal water-exchange rates for field strengths above 3 T. Both of these properties are desirable features of an effective contrast agent. In addition to the determination of the number of inner-sphere water molecules and water-exchange rate, EPR measurements were performed to determine electronic parameters including the *g* factor and transverse electronic relaxation time. With the relaxivity and NMR and EPR data, rotational-correlation rates were estimated and were found to limit the relaxivity of these small Eu^{2+}-containing cryptates.

With the understanding that these cryptates can potentially serve as contrast agents based on relaxivity data, I also determined the stability of these Eu^{2+}-containing complexes towards transmetallation in the presence of the biologically relevant metal ions Ca^{2+}, Mg^{2+}, and Zn^{2+}. This transmetallation experiment was important because of the toxicity of unchelated Eu^{2+}, the abundance of $Ca^{2+}$and Mg^{2+} in plasma, and the tendency of Zn^{2+} to chelate organic ligands. In this experiment, I found that amine-containing cryptates are inert to transmetallation and have longer transmetallation half-lives compared to non-macrocyclic, clinically approved Gd^{3+}-containing complexes including gadolinium(III) diethylenetriaminepentaacetate.

Finally, because I observed that the efficiency of small molecular weight cryptates increases with molecular weight, I studied the contrast-enhancing ability of a biphenyl-functionalized cryptate that can bind to macromolecules. I studied the relaxivity of this system in the presence of human serum albumin at multiple field strengths, performed albumin titration experiments, and used variable-temperature ^{17}O NMR and EPR spectroscopies to understand the effect of albumin binding on the molecular parameters that influence relaxivity. These studies revealed a decrease in relaxivity in the presence of albumin that was likely due to the displacement of an inner-sphere water molecule. However, an increase in relaxivity in the presence of albumin was observed at 1.4 T. This change was attributed to the enhanced contribution of rotational correlation rate to relaxivity. This work opens an avenue of research for understanding the effect of macromolecular binding to the efficiency of these cryptates as contrast agents and to gain an improved understanding of the relaxivity–molecular weight relationship for these cryptates.

6.2 Future Outlook

The increase in relaxivity for Eu^{2+}-containing cryptates at ultra-high field strengths is one of a few examples of paramagnetic materials exhibiting an increase in relaxivity as field strength increases in the ultra-high field strength regime. While the result is interesting, it is not yet fully understood why this increase in relaxivity is observed for these cryptates. Determining the relaxation profiles of other Eu^{2+}-containing cryptates with molecular weights of more than 500 Da could yield insight with respect to the relaxivity of these cryptates. These studies could be achieved by binding cryptates to supramolecular systems or by covalently attaching cryptates to polymers. Relaxation profiles of the

resulting macromolecular systems could be determined by nuclear magnetic relaxation dispersion (NMRD) relaxometry and high-field NMR spectroscopy.

In addition to the relaxometric studies in the preceding chapters, I synthesized dimeric and trimeric ligands to gain an understanding of the relaxivity–molecular weight relationship for Eu^{2+}-containing cryptates. However, obtaining pure ligands using size exclusion chromatography remained elusive, and unequivocal characterization of metalated ligands is a challenging task. I suggest using reverse phase chromatography as an alternative way of purifying these oligomers. Also, dialysis using membranes of 500–1000 molecular weight cutoff could also be used for purification. The metalated ligands could be characterized by elemental analysis. Differentiating bimetalated ligands to monometalated and unmetalated ligands could be made by comparing the sulfur to europium ratio in the elemental analysis. This characterization requires the metalation to be performed, using an excess of europium(II) to facilitate metalation, in water rather than in phosphate buffered saline. After metalation, dialysis should be performed using 500 Da molecular cutoff to remove unchelated europium.

To further boost the utility of Eu^{2+}-containing cryptates, I studied the relaxivity of a biphenyl-functionalized cryptate in the presence of human serum albumin. The albumin studies demonstrated that the decrease in relaxivity for the biphenyl-functionalized cryptate in the presence of albumin could be ascribed to displacement of an inner-sphere water molecule as indicated by the variable-temperature ^{17}O NMR spectroscopy results. This loss of an inner-sphere water molecule could be due to the short linker that connects the biphenyl moiety and Eu^{2+} in the cryptand. The use of longer linkers could prevent inner-sphere water molecules from being displaced from the complex.

In addition to the transmetallation studies that I performed in the presence of physiological cations, it is also important to study the effect of physiologically relevant anions such as citrate, malonate, carbonate, or lactate on the kinetic stability of Eu^{2+}-containing cryptates. These ions are of particular concern if the cryptates have net positive charges because the affinity of the anions would be higher. While the presence of phosphate does not displace inner-sphere water molecules from the cryptates that I studied, other anions could compete with the cryptand for Eu^{2+}, resulting in insoluble adducts. The transmetallation experiments described in this thesis could be adapted to study anions, and the results of these transmetallation studies would provide an understanding of the effect of different anions on the stability of Eu^{2+}-containing cryptates.

Finally, it is important to investigate the toxicity profile of the synthesized Eu^{2+}-containing cryptates by determining the maximum tolerated dose. These studies would help determine the effect of cryptate structure on toxicity. In addition, the use of antioxidants in the toxicity studies could provide information regarding the extent that antioxidants prolong the oxidation half-life of cryptates and lessen toxicity. Preliminary in vitro studies of cryptates in the presence of reduced glutathione demonstrated that reduced glutathione prolongs the oxidation half-life Eu^{2+}-containing cryptates. The information that will be obtained from toxicity studies of Eu^{2+}-containing cryptates would be useful for in vivo applications.

APPENDIX A

MATLAB CODES FOR GENERATING T_2^* AND T_1 MAPS

T_2*:

```
% function [T2map error_estimatemap]=flash_fit(fa,s,tr)
% s is the 3D matrix of # of slices equal to the nsumber of flip angles.
clear all;

clc
format long;

h=msgbox(' --------Please enter the information Asked for ---------');

waitfor(h);

rows=input('Enter Matrix size # ROWS: ');

cols=input('Enter Matrix size # COLS: ');

echonumber=input('Enter number of echoes: ');

slices=input('Enter the number of slices in each echo images: ');

s.fpathname=[];

%%%%%%%%%% FILE INFORMATION INPUT
for i=1:echonumber
    disp(' ');disp(' ');disp(' ')
    display('Select the first file in the series you want to calculate T2*');
    [fname, path]=uigetfile('C:\Archives\Ang Doktorado\Projects\Imaging
Experiments\2011 05 20 Phantom Imaging 3T\DICOM\5-
11Echo_SWI_FA5_.5x.5x2\TEsorted\*.*');
    s(i).fpathname=strcat(path,fname)
    disp(' ');disp(' ');disp(' ');
    TE(i)=input('\n Please enter the Corresponding echo time (TE) : ');
end

mm=zeros(rows,cols);
mm1=zeros(rows,cols);

%%%%%%%%%%%%%%%%%% ACTUAL CALCULATION WITH ALPHA MAP COMPENSATION INCLUDED
for i=1:slices

    mat=zeros(rows,cols); % IMAGE MATRIX SIZE
    xmat=zeros(size(TE,2),rows,cols); % IMAGE MATRIX SIZE
    ymat=zeros(size(TE,2),rows,cols); % IMAGE MATRIX SIZE

    for j=1:echonumber
```

```
        if s(j).fpathname(size(s(j).fpathname,2)-7)=='-'
            firstnum=str2num(s(j).fpathname(size(s(j).fpathname,2)-
6))*100+str2num(s(j).fpathname(size(s(j).fpathname,2)-
5))*10+str2num(s(j).fpathname(size(s(j).fpathname,2)-4));

mat(:,:)=dicomread(strcat(s(j).fpathname(1,1:(size(s(j).fpathname,2)-
7)),num2str(firstnum+i-1),'.dcm'));
        elseif s(j).fpathname(size(s(j).fpathname,2)-6)=='-'
            firstnum=str2num(s(j).fpathname(size(s(j).fpathname,2)-
5))*10+str2num(s(j).fpathname(size(s(j).fpathname,2)-4));

mat(:,:)=dicomread(strcat(s(j).fpathname(1,1:(size(s(j).fpathname,2)-
6)),num2str(firstnum+i-1),'.dcm'));
        else s(j).fpathname(size(s(j).fpathname,2)-5)=='-'
            firstnum=str2num(s(j).fpathname(size(s(j).fpathname,2)-4));

mat(:,:)=dicomread(strcat(s(j).fpathname(1,1:(size(s(j).fpathname,2)-
5)),num2str(firstnum+i-1),'.dcm'));
        end

        ymat(j,:,:)=log(mat);
        xmat(j,:,:)=-TE(j);

        %         end
    end

    clear  mat tmps tmpt;

    num=echonumber*sum((xmat.*ymat),1)-(sum(xmat,1).*sum(ymat,1));
    din=echonumber*(sum(xmat.^2,1))-(sum(xmat,1)).^2;

    b1=num./din;

    b2=(1/echonumber)*(sum(ymat,1)-b1.*sum(xmat,1));

    T2map=(1./b1);
    %     T1map=-tr./(log(b1)); %%%%% TR OF THE EXPERIMENT

    mm(:,:)=T2map(1,:,:);
    clear T2map;
    T2map=mm;

%     mm(:,:)=echoimagemat(1,:,:);
%     mm1(:,:)=echoimagemat(2,:,:);
%
%     T2_error= (T2map/dTE).*sqrt( (sigma1./mm).^2 + (sigma2./mm1).^2 );


    curntfname=strcat(s(1).fpathname(1,(1:size(s(1).fpathname,2)-
7)),'T2_map_mult10-',num2str(i),'.ima');
    writeima(curntfname, T2map*100);
%     dicomwrite(T2map*100,curntfname);
```

```
%     curntfname=strcat(s(1).fpathname(1,(1:size(s(1).fpathname,2)-
7)),'T2_errmap_mult10-',num2str(i),'.dcm');
%     %     writeima(curntfname, T2_error*10);
%     dicomwrite(T2map,curntfname);
end
```

T_1 map (with T_2* correction):

```
% function [T1map error_estimatemap]=flash_fit(fa,s,tr)
% s is the 3D matrix of # of slices equal to the number of flip angles.
clear all;

clc
format long;

h=msgbox(' --------Please enter the information Asked for ---------');

waitfor(h);

rows=input('Enter Matrix size # ROWS: ');

cols=input('Enter Matrix size # COLS: ');

TE=input('Enter Echo-time: ');

fanumber=input('Enter number of flip angles: ');
slices=input('Enter the number of slices in the Flip angle images: ');

s.fpathname=[];

display('Please input the T2starcorrection file (.ima)');
[fnameT2star, pathT2star]=uigetfile('C:\Archives\Ang
Doktorado\Projects\Imaging Experiments\2011 05 20 Phantom Imaging
3T\DICOM\*.*');
fpathnameT2star=strcat(pathT2star,fnameT2star)
t2starcorrection=showima(fpathnameT2star);


%%%%%%%%%% FILE INFORMATION INPUT
for i=1:fanumber
    disp(' ');disp(' ');disp(' ')
    display('Select the first file in the series you want to calculate T1');
    [fname, path]=uigetfile('C:\Archives\Ang Doktorado\Projects\Imaging
Experiments\2011 05 20 Phantom Imaging 3T\DICOM\*.*');
    s(i).fpathname=strcat(path,fname)
    disp(' ');disp(' ');disp(' ');
    fa(i)=input('\n Please enter the Corresponding Flip angle:    ');
end
```

```
% disp(' ');disp(' ');
% disp('Select the corresponding first reference flip angle image for
normalization:');
% fa=(fa)*(pi/180);

% [fname, path]= uigetfile('E:\Data_OM\Rahul1.5T_LOW FA data\');
% str=strcat(path,fname);
%
% disp(' ');disp(' ');
% normfactor=input('Enter the normalization peak/mode/mean value from the
normalization image:  ');

tr=input('Enter TR of the experiment: ');
%%%%%%%%%%%%%%%%%%%%%%%%%%%%%%%%%%%%

mm=zeros(rows,cols);



% flag=input(' ENTER 1 for alpha map normalisation: OR 2 for normal T1 map
calculation: ');

fa=fa*(pi/180);


%%%%%%%%%%%%%%%%%% ACTUAL CALCULATION WITH ALPHA MAP COMPENSATION INCLUDED
for i=1:slices

    %     alphamap=zeros(rows,cols);% IMAGE MATRIX SIZE
    mat=zeros(rows,cols); % IMAGE MATRIX SIZE
    xmat=zeros(size(fa,2),rows,cols); % IMAGE MATRIX SIZE
    ymat=zeros(size(fa,2),rows,cols); % IMAGE MATRIX SIZE
    %     faimagemat=zeros(size(fa,2),rows,cols); % IMAGE MATRIX SIZE


    for j=1:fanumber


        if s(j).fpathname(size(s(j).fpathname,2)-5)=='-'
            firstnum=str2num(s(j).fpathname(size(s(j).fpathname,2)-4));

mat(:,:)=dicomread(strcat(s(j).fpathname(1,1:(size(s(j).fpathname,2)-
5)),num2str(firstnum+i-1),'.dcm'));
            mat(:,:)=mat./exp(-TE./t2starcorrection);
        else
            firstnum=str2num(s(j).fpathname(size(s(j).fpathname,2)-4))+10;

mat(:,:)=dicomread(strcat(s(j).fpathname(1,1:(size(s(j).fpathname,2)-
6)),num2str(firstnum+i-1),'.dcm'));
            mat(:,:)=mat./exp(-TE./t2starcorrection);
        end


        faimagemat(j,:,:)=mat;
```

```
        tmps=sin(fa(j));
        tmpt=tan(fa(j));
        ymat(j,:,:)=mat./tmps;
        xmat(j,:,:)=mat./tmpt;

    end
    clear  mat tmps tmpt;


    num=fanumber*sum((xmat.*ymat),1)-(sum(xmat,1).*sum(ymat,1));
    din=fanumber*(sum(xmat.^2,1))-(sum(xmat,1)).^2;


    b1=num./din;

    b2=(1/fanumber)*(sum(ymat,1)-b1.*sum(xmat,1));


    T1map=-tr./(log(b1)); %%%%% TR OF THE EXPERIMENT

    mm(:,:)=T1map(1,:,:);
    clear T1map;
    T1map=mm;

    % Error MATRIX calculation

    yestimate=zeros(size(fa,2),rows,cols); % IMAGE MATRIX SIZE

    for j=1:fanumber
        num=b2.*sin(fa(j));
        din=1-cos(fa(j)).*b1;
        yestimate(j,:,:)=num./din;
    end
    sigma_y_error_estimate=sqrt((1/(fanumber-2))*sum((yestimate-
faimagemat).^2,1));

    din=fanumber*(sum(xmat.^2,1))-(sum(xmat,1)).^2;

    error_b1=sigma_y_error_estimate.*sqrt(fanumber./din);

    mm(:,:)=zeros(rows,cols);
    mm(:,:)=din(1,:,:);
    clear din;
    din=mm;clear mm;


    T1_error=(tr*error_b1)./(b1.*(log(b1)).^2);

    rho_e2=b2./(1-b1);


    mm(:,:)=zeros(rows,cols);
```

```
    mm(:,:)=T1_error(1,:,:);
    clear T1_error error_b1;
    T1_error=mm;


    curntfname=strcat(s(1).fpathname(1,(1:size(s(1).fpathname,2)-7)),'T1_map-
',num2str(i),'.ima');
    writeima(curntfname, T1map);

    curntfname=strcat(s(1).fpathname(1,(1:size(s(1).fpathname,2)-
7)),'T1_errmap_mult10-',num2str(i),'.ima');
    writeima(curntfname, T1_error*10);


end
```

APPENDIX B

CACULATED RELAXIVITY OF 5.1 AND 5.1–HSA AT DIFFERENT MAGNETIC FIELD STRENGTHS

Pertinent equations:

$$\text{relaxivity} = \frac{\frac{1}{T_1}}{1000c} = \frac{q}{55.5}\left(\frac{1}{T_{1m} + \tau_m}\right)$$

$$\frac{1}{T_{1m}} = \frac{1}{T_1^{DD}} + \frac{1}{T_1^{SC}} \quad \text{note: } \frac{1}{T_1^{SC}} \text{ goes to zero at frequencies above 10 MHz}$$

$$\frac{1}{T_1^{DD}} = \frac{2}{15}\left(\frac{\gamma^2 g^2 \mu_B^2}{r_{EuH}^6}\right) S(S+1)\left(\frac{\mu_o}{4\pi}\right)^2 \left(7\frac{\tau_{c2}}{1 + \omega_S^2\tau_{c2}^2} + 3\frac{\tau_{c1}}{1 + \omega_I^2\tau_{c1}^2}\right)$$

$$\frac{1}{\tau_{c1}} = \frac{1}{\tau_R} + \frac{1}{T_{1e}} + \frac{1}{\tau_m}$$

$$\frac{1}{\tau_{c2}} = \frac{1}{\tau_R} + \frac{1}{T_{2e}} + \frac{1}{\tau_m}$$

$$\frac{1}{T_{1e}} = 2C\left(\frac{1}{1 + \omega_S^2\tau_v^2} + \frac{4}{1 + \omega_S^2\tau_v^2}\right)$$

$$\frac{1}{T_{2e}} = C\left(\frac{5}{1 + \omega_S^2\tau_v^2} + \frac{2}{1 + \omega_S^2\tau_v^2} + 3\right)$$

$$C = \frac{1}{50}\Delta^2\tau_v[4S(S+1) - 3]$$

$$\omega_S = \gamma_S B$$

$$\omega_I = \gamma_I B$$

The calculated relaxivity decreases from 1.4 T to 11.7 T (**Table B.1**). Assumptions made in the calculations are that the electronic parameters, τ_v and Δ^2, do not change with magnetic field and that the values of τ_v and Δ^2 that were measured at 0.34 T are valid at higher field strengths. It was also assumed

that the τ_R for the biphenyl-modified cryptate in the presence of HSA is the same as that of MS-325 in the presence of HSA at 37 °C.

Constants		References
τ_m	4.0×10^{-8}	this work
q	1	this work
γ_I	2.67×10^{8}	http://physics.nist.gov/cgi-bin/cuu/Value?gammap
g	2	http://physics.nist.gov/cgi-bin/cuu/Value?gem|search_for=all!
μ_B	9.27×10^{-24}	http://physics.nist.gov/cgi-bin/cuu/Value?mub
$r_{\text{Eu–H}}$	3.22×10^{-10}	L. Burai, É. Tóth, S. Seibig, R. Scopelliti, A. E. Merbach, Chem. Eur. J. 6 (2000) 3761–3770.
μ_o	1.00×10^{-7}	http://physics.nist.gov/cgi-bin/cuu/Value?mu0
γ_S	1.76×10^{11}	L. Burai, É. Tóth, S. Seibig, R. Scopelliti, A. E. Merbach, Chem. Eur. J. 6 (2000) 3761–3770.
τ_R	1.33×10^{-8}	MS-325 with HSA from P. Caravan, N. J. Cloutier, M. T. Greenfield, S. A. McDermid, S. U. Dunham, J. W. M. Bulte, J. C. Amedio, Jr., R. J. Looby, R. M. Supkowski, W. DeW. Horrocks, Jr., T. J. McMurry, R. B. Lauffer, J. Am. Chem. Soc. 124 (2002) 3152–3162.
Δ^2	2.10×10^{19}	Eu^{2+}[2.2.2]cryptate from L. Burai, R. Scopelliti, É. Tóth, Chem. Commun. (2002) 2366–2367.
τ_v	1.70×10^{-11}	Eu^{2+}[2.2.2]cryptate from L. Burai, R. Scopelliti, É. Tóth, Chem. Commun. (2002) 2366–2367.

Table B.1. Calculated relaxivity values of **5.1** in the presence of HSA at different field strengths at 37 °C.

Field Strength (T)	**Relaxivity ($mM^{-1}s^{-1}$)**
1.4	16.10
3	3.80
7	0.71
9.4	0.40
11.7	0.26

APPENDIX C

Page	Contents
160	Table of contents
161–164	Copyright Permission for Reference 3 in Chapter 1
165–170	Copyright Permission for Reference 4 in Chapter 1
171–173	Copyright Permission for *Eur. J. Inorg. Chem.* **2012,** *2012,* 4550–4563.
174	Copyright Permission for Reference 18 in Chapter 2
175–178	Copyright Permission for Reference 12 in Chapter 2
179–181	Copyright Permission for *Chem. Commun.* **2011,** *47,* 12858–12860.
182–185	Copyright Permission for *Eur. J. Inorg. Chem.* **2012,** *2012,* 2135–2140.
186–190	Copyright Permission for *Inorg. Chim. Acta* **2012,** *393,* 324–327.

A1. Copyright Permission for Reference 3 in Chapter 1

JOHN WILEY AND SONS LICENSE
TERMS AND CONDITIONS

Feb 13, 2013

This is a License Agreement between Joel Garcia ("You") and John Wiley and Sons ("John Wiley and Sons") provided by Copyright Clearance Center ("CCC"). The license consists of your order details, the terms and conditions provided by John Wiley and Sons, and the payment terms and conditions.

All payments must be made in full to CCC. For payment instructions, please see information listed at the bottom of this form.

License Number

3080760752704

License date

Feb 02, 2013

Licensed content publisher

John Wiley and Sons

Licensed content publication

Journal of Magnetic Resonance Imaging

Licensed content title

7 tesla MRI of microbleeds and white matter lesions as seen in vascular dementia

Licensed copyright line

Copyright © 2011 Wiley-Liss, Inc.

Licensed content author

Jens M. Theysohn,Oliver Kraff,Stefan Maderwald,Markus Barth,Susanne C. Ladd,Michael Forsting,Mark E. Ladd,Elke R. Gizewski

Licensed content date

Mar 29, 2011

Start page

782

End page

791

Type of use

Dissertation/Thesis

Requestor type

University/Academic

Format

Print and electronic

Portion

Figure/table

Number of figures/tables

1

Original Wiley figure/table number(s)

Figure 1

Will you be translating?

No

Total

0.00 USD

Terms and Conditions

TERMS AND CONDITIONS

This copyrighted material is owned by or exclusively licensed to John Wiley & Sons, Inc. or one of its group companies (each a "Wiley Company") or a society for whom a Wiley Company has exclusive publishing rights in relation to a particular journal (collectively WILEY"). By clicking "accept" in connection with completing this licensing transaction, you agree that the following terms and conditions apply to this transaction (along with the billing and payment terms and conditions established by the Copyright Clearance Center Inc., ("CCC's Billing and Payment terms and conditions"), at the time that you opened your Rightslink account (these are available at any time at http://myaccount.copyright.com)

Terms and Conditions

1. The materials you have requested permission to reproduce (the "Materials") are protected by copyright.

2. You are hereby granted a personal, non-exclusive, non-sublicensable, non-transferable, worldwide, limited license to reproduce the Materials for the purpose specified in the licensing process. This license is for a one-time use only with a maximum distribution equal to the number that you identified in the licensing process. Any form of republication granted by this licence must be completed within two years of the date of the grant of this licence (although copies prepared before may be distributed thereafter). The Materials shall not be used in any other manner or for any other purpose. Permission is granted subject to an appropriate acknowledgement given to the author, title of the material/book/journal and the publisher. You shall also duplicate the copyright notice that appears in the Wiley publication in your use of the Material. Permission is also granted on the understanding that nowhere in the text is a previously published source acknowledged for all or part of this Material. Any third party material is expressly excluded from this permission.

3. With respect to the Materials, all rights are reserved. Except as expressly granted by the terms of the license, no part of the Materials may be copied, modified, adapted (except for minor reformatting required by the new Publication), translated, reproduced, transferred or distributed, in any form or by any means, and no derivative works may be made based on the Materials without the prior permission of the respective copyright owner. You may not alter, remove or suppress in any manner any copyright, trademark or other notices displayed by the Materials. You may not license, rent, sell, loan, lease, pledge, offer as security, transfer or assign the Materials, or any of the rights granted to you hereunder to any other person.

4. The Materials and all of the intellectual property rights therein shall at all times remain the exclusive property of John Wiley & Sons Inc or one of its related companies (WILEY) or their respective licensors, and your interest therein is only that of having possession of and the right to reproduce the Materials pursuant to Section 2 herein during the continuance of this Agreement. You agree that you own no right, title or interest in or to the Materials or any of the intellectual property rights therein. You shall have no rights hereunder other than the license as provided for above in Section 2. No right, license or interest to any trademark, trade name, service mark or other branding ("Marks") of WILEY or its licensors is granted hereunder, and you agree that you shall not assert any such right, license or interest with respect thereto.

5. NEITHER WILEY NOR ITS LICENSORS MAKES ANY WARRANTY OR REPRESENTATION OF ANY KIND TO YOU OR ANY THIRD PARTY, EXPRESS, IMPLIED OR STATUTORY, WITH RESPECT TO THE MATERIALS OR THE ACCURACY OF ANY INFORMATION CONTAINED IN THE MATERIALS, INCLUDING, WITHOUT LIMITATION, ANY IMPLIED WARRANTY OF MERCHANTABILITY, ACCURACY, SATISFACTORY QUALITY, FITNESS FOR A PARTICULAR PURPOSE, USABILITY, INTEGRATION OR NON-INFRINGEMENT AND ALL SUCH WARRANTIES ARE HEREBY EXCLUDED BY WILEY AND ITS LICENSORS AND WAIVED BY YOU.

6. WILEY shall have the right to terminate this Agreement immediately upon breach of this Agreement by you.

7. You shall indemnify, defend and hold harmless WILEY, its Licensors and their respective directors, officers, agents and employees, from and against any actual or threatened claims, demands, causes of action or proceedings arising from any breach of this Agreement by you.

8. IN NO EVENT SHALL WILEY OR ITS LICENSORS BE LIABLE TO YOU OR ANY OTHER PARTY OR ANY OTHER PERSON OR ENTITY FOR ANY SPECIAL, CONSEQUENTIAL, INCIDENTAL, INDIRECT, EXEMPLARY OR PUNITIVE DAMAGES, HOWEVER CAUSED, ARISING OUT OF OR IN CONNECTION WITH THE DOWNLOADING, PROVISIONING, VIEWING OR USE OF THE MATERIALS REGARDLESS OF THE FORM OF ACTION, WHETHER FOR BREACH OF CONTRACT, BREACH OF WARRANTY, TORT, NEGLIGENCE, INFRINGEMENT OR OTHERWISE (INCLUDING, WITHOUT LIMITATION, DAMAGES BASED ON LOSS OF PROFITS, DATA, FILES, USE, BUSINESS OPPORTUNITY OR

CLAIMS OF THIRD PARTIES), AND WHETHER OR NOT THE PARTY HAS BEEN ADVISED OF THE POSSIBILITY OF SUCH DAMAGES. THIS LIMITATION SHALL APPLY NOTWITHSTANDING ANY FAILURE OF ESSENTIAL PURPOSE OF ANY LIMITED REMEDY PROVIDED HEREIN.

9. Should any provision of this Agreement be held by a court of competent jurisdiction to be illegal, invalid, or unenforceable, that provision shall be deemed amended to achieve as nearly as possible the same economic effect as the original provision, and the legality, validity and enforceability of the remaining provisions of this Agreement shall not be affected or impaired thereby.

10. The failure of either party to enforce any term or condition of this Agreement shall not constitute a waiver of either party's right to enforce each and every term and condition of this Agreement. No breach under this agreement shall be deemed waived or excused by either party unless such waiver or consent is in writing signed by the party granting such waiver or consent. The waiver by or consent of a party to a breach of any provision of this Agreement shall not operate or be construed as a waiver of or consent to any other or subsequent breach by such other party.

11. This Agreement may not be assigned (including by operation of law or otherwise) by you without WILEY's prior written consent.

12. Any fee required for this permission shall be non-refundable after thirty (30) days from receipt.

13. These terms and conditions together with CCC's Billing and Payment terms and conditions (which are incorporated herein) form the entire agreement between you and WILEY concerning this licensing transaction and (in the absence of fraud) supersedes all prior agreements and representations of the parties, oral or written. This Agreement may not be amended except in writing signed by both parties. This Agreement shall be binding upon and inure to the benefit of the parties' successors, legal representatives, and authorized assigns.

14. In the event of any conflict between your obligations established by these terms and conditions and those established by CCC's Billing and Payment terms and conditions, these terms and conditions shall prevail.

15. WILEY expressly reserves all rights not specifically granted in the combination of (i) the license details provided by you and accepted in the course of this licensing transaction, (ii) these terms and conditions and (iii) CCC's Billing and Payment terms and conditions.

16. This Agreement will be void if the Type of Use, Format, Circulation, or Requestor Type was misrepresented during the licensing process.

17. This Agreement shall be governed by and construed in accordance with the laws of the State of New York, USA, without regards to such state's conflict of law rules. Any legal action, suit or proceeding arising out of or relating to these Terms and Conditions or the breach thereof shall be instituted in a court of competent jurisdiction in New York County in the State of New York in the United States of America and each party hereby consents and submits to the personal jurisdiction of such court, waives any objection to venue in such court and consents to service of process by registered or certified mail, return receipt requested, at the last known address of such party.

Wiley Open Access Terms and Conditions

All research articles published in Wiley Open Access journals are fully open access: immediately freely available to read, download and share. Articles are published under the terms of the Creative Commons Attribution Non Commercial License. which permits use, distribution and reproduction in any medium, provided the original work is properly cited and is not used for commercial purposes. The license is subject to the Wiley Open Access terms and conditions:
Wiley Open Access articles are protected by copyright and are posted to repositories and websites in accordance with the terms of the Creative Commons Attribution Non Commercial License. At the time of deposit, Wiley Open Access articles include all changes made during peer review, copyediting, and publishing. Repositories and websites that host the article are responsible for incorporating any publisher-supplied amendments or retractions issued subsequently.
Wiley Open Access articles are also available without charge on Wiley's publishing platform,**Wiley Online Library** or any successor sites.

Use by non-commercial users

For non-commercial and non-promotional purposes individual users may access, download, copy, display and redistribute to colleagues Wiley Open Access articles, as well as adapt, translate, text- and data-mine the content subject to the following conditions:

- The authors' moral rights are not compromised. These rights include the right of "paternity" (also known as "attribution" - the right for the author to be identified as such) and "integrity" (the right for the author not to have the work altered in such a way that the author's reputation or integrity may be impugned).
- Where content in the article is identified as belonging to a third party, it is the obligation of the user to ensure that any reuse complies with the copyright policies of the owner of that content.
- If article content is copied, downloaded or otherwise reused for non-commercial research and education purposes, a link to the appropriate bibliographic citation (authors, journal, article title, volume, issue, page numbers, DOI and the link to the definitive published version on Wiley Online Library) should be maintained. Copyright notices and disclaimers must not be deleted.
- Any translations, for which a prior translation agreement with Wiley has not been agreed, must prominently display the statement: "This is an unofficial translation of an article that appeared in a Wiley publication. The publisher has not endorsed this translation."

Use by commercial "for-profit" organisations

Use of Wiley Open Access articles for commercial, promotional, or marketing purposes requires further explicit permission from Wiley and will be subject to a fee. Commercial purposes include:

- Copying or downloading of articles, or linking to such articles for further redistribution, sale or licensing;

- Copying, downloading or posting by a site or service that incorporates advertising with such content;
- The inclusion or incorporation of article content in other works or services (other than normal quotations with an appropriate citation) that is then available for sale or licensing, for a fee (for example, a compilation produced for marketing purposes, inclusion in a sales pack)
- Use of article content (other than normal quotations with appropriate citation) by for-profit organisations for promotional purposes
- Linking to article content in e-mails redistributed for promotional, marketing or educational purposes;
- Use for the purposes of monetary reward by means of sale, resale, licence, loan, transfer or other form of commercial exploitation such as marketing products
- Print reprints of Wiley Open Access articles can be purchased from: corporatesales@wiley.com

Other Terms and Conditions:

BY CLICKING ON THE "I AGREE..." BOX, YOU ACKNOWLEDGE THAT YOU HAVE READ AND FULLY UNDERSTAND EACH OF THE SECTIONS OF AND PROVISIONS SET FORTH IN THIS AGREEMENT AND THAT YOU ARE IN AGREEMENT WITH AND ARE WILLING TO ACCEPT ALL OF YOUR OBLIGATIONS AS SET FORTH IN THIS AGREEMENT.

v1.7

If you would like to pay for this license now, please remit this license along with your payment made payable to "COPYRIGHT CLEARANCE CENTER" otherwise you will be invoiced within 48 hours of the license date. Payment should be in the form of a check or money order referencing your account number and this invoice number RLNK500948515.
Once you receive your invoice for this order, you may pay your invoice by credit card. Please follow instructions provided at that time.

Make Payment To:
Copyright Clearance Center
Dept 001
P.O. Box 843006
Boston, MA 02284-3006

For suggestions or comments regarding this order, contact RightsLink Customer Support:customercare@copyright.com or +1-877-622-5543 (toll free in the US) or +1-978-646-2777.

Gratis licenses (referencing $0 in the Total field) are free. Please retain this printable license for your reference. No payment is required.

A2. Copyright Permission for Reference 4 in Chapter 1

ELSEVIER LICENSE
TERMS AND CONDITIONS

Feb 13, 2013

This is a License Agreement between Joel Garcia ("You") and Elsevier ("Elsevier") provided by Copyright Clearance Center ("CCC"). The license consists of your order details, the terms and conditions provided by Elsevier, and the payment terms and conditions.

All payments must be made in full to CCC. For payment instructions, please see information listed at the bottom of this form.

Supplier

Elsevier Limited
The Boulevard,Langford Lane
Kidlington,Oxford,OX5 1GB,UK

Registered Company Number

1982084

Customer name

Joel Garcia

Customer address

5200 Anthony Wayne Drive APT 901

Detroit, MI 48202

License number

3076680104538

License date

Jan 26, 2013

Licensed content publisher

Elsevier

Licensed content publication

European Journal of Cancer

Licensed content title

Development of luciferase tagged brain tumour models in mice for chemotherapy intervention studies

Licensed content author

E.M. Kemper,W. Leenders,B. Küsters,S. Lyons,T. Buckle,A. Heerschap,W. Boogerd,J.H. Beijnen,O. van Tellingen

Licensed content date

December 2006

Licensed content volume number

42

Licensed content issue number

18

Number of pages

10

Start Page

3294

End Page

3303

Type of Use

reuse in a thesis/dissertation

Intended publisher of new work

other

Portion

figures/tables/illustrations

Number of figures/tables/illustrations

1

Format

both print and electronic

Are you the author of this Elsevier article?

No

Will you be translating?

No

Order reference number

Title of your thesis/dissertation

STUDIES ON THE PHYSICOCHEMICAL PROPERTIES OF Eu2+ CRYPTATES: IMPLICATIONS TO CONTRAST AGENTS FOR MAGNETIC RESONANCE IMAGING

Expected completion date

May 2013

Estimated size (number of pages)

200

Elsevier VAT number

GB 494 6272 12

Permissions price

0.00 USD

VAT/Local Sales Tax

0.0 USD / 0.0 GBP

Total

0.00 USD

Terms and Conditions

INTRODUCTION

1. The publisher for this copyrighted material is Elsevier. By clicking "accept" in connection with completing this licensing transaction, you agree that the following terms and conditions apply to this transaction (along with the Billing and Payment terms and conditions established by Copyright Clearance Center, Inc. ("CCC"), at the time that you opened your Rightslink account and that are available at any time at http://myaccount.copyright.com).

GENERAL TERMS

2. Elsevier hereby grants you permission to reproduce the aforementioned material subject to the terms and conditions indicated.

3. Acknowledgement: If any part of the material to be used (for example, figures) has appeared in our publication with credit or acknowledgement to another source, permission must also be sought from that source. If such permission is not obtained then that material may not be included in your publication/copies. Suitable acknowledgement to the source must be made, either as a footnote or in a reference list at the end of your publication, as follows:

“Reprinted from Publication title, Vol /edition number, Author(s), Title of article / title of chapter, Pages No., Copyright (Year), with permission from Elsevier [OR APPLICABLE SOCIETY COPYRIGHT OWNER].” Also Lancet special credit - “Reprinted from The Lancet, Vol. number, Author(s), Title of article, Pages No., Copyright (Year), with permission from Elsevier.”

4. Reproduction of this material is confined to the purpose and/or media for which permission is hereby given.

5. Altering/Modifying Material: Not Permitted. However figures and illustrations may be altered/adapted minimally to serve your work. Any other abbreviations, additions, deletions

and/or any other alterations shall be made only with prior written authorization of Elsevier Ltd. (Please contact Elsevier at permissions@elsevier.com)

6. If the permission fee for the requested use of our material is waived in this instance, please be advised that your future requests for Elsevier materials may attract a fee.

7. Reservation of Rights: Publisher reserves all rights not specifically granted in the combination of (i) the license details provided by you and accepted in the course of this licensing transaction, (ii) these terms and conditions and (iii) CCC's Billing and Payment terms and conditions.

8. License Contingent Upon Payment: While you may exercise the rights licensed immediately upon issuance of the license at the end of the licensing process for the transaction, provided that you have disclosed complete and accurate details of your proposed use, no license is finally effective unless and until full payment is received from you (either by publisher or by CCC) as provided in CCC's Billing and Payment terms and conditions. If full payment is not received on a timely basis, then any license preliminarily granted shall be deemed automatically revoked and shall be void as if never granted. Further, in the event that you breach any of these terms and conditions or any of CCC's Billing and Payment terms and conditions, the license is automatically revoked and shall be void as if never granted. Use of materials as described in a revoked license, as well as any use of the materials beyond the scope of an unrevoked license, may constitute copyright infringement and publisher reserves the right to take any and all action to protect its copyright in the materials.

9. Warranties: Publisher makes no representations or warranties with respect to the licensed material.

10. Indemnity: You hereby indemnify and agree to hold harmless publisher and CCC, and their respective officers, directors, employees and agents, from and against any and all claims arising out of your use of the licensed material other than as specifically authorized pursuant to this license.

11. No Transfer of License: This license is personal to you and may not be sublicensed, assigned, or transferred by you to any other person without publisher's written permission.

12. No Amendment Except in Writing: This license may not be amended except in a writing signed by both parties (or, in the case of publisher, by CCC on publisher's behalf).

13. Objection to Contrary Terms: Publisher hereby objects to any terms contained in any purchase order, acknowledgment, check endorsement or other writing prepared by you, which terms are inconsistent with these terms and conditions or CCC's Billing and Payment terms and conditions. These terms and conditions, together with CCC's Billing and Payment terms and conditions (which are incorporated herein), comprise the entire agreement between you and publisher (and CCC) concerning this licensing transaction. In the event of any conflict between your obligations established by these terms and conditions and those established by CCC's Billing and Payment terms and conditions, these terms and conditions shall control.

14. Revocation: Elsevier or Copyright Clearance Center may deny the permissions described in this License at their sole discretion, for any reason or no reason, with a full refund payable to you. Notice of such denial will be made using the contact information provided by you. Failure to receive such notice will not alter or invalidate the denial. In no event will Elsevier or Copyright Clearance Center be responsible or liable for any costs, expenses or damage incurred by you as a result of a denial of your permission request, other than a refund of the amount(s) paid by you to Elsevier and/or Copyright Clearance Center for denied permissions.

LIMITED LICENSE

The following terms and conditions apply only to specific license types:

15. **Translation**: This permission is granted for non-exclusive world **English** rights only unless your license was granted for translation rights. If you licensed translation rights you may only translate this content into the languages you requested. A professional translator must perform all translations and reproduce the content word for word preserving the integrity of the article. If this license is to re-use 1 or 2 figures then permission is granted for non-exclusive world rights in all languages.

16. **Website**: The following terms and conditions apply to electronic reserve and author websites:
Electronic reserve: If licensed material is to be posted to website, the web site is to be password-protected and made available only to bona fide students registered on a relevant course if:
This license was made in connection with a course,
This permission is granted for 1 year only. You may obtain a license for future website posting,
All content posted to the web site must maintain the copyright information line on the bottom of each image,
A hyper-text must be included to the Homepage of the journal from which you are licensing athttp://www.sciencedirect.com/science/journal/xxxxx or the Elsevier homepage for books athttp://www.elsevier.com , and
Central Storage: This license does not include permission for a scanned version of the material to be stored in a central repository such as that provided by Heron/XanEdu.

17. **Author website** for journals with the following additional clauses:

All content posted to the web site must maintain the copyright information line on the bottom of each image, and the permission granted is limited to the personal version of your paper. You are not allowed to download and post the published electronic version of your article (whether PDF or HTML, proof or final version), nor may you scan the printed edition to create an electronic version. A hyper-text must be included to the Homepage of the journal from which you are licensing athttp://www.sciencedirect.com/science/journal/xxxxx . As part of our normal production process, you will receive an e-mail notice when your article appears on Elsevier's online service ScienceDirect (www.sciencedirect.com). That e-mail will include the article's Digital Object Identifier (DOI). This number provides the electronic link to the published article

and should be included in the posting of your personal version. We ask that you wait until you receive this e-mail and have the DOI to do any posting.

Central Storage: This license does not include permission for a scanned version of the material to be stored in a central repository such as that provided by Heron/XanEdu.

18. **Author website** for books with the following additional clauses:
Authors are permitted to place a brief summary of their work online only.
A hyper-text must be included to the Elsevier homepage at http://www.elsevier.com . All content posted to the web site must maintain the copyright information line on the bottom of each image. You are not allowed to download and post the published electronic version of your chapter, nor may you scan the printed edition to create an electronic version.

Central Storage: This license does not include permission for a scanned version of the material to be stored in a central repository such as that provided by Heron/XanEdu.

19. **Website** (regular and for author): A hyper-text must be included to the Homepage of the journal from which you are licensing at http://www.sciencedirect.com/science/journal/xxxxx. or for books to the Elsevier homepage at http://www.elsevier.com

20. **Thesis/Dissertation**: If your license is for use in a thesis/dissertation your thesis may be submitted to your institution in either print or electronic form. Should your thesis be published commercially, please reapply for permission. These requirements include permission for the Library and Archives of Canada to supply single copies, on demand, of the complete thesis and include permission for UMI to supply single copies, on demand, of the complete thesis. Should your thesis be published commercially, please reapply for permission.

21. **Other Conditions**:

v1.6

If you would like to pay for this license now, please remit this license along with your payment made payable to "COPYRIGHT CLEARANCE CENTER" otherwise you will be invoiced within 48 hours of the license date. Payment should be in the form of a check or money order referencing your account number and this invoice number RLNK500942949.
Once you receive your invoice for this order, you may pay your invoice by credit card. Please follow instructions provided at that time.

Make Payment To:
Copyright Clearance Center
Dept 001
P.O. Box 843006
Boston, MA 02284-3006

For suggestions or comments regarding this order, contact RightsLink Customer Support:customercare@copyright.com or +1-877-622-5543 (toll free in the US) or +1-978-646-2777.

Gratis licenses (referencing $0 in the Total field) are free. Please retain this printable license for your reference. No payment is required.

A3. Copyright Permission for *Eur. J. Inorg. Chem.* 2012, *2012,* 4550–4563.

JOHN WILEY AND SONS LICENSE TERMS AND CONDITIONS

Feb 13, 2013

This is a License Agreement between Joel Garcia ("You") and John Wiley and Sons ("John Wiley and Sons") provided by Copyright Clearance Center ("CCC"). The license consists of your order details, the terms and conditions provided by John Wiley and Sons, and the payment terms and conditions.

All payments must be made in full to CCC. For payment instructions, please see information listed at the bottom of this form.

License Number

3066631094490

License date

Jan 12, 2013

Licensed content publisher

John Wiley and Sons

Licensed content publication

European Journal of Inorganic Chemistry

Licensed content title

Developments in the Coordination Chemistry of Europium(II)

Licensed copyright line

Copyright © 2012 WILEY-VCH Verlag GmbH & Co. KGaA, Weinheim

Licensed content author

Joel Garcia,Matthew J. Allen

Licensed content date

Jun 12, 2012

Start page

4550

End page

4563

Type of use

Dissertation/Thesis

Requestor type

Author of this Wiley article

Format

Electronic

Portion

Full article

Will you be translating?

No

Total

0.00 USD

Terms and Conditions

TERMS AND CONDITIONS

This copyrighted material is owned by or exclusively licensed to John Wiley & Sons, Inc. or one of its group companies (each a "Wiley Company") or a society for whom a Wiley Company has exclusive publishing rights in relation to a particular journal (collectively WILEY"). By clicking "accept" in connection with completing this licensing transaction, you agree that the following terms and conditions apply to this transaction (along with the billing and payment terms and conditions established by the Copyright Clearance Center Inc., ("CCC's Billing and Payment terms and conditions"), at the time that you opened your Rightslink account (these are available at any time at http://myaccount.copyright.com)

Terms and Conditions

1. The materials you have requested permission to reproduce (the "Materials") are protected by copyright.

2. You are hereby granted a personal, non-exclusive, non-sublicensable, non-transferable, worldwide, limited license to reproduce the Materials for the purpose specified in the licensing process. This license is for a one-time use only with a maximum distribution equal to the number that you identified in the licensing process. Any form of republication granted by this licence must be completed within two years of the date of the grant of this licence (although copies prepared before may be distributed thereafter). The Materials shall not be used in any other manner or for any other purpose. Permission is granted subject to an appropriate acknowledgement given to the author, title of the material/book/journal and the publisher. You shall also duplicate the copyright notice that appears in the Wiley publication in your use of the Material. Permission is also granted on the understanding that nowhere in the text is a previously published source acknowledged for all or part of this Material. Any third party material is expressly excluded from this permission.

3. With respect to the Materials, all rights are reserved. Except as expressly granted by the terms of the license, no part of the Materials may be copied, modified, adapted (except for minor reformatting required by the new Publication), translated, reproduced, transferred or distributed, in any form or by any means, and no derivative works may be made based on the Materials without the prior permission of the respective copyright owner. You may not alter, remove or suppress in any manner any copyright, trademark or other notices displayed by the Materials. You may not license, rent, sell, loan, lease, pledge, offer as security, transfer or assign the Materials, or any of the rights granted to you hereunder to any other person.

4. The Materials and all of the intellectual property rights therein shall at all times remain the exclusive property of John Wiley & Sons Inc or one of its related companies (WILEY) or their respective licensors, and your interest therein is only that of having possession of and the right to reproduce the Materials pursuant to Section 2 herein during the continuance of this Agreement. You agree that you own no right, title or interest in or to the Materials or any of the intellectual property rights therein. You shall have no rights hereunder other than the license as provided for above in Section 2. No right, license or interest to any trademark, trade name, service mark or other branding ("Marks") of WILEY or its licensors is granted hereunder, and you agree that you shall not assert any such right, license or interest with respect thereto.

5. NEITHER WILEY NOR ITS LICENSORS MAKES ANY WARRANTY OR REPRESENTATION OF ANY KIND TO YOU OR ANY THIRD PARTY, EXPRESS, IMPLIED OR STATUTORY, WITH RESPECT TO THE MATERIALS OR THE ACCURACY OF ANY INFORMATION CONTAINED IN THE MATERIALS, INCLUDING, WITHOUT LIMITATION, ANY IMPLIED WARRANTY OF MERCHANTABILITY, ACCURACY, SATISFACTORY QUALITY, FITNESS FOR A PARTICULAR PURPOSE, USABILITY, INTEGRATION OR NON-INFRINGEMENT AND ALL SUCH WARRANTIES ARE HEREBY EXCLUDED BY WILEY AND ITS LICENSORS AND WAIVED BY YOU.

6. WILEY shall have the right to terminate this Agreement immediately upon breach of this Agreement by you.

7. You shall indemnify, defend and hold harmless WILEY, its Licensors and their respective directors, officers, agents and employees, from and against any actual or threatened claims, demands, causes of action or proceedings arising from any breach of this Agreement by you.

8. IN NO EVENT SHALL WILEY OR ITS LICENSORS BE LIABLE TO YOU OR ANY OTHER PARTY OR ANY OTHER PERSON OR ENTITY FOR ANY SPECIAL, CONSEQUENTIAL, INCIDENTAL, INDIRECT, EXEMPLARY OR PUNITIVE DAMAGES, HOWEVER CAUSED, ARISING OUT OF OR IN CONNECTION WITH THE DOWNLOADING, PROVISIONING, VIEWING OR USE OF THE MATERIALS REGARDLESS OF THE FORM OF ACTION, WHETHER FOR BREACH OF CONTRACT, BREACH OF WARRANTY, TORT, NEGLIGENCE, INFRINGEMENT OR OTHERWISE (INCLUDING, WITHOUT LIMITATION, DAMAGES BASED ON LOSS OF PROFITS, DATA, FILES, USE, BUSINESS OPPORTUNITY OR CLAIMS OF THIRD PARTIES), AND WHETHER OR NOT THE PARTY HAS BEEN ADVISED OF THE POSSIBILITY OF SUCH DAMAGES. THIS LIMITATION SHALL APPLY NOTWITHSTANDING ANY FAILURE OF ESSENTIAL PURPOSE OF ANY LIMITED REMEDY PROVIDED HEREIN.

9. Should any provision of this Agreement be held by a court of competent jurisdiction to be illegal, invalid, or unenforceable, that provision shall be deemed amended to achieve as nearly as possible the same economic effect as the original provision, and the legality, validity and enforceability of the remaining provisions of this Agreement shall not be affected or impaired thereby.

10. The failure of either party to enforce any term or condition of this Agreement shall not constitute a waiver of either party's right to enforce each and every term and condition of this Agreement. No breach under this agreement shall be deemed waived or excused by either party unless such waiver or consent is in writing signed by the party granting such waiver or consent. The waiver by or consent of a party to a breach of any provision of this Agreement shall not operate or be construed as a waiver of or consent to any other or subsequent breach by such other party.

11. This Agreement may not be assigned (including by operation of law or otherwise) by you without WILEY's prior written consent.

12. Any fee required for this permission shall be non-refundable after thirty (30) days from receipt.

13. These terms and conditions together with CCC's Billing and Payment terms and conditions (which are incorporated herein) form the entire agreement between you and WILEY concerning this licensing transaction and (in the absence of fraud) supersedes all prior agreements and representations of the parties, oral or written. This Agreement may not be amended except in writing signed by both parties. This Agreement shall be binding upon and inure to the benefit of the parties' successors, legal representatives, and authorized assigns.

14. In the event of any conflict between your obligations established by these terms and conditions and those established by CCC's Billing and Payment terms and conditions, these terms and conditions shall prevail.

15. WILEY expressly reserves all rights not specifically granted in the combination of (i) the license details provided by you and accepted in the course of this licensing transaction, (ii) these terms and conditions and (iii) CCC's Billing and Payment terms and conditions.

16. This Agreement will be void if the Type of Use, Format, Circulation, or Requestor Type was misrepresented during the licensing process.

17. This Agreement shall be governed by and construed in accordance with the laws of the State of New York, USA, without regards to such state's conflict of law rules. Any legal action, suit or proceeding arising out of or relating to these Terms and Conditions or the breach thereof shall be instituted in a court of competent jurisdiction in New York County in the State of New York in the United States of America and each party hereby consents and submits to the personal jurisdiction of such court, waives any objection to venue in such court and consents to service of process by registered or certified mail, return receipt requested, at the last known address of such party.

Wiley Open Access Terms and Conditions

All research articles published in Wiley Open Access journals are fully open access: immediately freely available to read, download and share. Articles are published under the terms of the Creative Commons Attribution Non Commercial License. which permits use, distribution and reproduction in any medium, provided the original work is properly cited and is not used for commercial purposes. The license is subject to the Wiley Open Access terms and conditions:
Wiley Open Access articles are protected by copyright and are posted to repositories and websites in accordance with the terms of the Creative Commons Attribution Non Commercial License. At the time of deposit, Wiley Open Access articles include all changes made during peer review, copyediting, and publishing. Repositories and websites that host the article are responsible for incorporating any publisher-supplied amendments or retractions issued subsequently.
Wiley Open Access articles are also available without charge on Wiley's publishing platform, **Wiley Online Library** or any successor sites.

Use by non-commercial users

For non-commercial and non-promotional purposes individual users may access, download, copy, display and redistribute to colleagues Wiley Open Access articles, as well as adapt, translate, text- and data-mine the content subject to the following conditions:

- The authors' moral rights are not compromised. These rights include the right of "paternity" (also known as "attribution" - the right for the author to be identified as such) and "integrity" (the right for the author not to have the work altered in such a way that the author's reputation or integrity may be impugned).
- Where content in the article is identified as belonging to a third party, it is the obligation of the user to ensure that any reuse complies with the copyright policies of the owner of that content.
- If article content is copied, downloaded or otherwise reused for non-commercial research and education purposes, a link to the appropriate bibliographic citation (authors, journal, article title, volume, issue, page numbers, DOI and the link to the definitive published version on Wiley Online Library) should be maintained. Copyright notices and disclaimers must not be deleted.
- Any translations, for which a prior translation agreement with Wiley has not been agreed, must prominently display the statement: "This is an unofficial translation of an article that appeared in a Wiley publication. The publisher has not endorsed this translation."

Use by commercial "for-profit" organisations

Use of Wiley Open Access articles for commercial, promotional, or marketing purposes requires further explicit permission from Wiley and will be subject to a fee. Commercial purposes include:

- Copying or downloading of articles, or linking to such articles for further redistribution, sale or licensing;
- Copying, downloading or posting by a site or service that incorporates advertising with such content;
- The inclusion or incorporation of article content in other works or services (other than normal quotations with an appropriate citation) that is then available for sale or licensing, for a fee (for example, a compilation produced for marketing purposes, inclusion in a sales pack)
- Use of article content (other than normal quotations with appropriate citation) by for-profit organisations for promotional purposes
- Linking to article content in e-mails redistributed for promotional, marketing or educational purposes;
- Use for the purposes of monetary reward by means of sale, resale, licence, loan, transfer or other form of commercial exploitation such as marketing products
- Print reprints of Wiley Open Access articles can be purchased from: corporatesales@wiley.com

Other Terms and Conditions:

BY CLICKING ON THE "I AGREE..." BOX, YOU ACKNOWLEDGE THAT YOU HAVE READ AND FULLY UNDERSTAND EACH OF THE SECTIONS OF AND PROVISIONS SET FORTH IN THIS AGREEMENT AND THAT YOU ARE IN AGREEMENT WITH AND ARE WILLING TO ACCEPT ALL OF YOUR OBLIGATIONS AS SET FORTH IN THIS AGREEMENT.

v1.7

If you would like to pay for this license now, please remit this license along with your payment made payable to "COPYRIGHT CLEARANCE CENTER" otherwise you will be invoiced within 48 hours of the license date. Payment should be in the form of a check or money order referencing your account number and this invoice number RLNK500932956. Once you receive your invoice for this order, you may pay your invoice by credit card. Please follow instructions provided at that time.

Make Payment To:
Copyright Clearance Center
Dept 001
P.O. Box 843006
Boston, MA 02284-3006

For suggestions or comments regarding this order, contact RightsLink Customer Support: customercare@copyright.com or +1-877-622-5543 (toll free in the US) or +1-978-646-2777.

Gratis licenses (referencing $0 in the Total field) are free. Please retain this printable license for your reference. No payment is required.

A4. Copyright Permission for Reference 18 of Chapter 2.

RightsLink®

Home | Account Info | Help

Title: Lanthanide Phosphido Complexes: A Comparison of the Divalent Homoleptic Species Ln[(μ-PtBu2)2Li(thf)]2 (Ln = Yb, Eu, Sm) Including the Structural Characterization and a Europium-151 Mössbauer Spectrum of Eu[(μ-PtBu2)2Li(thf)]21

Author: Gerd W. Rabe,*,†, Glenn P. A. Yap,‡ and, and Arnold L. Rheingold‡

Publication: Inorganic Chemistry

Publisher: American Chemical Society

Date: Jul 1, 1997

Copyright © 1997, American Chemical Society

Logged in as:

Joel Garcia

Account #:

3000496330

LOGOUT

PERMISSION/LICENSE IS GRANTED FOR YOUR ORDER AT NO CHARGE

This type of permission/license, instead of the standard Terms & Conditions, is sent to you because no fee is being charged for your order. Please note the following:

- Permission is granted for your request in both print and electronic formats, and translations.
- If figures and/or tables were requested, they may be adapted or used in part.
- Please print this page for your records and send a copy of it to your publisher/graduate school.
- Appropriate credit for the requested material should be given as follows: "Reprinted (adapted) with permission from (COMPLETE REFERENCE CITATION). Copyright (YEAR) American Chemical Society." Insert appropriate information in place of the capitalized words.
- One-time permission is granted only for the use specified in your request. No additional uses are granted (such as derivative works or other editions). For any other uses, please submit a new request.

If credit is given to another source for the material you requested, permission must be obtained from that source.

BACK | CLOSE WINDOW

Copyright © 2013 Copyright Clearance Center, Inc. All Rights Reserved. Privacy statement.
Comments? We would like to hear from you. E-mail us at customercare@copyright.com

A5. Copyright Permission for Reference 12 of Chapter 2.

JOHN WILEY AND SONS LICENSE
TERMS AND CONDITIONS

Feb 13, 2013

This is a License Agreement between Joel Garcia ("You") and John Wiley and Sons ("John Wiley and Sons") provided by Copyright Clearance Center ("CCC"). The license consists of your order details, the terms and conditions provided by John Wiley and Sons, and the payment terms and conditions.

All payments must be made in full to CCC. For payment instructions, please see information listed at the bottom of this form.

License Number

3087200754996

License date

Feb 13, 2013

Licensed content publisher

John Wiley and Sons

Licensed content publication

European Journal of Inorganic Chemistry

Licensed content title

Synthesis, Characterization, and Catalytic Activity of Some Neodymium(III), Ytterbium(II), and Europium(II) Complexes with Pyrrolidinyl- and Piperidinyl-Functionalized Indenyl Ligands

Licensed copyright line

Copyright © 2007 WILEY-VCH Verlag GmbH & Co. KGaA, Weinheim

Licensed content author

Shuangliu Zhou,Shaowu Wang,Enhong Sheng,Lijun Zhang,Zeyan Yu,Xiaobing Xi,Guodong Chen,Wei Luo,Yan Li

Licensed content date

Mar 1, 2007

Start page

1519

End page

1528

Type of use

Dissertation/Thesis

Requestor type

University/Academic

Format

Print and electronic

Portion

Figure/table

Number of figures/tables

1

Original Wiley figure/table number(s)

Scheme 3

Will you be translating?

No

Total

0.00 USD

Terms and Conditions

TERMS AND CONDITIONS

This copyrighted material is owned by or exclusively licensed to John Wiley & Sons, Inc. or one of its group companies (each a "Wiley Company") or a society for whom a Wiley Company has exclusive publishing rights in relation to a particular journal (collectively WILEY"). By clicking "accept" in connection with completing this licensing transaction, you agree that the following terms and conditions apply to this transaction (along with the billing and payment terms and conditions established by the Copyright Clearance Center Inc., ("CCC's Billing and Payment terms and conditions"), at the time that you opened your Rightslink account (these are available at any time at http://myaccount.copyright.com)

Terms and Conditions

1. The materials you have requested permission to reproduce (the "Materials") are protected by copyright.

2. You are hereby granted a personal, non-exclusive, non-sublicensable, non-transferable, worldwide, limited license to reproduce the Materials for the purpose specified in the licensing process. This license is for a one-time use only with a maximum distribution equal to the number that you identified in the licensing process. Any form of republication granted by this licence must be completed within two years of the date of the grant of this licence (although copies prepared before may be distributed thereafter). The Materials shall not be used in any other manner or for any other purpose. Permission is granted subject to an appropriate acknowledgement given to the author, title of the material/book/journal and the publisher. You shall also duplicate the copyright notice that appears in the Wiley publication in your use of the Material. Permission is also granted on the understanding that nowhere in the text is a previously published source acknowledged for all or part of this Material. Any third party material is expressly excluded from this permission.

3. With respect to the Materials, all rights are reserved. Except as expressly granted by the terms of the license, no part of the Materials may be copied, modified, adapted (except for minor reformatting required by the new Publication), translated, reproduced, transferred or distributed, in any form or by any means, and no derivative works may be made based on the Materials without the prior permission of the respective copyright owner. You may not alter, remove or suppress in any manner any copyright, trademark or other notices displayed by the Materials. You may not license, rent, sell, loan, lease, pledge, offer as security, transfer or assign the Materials, or any of the rights granted to you hereunder to any other person.

4. The Materials and all of the intellectual property rights therein shall at all times remain the exclusive property of John Wiley & Sons Inc or one of its related companies (WILEY) or their respective licensors, and your interest therein is only that of having possession of and the right to reproduce the Materials pursuant to Section 2 herein during the continuance of this Agreement. You agree that you own no right, title or interest in or to the Materials or any of the intellectual property rights therein. You shall have no rights hereunder other than the license as provided for above in Section 2. No right, license or interest to any trademark, trade name, service mark or other branding ("Marks") of WILEY or its licensors is granted hereunder, and you agree that you shall not assert any such right, license or interest with respect thereto.

5. NEITHER WILEY NOR ITS LICENSORS MAKES ANY WARRANTY OR REPRESENTATION OF ANY KIND TO YOU OR ANY THIRD PARTY, EXPRESS, IMPLIED OR STATUTORY, WITH RESPECT TO THE MATERIALS OR THE ACCURACY OF ANY INFORMATION CONTAINED IN THE MATERIALS, INCLUDING, WITHOUT LIMITATION, ANY IMPLIED WARRANTY OF MERCHANTABILITY, ACCURACY, SATISFACTORY QUALITY, FITNESS FOR A PARTICULAR PURPOSE, USABILITY, INTEGRATION OR NON-INFRINGEMENT AND ALL SUCH WARRANTIES ARE HEREBY EXCLUDED BY WILEY AND ITS LICENSORS AND WAIVED BY YOU.

6. WILEY shall have the right to terminate this Agreement immediately upon breach of this Agreement by you.

7. You shall indemnify, defend and hold harmless WILEY, its Licensors and their respective directors, officers, agents and employees, from and against any actual or threatened claims, demands, causes of action or proceedings arising from any breach of this Agreement by you.

8. IN NO EVENT SHALL WILEY OR ITS LICENSORS BE LIABLE TO YOU OR ANY OTHER PARTY OR ANY OTHER PERSON OR ENTITY FOR ANY SPECIAL, CONSEQUENTIAL,

INCIDENTAL, INDIRECT, EXEMPLARY OR PUNITIVE DAMAGES, HOWEVER CAUSED, ARISING OUT OF OR IN CONNECTION WITH THE DOWNLOADING, PROVISIONING, VIEWING OR USE OF THE MATERIALS REGARDLESS OF THE FORM OF ACTION, WHETHER FOR BREACH OF CONTRACT, BREACH OF WARRANTY, TORT, NEGLIGENCE, INFRINGEMENT OR OTHERWISE (INCLUDING, WITHOUT LIMITATION, DAMAGES BASED ON LOSS OF PROFITS, DATA, FILES, USE, BUSINESS OPPORTUNITY OR CLAIMS OF THIRD PARTIES), AND WHETHER OR NOT THE PARTY HAS BEEN ADVISED OF THE POSSIBILITY OF SUCH DAMAGES. THIS LIMITATION SHALL APPLY NOTWITHSTANDING ANY FAILURE OF ESSENTIAL PURPOSE OF ANY LIMITED REMEDY PROVIDED HEREIN.

9. Should any provision of this Agreement be held by a court of competent jurisdiction to be illegal, invalid, or unenforceable, that provision shall be deemed amended to achieve as nearly as possible the same economic effect as the original provision, and the legality, validity and enforceability of the remaining provisions of this Agreement shall not be affected or impaired thereby.

10. The failure of either party to enforce any term or condition of this Agreement shall not constitute a waiver of either party's right to enforce each and every term and condition of this Agreement. No breach under this agreement shall be deemed waived or excused by either party unless such waiver or consent is in writing signed by the party granting such waiver or consent. The waiver by or consent of a party to a breach of any provision of this Agreement shall not operate or be construed as a waiver of or consent to any other or subsequent breach by such other party.

11. This Agreement may not be assigned (including by operation of law or otherwise) by you without WILEY's prior written consent.

12. Any fee required for this permission shall be non-refundable after thirty (30) days from receipt.

13. These terms and conditions together with CCC's Billing and Payment terms and conditions (which are incorporated herein) form the entire agreement between you and WILEY concerning this licensing transaction and (in the absence of fraud) supersedes all prior agreements and representations of the parties, oral or written. This Agreement may not be amended except in writing signed by both parties. This Agreement shall be binding upon and inure to the benefit of the parties' successors, legal representatives, and authorized assigns.

14. In the event of any conflict between your obligations established by these terms and conditions and those established by CCC's Billing and Payment terms and conditions, these terms and conditions shall prevail.

15. WILEY expressly reserves all rights not specifically granted in the combination of (i) the license details provided by you and accepted in the course of this licensing transaction, (ii) these terms and conditions and (iii) CCC's Billing and Payment terms and conditions.

16. This Agreement will be void if the Type of Use, Format, Circulation, or Requestor Type was misrepresented during the licensing process.

17. This Agreement shall be governed by and construed in accordance with the laws of the State of New York, USA, without regards to such state's conflict of law rules. Any legal action, suit or proceeding arising out of or relating to these Terms and Conditions or the breach thereof shall be instituted in a court of competent jurisdiction in New York County in the State of New York in the United States of America and each party hereby consents and submits to the personal jurisdiction of such court, waives any objection to venue in such court and consents to service of process by registered or certified mail, return receipt requested, at the last known address of such party.

Wiley Open Access Terms and Conditions

All research articles published in Wiley Open Access journals are fully open access: immediately freely available to read, download and share. Articles are published under the terms of the Creative Commons Attribution Non Commercial License. which permits use, distribution and reproduction in any medium, provided the original work is properly cited and is not used for commercial purposes. The license is subject to the Wiley Open Access terms and conditions:
Wiley Open Access articles are protected by copyright and are posted to repositories and websites in accordance with the terms of the Creative Commons Attribution Non Commercial License. At the time of deposit, Wiley Open Access articles include all changes made during peer review, copyediting, and publishing. Repositories and websites that host the article are responsible for incorporating any publisher-supplied amendments or retractions issued subsequently.
Wiley Open Access articles are also available without charge on Wiley's publishing platform,**Wiley Online Library** or any successor sites.

Use by non-commercial users

For non-commercial and non-promotional purposes individual users may access, download, copy, display and redistribute to colleagues Wiley Open Access articles, as well as adapt, translate, text- and data-mine the content subject to the following conditions:

- The authors' moral rights are not compromised. These rights include the right of "paternity" (also known as "attribution" - the right for the author to be identified as such) and "integrity" (the right for the author not to have the work altered in such a way that the author's reputation or integrity may be impugned).

- Where content in the article is identified as belonging to a third party, it is the obligation of the user to ensure that any reuse complies with the copyright policies of the owner of that content.

- If article content is copied, downloaded or otherwise reused for non-commercial research and education purposes, a link to the appropriate bibliographic citation (authors, journal, article title, volume, issue, page numbers, DOI and the link to the definitive published version on Wiley Online Library) should be maintained. Copyright notices and disclaimers must not be deleted.

- Any translations, for which a prior translation agreement with Wiley has not been agreed, must prominently display the statement: "This is an unofficial translation of an article that appeared in a Wiley publication. The publisher has not endorsed this translation."

Use by commercial "for-profit" organisations

Use of Wiley Open Access articles for commercial, promotional, or marketing purposes requires further explicit permission from Wiley and will be subject to a fee. Commercial purposes include:

- Copying or downloading of articles, or linking to such articles for further redistribution, sale or licensing;
- Copying, downloading or posting by a site or service that incorporates advertising with such content;
- The inclusion or incorporation of article content in other works or services (other than normal quotations with an appropriate citation) that is then available for sale or licensing, for a fee (for example, a compilation produced for marketing purposes, inclusion in a sales pack)
- Use of article content (other than normal quotations with appropriate citation) by for-profit organisations for promotional purposes
- Linking to article content in e-mails redistributed for promotional, marketing or educational purposes;
- Use for the purposes of monetary reward by means of sale, resale, licence, loan, transfer or other form of commercial exploitation such as marketing products
- Print reprints of Wiley Open Access articles can be purchased from: corporatesales@wiley.com

Other Terms and Conditions:

BY CLICKING ON THE "I AGREE..." BOX, YOU ACKNOWLEDGE THAT YOU HAVE READ AND FULLY UNDERSTAND EACH OF THE SECTIONS OF AND PROVISIONS SET FORTH IN THIS AGREEMENT AND THAT YOU ARE IN AGREEMENT WITH AND ARE WILLING TO ACCEPT ALL OF YOUR OBLIGATIONS AS SET FORTH IN THIS AGREEMENT.

v1.7

If you would like to pay for this license now, please remit this license along with your payment made payable to "COPYRIGHT CLEARANCE CENTER" otherwise you will be invoiced within 48 hours of the license date. Payment should be in the form of a check or money order referencing your account number and this invoice number RLNK500956261.
Once you receive your invoice for this order, you may pay your invoice by credit card. Please follow instructions provided at that time.

Make Payment To:
Copyright Clearance Center
Dept 001
P.O. Box 843006
Boston, MA 02284-3006

For suggestions or comments regarding this order, contact RightsLink Customer Support:customercare@copyright.com or +1-877-622-5543 (toll free in the US) or +1-978-646-2777.

Gratis licenses (referencing $0 in the Total field) are free. Please retain this printable license for your reference. No payment is required.

A6. Copyright Permission for *Chem. Commun.* 2011, *47*, 12858–12860.

Date: Wed, 30 Jan 2013 13:19:00 +0000 [01/30/2013 08:19:00 AM EST]

From: CONTRACTS-COPYRIGHT (shared) <Contracts-Copyright@rsc.org>

To: 'Joel Garcia' <jgarcia@chem.wayne.edu>

Subject: RE: reuse of my paper in my dissertation

Dear Joel

The Royal Society of Chemistry (RSC) hereby grants permission for the use of your paper(s) specified below in the printed and microfilm version of your thesis. You may also make available the PDF version of your paper(s) that the RSC sent to the corresponding author(s) of your paper(s) upon publication of the paper(s) in the following ways: in your thesis via any website that your university may have for the deposition of theses, via your university's Intranet or via your own personal website. We are however unable to grant you permission to include the PDF version of the paper(s) on its own in your institutional repository. The Royal Society of Chemistry is a signatory to the STM Guidelines on Permissions (available on request).

Please note that if the material specified below or any part of it appears with credit or acknowledgement to a third party then you must also secure permission from that third party before reproducing that material.

Please ensure that the thesis states the following:

Reproduced by permission of The Royal Society of Chemistry

and include a link to the paper on the Royal Society of Chemistry's website.

Please ensure that your co-authors are aware that you are including the paper in your thesis.

Regards

Gill Cockhead
Publishing Contracts & Copyright Executive

Gill Cockhead (Mrs), Publishing Contracts & Copyright Executive
Royal Society of Chemistry, Thomas Graham House
Science Park, Milton Road, Cambridge CB4 0WF, UK
Tel +44 (0) 1223 432134, Fax +44 (0) 1223 423623
http://www.rsc.org<http://www.rsc.org/>

-----Original Message-----

From: Joel Garcia [mailto:jgarcia@chem.wayne.edu]

Sent: 22 January 2013 18:35

To: CONTRACTS-COPYRIGHT (shared)

Subject: reuse of my paper in my dissertation

Hi! I would like to ask for permission to reuse my paper:

EuII-containing cryptates as contrast agents for ultra-high field strength magnetic resonance imaging Joel Garcia, Jaladhar Neelavalli, E. Mark Haacke and Matthew J. Allen Chem. Commun., 2011, 47, 12858-12860.

DOI: 10.1039/C1CC15219J

to my dissertation. I am the author of the original worrk. The portion I would like to use is the full article. My format is print and electronic. My distribution is about 10. I won't be translating.

Thank you,

Joel

--
Joel Garcia
Graduate Research Assistant
Professor Matthew J. Allen Laboratory
Department of Chemistry

Wayne State University

5101 Cass Avenue

Detroit, MI 48202

Lab Phone: 313-577-2042

DISCLAIMER:

This communication (including any attachments) is intended for the use of the addressee only and may contain confidential, privileged or copyright material. It may not be relied upon or disclosed to any other person without the consent of the RSC. If you have received it in error, please contact us immediately. Any advice given by the RSC has been carefully formulated but is necessarily based on the information available, and the RSC cannot be held responsible for accuracy or completeness. In this respect, the RSC owes no duty of care and shall not be liable for any resulting damage or loss. The RSC acknowledges that a disclaimer cannot restrict liability at law for personal injury or death arising through a finding of negligence. The RSC does not warrant that its emails or attachments are Virus-free: Please rely on your own screening. The Royal Society of Chemistry is a charity, registered in England and Wales, number 207890 - Registered office: Thomas Graham House, Science Park, Milton Road, Cambridge CB4 0WF

Date: Wed, 30 Jan 2013 10:07:12 -0500 [01/30/2013 10:07:12 AM EST]

From: Joel Garcia <jgarcia@chem.wayne.edu>

To: mallen@chem.wayne.edu

Subject: Fwd: RE: reuse of my paper in my dissertation

Dear Professor Allen,

This is to inform you that I will be using the following paper:

EuII-containing cryptates as contrast agents for ultra-high field strength magnetic resonance imaging Joel Garcia, Jaladhar Neelavalli, E. Mark Haacke and Matthew J. Allen Chem. Commun., 2011, 47, 12858-12860.

in my dissertation.

Sincerely,

Joel

Date: Wed, 30 Jan 2013 10:10:03 -0500 [01/30/2013 10:10:03 AM EST]

From: Joel Garcia <jgarcia@chem.wayne.edu>

To: Nmrimaging@aol.com

Subject: RE: reuse of my paper in my dissertation

Dear Professor Haacke,

This is to inform you that I will be using the following paper:

EuII-containing cryptates as contrast agents for ultra-high field strength magnetic resonance imaging Joel Garcia, Jaladhar Neelavalli, E. Mark Haacke and Matthew J. Allen Chem. Commun., 2011, 47, 12858-12860.

in my dissertation.

Sincerely,

Joel

Date: Wed, 30 Jan 2013 10:11:31 -0500 [01/30/2013 10:11:31 AM EST]

From: Joel Garcia <jgarcia@chem.wayne.edu>

To: jaladhar@gmail.com

Subject: RE: reuse of my paper in my dissertation

Dear Professor Neelavalli,

This is to inform you that I will be using the following paper:

EuII-containing cryptates as contrast agents for ultra-high field strength magnetic resonance imaging Joel Garcia, Jaladhar Neelavalli, E. Mark Haacke and Matthew J. Allen Chem. Commun., 2011, 47, 12858-12860.

in my dissertation.

Sincerely,

Joel

A7. Copyright Permission for *Eur. J. Inorg. Chem.* 2012, *2012*, 2135–2140.

JOHN WILEY AND SONS LICENSE
TERMS AND CONDITIONS

Feb 13, 2013

This is a License Agreement between Joel Garcia ("You") and John Wiley and Sons ("John Wiley and Sons") provided by Copyright Clearance Center ("CCC"). The license consists of your order details, the terms and conditions provided by John Wiley and Sons, and the payment terms and conditions.

All payments must be made in full to CCC. For payment instructions, please see information listed at the bottom of this form.

License Number

3087201280408

License date

Feb 13, 2013

Licensed content publisher

John Wiley and Sons

Licensed content publication

European Journal of Inorganic Chemistry

Licensed content title

Physical Properties of Eu2 -Containing Cryptates as Contrast Agents for Ultrahigh-Field Magnetic Resonance Imaging

Licensed copyright line

Copyright © 2012 WILEY-VCH Verlag GmbH & Co. KGaA, Weinheim

Licensed content author

Joel Garcia,Akhila N. W. Kuda-Wedagedara,Matthew J. Allen

Licensed content date

Feb 8, 2012

Start page

2135

End page

2140

Type of use

Dissertation/Thesis

Requestor type

Author of this Wiley article

Format

Print and electronic

Portion

Full article

Will you be translating?

No

Total

0.00 USD

Terms and Conditions

TERMS AND CONDITIONS

This copyrighted material is owned by or exclusively licensed to John Wiley & Sons, Inc. or one of its group companies (each a "Wiley Company") or a society for whom a Wiley Company has exclusive publishing rights in relation to a particular journal (collectively WILEY"). By clicking "accept" in connection with completing this licensing transaction, you agree that the following terms and conditions apply to this transaction (along with the billing and payment terms and conditions established by the Copyright Clearance Center Inc., ("CCC's Billing and Payment terms and conditions"), at the time that you opened your Rightslink account (these are available at any time at http://myaccount.copyright.com)

Terms and Conditions

1. The materials you have requested permission to reproduce (the "Materials") are protected by copyright.

2. You are hereby granted a personal, non-exclusive, non-sublicensable, non-transferable, worldwide, limited license to reproduce the Materials for the purpose specified in the licensing process. This license is for a one-time use only with a maximum distribution equal to the number that you identified in the licensing process. Any form of republication granted by this licence must be completed within two years of the date of the grant of this licence (although copies prepared before may be distributed thereafter). The Materials shall not be used in any other manner or for any other purpose. Permission is granted subject to an appropriate acknowledgement given to the author, title of the material/book/journal and the publisher. You shall also duplicate the copyright notice that appears in the Wiley publication in your use of the Material. Permission is also granted on the understanding that nowhere in the text is a previously published source acknowledged for all or part of this Material. Any third party material is expressly excluded from this permission.

3. With respect to the Materials, all rights are reserved. Except as expressly granted by the terms of the license, no part of the Materials may be copied, modified, adapted (except for minor reformatting required by the new Publication), translated, reproduced, transferred or distributed, in any form or by any means, and no derivative works may be made based on the Materials without the prior permission of the respective copyright owner. You may not alter, remove or suppress in any manner any copyright, trademark or other notices displayed by the Materials. You may not license, rent, sell, loan, lease, pledge, offer as security, transfer or assign the Materials, or any of the rights granted to you hereunder to any other person.

4. The Materials and all of the intellectual property rights therein shall at all times remain the exclusive property of John Wiley & Sons Inc or one of its related companies (WILEY) or their respective licensors, and your interest therein is only that of having possession of and the right to reproduce the Materials pursuant to Section 2 herein during the continuance of this Agreement. You agree that you own no right, title or interest in or to the Materials or any of the intellectual property rights therein. You shall have no rights hereunder other than the license as provided for above in Section 2. No right, license or interest to any trademark, trade name, service mark or other branding ("Marks") of WILEY or its licensors is granted hereunder, and you agree that you shall not assert any such right, license or interest with respect thereto.

5. NEITHER WILEY NOR ITS LICENSORS MAKES ANY WARRANTY OR REPRESENTATION OF ANY KIND TO YOU OR ANY THIRD PARTY, EXPRESS, IMPLIED OR STATUTORY, WITH RESPECT TO THE MATERIALS OR THE ACCURACY OF ANY INFORMATION CONTAINED IN THE MATERIALS, INCLUDING, WITHOUT LIMITATION, ANY IMPLIED WARRANTY OF MERCHANTABILITY, ACCURACY, SATISFACTORY QUALITY, FITNESS FOR A PARTICULAR PURPOSE, USABILITY, INTEGRATION OR NON-INFRINGEMENT AND ALL SUCH WARRANTIES ARE HEREBY EXCLUDED BY WILEY AND ITS LICENSORS AND WAIVED BY YOU.

6. WILEY shall have the right to terminate this Agreement immediately upon breach of this Agreement by you.

7. You shall indemnify, defend and hold harmless WILEY, its Licensors and their respective directors, officers, agents and employees, from and against any actual or threatened claims, demands, causes of action or proceedings arising from any breach of this Agreement by you.

8. IN NO EVENT SHALL WILEY OR ITS LICENSORS BE LIABLE TO YOU OR ANY OTHER PARTY OR ANY OTHER PERSON OR ENTITY FOR ANY SPECIAL, CONSEQUENTIAL, INCIDENTAL, INDIRECT, EXEMPLARY OR PUNITIVE DAMAGES, HOWEVER CAUSED, ARISING OUT OF OR IN CONNECTION WITH THE DOWNLOADING, PROVISIONING, VIEWING OR USE OF THE MATERIALS REGARDLESS OF THE FORM OF ACTION, WHETHER FOR BREACH OF CONTRACT, BREACH OF WARRANTY, TORT, NEGLIGENCE, INFRINGEMENT OR OTHERWISE (INCLUDING, WITHOUT LIMITATION, DAMAGES BASED ON LOSS OF PROFITS, DATA, FILES, USE, BUSINESS OPPORTUNITY OR CLAIMS OF THIRD PARTIES), AND WHETHER OR NOT THE PARTY HAS BEEN ADVISED OF THE POSSIBILITY OF SUCH DAMAGES. THIS LIMITATION SHALL APPLY NOTWITHSTANDING ANY FAILURE OF ESSENTIAL PURPOSE OF ANY LIMITED REMEDY PROVIDED HEREIN.

9. Should any provision of this Agreement be held by a court of competent jurisdiction to be illegal, invalid, or unenforceable, that provision shall be deemed amended to achieve as nearly as possible the same economic effect as the original provision, and the legality, validity and enforceability of the remaining provisions of this Agreement shall not be affected or impaired thereby.

10. The failure of either party to enforce any term or condition of this Agreement shall not constitute a waiver of either party's right to enforce each and every term and condition of this Agreement. No breach under this agreement shall be deemed waived or excused by either party unless such waiver or consent is in writing signed by the party granting such waiver or consent. The waiver by or consent of a party to a breach of any provision of this Agreement shall not operate or be construed as a waiver of or consent to any other or subsequent breach by such other party.

11. This Agreement may not be assigned (including by operation of law or otherwise) by you without WILEY's prior written consent.

12. Any fee required for this permission shall be non-refundable after thirty (30) days from receipt.

13. These terms and conditions together with CCC's Billing and Payment terms and conditions (which are incorporated herein) form the entire agreement between you and WILEY concerning this licensing transaction and (in the absence of fraud) supersedes all prior agreements and representations of the parties, oral or written. This Agreement may not be amended except in writing signed by both parties. This Agreement shall be binding upon and inure to the benefit of the parties' successors, legal representatives, and authorized assigns.

14. In the event of any conflict between your obligations established by these terms and conditions and those established by CCC's Billing and Payment terms and conditions, these terms and conditions shall prevail.

15. WILEY expressly reserves all rights not specifically granted in the combination of (i) the license details provided by you and accepted in the course of this licensing transaction, (ii) these terms and conditions and (iii) CCC's Billing and Payment terms and conditions.

16. This Agreement will be void if the Type of Use, Format, Circulation, or Requestor Type was misrepresented during the licensing process.

17. This Agreement shall be governed by and construed in accordance with the laws of the State of New York, USA, without regards to such state's conflict of law rules. Any legal action, suit or proceeding arising out of or relating to these Terms and Conditions or the breach thereof shall be instituted in a court of competent jurisdiction in New York County in the State of New York in the United States of America and each party hereby consents and submits to the personal jurisdiction of such court, waives any objection to venue in such court and consents to service of process by registered or certified mail, return receipt requested, at the last known address of such party.

Wiley Open Access Terms and Conditions

All research articles published in Wiley Open Access journals are fully open access: immediately freely available to read, download and share. Articles are published under the terms of the Creative Commons Attribution Non Commercial License. which permits use, distribution and reproduction in any medium, provided the original work is properly cited and is not used for commercial purposes. The license is subject to the Wiley Open Access terms and conditions:
Wiley Open Access articles are protected by copyright and are posted to repositories and websites in accordance with the terms of the Creative Commons Attribution Non Commercial License. At the time of deposit, Wiley Open Access articles include all changes made during peer review, copyediting, and publishing. Repositories and websites that host the article are responsible for incorporating any publisher-supplied amendments or retractions issued subsequently.
Wiley Open Access articles are also available without charge on Wiley's publishing platform,**Wiley Online Library** or any successor sites.

Use by non-commercial users

For non-commercial and non-promotional purposes individual users may access, download, copy, display and redistribute to colleagues Wiley Open Access articles, as well as adapt, translate, text- and data-mine the content subject to the following conditions:

- The authors' moral rights are not compromised. These rights include the right of "paternity" (also known as "attribution" - the right for the author to be identified as such) and "integrity" (the right for the author not to have the work altered in such a way that the author's reputation or integrity may be impugned).

- Where content in the article is identified as belonging to a third party, it is the obligation of the user to ensure that any reuse complies with the copyright policies of the owner of that content.

- If article content is copied, downloaded or otherwise reused for non-commercial research and education purposes, a link to the appropriate bibliographic citation (authors, journal, article title, volume, issue, page numbers, DOI and the link to the definitive published version on Wiley Online Library) should be maintained. Copyright notices and disclaimers must not be deleted.

- Any translations, for which a prior translation agreement with Wiley has not been agreed, must prominently display the statement: "This is an unofficial translation of an article that appeared in a Wiley publication. The publisher has not endorsed this translation."

Use by commercial "for-profit" organisations

Use of Wiley Open Access articles for commercial, promotional, or marketing purposes requires further explicit permission from Wiley and will be subject to a fee. Commercial purposes include:

- Copying or downloading of articles, or linking to such articles for further redistribution, sale or licensing;
- Copying, downloading or posting by a site or service that incorporates advertising with such content;

- The inclusion or incorporation of article content in other works or services (other than normal quotations with an appropriate citation) that is then available for sale or licensing, for a fee (for example, a compilation produced for marketing purposes, inclusion in a sales pack)

- Use of article content (other than normal quotations with appropriate citation) by for-profit organisations for promotional purposes

- Linking to article content in e-mails redistributed for promotional, marketing or educational purposes;

- Use for the purposes of monetary reward by means of sale, resale, licence, loan, transfer or other form of commercial exploitation such as marketing products

- Print reprints of Wiley Open Access articles can be purchased from: corporatesales@wiley.com

Other Terms and Conditions:

BY CLICKING ON THE "I AGREE..." BOX, YOU ACKNOWLEDGE THAT YOU HAVE READ AND FULLY UNDERSTAND EACH OF THE SECTIONS OF AND PROVISIONS SET FORTH IN THIS AGREEMENT AND THAT YOU ARE IN AGREEMENT WITH AND ARE WILLING TO ACCEPT ALL OF YOUR OBLIGATIONS AS SET FORTH IN THIS AGREEMENT.

v1.7

If you would like to pay for this license now, please remit this license along with your payment made payable to "COPYRIGHT CLEARANCE CENTER" otherwise you will be invoiced within 48 hours of the license date. Payment should be in the form of a check or money order referencing your account number and this invoice number RLNK500956269.
Once you receive your invoice for this order, you may pay your invoice by credit card. Please follow instructions provided at that time.

Make Payment To:
Copyright Clearance Center
Dept 001
P.O. Box 843006
Boston, MA 02284-3006

For suggestions or comments regarding this order, contact RightsLink Customer Support:customercare@copyright.com or +1-877-622-5543 (toll free in the US) or +1-978-646-2777.

Gratis licenses (referencing $0 in the Total field) are free. Please retain this printable license for your reference. No payment is required.

A8. Copyright Permission for *Inorg. Chim. Acta* 2012, *393*, 324–327.

ELSEVIER LICENSE
TERMS AND CONDITIONS

Feb 13, 2013

This is a License Agreement between Joel Garcia ("You") and Elsevier ("Elsevier") provided by Copyright Clearance Center ("CCC"). The license consists of your order details, the terms and conditions provided by Elsevier, and the payment terms and conditions.

All payments must be made in full to CCC. For payment instructions, please see information listed at the bottom of this form.

Supplier

Elsevier Limited
The Boulevard,Langford Lane
Kidlington,Oxford,OX5 1GB,UK

Registered Company Number

1982084

Customer name

Joel Garcia

Customer address

5200 Anthony Wayne Drive APT 901

Detroit, MI 48202

License number

3075921389123

License date

Jan 25, 2013

Licensed content publisher

Elsevier

Licensed content publication

Inorganica Chimica Acta

Licensed content title

Interaction of biphenyl-functionalized Eu-containing cryptate with albumin: Implications to contrast agents in magnetic resonance imaging

Licensed content author

Joel Garcia,Matthew J. Allen

Licensed content date

1 December 2012

Licensed content volume number

393

Licensed content issue number

None

Number of pages

4

Start Page

324

End Page

327

Type of Use

reuse in a thesis/dissertation

Portion

full article

Format

both print and electronic

Are you the author of this Elsevier article?

Yes

Will you be translating?

No

Order reference number

None

Title of your thesis/dissertation

STUDIES ON THE PHYSICOCHEMICAL PROPERTIES OF Eu2+ CRYPTATES: IMPLICATIONS TO CONTRAST AGENTS FOR MAGNETIC RESONANCE IMAGING

Expected completion date

May 2013

Estimated size (number of pages)

200

Elsevier VAT number

GB 494 6272 12

Permissions price

0.00 USD

VAT/Local Sales Tax

0.0 USD / 0.0 GBP

Total

0.00 USD

Terms and Conditions

INTRODUCTION

1. The publisher for this copyrighted material is Elsevier. By clicking "accept" in connection with completing this licensing transaction, you agree that the following terms and conditions apply to this transaction (along with the Billing and Payment terms and conditions established by Copyright Clearance Center, Inc. ("CCC"), at the time that you opened your Rightslink account and that are available at any time at http://myaccount.copyright.com).

GENERAL TERMS

2. Elsevier hereby grants you permission to reproduce the aforementioned material subject to the terms and conditions indicated.

3. Acknowledgement: If any part of the material to be used (for example, figures) has appeared in our publication with credit or acknowledgement to another source, permission must also be sought from that source. If such permission is not obtained then that material may not be included in your publication/copies. Suitable acknowledgement to the source must be made, either as a footnote or in a reference list at the end of your publication, as follows:

"Reprinted from Publication title, Vol /edition number, Author(s), Title of article / title of chapter, Pages No., Copyright (Year), with permission from Elsevier [OR APPLICABLE SOCIETY COPYRIGHT OWNER]." Also Lancet special credit - "Reprinted from The Lancet, Vol. number, Author(s), Title of article, Pages No., Copyright (Year), with permission from Elsevier."

4. Reproduction of this material is confined to the purpose and/or media for which permission is hereby given.

5. Altering/Modifying Material: Not Permitted. However figures and illustrations may be altered/adapted minimally to serve your work. Any other abbreviations, additions, deletions and/or any other alterations shall be made only with prior written authorization of Elsevier Ltd. (Please contact Elsevier at permissions@elsevier.com)

6. If the permission fee for the requested use of our material is waived in this instance, please be advised that your future requests for Elsevier materials may attract a fee.

7. Reservation of Rights: Publisher reserves all rights not specifically granted in the combination of (i) the license details provided by you and accepted in the course of this licensing transaction, (ii) these terms and conditions and (iii) CCC's Billing and Payment terms and conditions.

8. License Contingent Upon Payment: While you may exercise the rights licensed immediately upon issuance of the license at the end of the licensing process for the transaction, provided that you have disclosed complete and accurate details of your proposed use, no license is finally effective unless and until full payment is received from you (either by publisher or by CCC) as provided in CCC's Billing and Payment terms and conditions. If full payment is not received on a timely basis, then any license preliminarily granted shall be deemed automatically revoked and shall be void as if never granted. Further, in the event that you breach any of these terms and conditions or any of CCC's Billing and Payment terms and conditions, the license is automatically revoked and shall be void as if never granted. Use of materials as described in a revoked license, as well as any use of the materials beyond the scope of an unrevoked license, may constitute copyright infringement and publisher reserves the right to take any and all action to protect its copyright in the materials.

9. Warranties: Publisher makes no representations or warranties with respect to the licensed material.

10. Indemnity: You hereby indemnify and agree to hold harmless publisher and CCC, and their respective officers, directors, employees and agents, from and against any and all claims arising out of your use of the licensed material other than as specifically authorized pursuant to this license.

11. No Transfer of License: This license is personal to you and may not be sublicensed, assigned, or transferred by you to any other person without publisher's written permission.

12. No Amendment Except in Writing: This license may not be amended except in a writing signed by both parties (or, in the case of publisher, by CCC on publisher's behalf).

13. Objection to Contrary Terms: Publisher hereby objects to any terms contained in any purchase order, acknowledgment, check endorsement or other writing prepared by you, which terms are inconsistent with these terms and conditions or CCC's Billing and Payment terms and conditions. These terms and conditions, together with CCC's Billing and Payment terms and

conditions (which are incorporated herein), comprise the entire agreement between you and publisher (and CCC) concerning this licensing transaction. In the event of any conflict between your obligations established by these terms and conditions and those established by CCC's Billing and Payment terms and conditions, these terms and conditions shall control.

14. Revocation: Elsevier or Copyright Clearance Center may deny the permissions described in this License at their sole discretion, for any reason or no reason, with a full refund payable to you. Notice of such denial will be made using the contact information provided by you. Failure to receive such notice will not alter or invalidate the denial. In no event will Elsevier or Copyright Clearance Center be responsible or liable for any costs, expenses or damage incurred by you as a result of a denial of your permission request, other than a refund of the amount(s) paid by you to Elsevier and/or Copyright Clearance Center for denied permissions.

LIMITED LICENSE

The following terms and conditions apply only to specific license types:

15. **Translation**: This permission is granted for non-exclusive world **English** rights only unless your license was granted for translation rights. If you licensed translation rights you may only translate this content into the languages you requested. A professional translator must perform all translations and reproduce the content word for word preserving the integrity of the article. If this license is to re-use 1 or 2 figures then permission is granted for non-exclusive world rights in all languages.

16. **Website**: The following terms and conditions apply to electronic reserve and author websites:
Electronic reserve: If licensed material is to be posted to website, the web site is to be password-protected and made available only to bona fide students registered on a relevant course if:
This license was made in connection with a course,
This permission is granted for 1 year only. You may obtain a license for future website posting,
All content posted to the web site must maintain the copyright information line on the bottom of each image,
A hyper-text must be included to the Homepage of the journal from which you are licensing at http://www.sciencedirect.com/science/journal/xxxxx or the Elsevier homepage for books at http://www.elsevier.com , and
Central Storage: This license does not include permission for a scanned version of the material to be stored in a central repository such as that provided by Heron/XanEdu.

17. **Author website** for journals with the following additional clauses:

All content posted to the web site must maintain the copyright information line on the bottom of each image, and the permission granted is limited to the personal version of your paper. You are not allowed to download and post the published electronic version of your article (whether PDF or HTML, proof or final version), nor may you scan the printed edition to create an electronic version. A hyper-text must be included to the Homepage of the journal from which you are licensing athttp://www.sciencedirect.com/science/journal/xxxxx . As part of our normal production process, you will receive an e-mail notice when your article appears on Elsevier's online service ScienceDirect (www.sciencedirect.com). That e-mail will include the article's Digital Object Identifier (DOI). This number provides the electronic link to the published article and should be included in the posting of your personal version. We ask that you wait until you receive this e-mail and have the DOI to do any posting.

Central Storage: This license does not include permission for a scanned version of the material to be stored in a central repository such as that provided by Heron/XanEdu.

18. **Author website** for books with the following additional clauses:
Authors are permitted to place a brief summary of their work online only.
A hyper-text must be included to the Elsevier homepage at http://www.elsevier.com . All content posted to the web site must maintain the copyright information line on the bottom of each image. You are not allowed to download and post the published electronic version of your chapter, nor may you scan the printed edition to create an electronic version.

Central Storage: This license does not include permission for a scanned version of the material to be stored in a central repository such as that provided by Heron/XanEdu.

19. **Website** (regular and for author): A hyper-text must be included to the Homepage of the journal from which you are licensing at http://www.sciencedirect.com/science/journal/xxxxx. or for books to the Elsevier homepage at http://www.elsevier.com

20. **Thesis/Dissertation**: If your license is for use in a thesis/dissertation your thesis may be submitted to your institution in either print or electronic form. Should your thesis be published commercially, please reapply for permission. These requirements include permission for the Library and Archives of Canada to supply single copies, on demand, of the complete thesis and include permission for UMI to supply single copies, on demand, of the complete thesis. Should your thesis be published commercially, please reapply for permission.

21. **Other Conditions**:

v1.6

If you would like to pay for this license now, please remit this license along with your payment made payable to "COPYRIGHT CLEARANCE CENTER" otherwise you will be invoiced within 48 hours of the license date. Payment should be in the form of a check or money order referencing your account number and this invoice number RLNK500941965. Once you receive your invoice for this order, you may pay your invoice by credit card. Please follow instructions provided at that time.

Make Payment To:
Copyright Clearance Center
Dept 001
P.O. Box 843006
Boston, MA 02284-3006

For suggestions or comments regarding this order, contact RightsLink Customer Support: customercare@copyright.com or +1-877-622-5543 (toll free in the US) or +1-978-646-2777.

Gratis licenses (referencing $0 in the Total field) are free. Please retain this printable license for your reference. No payment is required.

ABSTRACT

STUDIES ON THE PHYSICOCHEMICAL PROPERTIES OF Eu^{2+} CRYPTATES: IMPLICATIONS TO CONTRAST AGENTS FOR MAGNETIC RESONANCE IMAGING

by

JOEL GARCIA

May 2013

Advisor: Professor Matthew J. Allen

Major: Chemistry

Degree: Doctor of Philosophy

Magnetic resonance imaging (MRI) is a powerful medical imaging technique that can be enhanced using metal complexes called contrast agents. Most clinically approved contrast agents contain Gd^{3+}. However, the efficiency (also known as relaxivity) of these Gd^{3+}-containing complexes decreases as field strength increases, and in the ultra-high field strength regime, the relaxivity of these complexes is decreased considerably. Because of the slow water-exchange rate of most Gd^{3+}-containing complexes ($\sim 10^6$ s^{-1}), I used Eu^{2+} instead of Gd^{3+} and adapted the ligand modification strategies that have been used for Gd^{3+}-containing contrast agents to my Eu^{2+}-containing complexes. Eu^{2+} is isoelectronic to Gd^{3+} and has fast water-exchange rate ($\sim 10^9$ s^{-1}); however, the propensity of Eu^{2+} to oxidize in aerobic conditions limits its utility. Earlier work in the Allen lab demonstrated that modified cryptands can stabilize the divalent state of Eu. Because of the favorable properties of Eu^{2+} and the ability of cryptands to oxidatively stabilize Eu^{2+}, I hypothesized that Eu^{2+}-containing cryptates could serve as good candidates for use as contrast agents for MRI. Relaxometric studies revealed higher efficacy of small Eu^{2+}-containing cryptates

compared to the clinically approved contrast agent gadolinium(III) 1,4,7,10-tetraazacyclododecane-1,4,7,10-tetraacetate at ultra-high field strengths. Also, an increase in relaxivity with increasing field strength was observed for these cryptates. Further, the relaxivity of Eu^{2+}-containing cryptates decreases as temperature increases, but is not affected by changes in pH in a physiologically relevant range.

Variable-temperature ^{17}O NMR and electron paramagnetic resonance spectroscopy were used to understand these observations in relaxivity. Variable-temperature ^{17}O NMR experiments revealed the presence of two inner-sphere water molecules and fast water-exchange rates ($\sim 10^7$–10^8 s^{-1}) for small Eu^{2+}-containing cryptates. With the relaxivity and ^{17}O NMR and EPR data, rotational-correlation rates for these cryptates were estimated and were found to limit relaxivity.

In addition to relaxometric studies, transmetallation experiments were performed in the presence of Ca^{2+}, Mg^{2+}, and Zn^{2+} because of their relative abundance in plasma and the affinity of these ions for ligands. The transmetallation experiments demonstrated that amine-based cryptates are stable to transmetallation in the presence of Ca^{2+}, Mg^{2+}, and Zn^{2+} and are more stable than the clinically approved gadolinium(III) diethylenetriaminepentaacetate, a promising result for their potential use for in vivo applications.

Because relaxivity of small Eu^{2+}-containing cryptates increases with molecular weight, I also investigated the effect of albumin on the relaxivity of a biphenyl-containing cryptate. While relaxivity enhancement was observed in the presence of albumin at 1.4 T, the relaxivity of the biphenyl-based cryptate in the presence of albumin at 3, 7, 9.4, and 11.7 T was lower compared to in the absence of albumin. This decrease in relaxivity was attributed to a displacement of one inner-sphere water molecule upon protein binding.

These studies of the physicochemical properties of Eu^{2+}-containing cryptates provide a better understanding of how relaxivity is influenced by molecular parameters including the number of inner-sphere water molecules, water-exchange rate, and rotational-correlation rate for these cryptates and pave the way for designing more efficient Eu^{2+}-containing cryptates for use as contrast agents for MRI.

AUTOBIOGRAPHICAL STATEMENT

Education

Wayne State University, Detroit, MI, USA: Chemistry, Ph. D. 2008–2013
University of the Philippines, Diliman, Quezon City, Philippines: Chemistry, B.Sc. 1999–2004

Fellowships and Awards

Thomas C. Rumble University Graduate Fellowship, Wayne State University: 2012–2013
Gordon Research Conference Travel Award: June 2012
Esther and Stanley Kirschner Graduate Inorganic Chemistry Award, Wayne State University: April 2012
Summer 2012 Dissertation Fellowship, Wayne State University: May 2012–August 2012
Paul and Carol Schaap Graduate Fellowship, Wayne State University: 2011–2012
Graduate and Professional School Travel Award, Wayne State University: 2011
Thomas C. Rumble University Graduate Fellowship, Wayne State University: 2010–2011
Departmental Citation for Excellence in Teaching Service, Wayne State University: April 2010
Graduate School Citation for Excellence in Teaching, Wayne State University: April 2009
Cum Laude, University of the Philippines: April 2004
University Scholar, University of the Philippines: four semesters
College Scholar, University of the Philippines: two semesters

Professional Affiliations

American Chemical Society—Member	2011–Present
Phi Lambda Upsilon (Chemistry Honor Society)	2010–Present

Publications

Garcia, J.; Allen, M. J. *Inorg. Chim. Acta* **2012,** *393,* 324–327.
Garcia, J.; Allen, M. J. *Eur. J. Inorg. Chem.* **2012,** *2012,* 4550–4563. (review article)
Garcia, J.; Kuda-Wedagedara, A. N. W.; Allen, M. J. *Eur. J. Inorg. Chem.* **2012,** *2012,* 2135–2140.
Garcia, J.; Neelavalli, J.; Haacke, E. M.; Allen, M. J. *Chem. Commun.* **2011,** *47,* 12858–12860.
Garcia, J.; Kuda-Wedagedara, A.; Gamage, N.-D.; Haacke, E. M.; Allen, M. J. *Invest. Radiol.* **2011,** *46,* 742–743. (published abstract)
Averill, D. J.; **Garcia, J.**;* Siriwardena-Mahanama, B. N.; Vithanarachchi, S. M.; Allen, M. J. *J. Vis. Exp.* **2011,** *53,* e2844. (* co-first author)
Gamage, N.-D. H.; Mei, Y.; **Garcia, J.**; Allen, M. J. *Angew. Chem., Int. Ed.* **2010,** *49,* 8923–8925.

Presentations/Conferences Attended

Metals in Medicine Gordon Research Conference. Andover, NH. June 24–29, 2012; Poster.
242nd American Chemical Society National Meeting & Exposition. Denver, CO. August 28–September 1, 2011; Poster.
Ohio Inorganic Weekend 2012. Wayne State University, Detroit, MI. October 19–20, 2012; Poster.
14th Annual Chemistry Graduate Research Symposium 2012. Wayne State University, Detroit, MI. October 13, 2012; Poster.
Proteases and Cancer Program Annual Retreat 2011. Wayne State University, Detroit, MI. December 1, 2011; Poster.
Ohio Inorganic Weekend 2011. University of Cincinnati, Cincinnati, OH. October 28–29, 2011; Poster.
Schaap Chemistry Symposium. Wayne State University, Detroit, MI. September 17, 2011; Talk.
Joint Scientific Retreat of the Breast Cancer Biology and Proteases and Cancer Programs. Wayne State University, Detroit, MI. December 14, 2010; Poster.
Ohio Inorganic Weekend 2010. The Ohio State University, Columbus, OH. October 29–30, 2010; Talk.
Ohio Inorganic Weekend 2009. Case Western Reserve University, Cleveland, OH. November 13–14, 2009; Poster.
12th Annual Chemistry Graduate Research Symposium 2010. Wayne State University, Detroit, MI. October 9, 2010; Poster.
11th Annual Chemistry Graduate Research Symposium 2009. Wayne State University, Detroit, MI. October 3, 2009; Poster.